# The cardiac fetal gene program in heart failure

from OPLAH to 5-oxoproline and beyond

Atze van der Pol

2018

Financial support by the Groningen University Institute for Drug Exploration (GUIDE) and University of Groningen is gratefully acknowledged.

Financial support by the Dutch Heart Foundation for the publication of this thesis is gratefully acknowledged.

Financial support for the publication of this thesis is gratefully acknowledged:
Pfizer Nederland B.V.
Servier Nederland Frama B.V.

Cover design: Atze van der Pol
Lay-out: Atze van der Pol

Printed by: Gildepring, Enschede

ISBN: 978-94-034-0712-8; printed version
ISBN: 978-94-034-0711-1; electronic version

The cardiac fetal gene program in heart failure: from OPLAH to 5-oxoproline and beyond

rijksuniversiteit groningen

# The cardiac fetal gene program in heart failure

From OPLAH to 5-oxoproline and beyond

**Proefschrift**

ter verkrijging van de graad van doctor aan de
Rijksuniversiteit Groningen
op gezag van de
Rector Magnificus prof. dr. E. Sterken
en volgens besluit van het College voor Promoties

De openbare verdediging zal plaatsvinden op

woensdag 4 juli 2018 om 9:00

door

**Atze van der Pol**

geboren op 28 april 1986
te Yaoundé, Kameroen

**Promotores:**
Prof. dr. P. van der Meer
Prof. dr. W.H. van Gilst
Prof. dr. R.A. de Boer

**Beoordelingscommissie:**
Prof. dr. J.P.G. Sluijter
Prof. dr. E.A.A. Nollen
Prof. dr. G.J. Navis

**Paranimfen:**
Martijn Hoes
Jasper Tromp

Para mi Familia

Foar myn Famylje

For my Family

Voor mijn Familie

| | | |
|---|---|---|
| **Chapter 1** | Introduction and Aims | 11 |
| **Chapter 2** | Cardiac fetal reprogramming: a tool to exploit novel treatment targets for the failing heart | 15 |
| **Chapter 3** | Accumulation of 5-oxoproline in myocardial dysfunction and the protective effects of OPLAH | 39 |
| **Chapter 4** | OPLAH ablation leads to accumulation of 5-oxoproline, oxidative stress, fibrosis and elevated filling pressures in a murine model for heart failure with a preserved ejection fraction | 91 |
| **Chapter 5** | LC-MS Analysis of Key Components of the γ-Glutamyl Cycle in Tissues and Body Fluids from Mice with Myocardial Infarction | 123 |
| **Chapter 6** | Treating oxidative stress in heart failure: past, present and future | 143 |
| **Chapter 7** | Discussion and future perspectives | 161 |
| **Chapter 8** | Summary | 175 |
| **Chapter 9** | Nederlandse samenvatting | 181 |
| **Appendices**: | | 187 |
| | Curriculum vitae & publications | 189 |
| | Acknowledgments | 193 |

# Chapter 1

## Introduction and Aims

Heart failure (HF) as a result of myocardial infarction (MI) and ischemic heart disease remains the most prominent health challenge of the developed world, with a five year survival rate of less than 50%. HF is defined as the complex end stage clinical syndrome that can result from numerous cardiac disorders, including myocardial infarction (MI), hypertension, cardiomyopathies, and valvular disease. HF is characterized by the acute or gradual loss of functional cardiomyocytes. The remaining cardiomyocytes ineffectively attempt to compensate for the loss of myocardium, initiating a cascade of processes which eventually lead to cardiac remodeling. Cardiac remodeling induces scar tissue formation, ventricular wall thickening, and eventually diminished cardiac muscle functionality. Current clinical therapeutic interventions are successful in slowing down the progression of HF. Such therapies include several forms of drug treatments (e.g. ACE inhibitors), lifestyle modifications, surgery and ultimately heart transplantation. Cardiac transplantation is to date the only therapeutic option for end-stage HF but due to the low number of organ donors only a few thousand patients a year have access to a transplantation program. Therefore, novel strategies aimed at identifying the pathophysiological pathways involved in HF development and progression may lead to novel therapeutic strategies to help patient prognosis.

Over the past decade multiple advances in myocardial cell homeostasis and stem cell biology have enhanced our understanding of cardiac development and maturation. These findings coupled to our knowledge of HF has led to the discovery that cardiac injury in the adult heart leads to a switch in gene expression which to some extend resembles the expression pattern observed in the fetal heart. This process has been described as cardiac fetal reprogramming, and is defined as the reversion from an adult gene expression profile to a fetal gene expression profile in the diseased myocardium. The exact reasons and mechanisms as to why the adult heart reverts back to a fetal-like expression pattern remains unknown. However, it has been suggested that this process is an adaptive response to cope with adverse remodeling in the heart. Furthermore, it is unknown if the expression of fetal gene profile protects the heart during HF or whether this adds further insult to the already weakened heart.

**Aims and outline of this thesis**

The primary aims of this thesis are:

1. To identify novel members of the cardiac fetal gene program.
2. To characterize the pathophysiology of identified novel cardiac fetal genes
3. To characterize the therapeutic potential of these novel cardiac fetal genes

In **chapter 2** we describe the current knowledge regarding the cardiac fetal gene program, and how targeting this process might lead to novel therapeutic strategies to

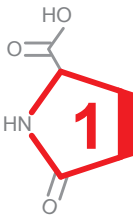


improve patient outcome. In **chapter 3** we sought out to identify novel members of the cardiac fetal gene program in HF, by looking at gene expression during murine cardiac development and ischemic HF. Furthermore, in **chapter 3**, we were also interested in characterizing the therapeutic potential of these novel cardiac fetal genes, in particular that of our top candidate gene *Oplah*, encoding for 5-oxoprolinase, and its substrate 5-oxoprolinase. OPLAH is a member of the γ-glutamyl cycle, responsible for the homeostasis of the major antioxidant glutathione, where it converts 5-oxoproline, a degradation product of glutathione (GSH) and an oxidative stress inducing agent, into glutamate. To study the effects of OPLAH depletion, and therefore 5-oxoproline induced oxidative stress, on the heart, in **chapter 4** we developed an *Oplah* knock-out mouse model. Of particular interest was to identify whether OPLAH ablation coupled to 5-oxoproline accumulation, resulting in oxidative stress, could lead to the development of HF with a preserved ejection fraction (HFpEF). Currently there is limited knowledge regarding the pathiophysiology of HFpEF and therefore there are also limited therapeutic strategies targeting this form of HF. However, oxidative stress is suggested to play an important role in the pathophysiology of HFpEF.

Since OPLAH and 5-oxoproline are members of the γ-glutamyl cycle, in **chapter 5** we were interested in developing a LC-MS method for the quantification of 5-oxoproline, glutamate, GSH and GSSG (oxidized GSH), key components of the γ-glutamyl cycle, in several biological samples of mice with HF and healthy controls. This might lead to new information regarding the involvement of the γ-glutamyl cycle in HF, and potentially novel biomarkers and therapeutic targets for HF. Finally, following the observations made in this thesis that OPLAH and 5-oxoproline, members of the γ-glutamyl cycle, are involved in HF, in **chapter 6** we were interested in further characterizing this cycle in HF and uncover whether other members of this cycle could also serve as possible therapeutic targets for patients with HF.

Finally, the relevance of this thesis for the field of cardiovascular research is discussed in the **Discussion and future perspectives**.

# Chapter 2

## Cardiac fetal reprogramming: a tool to exploit novel treatment targets for the failing heart

Atze van der Pol[1], Martijn Hoes[1], Rudolf A. de Boer[1],
Ibrahim Domian[2,3], Peter van der Meer[1]

[1]Department of Cardiology, University Medical Center Groningen, University of Groningen
[2]Cardiovascular Research Center, Department of Medicine, Massachusetts General Hospital, Harvard Medical School, Boston, MA 02114, USA.
[3]Harvard Stem Cell Institute, Cambridge, MA 02138, USA.

*Manuscript in preparation*

## Abstract

As the heart matures during embryogenesis from its fetal stages, several structural and functional modifications take place to form the adult heart. This process of maturation is in large part a result of increased volume and work load of the heart to maintain proper circulation throughout the growing body. It has been observed that these changes during cardiac development are reversed to some extent as a result of cardiac disease in adult life. The process by which this occurs has been characterized as cardiac fetal reprogramming, and is defined as the suppression of adult and re-expression of fetal genes in the diseased myocardium. The reasons as to why this process occurs in the diseased myocardium is unknown, however it has been suggested to be an adaptive process to counteract deleterious events taking place during cardiac remodeling. In this review we will highlight the most important aspects of cardiac fetal reprogramming, and will discuss whether this process is a cause or consequence of heart failure. Furthermore, we will explain why a deeper understanding of this process may result in novel therapeutic strategies in heart failure.

## Introduction

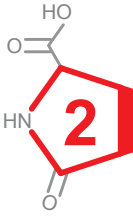


The mammalian heart is the first organ to develop during embryogenesis. As the fetal heart develops, several structural and functional modifications take place to form the four-chambered adult heart. This process of maturation is in large part a result of increased volume and work load of the heart to maintain proper circulation throughout the growing body (1–4). Over the past decade multiple advances in myocardial cell homeostasis and stem cell biology have enhanced our understanding of cardiac cellular differentiation and maturation. These findings coupled to our knowledge of heart failure (HF) have led to the discovery that cardiac injury in the adult heart leads to a switch in gene expression which to some extent resembles the expression pattern observed in the fetal heart, a process known as 'cardiac fetal reprogramming'. The exact reasons and mechanisms as to why the adult heart reverts back to a fetal-like expression pattern remains unknown. However, it has been suggested that this process is an adaptive response to cope with adverse remodeling in the heart. Strikingly, it remains unknown if the re-expression of fetal genes is an adaptive response that protects the heart during HF, or a maladaptive response that compounds the insult an already weakened heart. In the present review we summarize the current knowledge of the cardiac fetal gene program, by looking at the expression profiles during cardiac development and disease, with a particular focus on cardiac metabolism, contractile machinery, electrophysiology, and neurohormonal expression. We then examine how this process may lead to improved therapies for HF patients.

## Fetal Reprogramming in Cardiac Metabolism

Each contraction of the heart requires relatively large amounts of ATP (5). With very low energy stores and a high ATP turnover, the metabolic activity of the heart is the highest of all organs in the body (6). To meet energetic needs, the mature myocardium of the adult heart primarily utilizes fatty acids. Under certain conditions, the heart can also use pyruvate, lactate, acetate, amino acids, ketone bodies, and phospho-creatine (7). Each of these substrates can be metabolized to generate acetyl coenzyme A (acetyl-CoA), which in turn is essential for the production of substrates used in the oxidative phosphorylation pathway.

**From Glycolysis (fetal) to fatty acid oxidation (adult)**

Fetal development occurs in a relative hypoxic environment (8), therefore ATP is ultimately generated through anaerobic glycolysis during fetal development. This

hypoxic state results in high levels of HIF-1α protein, which induces the transcription of major glycolysis key factors like glucose transporter (GLUT)-1 and GLUT-4 (9–11), hexokinase (HK)-1 (9), lactate dehydrogenase (LDH)-A (9,10), and pyruvate dehydrogenase kinase (PDK)-1 and PDK-2 (12,13). In the fetal heart, GLUT-1 is the major transporter of extracellular glucose, which is intracellularly converted to glucose-6-phosphate by HK-1 (14,15). Furthermore, high expression levels of LDH-A greatly contributes to the conversion of glycolysis-derived pyruvate to lactate, consequently regenerating nicotinamide adenine dinucleotide ($NAD^+$) from its reduced form (NADH), which is needed to sustain glycolysis (16). Additionally, the fetal heart can utilize lactate as main energy source (17,18). Combined, any additional lactate produced by LDH-A can be efficiently oxidized in order to produce pyruvate and restore the NADH stores required for continued ATP production through glycolysis.

After birth, cardiac metabolism does not switch to different substrates until 7 days postpartum, in lambs (18,19). In rabbits it has been observed that circulating lactate levels fall 5-7 mM to 0.5 mM in the first 2 hours after birth (20). As such, lactate oxidation contributes notably less to ATP production. Moreover, glycolytic rates decrease from 44% to only 10% by day 7 after birth, in rabbits (21). In concert with reduced glycolytic rates, fatty acid oxidation rates gradually increase towards levels observed in hearts from adult animals (22). Metabolic contribution by the various ATP generating pathways stabilizes around 3 weeks after birth with fatty acid oxidation as the main metabolic pathway, contributing to 89% of total ATP production (23,24).

The transition from glycolysis to fatty acid oxidation is brought about by the shift from a relatively hypoxic environment of the fetus to physiological normoxia attained shortly after birth (Fig. 1) (25). Subsequently, normalized oxygen tension allows for prolyl hydroxylase-mediated degradation of HIF-1α, leading to abrogated expression of the aforementioned HIF-1α target genes. Among these target genes is HAND1, a transcription factor that inhibits lipid oxidation, leading to repression of mitochondrial energy generation (26). Additionally, HIF-1α hampers lipid oxidation through inhibition of the peroxisome proliferator-activated receptor alpha (PPARα)/retinoid X receptor (RXR) heterodimer (27). The transitions into a more mature heart coincides with a dramatic increase in the expression levels of PPAR-α and PPAR-β/δ, which are the key regulators of fatty acid metabolism (28–30).

**From fatty acid oxidation (adult) to glycolysis (disease)**

In the event of various pathophysiological conditions, genes that have been active during fetal development are re-expressed (Fig. 1) (31). Protein levels of glycolysis genes (i.a. GLUTs, PDKs, and HK-1) are lower in healthy mature hearts than in fetal hearts. Expression of these genes increase to fetal levels in failing mature hearts

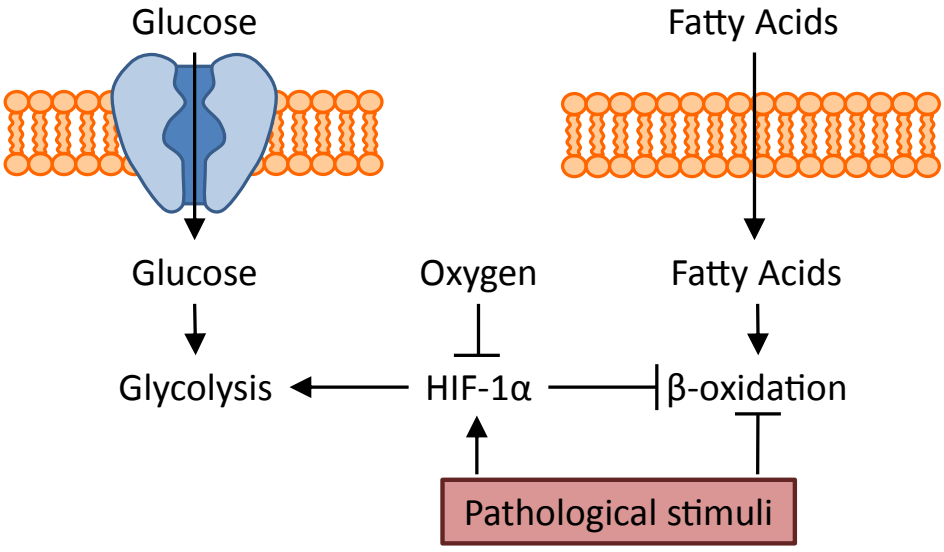


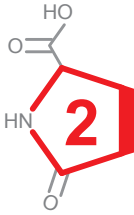


**Fig. 1. Schematic representation of the metabolic cardiac fetal reprogramming.**
During cardiogenesis the cardiac tissue is primarily reliant on glycolysis for its energy requirements. This reliance on glycolysis is regulated by the relative hypoxic environment and therefore the expression of HIF-1α, which induces the expression of glycolysis related genes and suppresses the expression of gens involved in fatty acid oxidation (β-oxidation). Following birth, and the influx of oxygen, HIF-1α is suppressed, leading to an increase in β-oxidation, and a reduced utilization of glycolysis for energy production. Upon the induction of cardiac injury, there is a re-expression of HIF-1α leading to the inhibition of β-oxidation, and an increased reliance on glycolysis.

(32). With the re-emergence of glycolysis as the main ATP-generating metabolic pathway, fatty acid oxidation rates are greatly reduced (the Randle cycle) (33).

During HF, cardiac metabolism reverts to a fetal pattern in which glycolysis primarily contributes to ATP production as opposed to fatty acid oxidation (34,35). It has been shown that glycolysis increases as fatty acid oxidation decreases during pathological hypertrophy (36,37). Activity levels of mediating protein change or protein expression is altered in concert with the changes of each metabolic pathway (38–41). During HF, PPAR-α and PGC-1α levels decrease, consequently reducing fatty acid oxidation (42). It is hypothesized that this reduction in PPAR-α and PGC-1α levels is due to rising levels of HIF-1α. Most forms of HF result in cardiac hypoxia, e.g. hypertrophic cardiomyocytes increase in size and consequently oxygen tension per cell decreases. Moreover, HIF-1α were found to be increased in pressure-overload hypertrophy (42). As previously mentioned, HIF-1α is a master switch between glycolysis and fatty acid oxidation. Once HIF-1α levels increase in the adult heart, expression of 6-phosphofructo-2-kinase (PFK2) increases, resulting in increased

levels of fructose-2,6-biphosphate, thereby activating PFK1 and ultimately glycolysis (43).

## Fetal Reprogramming in Cardiac Contractile Machinery

The re-emergence of fetal gene expression in the heart is not only limited to a switch in energy substrate. Maturation from a fetal to an adult heart involves a steady shift from compliant (fetal) to stiffer (adult) contractile proteins. As a result of cardiac disease, the adult heart undergoes a reversion to a more complaint fetal contractile machinery (Fig. 1). This turnover has been highly studied in the sarcomere, which gives cardiac muscles their striated appearance and is responsible for the contractile function. The most abundant sarcomeric proteins are myofilament proteins (myosin and actin), regulatory proteins (troponins and tropomyosin), and cytoskeletal proteins (myosin binding protein C and titin). Several isoforms exist of each sarcomeric protein and it is the level of expression of these isoforms that determine the function of the cardiac sarcomere. The turn-over of the sarcomeric proteins during cardiac development and disease has been extensively studied in rodent models, and to a lesser extent in the human setting (Table 1). The sarcomeric protein composition and distribution in rodent models is somewhat different from that from the human setting and it is therefore not always possible to extrapolate the rodent findings to the human clinical setting.

**Myosin**

Myosin heavy chain (MHC) is the so-called "molecular motor" protein of the sarcomere, which together with actin is responsible for the contraction of the cardiomyocyte, consuming ATP as the energy source to produce tension. Within cardiomyocytes there are two main isoforms of MHC, the slow twitch, β-MHC, and the fast α-MHC. α-MHC has a higher ATPase activity and shortening velocity, compared to β-MHC, therefore, hearts expressing α-MHC possess more rapid contractile velocity than hearts expressing β-MHC. Besides the MHC isoforms, the motor function of myosin is also regulated by the myosin light chain (MLC). Similar to MHC, the human heart expresses two isoforms of MLC, the essential (MLC-1) and regulatory (MLC-2). MLC-1 has been suggested to act as a MHC/actin tether, while MLC-2 slows the rate of tension development of myosin (44,45).

The turn-over in MHC in the rodent heart has been extensively studied. During cardiac development, the rodent heart switches from MHC-β to MHC-α, and upon cardiac injury the heart reverts back to the expression of MHC-β. On the other hand, in human cardiac development, both α-MHC and β-MHC are expressed, and as

**Table 1. Expression of sarcomeric proteins in fetal, adult, and diseased hearts**

| | Fetal | Adult | Disease |
|---|---|---|---|
| Myosin heavy chain* | | | |
| α-MHC | ↓ | ↑ | ↓ |
| β-MHC | ↑ | ↓ | ↑ |
| Myosin light chain | | | |
| MLC-1 | ↑ | ↓ | ↑ |
| MLC-2 | ↓ | ↑ | ↓ |
| Actin** | | | |
| α-Skeletal actin | ↑ | ↓ | ↑ |
| α-Cardiac actin | ↓ | ↑ | ↓ |
| Troponin | | | |
| $TnT_{fetal}$ | ↑ | ↓ | ↑ |
| $TnT_{adult}$ | ↓ | ↑ | ↓ |
| $TnI_{fetal}$ | ↑ | ↓ | ↑ |
| $TnI_{adult}$ | ↓ | ↑ | ↓ |
| Titin | | | |
| N2BA | ↑ | ↓ | ↑ |
| N2B | ↓ | ↑ | ↓ |

*The ratio of α/β-MHC is different in humans

**It is unknown if this switch occurs in the human setting

the heart matures β-MHC becomes the predominant isoform. As a result of cardiac damage the expression levels of both isoforms is reduced and reverts back to a fetal-like expression pattern (36,45–49).

Similar to the MHC, the human heart expresses both MLC-1 and MLC-2 isoforms. During development, MLC-1 is primarily expressed in the whole heart. After birth MLC-1 expression declines rapidly and is replaced by MLC-2 in the ventricles. However, in response to hypertrophy, ischemia, or dilated cardiomyopathies, MLC-1 is re-expressed (45). Recently it has been observed that this switch to MLC-1 expression results in a structural change enabling cardiomyocytes to adjust to

enhanced work load, by improving power output and cardiac contractility (44,45).

These findings suggest that the re-expression of the fetal-like myosin, both MHC and MLC, isoforms can be considered a molecular adaptation mechanisms to compensate for an increased work demand or impaired sarcomeric function.

**Actin**

In mammals actins are encoded by a multigene family and in cardiomyocytes two main sarcomeric actin isoforms exist: α-skeletal and α-cardiac actin. During cardiac development, α-skeletal actin is primarily expressed in the fetal and neonatal hearts and as the heart matures α-skeletal actin is slowly replaced by α-cardiac actin (48,50–53). In rats exposed to pressure-overload hypertrophy, a turn-over was observed from α-cardiac actin to α-skeletal actin expression (48,52–54). Similarly, in cultured neonatal cardiomyocytes exposed to α1-adrenergic agonists or growth factors TGFβ1 and bFGF, α-skeletal actin mRNA was significantly increased (55). Several studies have examined if in humans an actin isoform switch takes place during development and disease, however the results have been contradictory and as such it still remains unclear if in humans this switch takes place (48,49,56–58). Noteworthy is the observation that α-skeletal actin, when compared to α-cardiac acting, can strongly promote the contractility of the myocardium by activating α-MHC's ATPase activity to a larger extend (59). This suggest that the switch from α-cardiac to α-skeletal actin is an adaptive response to maintain cardiac contractility due to the increased presence of α-MHC in the myocardium.

**Troponin**

Troponin is part of the myofibrillar contractile complex, involved in controlling muscular contraction by regulating the myofibrillar responsiveness to calcium and adrenergic stimulation. Troponin consists of 3 subunits, troponin C, T, and I (TnC, TnT, and TnI, respectively). During normal cardiac development in rats, both TnT and TnI switch from their respective fetal to the adult isovorms (58,60,61). Rat hearts when exposed to cardiac injury, demonstrate a re-expression of the fetal isoforms of TnT and TnI (58,61,62). Several studies have shown that the fetal TnT and TnI isoforms have a lowered calcium sensitivity, adrenergic sensitivity, ATPase activity and cardiac muscle relaxation (58,61). This suggests that the re-expression of the fetal TnT and TnI is either a mechanism of pathologic change or a maladaptive process induced by the pathological changes of HF.

**Titin**

Titin is a large protein that has been characterized as molecular spring, with its elastic properties defining the passive mechanical properties of cardiomyocytes. In humans, titin is encoded by a single gene (*TTN*) containing 363 exons that are differentially

spliced, creating the stiffer N2B (short molecular spring) and the more compliant N2BA (long molecular spring) isoforms (58,63,64). Both isoforms are co-expressed in the sarcomere, and the degree of expression of each isoform adjusts the passive stiffness (58,63,64). When looking at neonatal pig hearts it was observed that these had a higher abundance of the complaint, N2BA, titin isoform, while adult pig hearts demonstrated a shift towards the stiffer N2B isoform (58,63). This finding suggest that as the heart matures there is an increase in passive myocardial stiffness, which could play a role in adjusting for diastolic function during development. Upon cardiac damage, it has been observed that in both rats and humans there is a shift from the N2B to N2BA (58,63–65). This shift causes a reduction in titin-drived myofibrillar stiffness, which can lead to a decrease in cardiac output.

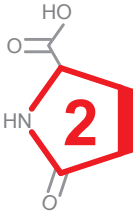


## Fetal Reprogramming in Cardiac Electrophysiology

Besides the switches in metabolism and contractile machinery, the reversion to a more fetal-like state in response to cardiac injury has also been observed in the mechanisms regulating the electrophysiology of cardiomyocytes. Cardiac electrophysiology is in large part governed by the expression of ion channels, gap junctions, and the calcium homeostasis.

**Ion channels**

Ion channels are essential for the generation and propagation of the current that enables the heart to perform its function. Extensive research has been done to understand the electrophysiological changes that occur during cardiac maturation. It has been observed that the excitability, action potential properties, contractility and relaxation of the fetal and adult heart differ significantly from each other (66). As a result the fetal heart expresses different genes involved in the generation and propagation of the action potential then the adult heart. In mice during cardiac development from fetal to adult, there is an up-regulation of genes involved in the $I_{k1}$ (*KCNH2*), $I_{to}$ (*KCND2* and *KCND3*), $I_{kr}$ (*KCNH2*), $I_{ks}$ (*KCNQ1*), $I_{Ca,L}$ (*CACNA1C*), $I_{Na}$ (*SCN5A*), $I_f$ (*HCN1* and *HCN4*) currents, and a down-regulation of genes involved in the $I_{Ca,T}$ (*CACNA1H*) and NCX (*NCX1*) currents (66–70). The reduced expression of potassium channels in the fetal heart coincides with the observation that these hearts have a less negative resting and longer action potentials compared to adult hearts (66). The observed lower expression of $I_{Ca,L}$ and higher $I_{Ca,T}$ and NCX is consistent with the greater importance of alternate calcium-entry pathways in the fetal versus adult hearts (66). The increase in sodium channel expression in adult mouse hearts may be necessary for rapid activation of the much larger heart (66). Similarly, studies comparing human cardiomyocytes derived from human induced pluripotent stem cells (hiPSC) or from human embryonic stem cells (hESC), to adult tissue have

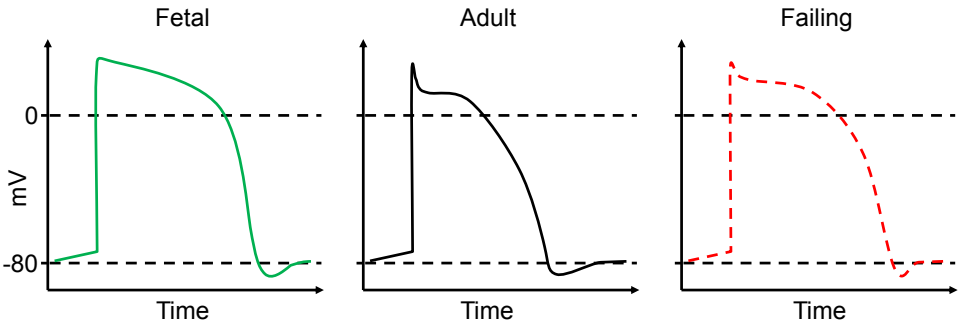


**Fig. 2. Schematic representations of the fetal, adult, and diseased action potential.**
(**LEFT**) In the fetal stages of cardiac development, the heart has a prolonged action potential primarily due to a reduced expression of potassium channels. (**MIDDLE**) A schematic representation of an adult heart action potential. Compared to the fetal heart, the adult heart has an increased expression of potassium channels, sodium channels, and a reduction in calcium channels. (**RIGHT**) Following cardiac injury, the myocardium has a reduced expression of potassium channels and sodium channels coupled to an increase in the expression of calcium-sensitive channels. This switch leads to an increase in action potential, reminiscent of the fetal action potential.

shown similar findings (71,72). Interestingly, in cardiac tissue of patients diagnosed with end stage HF, the major sodium ($I_{Na}$), potassium ($I_{to}$, $I_{K1}$, $I_{Kr}$, and $I_{Ks}$), and calcium ($I_{Ca,L}$) ion channels are significantly repressed, while $I_{Ca,T}$, NCX, and $I_f$ (*HCN4*) are up-regulated (70,73,74). Therefore, the heart responds to an increased load by decreasing the potassium currents, thereby prolonging the action potential and increasing the calcium within the cardiomyocytes, leading to increased contractility (Fig. 2). These findings suggest that as a result of cardiac injury, the heart undergoes ion channel remodeling, resulting in an expression profile similar to that of the fetal heart. Initially, these changes are adaptive, however in the long run they can become maladaptive by increasing the changes of arrhythmias (75,76).

### Gap junctions

Gap junctions are clusters of intercellular channels, assembled forming connexins, which are the pathways through which electrical current propagation takes place that control the rhythm of the heart. As is the case in most tissues and organs, multiple connexins are expressed in the heart, primarily; connexin 43, connexin 40, and connexin 45 (77,78). The presence of each connexin type varies in relative quantities depending on the functional specialization of each subsets of cardiomyocytes. The most predominant gap junction protein in the adult heart is connexin 43, expressed highly in all cardiomyocytes subsets of the heart (77,78). In the sinoatrial node, the site of impulse generation, and the atrioventricular node, the site where impulse is slowed before being routed to the ventricles, cardiomyocyte gap junctions are formed by connexin 43 and connexin 45, associated with slow conductance channels (78).

Cardiomyocytes of the His-Purkinje conduction systems are mainly characterized by the expression of connexin 40, a connexin associated with high conductance channels, which facilitates rapid distribution of the impulse throughout the working ventricular myocardium (78).

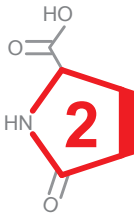


It has been well established that during cardiac development in both rodent models and in the human setting, the expression of connexin 43, connexin 40, and connexin 45 are progressively increased as the heart matures (77–80). This increase in the density of gap junctions in the developing heart results in an increase in conduction velocity. Upon cardiac damage in both rodent models and in the human setting, connexin 43 expression is not only drastically reduced (±50%), but the remaining connexin 43 gap junctions are also highly disorganized (78,81,82). This decrease in connexin 43 expression is also associated with an increase in connexin40 expression (78,81,82). Whether this increase in connexin 40 expression is a result of reduced connexin 43 levels, of whether it is an adaptive response leading to increased impulse propagation throughout the myocardium is unknown (78,81,82). It has been suggested, that the reduction in cell-to-cell coupling in HF results in an increase in the QT-interval and action potential prolongation, and increased risk of arrythmias (78,81,82).

**Calcium homeostasis**

Intracellular calcium homeostasis (release and uptake) plays an essential role in regulating excitation-contraction coupling and in modulating systolic and diastolic function in the heart. Calcium ions are initially imported into the cell through the plasma membrane by means of the $I_{Ca,L}$ current, which is generated as a result of the depolarization of the plasma membrane (see above). Calcium entry from the plasma membrane activate the ryanodine receptors (RyR), which results in an efflux of calcium ions from the sarcoplasmic reticulum (SR), in a process known as calcium-induced calcium release. The released cytoplasmic calcium interacts with calcium-sensitive proteins (TnC) controlling the force and rate of contraction (see previous section). The cytoplasmic calcium is then pumped back into the SR, by SR calcium-ATPases (SERCA) activity, and out through the plasma membrane, by NCX activity (see above). The expression of the $I_{Ca,L}$ current, TnC, and NCX in cardiac development and disease have already been described above, here we will focus on the expression of RyR and SERCA during cardiac development and disease.

Calcium homeostasis has been extensively studies in both cardiac development and cardiac disease, especially in terms of the expression of RyR and SERCA. There are three major isoforms of the RyR, of which RyR2 is the major SR calcium-release channel involved in excitation-contraction coupling in the heart. SERCA functions by transferring calcium from the cytosol to the SR at the expense of ATP during muscle

contraction, in the cardiomyocytes the major SERCA isoform is SERCA2, encoded by *ATP2A2*. In studies exploring cardiac development in rodents and in hESC/hIPCS cardiac differentiation it has been observed that the expression of both RyR2 and SERCA2 is up-regulated (66,83–85). The greater expression of the calcium handling proteins (ATP2A2, RyR2, and CACNA1C) during cardiac development may be essential for the stronger mechanical function required to provide the blood supply to much larger adult bodies (66,83–85).

The expression of RyR2 in HF has been controversial, several studies have shown a reduction in the expression levels, back to fetal levels, in rodent and human HF (86,87), however numerous studies have also shown no change in the expression of RyR2 in HF (86,87). Therefore the exact expression and involvement of RyR2 during HF remains uncertain. Interestingly, several studies have demonstrated that during HF, RyR2 are hyperphosphorylated resulting in a leaky RyR2 channel and reduced SR calcium content (86,88). On the other hand, SERCA2 expression, which is increased during cardiac developing, has been shown to be substantially reduced in HF, in both rodent and human models (66,89,90). Furthermore, a decrease in phospholamban (PLN), a regulator of SERCA2 activity, phosphorylation in HF has been described, which further depresses the function of SERCA2 (88). Combined, the reduction of SERCA2 expression/activity and SR leakage by hyperphosphorylated RyR2 channels lead to reduced SR calcium content, resulting in reduced SR calcium release, myofilament activation, and contractility (88).

## Cardiac Neurohormonal Fetal Reprogramming

Cardiac fetal reprogramming is not only limited to metabolism, contractile machinery, and electrophysiological, but also occurs in the expression of cardiac neurohormones. Specifically fetal reprogramming has been observed in the expression of atrial and brain natriuretic peptides.

The atrial natriuretic peptide (ANP) was the first natriuretic peptide identified in 1981 (91). Since then extensive research has been done on ANP, whose primary function has been identified to reduce plasma volume, and therefore blood pressure, by increased renal excretion of salt and water, vasodilation, increased vascular permeability (92). In the adult murine and human heart, the atrium is the major source of ANP expression, however during cardiac development ANP expression is primarily localized to the ventricles (93). As the heart matures, the expression of ANP in the ventricles is significantly reduced in the ventricles (93). The primary stimuli for ANP expression is stretch, thus as a result of cardiac hypertrophy, remodeling

and HF, ANP is significantly expressed in the ventricles returning to fetal expression levels (93,94).

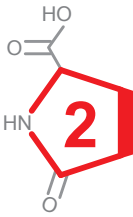


Following the discovery of ANP a second natriuretic peptide was identified in the brain, brain natriuretic peptide (BNP) (93). Although initially isolated and characterized in the brain, BNP was later identified as being predominantly expressed in the heart ventricles (93). Furthermore, BNP has a similar mode of action as ANP, that is to lower blood volume, reduce cardiac output and systemic blood pressure. Additionally, BNP mimics the expression profile of ANP during cardiac development, with BNP levels being significantly reduced in the adult compared to the fetal myocardium (93,94). Upon myocardial stretch, BNP, like ANP, is re-expressed by the ventricles (93,94).

In recent years it has been well established that the re-expression of both ANP and BNP has a cardioprotective effect in the failing myocardium (95). In the human setting, the actions of BNP are of particular interest. BNP not only helps unload the failing heart, by reducing preload, facilitate renal excretion of salt and water, and to inhibit the renin-angiotensin system, but it is also involved in the inhibition of the sympathetic drive to the heart, enhancement of the parasympathetic cardiac reflex, and inhibition of pathological cardiac hypertrophy (95). Thus, the re-expression of ANP and BNP in the failing heart is an adaptive response that helps to protect the failing heart.

## Discussion and Clinical implications

The heart exposed to stress undergoes physiological changes bringing it back to a more fetal like state, in other words cardiac fetal reprogramming. Cardiac damage leading to HF results in a switch in energy substrate, from fatty acids (post-natal) to carbohydrates (fetal). Similarly, the contractile machinery of the heart reverts back to a more compliant state, as observed in the fetal heart. Finally, cardiac electrophysiology, governed by ion channels, gap junctions, and calcium homeostasis, also switches to a state similar to that observed in the fetal heart. Initially, the process of cardiac fetal reprogramming seems to be an adaptive response to cope with adverse remodeling in the heart, and as such a consequence of cardiac injury. However, as time progresses these changes are detrimental to the myocardium and add further insult leading to disease progression. Therefore, targeting cardiac fetal reprogramming could be ideal for therapeutic interventions.

To date, several aspects of the cardiac fetal gene program have been studied for their potential as targets for therapeutic intervention. An number of studies have

explored to modulate ion channels and calcium handling in the failing heart. Such studies have demonstrated that by overexpressing SERCA2, thus reverting cardiac fetal reprograming, in transgenic rodent models for HF, these animals have improved cardiac function and are less prone to develop HF following myocardial injury (96–98). Similarly, overexpression of SERCA2 by means of adenoviral gene transfer, in HF models, has also demonstrated beneficial effects (99,100). Due to these positive experimental results observed by modulating cardiac fetal reprograming of SERCA2, human trials with SERCA2 gene therapy have been performed. The initial findings were positive, demonstrating improved cardiac function, decreased HF symptoms, and reduced mortality in patients with advanced HF (101,102). However, a recent study utilizing the same SERCA2 gene therapy showed no improvement on ventricular remodeling in patients with advanced systolic HF (103). Besides utilizing gene therapy as a therapeutic strategy, pharmacological agents that restore SERCA2 function have also been explored. One such agent is Istaroxime, which functions by stimulating SERCA2 activity and indirectly inhibiting NCX function by increasing intracellular sodium levels104. Treatment with istaroxime in animal models of HF have shown improved cardiac function with no adverse effects (105,106). Following these animal studies, a clinical trial evaluating the effects of istaroxime acute administration in HF patients, has demonstrated an improvement in cardiac function in these patients (107,108). Although such a pharmacological intervention does not directly target cardiac fetal reprograming, like direct gene therapy does, it does ensures that the remaining SERCA2 is more active, therefore compensating for the lack of SERCA2 expression.

Besides looking at ion channels and calcium handling, studies have also looked that improving the contractility of the cardiomyocytes in the failing heart by targeting myosin. Similar to the fetal human heart, the diseased adult myocardium predominantly expresses more β-MHC, an MHC isoform characterized for lower ATPase activity and reduced shortening velocity when compared to α-MHC. Therefore, the diseased myocardium has a reduced contractile capacity. Omecamtiv Mecarbil (OM) is a selective, small-molecule cardiac myosin activator that binds to the catalytic domain of myosin, thereby increasing cardiac contractility without affecting cardiomyocyte calcium concentrations or myocardial oxygen consumption (109). OM has been shown in animal models for HF to improve cardiac muscle function (110–113). OM doesn't directly reverse cardiac fetal reprograming of the myosin, however it ensures that the present β-MHC has an improved contractile capacity, similar to that of α-MHC (111,114). Following these positive results in the experimental setting, several clinical trials have been performed with the administration of OM to HF patients. The studies performed to date have all shown that OM treatment leads to improvement in cardiac function (115–118).

Another aspect of the cardiac fetal gene program that has been studied for its potential as a treatment target have been the natriuretic peptides, specifically BNP. As previously mentioned, the re-expression of BNP results in several cardioprotective effects. Based on this two main therapeutic strategies have been employed to further increase the levels of natriuretic peptides in HF patients. The first approach has been to target neprilysin, the enzyme responsible for the degradation of natriuretic peptides. Sacubitril, a prodrug that strongly inhibits the activity of neprilysin, and has been shown to have beneficial effects in models for heart failure and also in the clinical setting (119,120). The second approach has been to administer engineered recombinant natriuretic peptides, which mimic the effects of the endogenous natriuretic peptides. These recombinant natriuretic peptides have also demonstrated beneficial effects in both heart failure animal models and in the clinical setting (121–123).

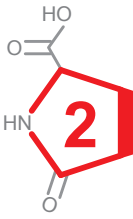


Together these studies demonstrate that targeting the cardiac fetal gene program can improve patients outcome, and therefore a better understanding of this process may eventually lead to better therapeutic options for HF patients.

## Exploring unknown elements of the fetal program to uncover new therapeutic avenues

To obtain a better understanding of cardiac fetal reprogramming studies in the field of cardiovascular research should focus on further elucidating this process. There are several ways one could go about characterizing the cardiac fetal gene program, especially with the current improvements in the “omics” techniques (i.e. genomics, proteomics, and metabolomics). These techniques could lead to a better understanding of how diseased myocardium mimics the developing heart. Furthermore, pathophysiological pathways implicated in cardiac fetal reprogramming could be uncovered, leading to novel therapeutic targets. Recently, we focused on characterizing the murine cardiac fetal gene program, by means of RNA sequencing, this has led to the identification of several new cardiac fetal genes, including OPLAH (Table 2) (124). OPLAH is a gene that encodes for 5-oxoprolinase, and enzyme involved in the γ-glutamyl cycle, where it is responsible for the conversion of 5-oxoproline, a degradation product of glutathione, into glutamate (125,126). OPLAH was found to be expressed during cardiac development and repressed in cardiac disease, in both the experimental and clinical settings (124,127). By over-expressing OPLAH, and reversing cardiac fetal reprogramming of the gene, mice were found to have improved cardiac function following myocardial infarction (124). The improvement in cardiac function was found to result from a reduction in

**Table 2. Several known and novel members of the cardiac fetal gene program recently identified.**

| Known members of the cardiac fetal gene program | | | |
|---|---|---|---|
| **Gene** | **Annodation** | **Developmental** | **Diseased** |
| *RYR2* | Ryanodine receptor 2, cardiac | ↑ | ↓ |
| *CACNA2D1* | Calcium channel, voltage-dependent, alpha2/delta subunit 1 | ↑ | ↓ |
| *ATP2A2* | ATPase, Ca++ transporting, cardiac muscle, slow twitch 2 | ↑ | ↓ |

| Novel members of the cardiac fetal gene program | | | |
|---|---|---|---|
| **Gene** | **Annodation** | **Developmental** | **Diseased** |
| *OPLAH* | 5-Oxoprolinase (ATP-hydrolysing) | ↑ | ↓ |
| *ANXA11* | Annexin A11 | ↑ | ↓ |
| *HADH* | Hydroxyacyl-Coenzyme A dehydrogenase | ↑ | ↓ |
| *CD300LG* | CD300 antigen like family member G | ↑ | ↓ |
| *MCCC1* | Methylcrotonoyl-Coenzyme A carboxylase 1 (alpha) | ↑ | ↓ |
| *LGALS4* | Lectin, galactose binding, soluble 4 | ↑ | ↓ |
| *CYYR1* | Cysteine and tyrosine-rich protein 1 | ↑ | ↓ |
| *SLCO2B1* | Solute carrier organic anion transporter family, member 2b1 | ↑ | ↓ |
| *RALGAPA2* | Ral GTPase activating protein, alpha subunit 2 (catalytic) | ↑ | ↓ |
| *DNAJB1* | DnaJ (Hsp40) homolog, subfamily B, member 1 | ↓ | ↑ |
| *THEM6* | Thioesterase superfamily member 6 | ↑ | ↓ |
| *ETL4* | Enhancer trap locus 4 | ↑ | ↓ |
| *ABHD14B* | Abhydrolase domain containing 14b | ↑ | ↓ |
| *VPS13C* | Vacuolar protein sorting 13C (yeast) | ↑ | ↓ |
| *OSTC* | Oligosaccharyltransferase complex subunit | ↓ | ↑ |
| *FREM1* | Fras1 related extracellular matrix protein 1 | ↓ | ↑ |
| *DENND4C* | DENN/MADD domain containing 4C | ↑ | ↓ |
| *SNX6* | Sorting nexin 6 | ↓ | ↑ |
| *HSP90AA1* | Heat shock protein 90, alpha (cytosolic), class A member 1 | ↓ | ↑ |
| *PSMC3IP* | Proteasome (prosome, macropain) 26S subunit, ATPase 3, interacting protein | ↓ | ↑ |
| *DNAJA1* | DnaJ (Hsp40) homolog, subfamily A, member 1 | ↓ | ↑ |
| *ITM2A* | Integral membrane protein 2A | ↓ | ↑ |
| *VPS13D* | Vacuolar protein sorting 13 D (yeast) | ↑ | ↓ |
| *PPRC1* | Peroxisome proliferative activated receptor, gamma, coactivator-related 1 | ↓ | ↑ |
| *SLC25A22* | Solute carrier family 25 (mitochondrial carrier, glutamate), member 22 | ↑ | ↓ |
| *LSM1* | LSM1 homolog, U6 small nuclear RNA associated (S. cerevisiae) | ↓ | ↑ |
| *BANP* | BTG3 associated nuclear protein | ↓ | ↑ |
| *KIF26B* | Kinesin family member 26B | ↓ | ↑ |
| *GRB10* | Growth factor receptor bound protein 10 | ↓ | ↑ |

oxidative stress, due to a decrease in 5-oxoproline, a strong mediator of oxidative stress (124,128,129). These findings suggest OPLAH may be an ideal candidate for therapeutic intervention. Identifying drugs and or small molecules capable of improving OPLAH expression or activity may therefore lead to novel therapeutic strategies for HF patients. Interestingly, 5-oxoproline was also found to be a potential novel biomarker for HF (124). Combined, this study demonstrates the potential of characterizing cardiac fetal reprogramming to help uncover novel pathophysiological pathways which may lead to new therapeutic strategies and improved patient outcome.

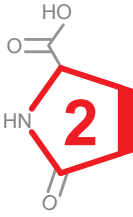

# References


1. Jonker, S. S. et al. Cardiomyocyte enlargement, proliferation and maturation during chronic fetal anaemia in sheep. Exp. Physiol. 95, 131–139 (2010).
2. Jonker, S. S. et al. Myocyte enlargement, differentiation, and proliferation kinetics in the fetal sheep heart. J. Appl. Physiol. 102, 1130–1142 (2007).
3. Smolich, J. J., Walker, A. M., Campbell, G. R. & Adamson, T. M. Left and right ventricular myocardial morphometry in fetal, neonatal, and adult sheep. Am. J. Physiol. Circ. Physiol. 257, H1–H9 (1989).
4. Maillet, M., van Berlo, J. H. & Molkentin, J. D. Molecular basis of physiological heart growth: fundamental concepts and new players. Nat. Rev. Mol. Cell Biol. 14, 38–48 (2013).
5. Kolwicz, S. C., Purohit, S. & Tian, R. Cardiac Metabolism and its Interactions With Contraction, Growth, and Survival of Cardiomyocytes. Circ. Res. 113, 603–616 (2013).
6. Wang, Z. et al. Specific metabolic rates of major organs and tissues across adulthood: evaluation by mechanistic model of resting energy expenditure. Am. J. Clin. Nutr. 92, 1369–1377 (2010).
7. Kodde, I. F., van der Stok, J., Smolenski, R. T. & de Jong, J. W. Metabolic and genetic regulation of cardiac energy substrate preference. Comp. Biochem. Physiol. Part A Mol. Integr. Physiol. 146, 26–39 (2007).
8. Fischer, B. & Bavister, B. D. Oxygen tension in the oviduct and uterus of rhesus monkeys, hamsters and rabbits. J. Reprod. Fertil. 99, 673–9 (1993).
9. Iyer, N. V et al. Cellular and developmental control of O2 homeostasis by hypoxia-inducible factor 1 alpha. Genes Dev. 12, 149–62 (1998).
10. Ryan, H. E., Lo, J. & Johnson, R. S. HIF-1 alpha is required for solid tumor formation and embryonic vascularization. EMBO J. 17, 3005–15 (1998).
11. Wood, S. M. et al. Selection and analysis of a mutant cell line defective in the hypoxia-inducible factor-1 alpha-subunit (HIF-1alpha). Characterization of hif-1alpha-dependent and -independent hypoxia-inducible gene expression. J. Biol. Chem. 273, 8360–8 (1998).
12. Kim, J., Tchernyshyov, I., Semenza, G. L. & Dang, C. V. HIF-1-mediated expression of pyruvate dehydrogenase kinase: a metabolic switch required for cellular adaptation to hypoxia. Cell Metab. 3, 177–85 (2006).
13. Papandreou, I., Cairns, R. A., Fontana, L., Lim, A. L. & Denko, N. C. HIF-1 mediates adaptation to hypoxia by actively downregulating mitochondrial oxygen consumption. Cell Metab. 3, 187–97 (2006).
14. Santalucía, T. et al. Developmental regulation of GLUT-1 (erythroid/Hep G2) and GLUT-4 (muscle/fat) glucose transporter expression in rat heart, skeletal muscle, and brown adipose tissue. Endocrinology 130, 837–46 (1992).
15. Postic, C. et al. Development and regulation of glucose transporter and hexokinase expression in rat. Am. J. Physiol. 266, E548-59 (1994).
16. Bishop, S. P. & Altschuld, R. A. Increased glycolytic metabolism in cardiac hypertrophy and congestive failure. Am. J. Physiol. 218, 153–9 (1970).
17. Neely, J. R. & Morgan, H. E. Relationship between carbohydrate and lipid metabolism and the energy balance of heart muscle. Annu. Rev. Physiol. 36, 413–59 (1974).
18. Werner, J. C. & Sicard, R. E. Lactate metabolism of isolated, perfused fetal, and newborn pig hearts. Pediatr. Res. 22, 552–6 (1987).
19. Bartelds, B. et al. Perinatal changes in myocardial supply and flux of fatty acids, carbohydrates, and ketone bodies in lambs. Am J Physiol 274, H1962-9 (1998).
20. Medina, J. M. The role of lactate as an energy substrate for the brain during the early neonatal period. Biol. Neonate 48, 237–44 (1985).
21. Lopaschuk, G. D., Spafford, M. A. & Marsh, D. R. Glycolysis is predominant source of myocardial ATP production immediately after birth. Am. J. Physiol. 261, H1698-705 (1991).
22. Itoi, T. & Lopaschuk, G. D. The contribution of glycolysis, glucose oxidation, lactate oxidation, and fatty acid oxidation to ATP production in isolated biventricular working hearts from 2-week-old rabbits. Pediatr. Res. 34, 735–41 (1993).
23. Fukushima, A. et al. Acetylation and succinylation contribute to maturational alterations in energy metabolism in the newborn heart. Am. J. Physiol. Heart Circ. Physiol. 311, H347-63 (2016).
24. Lopaschuk, G. D. & Jaswal, J. S. Energy metabolic phenotype of the cardiomyocyte during development, differentiation, and postnatal maturation. J. Cardiovasc. Pharmacol. 56, 130–40 (2010).

25. Rabi, Y., Yee, W., Chen, S. Y. & Singhal, N. Oxygen saturation trends immediately after birth. J. Pediatr. 148, 590–4 (2006).
26. Breckenridge, R. A. et al. Hypoxic Regulation of Hand1 Controls the Fetal-Neonatal Switch in Cardiac Metabolism. PLoS Biol. 11, 4–7 (2013).
27. Belanger, A. J. et al. Hypoxia-inducible factor 1 mediates hypoxia-induced cardiomyocyte lipid accumulation by reducing the DNA binding activity of peroxisome proliferator-activated receptor alpha/retinoid X receptor. Biochem. Biophys. Res. Commun. 364, 567–72 (2007).
28. Panadero, M., Herrera, E. & Bocos, C. Peroxisome proliferator-activated receptor-alpha expression in rat liver during postnatal development. Biochimie 82, 723–6 (2000).
29. Wang, Y.-X. et al. Peroxisome-proliferator-activated receptor delta activates fat metabolism to prevent obesity. Cell 113, 159–70 (2003).
30. Gilde, A. J. et al. Peroxisome proliferator-activated receptor (PPAR) alpha and PPARbeta/delta, but not PPARgamma, modulate the expression of genes involved in cardiac lipid metabolism. Circ. Res. 92, 518–24 (2003).
31. Taegtmeyer, H., Sen, S. & Vela, D. Return to the fetal gene program. Ann. N. Y. Acad. Sci. 1188, 191–198 (2010).
32. Sugden, M. C., Langdown, M. L., Harris, R. A. & Holness, M. J. Expression and regulation of pyruvate dehydrogenase kinase isoforms in the developing rat heart and in adulthood: role of thyroid hormone status and lipid supply. Biochem. J. 352 Pt 3, 731–8 (2000).
33. Randle, P. J. Regulatory interactions between lipids and carbohydrates: the glucose fatty acid cycle after 35 years. Diabetes. Metab. Rev. 14, 263–83 (1998).
34. Clerk, A. et al. Signaling pathways mediating cardiac myocyte gene expression in physiological and stress responses. J. Cell. Physiol. 212, 311–22 (2007).
35. van Bilsen, M., Smeets, P. J. H., Gilde, A. J. & van der Vusse, G. J. Metabolic remodelling of the failing heart: the cardiac burn-out syndrome? Cardiovasc. Res. 61, 218–26 (2004).
36. Razeghi, P. et al. Metabolic gene expression in fetal and failing human heart. Circulation 104, 2923–31 (2001).
37. Depre, C. et al. Unloaded heart in vivo replicates fetal gene expression of cardiac hypertrophy. Nat. Med. 4, 1269–75 (1998).
38. el Alaoui-Talibi, Z., Landormy, S., Loireau, A. & Moravec, J. Fatty acid oxidation and mechanical performance of volume-overloaded rat hearts. Am. J. Physiol. 262, H1068-74 (1992).
39. El Alaoui-Talibi, Z., Guendouz, A., Moravec, M. & Moravec, J. Control of oxidative metabolism in volume-overloaded rat hearts: effect of propionyl-L-carnitine. Am. J. Physiol. 272, H1615-24 (1997).
40. Wambolt, R. B. et al. Glucose utilization and glycogen turnover are accelerated in hypertrophied rat hearts during severe low-flow ischemia. J. Mol. Cell. Cardiol. 31, 493–502 (1999).
41. Allard, M. F., Schönekess, B. O., Henning, S. L., English, D. R. & Lopaschuk, G. D. Contribution of oxidative metabolism and glycolysis to ATP production in hypertrophied hearts. Am. J. Physiol. 267, H742-50 (1994).
42. Young, M. E. et al. Uncoupling protein 3 transcription is regulated by peroxisome proliferator-activated receptor (alpha) in the adult rodent heart. FASEB J. 15, 833–45 (2001).
43. Minchenko, O., Opentanova, I. & Caro, J. Hypoxic regulation of the 6-phosphofructo-2-kinase/fructose-2,6-bisphosphatase gene family (PFKFB-1-4) expression in vivo. FEBS Lett. 554, 264–70 (2003).
44. Ritter, O. et al. Expression of atrial myosin light chains but not α -myosin heavy chains is correlated in vivo with increased ventricular function in patients with hypertrophic obstructive cardiomyopathy. 677–685 (1999).
45. Morano, I. Tuning the human heart molecular motors by myosin light chains. J. Mol. Med. 77, 544–555 (1999).
46. Miyata, S., Minobe, W., Bristow, M. R. & Leinwand, L. A. Myosin heavy chain isoform expression in the failing and nonfailing human heart. Circ. Res. 86, 386–390 (2000).
47. Lompre, A. M. et al. Myosin isoenzyme redistribution in chronic heart overload. Nature 282, 105–7 (1979).
48. Schwartz, K., Carrier, L., Chassagne, C., Wisnewsky, C. & Boheler, K. R. Regulation of myosin heavy chain and actin isogenes during cardiac growth and hypertrophy. Symp. Soc. Exp. Biol. 46, 265–72 (1992).
49. Schwartz, K., Boheler, K. R., de la Bastie, D., Lompre, A. M. & Mercadier, J. J. Switches in cardiac muscle gene expression as a result of pressure and volume overload. Am J Physiol 262, R364-9


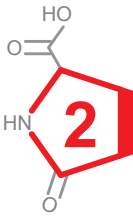

(1992).
50. Mayer, Y., Czosnek, H., Zeelon, P. E., Yaffe, D. & Nudel, U. Expression of the genes coding for the skeletal muscle and cardiac actions in the heart. Nucleic Acids Res. 12, 1087–100 (1984).
51. Tondeleir, D., Vandamme, D., Vandekerckhove, J., Ampe, C. & Lambrechts, A. Actin isoform expression patterns during mammalian development and in pathology: Insights from mouse models. Cell Motil. Cytoskeleton 66, 798–815 (2009).
52. Suurmeijer, A. J. et al. α-Actin isoform distribution in normal and failing human heart: a morphological, morphometric, and biochemical study. J. Pathol. 199, 387–397 (2003).
53. Franco, D., Lamers, W. H. & Moorman, A. F. M. Patterns of expression in the developing myocardium: towards a morphologically intergrated transcriptional model. Cardiovasc. Res. 38, 25 (1998).
54. Schwartz, K. et al. Alpha-skeletal muscle actin mRNA's accumulate in hypertrophied adult rat hearts. Circ. Res. 59, 551–5 (1986).
55. Parker, T. G., Packer, S. E. & Schneider, M. D. Peptide growth factors can provoke 'fetal' contractile protein gene expression in rat cardiac myocytes. J. Clin. Invest. 85, 507–14 (1990).
56. Boheler, K. R. et al. Skeletal actin mRNA increases in the human heart during ontogenic development and is the major isoform of control and failing adult hearts. J. Clin. Invest. 88, 323–330 (1991).
57. Kuwahara, K., Nishikimi, T. & Nakao, K. Transcriptional regulation of the fetal cardiac gene program. J Pharmacol Sci 119, 198–203 (2012).
58. Yin, Z., Ren, J. & Guo, W. Sarcomeric protein isoform transitions in cardiac muscle: A journey to heart failure. Biochim. Biophys. Acta - Mol. Basis Dis. 1852, 47–52 (2015).
59. Hewett, T. E., Grupp, I. L., Grupp, G. & Robbins, J. Alpha-skeletal actin is associated with increased contractility in the mouse heart. Circ. Res. 74, 740–6 (1994).
60. Ausoni, S., De Nardi, C., Moretti, P., Gorza, L. & Schiaffino, S. Developmental Expression of Rat Cardiac Troponin-I Messenger-Rna. Development 112, 1041–1051 (1991).
61. Schiaffino, S., Gorza, L. & Ausoni, S. Troponin isoform switching in the developing heart and its functional consequences. Trends Cardiovasc. Med. 3, 12–17 (1993).
62. Kim, S.-H., Kim, H.-S. & Lee, M.-M. Re-expression of fetal troponin isoforms in the postinfarction failing heart of the rat. Circ. J. 66, 959–64 (2002).
63. Lahmers, S., Wu, Y., Call, D. R., Labeit, S. & Granzier, H. Developmental Control of Titin Isoform Expression and Passive Stiffness in Fetal and Neonatal Myocardium. Circ. Res. 94, 505–513 (2004).
64. Neagoe, C. et al. Titin isoform switch in ischemic human heart disease. Circulation 106, 1333–1341 (2002).
65. Rajabi, M., Kassiotis, C., Razeghi, P. & Taegtmeyer, H. Return to the fetal gene program protects the stressed heart: a strong hypothesis. Heart Fail. Rev. 12, 331–43 (2007).
66. Harrell, M. D., Harbi, S., Hoffman, J. F., Zavadil, J. & Coetzee, W. A. Large-scale analysis of ion channel gene expression in the mouse heart during perinatal development. Genomics 273–283 (2007). doi:10.1152/physiolgenomics.00163.2006.
67. Schweizer, P. A. et al. Transcription profiling of HCN-channel isotypes throughout mouse cardiac development. Basic Res. Cardiol. 104, 621–629 (2009).
68. Domínguez, J. N., de la Rosa, A., Navarro, F., Franco, D. & Aránega, A. E. Tissue distribution and subcellular localization of the cardiac sodium channel during mouse heart development. Cardiovasc. Res. 78, 45–52 (2008).
69. Despa, S. & Bers, D. M. Na+ transport in the normal and failing heart - Remember the balance. J. Mol. Cell. Cardiol. 61, 2–10 (2013).
70. Nattel, S., Frelin, Y., Gaborit, N., Louault, C. & Demolombe, S. Ion-channel mRNA-expression profiling: Insights into cardiac remodeling and arrhythmic substrates. J. Mol. Cell. Cardiol. 48, 96–105 (2010).
71. Robertson, C., Tran, D. & George, S. Concise Review: Maturation Phases of Human Pluripotent Stem Cell-Derived Cardiomyocytes. Stem Cells 31, 1–17 (2013).
72. van den Berg, C. W. et al. Transcriptome of human foetal heart compared with cardiomyocytes from pluripotent stem cells. Development 3231–3238 (2015). doi:10.1242/dev.123810
73. Borlak, J. & Thum, T. Hallmarks of ion channel gene expression in end-stage heart failure. FASEB J. 17, 1592–608 (2003).
74. Nattel, S., Maguy, A., Le Bouter, S. & Yeh, Y.-H. Arrhythmogenic ion-channel remodeling in the heart: heart failure, myocardial infarction, and atrial fibrillation. Physiol. Rev. 87, 425–56 (2007).
75. Tomaselli, G. F. et al. Sudden cardiac death in heart failure. The role of abnormal repolarization. Circulation 90, 2534–2539 (1994).

76. Wickenden, a D. et al. The role of action potential prolongation and altered intracellular calcium handling in the pathogenesis of heart failure. Cardiovasc. Res. 37, 312–323 (1998).
77. Hertzberg, E. L., Spray, D. C. & Leinwand, L. A. Expression of Connexin43 in the Developing Rat Heart. Circ. Res. 68, 782–787 (1991).
78. Severs, N. J. et al. Gap junction alterations in human cardiac disease. Cardiovasc. Res. 62, 368–377 (2004).
79. Kempen, M. J. A. Van, Fromaget, C., Gros, D., Moorman, A. F. M. & Lamers, W. H. Spatial Distribution of Connexin43 , the Major Cardiac Gap Junction Protein , in the Developing and Adult Rat Heart. 1638–1651 (1991). doi:10.1161/01.RES.68.6.1638
80. Fromaget, C., el Aoumari, A., Dupont, E., Briand, J. P. & Gros, D. Changes in the expression of connexin 43, a cardiac gap junctional protein, during mouse heart development. J Mol Cell Cardiol 22, 1245–1258 (1990).
81. Wang, Y., Hill, J. A., Akar, F. G. & Tomaselli, G. F. Electrophysiological remodeling in heart failure. Electr. Dis. Hear. Vol. 1 Basic Found. Prim. Electr. Dis. 48, 369–386 (2013).
82. Severs, N. J., Bruce, A. F., Dupont, E. & Rothery, S. Remodelling of gap junctions and connexin expression in diseased myocardium. Cardiovasc. Res. 80, 9–19 (2008).
83. ITZHAKI, I., SCHILLER, J., BEYAR, R., SATIN, J. & GEPSTEIN, L. Calcium Handling in Embryonic Stem Cell-Derived Cardiac Myocytes: Of Mice and Men. Ann. N. Y. Acad. Sci. 1080, 207–215 (2006).
84. Tyser, R. C. V et al. Calcium handling precedes cardiac differentiation to initiate the first heartbeat. Elife 5, 1–25 (2016).
85. Liu, J., Fu, J. D., Siu, C. W. & Li, R. A. Functional sarcoplasmic reticulum for calcium handling of human embryonic stem cell-derived cardiomyocytes: insights for driven maturation. Stem Cells 25, 3038–44 (2007).
86. Ather, S., Respress, J. L., Li, N. & Wehrens, X. H. T. Alterations in ryanodine receptors and related proteins in heart failure. Biochim. Biophys. Acta - Mol. Basis Dis. 1832, 2425–2431 (2013).
87. Scoote, M. & Williams, A. J. The cardiac ryanodine receptor (calcium release channel): emerging role in heart failure and arrhythmia pathogenesis. Cardiovasc.Res. 56, 359–372 (2002).
88. Dobrev, D. & Wehrens, X. H. T. Role of RyR2 Phosphorylation in Heart Failure and Arrhythmias Response to Dobrev and Wehrens. Circ. Res. 114, (2014).
89. Balke, C. W. & Shorofsky, S. R. Alterations in calcium handling in cardiac hypertrophy and heart failure. Cardiovasc. Res. 37, (1998).
90. Lou, Q., Janardhan, A. & Efimov, I. R. Remodeling of calcium handling in human heart failure. Adv. Exp. Med. Biol. 740, 1145–74 (2012).
91. de Bold, A. J., Borenstein, H. B., Veress, A. T. & Sonnenberg, H. A rapid and potent natriuretic response to intravenous injection of atrial myocardial extract in rats. Life Sci. 28, 89–94 (1981).
92. Curry, F.-R. E. Atrial natriuretic peptide: an essential physiological regulator of transvascular fluid, protein transport, and plasma volume. J. Clin. Invest. 115, 1458–1461 (2005).
93. Cameron, V. A. & Ellmers, L. J. Minireview: Natriuretic Peptides during Development of the Fetal Heart and Circulation. Endocrinology 144, 2191–2194 (2003).
94. Sergeeva, I. A. & Christoffels, V. M. Regulation of expression of atrial and brain natriuretic peptide, biomarkers for heart development and disease. Biochim. Biophys. Acta - Mol. Basis Dis. 1832, 2403–2413 (2013).
95. Woods, R. L. CARDIOPROTECTIVE FUNCTIONS OF ATRIAL NATRIURETIC PEPTIDE AND B-TYPE NATRIURETIC PEPTIDE: A BRIEF REVIEW. Clin. Exp. Pharmacol. Physiol. 31, 791–794 (2004).
96. He, H. et al. Overexpression of the rat sarcoplasmic reticulum Ca2+ ATPase gene in the heart of transgenic mice accelerates calcium transients and cardiac relaxation. J. Clin. Invest. 100, 380–389 (1997).
97. Chen, Y. et al. Constitutive Cardiac Overexpression of Sarcoplasmic/Endoplasmic Reticulum Ca2+-ATPase Delays Myocardial Failure After Myocardial Infarction in Rats at a Cost of Increased Acute Arrhythmias. Circulation 109, 1898–1903 (2004).
98. Müller, O. J. et al. Transgenic rat hearts overexpressing SERCA2a show improved contractility under baseline conditions and pressure overload. Cardiovasc. Res. 59, 380–9 (2003).
99. del Monte, F. et al. Improvement in survival and cardiac metabolism after gene transfer of sarcoplasmic reticulum Ca(2+)-ATPase in a rat model of heart failure. Circulation 104, 1424–9 (2001).
100. Sakata, S. et al. Restoration of mechanical and energetic function in failing aortic-banded rat hearts by gene transfer of calcium cycling proteins. J. Mol. Cell. Cardiol. 42, 852–861 (2007).

101. Jessup, M. et al. Calcium Upregulation by Percutaneous Administration of Gene Therapy in Cardiac Disease (CUPID): A Phase 2 Trial of Intracoronary Gene Therapy of Sarcoplasmic Reticulum Ca2+-ATPase in Patients With Advanced Heart Failure. Circulation 124, 304–313 (2011).
102. Zsebo, K. et al. Long-Term Effects of AAV1/SERCA2a Gene Transfer in Patients With Severe Heart FailureNovelty and Significance. Circ. Res. 114, 101–108 (2014).
103. Hulot, J.-S. et al. Effect of intracoronary administration of AAV1/SERCA2a on ventricular remodelling in patients with advanced systolic heart failure: results from the AGENT-HF randomized phase 2 trial. Eur. J. Heart Fail. 19, 1534–1541 (2017).
104. Roe, A. T., Frisk, M. & Louch, W. E. Targeting cardiomyocyte Ca2+ homeostasis in heart failure. Curr. Pharm. Des. 21, 431–48 (2015).
105. Lo Giudice, P., Mattera, G. G., Gagnol, J.-P. & Borsini, F. Chronic Istaroxime Improves Cardiac Function and Heart Rate Variability in Cardiomyopathic Hamsters. Cardiovasc. Drugs Ther. 25, 133–138 (2011).
106. Mattera, G. G. et al. Istaroxime: A New Luso-Inotropic Agent for Heart Failure. Am. J. Cardiol. 99, S33–S40 (2007).
107. Shah, S. J. et al. Effects of istaroxime on diastolic stiffness in acute heart failure syndromes: Results from the Hemodynamic, Echocardiographic, and Neurohormonal Effects of Istaroxime, a Novel Intravenous Inotropic and Lusitropic Agent: a Randomized Controlled Trial in Patients Hospitalized with Heart Failure (HORIZON-HF) trial. Am. Heart J. 157, 1035–1041 (2009).
108. Gheorghiade, M. et al. Hemodynamic, Echocardiographic, and Neurohormonal Effects of Istaroxime, a Novel Intravenous Inotropic and Lusitropic Agent. J. Am. Coll. Cardiol. 51, 2276–2285 (2008).
109. Planelles-Herrero, V. J., Hartman, J. J., Robert-Paganin, J., Malik, F. I. & Houdusse, A. Mechanistic and structural basis for activation of cardiac myosin force production by omecamtiv mecarbil. Nat. Commun. 8, 190 (2017).
110. Liu, L. C., Dorhout, B., van der Meer, P., Teerlink, J. R. & Voors, A. A. Omecamtiv mecarbil: a new cardiac myosin activator for the treatment of heart failure. Expert Opin. Investig. Drugs 25, 117–127 (2016).
111. Winkelmann, D. A., Forgacs, E., Miller, M. T. & Stock, A. M. Structural basis for drug-induced allosteric changes to human β-cardiac myosin motor activity. Nat. Commun. 6, 7974 (2015).
112. Bakkehaug, J. P. et al. Myosin Activator Omecamtiv Mecarbil Increases Myocardial Oxygen Consumption and Impairs Cardiac Efficiency Mediated by Resting Myosin ATPase ActivityCLINICAL PERSPECTIVE. Circ. Hear. Fail. 8, 766–775 (2015).
113. Shen, Y.-T. et al. Improvement of Cardiac Function by a Cardiac Myosin Activator in Conscious Dogs With Systolic Heart Failure. Circ. Hear. Fail. 3, 522–527 (2010).
114. Liu, Y., White, H. D., Belknap, B., Winkelmann, D. A. & Forgacs, E. Omecamtiv Mecarbil Modulates the Kinetic and Motile Properties of Porcine β-Cardiac Myosin. Biochemistry 54, 1963–1975 (2015).
115. Cleland, J. G. et al. The effects of the cardiac myosin activator, omecamtiv mecarbil, on cardiac function in systolic heart failure: a double-blind, placebo-controlled, crossover, dose-ranging phase 2 trial. Lancet 378, 676–683 (2011).
116. Greenberg, B. H. et al. Safety and Tolerability of Omecamtiv Mecarbil During Exercise in Patients With Ischemic Cardiomyopathy and Angina. JACC Hear. Fail. 3, 22–29 (2015).
117. Teerlink, J. R. et al. Dose-dependent augmentation of cardiac systolic function with the selective cardiac myosin activator, omecamtiv mecarbil: a first-in-man study. Lancet 378, 667–675 (2011).
118. Teerlink, J. R. A novel approach to improve cardiac performance: cardiac myosin activators. Heart Fail. Rev. 14, 289–298 (2009).
119. Almufleh, A. et al. Ejection fraction improvement and reverse remodeling achieved with Sacubitril/Valsartan in heart failure with reduced ejection fraction patients. Am. J. Cardiovasc. Dis. 7, 108–113 (2017).
120. Suematsu, Y. et al. LCZ696 (Sacubitril/Valsartan), an Angiotensin-Receptor Neprilysin Inhibitor, Attenuates Cardiac Hypertrophy, Fibrosis, and Vasculopathy in a Rat Model of Chronic Kidney Disease. J. Card. Fail. 24, 266–275 (2018).
121. Chen, B.-Y. et al. AC-NP: A Novel Chimeric Peptide with Natriuretic and Vasorelaxing Actions. PLoS One 6, e20477 (2011).
122. From, A. H. L. Do engineered natriuretic peptides have greater therapeutic potential than do native peptides? Cardiovasc. Res. 88, 391–392 (2010).
123. Wylie, J. V & Tsao, L. Nesiritide for the treatment of decompensated heart failure. Expert Rev. Cardiovasc. Ther. 2, 803–813 (2004).

124. van der Pol, A. et al. Accumulation of 5-oxoproline in myocardial dysfunction and the protective effects of OPLAH. Sci. Transl. Med. 9, eaam8574 (2017).
125. Meister, A. & Anderson, M. E. Glutathione. Annu. Rev. Biochem. 52, 711–760 (1983).
126. Liu, Y., Hyde, A. S., Simpson, M. A. & Barycki, J. J. Emerging regulatory paradigms in glutathione metabolism. Advances in Cancer Research 122, 69–101 (2014).
127. Yang, K.-C. et al. Deep RNA sequencing reveals dynamic regulation of myocardial noncoding RNAs in failing human heart and remodeling with mechanical circulatory support. Circulation 129, 1009–21 (2014).
128. Pederzolli, C. D. et al. 5-Oxoproline reduces non-enzymatic antioxidant defenses in vitro in rat brain. Metab. Brain Dis. 22, 51–65 (2007).
129. Pederzolli, C. D. et al. Acute administration of 5-oxoproline induces oxidative damage to lipids and proteins and impairs antioxidant defenses in cerebral cortex and cerebellum of young rats. Metab. Brain Dis. 25, 145–54 (2010).

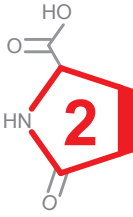

# Chapter 3

## Accumulation of 5-oxoproline in myocardial dysfunction and the protective effects of OPLAH

Atze van der Pol[1], Andres Gil[2], Herman H.W. Silljé[1], Jasper Tromp[1,3], Ekaterina S. Ovchinnikova[1,4], Inge Vreeswijk-Baudoin[1], Martijn Hoes[1], Ibrahim J. Domian[5,6], Bart van de Sluis[7], Jan M. van Deursen[8], Adriaan A. Voors[1], Dirk J. van Veldhuisen[1], Wiek H. van Gilst[1], Eugene Berezikov[4], Pim van der Harst[1], Rudolf A. de Boer[1], Rainer Bischoff[2], Peter van der Meer[1]

[1]Department of Cardiology, University Medical Center Groningen, University of Groningen
[2]Department of Pharmacy, Analytical Biochemistry, University of Groningen
[3]National Heart Centre Singapore
[4]European Research Institute for the Biology of Aging, Laboratory of Stem Cell Regulation and Mechanisms of Regeneration, University of Groningen
[5]Cardiovascular Research Center, Department of Medicine, Massachusetts General Hospital, Harvard Medical School
[6]Harvard Stem Cell Institute
[7]Molecular Genetics Section, Department of Pediatrics, University Medical Center Groningen, University of Groningen
[8]Department of Pediatrics, Mayo Clinic

*Science Translational Medicine 2017 Nov 8; 9(415): eaam8574*

## ABSTRACT

In response to heart failure (HF), the heart reacts by repressing adult genes and expressing fetal genes, thereby returning to a more fetal-like gene profile. To identify genes involved in this process, we carried out transcriptional analysis on murine hearts at different stages of development and on hearts from adult mice with HF. Our screen identified *Oplah*, encoding for 5-oxoprolinase, a member of the γ-glutamyl cycle that functions by scavenging 5-oxoproline. OPLAH depletion occurred as a result of cardiac injury, leading to elevated 5-oxoproline and oxidative stress, whereas OPLAH overexpression improved cardiac function after ischemic injury. In HF patients, we observed elevated plasma 5-oxoproline, which was associated with a worse clinical outcome. Understanding and modulating fetal-like genes in the failing heart may lead to potential diagnostic, prognostic, and therapeutic options in HF.

## INTRODUCTION

Heart failure (HF) is one the most challenging health problems of the developed world, with a 5-year survival rate of less than 50% (1). Cellular responses to cardiac injury in the failing heart lead to changes in cardiac gene expression and are comparable to patterns observed in the fetal heart (2). Most notable is the metabolic switch in energy substrate from fatty acids (postnatal) to carbohydrates (fetal), which is thought to take place by repression of adult and re-expression of fetal genes (2, 3). During HF, several proteins switch back to fetal-like isoforms, including sarcomeric proteins myosin heavy chains and α-actins (4). It has been suggested that expression of these fetal-like genes, including several well-known HF-related genes, contributes to the progression of cardiac dysfunction (2). Although several aspects of the cardiac fetal-like gene program have been identified, the reoccurrence of the fetal-like gene program in the failing heart remains poorly characterized. The identification of novel genes associated with this process may lead to the identification of novel therapeutic targets in HF.

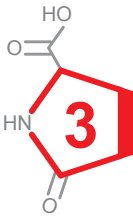


Here, we setout to further characterize the fetal-like gene programin HFand investigate whether identified genes can affect cardiac function after myocardial infarction (MI). Genes were identified by next-generation RNA-sequencing (RNA-seq) of murine cardiac tissue during development and adult HF. Of the identified genes, we further investigated the role of *Oplah* in murine and human cardiac disease. Oplah encodes for 5-oxoprolinase, an enzyme involved in the γ-glutamyl cycle (5, 6), and was shown to be expressed during cardiac development but repressed in HF. OPLAH functions by converting 5-oxoproline, a degradation product of glutathione, to glutamate. The role of the γ-glutamyl cycle in HF has been well established, where dysregulation of several members of this cycle has been associated with the progression and severity of HF, including γ-glutamylcysteine synthetase, glutathione peroxidase, and γ-glutamyltransferase (7–12). However, the role of OPLAH and 5-oxoproline in cardiovascular diseases has, to date, remained unclear.

## MATERIAL AND METHODS

### Study design

The main research objective was to identify genes associated with the fetal gene program, leading to the identification of OPLAH as a relevant gene in cardiac development and HF. We used rodent disease models, genetically modified mice, and human plasma samples to study its importance in cardiac disease and protection supported by *in vitro* mechanistic data. The mice were assigned randomly to the experimental groups and were analyzed in a blinded fashion. The number of animals,

experimental replicates, and patient samples is described in the figure legends.

**Next-generation sequencing tissue acquisition and RNA extraction**

All animal protocols were approved by the Animal Ethical Committee of the University of Groningen (permit number DEC6002AA). A total of four stages of murine cardiac development (E12, E18, PP2, and 4 weeks) were used in this study. Female mice at days 12 and18 of pregnancy were sacrificed, followed by the excision of the embryos. For E12, the whole heart was removed for each embryo. At E18, the left ventricle was excised from the embryos. The left ventricle of PP2 pups were removed after decapitation. Four-week-old mice were sacrificed after which the left ventricle was isolated.We also included 20-week-old mice that had undergone IR injury or sham treatment. For each time point, we used n = 3 samples, and all tissue samples were snap-frozen after excision and stored at −80°C until total RNA was isolated by the TRIzol RNA isolation protocol.

**RNA-seq library preparation and sequencing**

RNA-seq was performed on the same 18 mice samples that were used for the qRT-PCR analysis. The quality of extracted RNA was accessed on a Bioanalyzer 2100 (Agilent) using a Pico RNA chip (Agilent). All samples passed quality control, exceeding a minimum RNA integrity number of 8. Then, 1 mg of total RNA from each sample was processed with the NEXTflex Poly(A) Beads kit (Bioo Life Science) to pull down them RNA from the total RNA samples. Eluted mRNA was further used for library preparation. Libraries were generated by strictly following NEXTflex Illumina RNA-Seq Library Prep version 2 kit recommendations (Bioo Life Science). At the end of the procedure, libraries were purified with AMPure XP beads, and the DNA was eluted with 30 ml of resuspension buffer. The size and quality of the libraries were controlled by running them on a Bioanalyzer 2100 using the High Sensitivity DNAassay. For sequencing, all 18 samples were pooled together. This 2 nM pool was made equimolar with individual library concentrations calculated from Qubit dsDNA HS Assay kit data and library peak size derived from Bioanalyzer data. The libraries were sequenced on the Illumina HiSeq 2500 machine in the RapidRun mode.

**Analysis of RNA-seq data**

Reads were mapped to the mouse genome assembly GRCm38 using STAR aligner version 2.5.2b (31). Gene counts were derived from the alignment files using the htseq-count program version 0.6.1p1 from HTSeq package (32) and Ensembl gene annotations. Differential gene expression between pairs of conditions was calculated using edgeR package (33) with batch effects correction and upper quartile normalization. Genes with FDR of ≤ 0.05 were considered as statistically significant. For linear regression analysis of gene expression during development, a custom script based on Perl::PDL library (http://pdl.perl.org) was used. Genes with P values

of ≤ 0.05 after Bonferroni correction were considered as statistically significant.

**Cell culture**

For a detailed description of cell lines and culturing protocols, see Supplementary Materials and Methods.

**Viral constructs**

To generate recombinant adenoviral vectors, the ViraPower Adenoviral Expression System (Invitrogen) was used according to the manufacturer's instructions. OPLAH-specific shRNA–targeting oligonucleotides (Table S14) were cloned into a pENTR4 vector containing an H1 promoter and a green fluorescent protein marker gene. For theOPLAH overexpression construct, the full-length human OPLAH complementary DNA (cDNA) was N-terminally fused with a myc tag and cloned into the pENTR4 vector. Recombinant adenovirus was generated as previously described (34). All constructs were verified by sequencing, and NRVCs were infected with an adenoviral multiplicity of infection of 50.

**In vitro oxidative stress**

*In vitro* oxidative stress was achieved by culturing cells under hypoxic conditions or by the addition of $H_2O_2$. Additional information is provided in Supplementary Materials and Methods.

**CellROX**

Oxidative stress was measured by means of CellROX Orange Reagent (Thermo Fisher Scientific), as per the manufacturer's instructions. For additional information, see Supplementary Materials and Methods.

**Total antioxidant capacity**

The antioxidant capacity of tissue samples was measured by means of the Total Antioxidant Capacity Assay kit (ab65329, Abcam), as per the manufacturer's instructions. For additional information, see Supplementary Materials and Methods.

**GSH/GSSG measurements**

GSH and GSSG were measured by means of the Glutathione Fluorometric Assay kit (#K26-100, BioVision), as per the manufacturer's instructions. See Supplementary Materials and Methods for details.

**Quantitative real-time PCR**

Details of qRT-PCR are provided in Supplementary Materials and Methods. Primer sequences can be found in Table S15.

**Western blotting**

Details regarding Western blotting are provided in Supplementary Materials and Methods. Antibodies used are described in Table S16.

**TG renin overexpression rats**

Animal protocol was approved by the Animal Ethical Committee of the University of Groningen (permit number DEC5163). The male homozygous TGR (mREN2)27 rats (denoted as REN2) were bred and obtained from the Max Delbrück Center for Molecular Medicine. These rats have an overexpression of the mouse renin and develop severe hypertension and LV hypertrophy, leading to HF at 13 to 15 weeks of age (35). We used five 12- to 14-week-old male REN2 rats and four male age-matched Sprague Dawley rats as control (Harlan). Before scarification, an echocardiogram and hemodynamic measurements were performed. Animals were housed under standard conditions.

**OPLAH-TG mice**

The animal protocol was approved by the Animal Ethical Committee of the University of Groningen (permit number DEC6632A). The animal experiments that were performed conform with the ARRIVE (Animal Research: Reporting of In Vivo Experiments) guidelines. The human OPLAH gene (GenBank no. NM_017570.4) was amplified by PCR using primers containing Sal I and Hind III restriction sites (Table S14). The PCR product was cloned into a previously described vector containing the cardiac-specific myosin heavy chain (α-MHC) promoter (36). The BamH I fragment of this construct, containing the α-MHC promoter and human OPLAH cDNA sequence, was subsequently used for pronuclear injection to generate cardiac-specific human OPLAH-TG mice (FVB background). These TG mice were made by the mouse clinic for aging research (University Medical Center Groningen) in collaboration with Mayo Clinic. The mice were backcrossed with C57BL/6 mice, and third generation backcrossed animals (N3) were used in this study. In all experiments performed in this study, age- and sex-matched non-TG (WT) littermates were used for comparison with the OPLAH TG mice.

**Rodent models of HF**

All animal protocols were approved by the Animal Ethical Committee of the University of Groningen. The animal experiments that were performed conform with the ARRIVE guidelines. Animals were housed under standard conditions. For animal experiments involving TG animals, the surgeon tried to achieve a ±30% area at risk of the left ventricle and was blinded to which animal was WT and which was TG. Details regarding the implementation of rat MI, murine MI, and murine IR models are described in Supplementary Materials and Methods.

### Echocardiography and cardiac MRI measurements

Cardiac function of rats was assessed by means of echocardiography at baseline and before scarificationwith aVivid 7 (GE Healthcare) equipped with a 10-MHz phase array linear transducer, as previously described (36). CardiacMRI was performed as previously described (37). For additional information, see Supplementary Materials and Methods.


### Hemodynamic measurements

Heart rate and pressures of the aorta and left ventricle were measured after 4 weeks using the Scisense ADVantage pressure-volume (PV) measurement system with a PV catheter, as previously described (38). For additional information, see Supplementary Materials and Methods.

### Histology

For immunohistochemical analysis, hearts were fixed overnight with 10% neutral-buffered formalin at 4°C. After fixation, samples were subjected to a dehydration series, embedded in paraffin, and cut into 4 mM sections. Masson's trichrome, fluorescein isothiocyanate–labeled wheat germ agglutinin (WGA), and cleaved Caspase-3 stainings were performed. Quantification was performed with the Aperio ImageScope software (Masson's trichrome) and Fiji for the WGA and cleaved Caspase-3 stainings (39). The investigators were blinded to experimental settings during data analysis. For additional information, see Supplementary Materials and Methods.

### Human patient population and plasma samples

A subpopulation of the Coordinating Study Evaluating Outcomes of Advising and Counseling in Heart Failure (COACH) was used. Briefly, 1023 patients were included to participate in a prospective randomized disease management study. The rationale and outcomes of this trail have been reported elsewhere (26–28). Samples for biomarker analysis were obtained from a subset of 567 patients, who were representative of the entire study population on baseline characteristics. Blood sampling was performed before discharge, when patients were stabilized after an acute HF admission, and samples were immediately stored at −80°C until the analysis was performed. This study complies with the Declaration of Helsinki, and local medical ethics committees approved the study. All patients provided written informed consent.

Here, 535 patient plasma samples from the 567 previously described samples were analyzed. Of the remaining 32 patients, no plasma was available for 5-oxoproline measurements, and these patients were excluded from this analysis. The subpopulation of 535 patients remained representative for the entire study

population on baseline characteristics (Table S9). The primary end point of the COACH study was the combined end point of all-cause mortality or rehospitalization at 18 months, where rehospitalizationwas defined as an unplanned overnight hospital stay connected to worsening HF. All events were evaluated and adjudicated by an independent end point committee. Blood sampling was performed before discharge, and samples were immediately stored at −80°C until the analysis was performed. Measurements of the available biomarkers have been previously described (25).

**Internal standard preparation ($^{13}$C-5-oxoproline and L-glutamic acid) and validation of the analytical method**

5-Oxoproline internal standard (IS) was prepared from $^{13}$C-labeled L-glutamic acid (40). Following international guidelines (41, 42), method validation was performed by evaluating the following parameters: intraday variability (repeatability), interday variability (intermediate precision), lower limit of quantification, linearity, and accuracy (fig. S14 and Tables S17 and S18). For additional information, see Supplementary Materials and Methods.

**Sample preparation procedure**

For plasma sample preparation, 5 µl of animal plasma or 25 µl of human plasma was mixed with 200 µl of the extraction solution (25 µl of 5-oxoproline IS in 75% methanol). For murine LV tissue sample preparation, about 1 mg of powdered tissue was homogenized in 200 µl of extraction solution. Samples were vortex-mixed and centrifuged for 10 min at 20,000g. Supernatant was dried under a streamof nitrogen gas at roomtemperature, followed by resuspension in 100 µl of water. At this stage, samples were stored at −80°C until LC-MS measurements were performed. For tissue samples, 5-oxoproline and L-glutamic acid concentrations were corrected for the amount of total protein (per microgram).

**LC-MS of 5-oxoproline and L-glutamic acid**

5-Oxoproline and L-glutamic acid were separated in the HILIC (hydrophilic interaction liquid chromatography) mode using a Luna NH2 column (3 mm; 100 × 2 mm; Phenomenex) on an Agilent 1290 Infinity LC system. Mass spectrometry detection was performed using an Agilent 6410 triple quadrupole system. For additional information, see Supplementary Materials and Methods.

**Statistical analysis**

All animal and cell experimental data are represented as means ± SEM. To compare the difference between two groups, Student's t test was performed. Comparisons between more than two groups were carried out using one-way ANOVA with post hoc Bonferroni test. P values of $<0.05$ were considered statistically significant. All analyses were carried out using the GraphPad Prism software version 5.04

(GraphPad Software Inc.). For the animal experiments, we chose the sample sizes for all the groups based on the feasibility and prior knowledge of statistical power from previously published experiments (35–37,43,44). Parametric tests were chosen only when variances between the compared groups were not significantly different. With small sample sizes, we did not apply statistical tests for normality or equality of variances.


All human plasma data are represented as means ± SD or medians with interquartile ranges where appropriate. Comparisons between two or more groups were performed using one-way ANOVA or the Kruskal-Wallis test or c2 test where appropriate. For further analyses, concentrations of 5-oxoproline were log2-transformed to acquire a normal distribution. To investigate the relationship of 5-oxoproline with other biochemicalmarkers, a linear regressionwas performed. A Kaplan-Meier graph shows the relationship of tertiles of 5-oxorpoline with the primary end point of all-cause mortality and HF-related rehospitalizations at 18 months. For multivariable outcome analyses, the relationship of tertiles of 5-oxoproline with outcome was studied using Cox regression analysis. The risk nadir was used as the reference group. Analyses were corrected for clinically relevant variables. $P < 0.05$ was considered statistically significant. All analyses were carried out using the Stata version 13.0 for Windows. For experiments where the total n was smaller than 20, individual subject level data are shown in table S19.

## RESULTS

**OPLAH is a novel member of the cardiac fetal-like gene program**

To identify genes associated with the cardiac fetal-like gene program, we performed RNA-seq on RNA from murine whole-heart embryonic day 12 (E12), left ventricular (LV) tissue at four different stages of cardiac development [E18, postpartum day 2 (PP2), week 4, and week 20 sham], and LV tissue of ischemia/reperfusion (IR)–induced HF (week 20 IR) (Fig. 1A). To specifically target stepwise up-regulated or down-regulated genes, we performed linear regression analysis on the five developmental stages (E12 to week 20 sham). We identified 1266 up-regulated and 1373 down-regulated genes [false discovery rate (FDR), ≤ 0.05]. The up-regulated genes were highly enriched for genes involved in metabolism and cardiac development, including *Ppar-α*, *Atp2a22* (*Serca2a*), *Atp5b*, and *Pdk2* (Table S1), whereas the down-regulated geneswere highly enriched for genes involved in cell cycle, including *c-Myc*, *Smad2/3*, and *E2f* (Table S2).

To identify genes that were differentially expressed in HF, we compared week 20 sham with week 20 IR. We identified a total of 673 differentially expressed genes

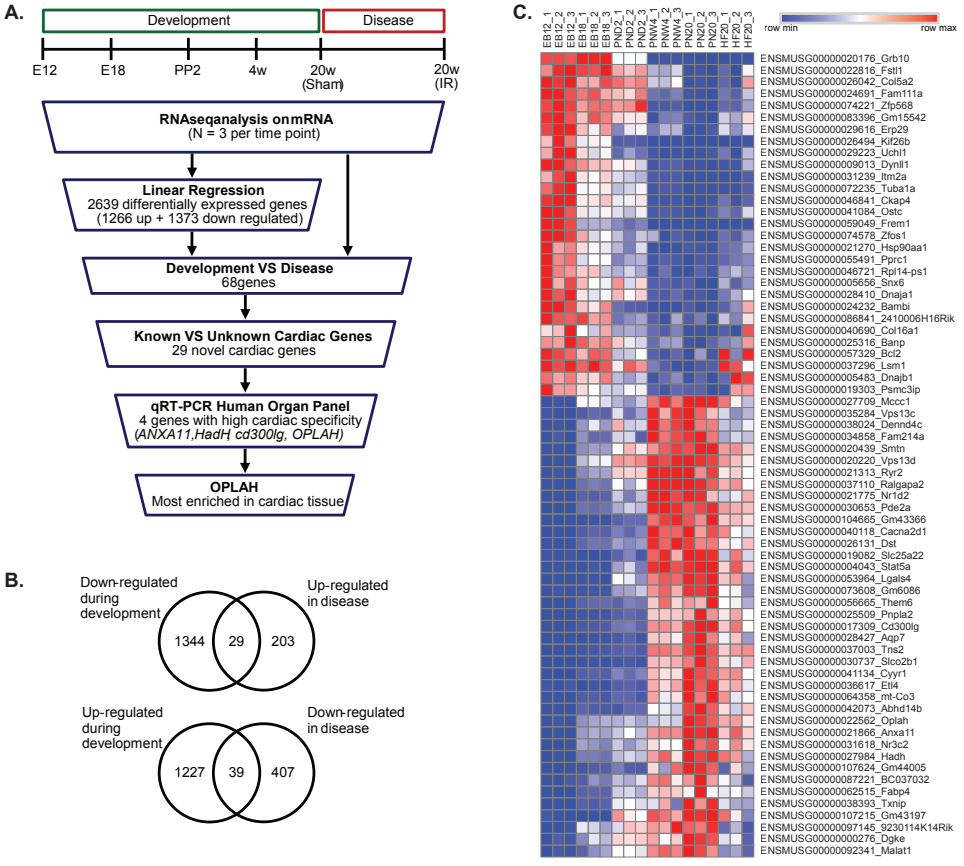


**Fig. 1. RNA-seq analysis on the reactivation of the cardiac fetal program.**
**(A)** Flow chart displaying the steps taken for the identification of novel cardiac fetal genes (n indicates the number of murine hearts/left ventricles used). qRT-PCR, quantitative real-time polymerase chain reaction. **(B)** Venn diagram of the number of differentially expressed genes identified in the different groups: up-regulated in development, down-regulated in development, down-regulated in HF, and up-regulated in HF. **(C)** Heat map depicting the expression profiles of the 68 identified cardiac fetal genes during murine development (E12, E18, PP2, 4 weeks old, and 20 weeks old) and cardiac injury (20 weeks old after IR).

(FDR, ≤ 0.05) in IR-induced HF (203 up-regulated genes and 470 down-regulated genes, including *Myh7*, *Acta1*, *Nppb*, *Ryr2*, and *Fgf2*). Genes involved in the reactivation of the fetal-like gene program were defined as genes that demonstrated inverse expression in HF than during development. Of the 1266 up-regulated genes during development, 39 were down-regulated in HF, and of the 1373 down-regulated genes during development, 29 were up-regulated in HF (Fig. 1, B and C, and Table S3).Onthe basis of KEGG (Kyoto Encyclopedia of Genes and Genomes) pathway analysis, these 68 genes were highly enriched for metabolic and cardiac disease pathways. Of these 68 putative cardiac fetal genes, 39 had already been described

in the literature to be associated with cardiac disease or development (including *Ryr2*, *Cacna2d1*, *Fstl1*, and *Bambi*) (13–16). The remaining 29 genes had been associated with neither cardiac development nor cardiac disease to date and were considered novel genes associated with the cardiac fetal-like gene program.

To evaluate whether these 29 putative cardiac fetal-like genes were also relevant in humans, we screened the expression of these genes across an adult human organ panel using qRT-PCR. *ANXA11*, *HADH*, *CD300LG*, and *OPLAH* were predominantly expressed in the human heart (Fig. S1). *CD300LG* was predominantly expressed in adult cardiac tissue, but the expression was barely detectable by qRT-PCR. *ANXA11*, *HADH*, and *OPLAH* were highly expressed in the human adult heart. However, *ANXA11* and *HADH* also had relative high expression in other tissues, compared to *OPLAH*. Therefore, we further explored the role of OPLAH in the heart. To test whether OPLAH was also induced during human cardiac development, we differentiated human embryonic stem cells (hESCs) to cardiomyocytes. OPLAH protein expression was found to coincide with the expression of the cardiomyocyte marker α-actinin (Fig. 2A). To determine which cellular component of the heart expressed OPLAH,we performed immunoblotting and qRT-PCR on cardiomyocytes, fibroblasts, and endothelial and smooth muscle cells. OPLAH was found to be predominantly expressed by cardiomyocytes (Fig. 2, B to D). Analysis on isolated neonatal rat ventricular cardiomyocytes (NRVCs) revealed that OPLAH was expressed solely in the cytoplasm of cardiomyocytes (Fig. S2). To explore the association between cardiac dysfunction and OPLAH expression, we measured OPLAH in three different animal models of HF: IR injury, permanent MI, and pressure overload. In all HF models, OPLAH expression was found to be 50 to 80% lower in failing hearts compared to controls (Fig. 2E, Tables S4 to S6, and Fig. S3).

**Oxidative stress and mechanical stretch deplete OPLAH *in vitro***

To determine which HF-associated stressors induce OPLAH depletion, we exposed NRVCs to mechanical stretch, isoproterenol (ISO), phenylephrine (PE), and oxidative stress (by administration of hypoxia or $H_2O_2$). Both ISO and PE are adrenergic stimuli that result in hypertrophy in cardiomyocytes. Neither ISO nor PE administration had an effect on *Oplah* expression (Fig. 2F).With the application of mechanical stretch to NRVCs, we observed a clear reduction in *Oplah* (Fig. 2F and Fig. S4), which coincides with an increase in oxidative stress. Similarly, hypoxia resulted in a significant reduction in OPLAH expression ($P < 0.0001$; Fig. 2F and Fig. S5). Hypoxic culture conditions were maintained for 24 hours, resulting in a significant increase in oxidative stress ($P < 0.001$) and a reduction in medium pH and oxygen concentrations, when compared to controls (Fig. S5). To test whether other forms of oxidative stress could also reduce OPLAH expression, we applied $H_2O_2$ to NRVCs. Exposure to a concentration of 500 mM of $H_2O_2$ for 12 hours was sufficient to induce

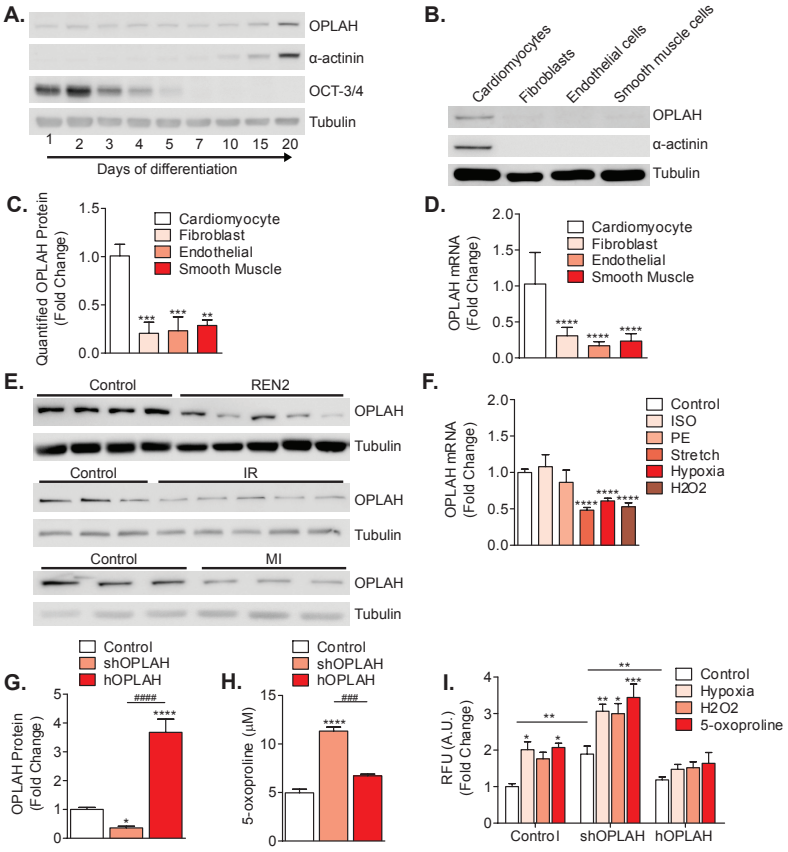


**Fig. 2. OPLAH *in vitro* characterization.**
**(A)** Representative immunoblotting analysis of OPLAH expression during hESC cardiomyocyte differentiation. **(B)** Representative immunoblotting analysis of OPLAH protein expression in NRVCs, rat fibroblasts,murine endothelioma cells, and rat smoothmuscle cells. **(C)** Quantified OPLAH protein expression in NRVCs (n = 4), rat fibroblasts (n = 4), murine endothelioma cells (n = 4), and rat smooth muscle cells (n = 5). **(D)** qRT-PCR mRNA expression of OPLAH in NRVCs (n = 7), rat fibroblasts (n = 8), murine endothelioma cells (n = 8), and rat smooth muscle cells (n = 8). **(E)** Immunoblotting analysis of OPLAH expression in three animal models for HF. Top: OPLAH expression in Sprague Dawley rats (control; n = 4) versus renin overexpression TG rats (REN2; n = 5). Middle: OPLAH expression in sham (control; n = 3) versus IR (n = 5) C57BL/6mice. Bottom: OPLAH expression in sham (control; n = 3) versus MI (n = 3) rats. **(F)** qRT-PCR mRNA expression of OPLAH in NRVM exposed to ISO (n = 4), PE (n = 4), stretch (n = 17), hypoxia (n = 31), $H_2O_2$ (n = 16), and no-treatment controls (n = 23). **(G)** Quantified OPLAH protein expression in NRVCs infected with the control, short hairpin OPLAH (shOPLAH), or human OPLAH overexpression (hOPLAH) constructs (n = 6, 11, and 5, respectively). **(H)** 5-Oxoproline concentrations in NRVCs infected with the control, shOPLAH, or hOPLAH adenoviral construct (n = 3). **(I)** CellROX analysis of adenoviral-infected NRVCs with control, shOPLAH, or hOPLAH vector exposed to 24 hours of hypoxia, 24 hours of $H_2O_2$ (500 mM), or 2 hours of 5-oxoproline (10 mM) culture conditions [for all conditions, n = 10 (control), 15 (shOPLAH), and 15 (hOPLAH)]. CellROX data are presented as fold change of relative fluorescence units (RFU) [arbitrary units (A.U.)] per microgram protein. Data are presented as means ± SEM. * P < 0.05; ** P < 0.01; *** P < 0.001; **** P < 0.0001; ### P < 0.001; #### P < 0.0001, as calculated by Student's t test or one-way analysis of variance (ANOVA). "*" indicates significant difference compared to control, whereas "#" denotes differences between groups other than control. n indicates the number of biological replicates of cell experiments or the number of animals.

a significant reduction in OPLAH ($P < 0.0001$) coupled to a significant increase in oxidative stress ($P < 0.01$; Fig. 2E and Fig. S6). Stretch, hypoxia, and $H_2O_2$ are stressors that can inducemyocyte death; to exclude myocyte death as the cause of *Oplah* reduction, we measured trypan blue–positive cells and lactate dehydrogenase release and performed qRT-PCR for *BCL2* and *BAX* expression (Figs. S4, B to D, S5, C to E, and S6, A to C). In all cases, we found an increase in cardiomyocyte death. However, the percentage of cell death could only partially explain the reduction in *Oplah* expression observed. Finally, because we found OPLAH to be markedly depleted with the induction of oxidative stress, we investigated whether mechanical stretch, which depleted OPLAH, also resulted in an increase in oxidative stress. We found a 25% increase in oxidative stress in stretched cardiomyocytes compared to controls (Fig. S4A). These findings indicate that OPLAH depletion is influenced by stretch and oxidative stress. The latter is of particular interest because OPLAH is associated with the formation of the antioxidant glutathione.

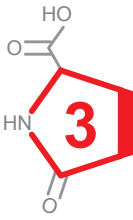


**OPLAH expression is associated with oxidative stress *in vitro***

To identify whether OPLAH had an *in vitro* effect on oxidative stress in cardiomyocytes, we developed adenovirus harboring short hairpin RNA (shRNA) knockdown vectors of *Oplah* (shOPLAH) and cardiacspecific human *OPLAH* overexpression vectors (hOPLAH) (Fig. 2G and Fig. S7). To test whether our shOPLAH and hOPLAH constructs were functional in vitro, we developed a liquid chromatography–mass spectrometry (LC-MS) method to measure 5-oxoproline, the substrate for OPLAH. In cell lysates of NRVCs infected with shOPLAH, we found a significant increase in intracellular 5-oxoproline ($P < 0.0001$; Fig. 2H). This increase in 5-oxoproline was coupled to an increase in reactive oxygen species (ROS) (Fig. 2I). The increase in ROS was more pronounced under hypoxic or $H_2O_2$ culturing conditions (Fig. 2I). NRVCs infected with hOPLAH were protected, to a large extent, from hypoxia and $H_2O_2$-induced oxidative stress (Fig. 2I). Previous publications have demonstrated that 5-oxoproline can itself induce oxidative stress in neurons (17, 18). This finding is supported by our data, where a decrease in OPLAH leads to increased 5-oxoproline and oxidative stress. To further demonstrate that 5-oxoproline is an oxidative stress–inducing agent, we exposed NRVCs to exogenous 5-oxoproline. The administration of 5-oxoproline resulted in an increase in ROS production in cardiomyocytes under control culture conditions, which was amplified when OPLAH was depleted, but diminished when OPLAH was overexpressed (Fig. 2I).

**ERRα, and not ERRγ, transcriptionally regulates OPLAH expression *in vitro***

To understand the regulation of *Oplah*, wewere interested in identifying transcription factors involved in the expression of OPLAH. A recent study has shown by means of ChIP (chromatin immunoprecipitation)–on–chip analysis that the estrogen-related receptor a (ERRα) and ERRγ both have high affinity for the *Oplah* promoter (19).

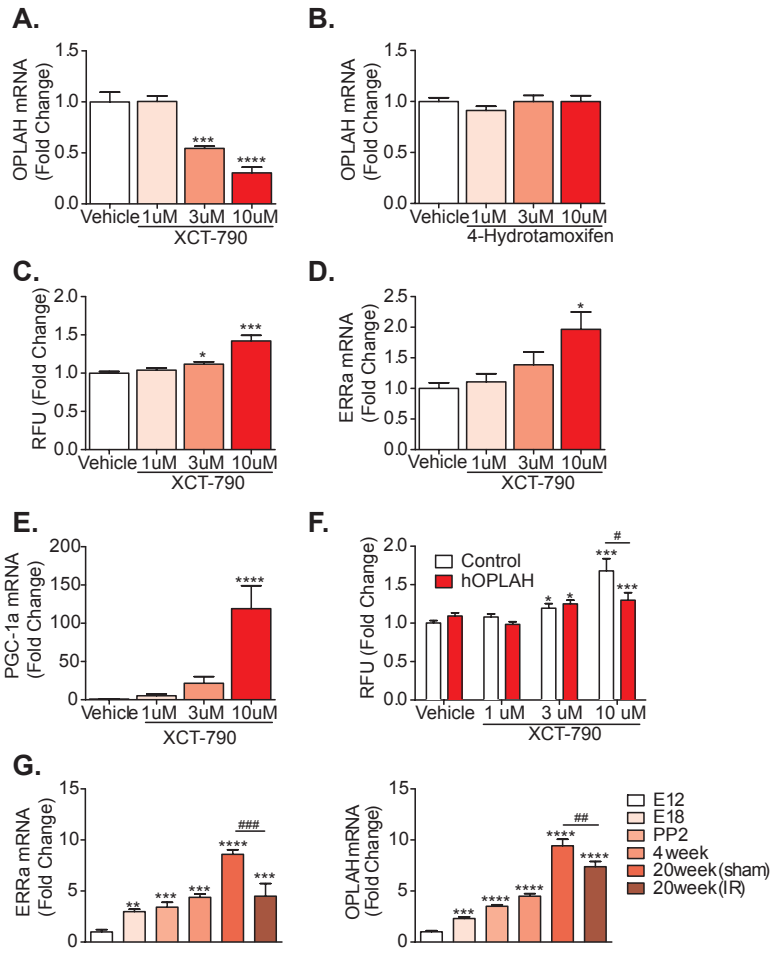


**Fig. 3. ERR*α* is involved in the regulation ofOPLAH.**
**(A)** OPLAH expression in hESC-derived cardiomyocytes exposed to increasing concentrations of XCT-790 (vehicle, n = 6; 1 mM, n = 6; 3 mM, n = 6; 10 mM, n = 4). **(B)** OPLAH expression in hESC-derived cardiomyocytes exposed to increasing concentration of 4-hydroxytamoxifen (vehicle, n = 5; 1 mM, n = 6; 3 mM, n = 6; 10 mM, n = 5). **(C)** CellROX analysis of hESC-derived cardiomyocytes exposed to increasing concentrations of XCT-790 (vehicle, n = 48; 1 mM, n = 48; 3 mM, n = 64; 10 mM, n = 39; n indicates technical replicates). **(D)** ERRα mRNA expression in hESC-derived cardiomyocytes exposed to increasing concentrations of XCT-790 (vehicle, n = 3; 1 mM, n = 6; 3 mM, n = 4; 10 mM, n = 4). **(E)** Peroxisome proliferator–activated receptor γ coactivator 1α (PGC-1α) mRNA expression in hESC-derived cardiomyocytes exposed to increasing concentrations of XCT-790 (vehicle, n = 4; 1 mM, n = 6; 3 mM, n = 6; 10 mM, n = 3). **(F)** CellROX analysis of adenoviral-infected H9C2 cells with control or hOPLAH adenoviral vector exposed to increasing concentration of XCT-790 (vehicle, n = 24; 1 mM, n = 24; 3 mM, n = 24; 10 mM, n = 16; n indicates technical replicates). **(G)** qRT-PCR mRNA expression of ERRα and OPLAH at different stages of development and IR injury [E12, n = 8; E18, n = 11; PP2, n = 7; 4 weeks, n = 3; 20 weeks (sham), n = 3; 20 weeks (IR), n = 3]. CellROX data are presented as fold change of RFU (A.U.) per microgram protein. Data are presented as means ± SEM. *P < 0.05; **P < 0.01; ***P < 0.001; ****P < 0.0001; #P < 0.05; ##P < 0.01; ###P < 0.001, as calculated by Student's t test or one-way ANOVA. "*" indicates significant difference compared to control, whereas "#" denotes differences between groups other than control. n indicates the number of biological replicates of cell experiments.

However, direct regulation of *Oplah* by these transcription factors has not been demonstrated. To study the effects of ERRα and ERRγ on OPLAH expression, we exposed NRVCs to XCT-790 [ERRα antagonist (20)] and 4-hydroxytamoxifen [ERRγ antagonist (21)]. 4-Hydroxytamoxifen demonstrated no effect on *Oplah* expression, whereas exposure to XCT-790 resulted in a dose-dependent reduction in *Oplah* coupled to an increase in ROS (Fig. S8). To test whether this mechanism was also present in human cardiomyocytes, we exposed cardiomyocytes derived from hESCs to XCT-790 and 4-hydroxytamoxifen and observed similar results (Fig. 3, A to C). Inhibition of ERRα in the human cardiomyocytes led to an increase in transcription of *ERRα* and *PGC-1α* [a coactivator and transcriptional regulator of ERRα (22, 23)], suggesting a compensatory mechanism for the lack of functional ERRα (Fig. 3, D to E). To determine whether the increase in ROS by the ERRα antagonist was a consequence of a reduction in OPLAH, we administered hOPLAH adenovirus to cardiomyoblasts before treatment with XCT-790. OPLAH overexpression reduced the XCT-790–induced oxidative stress (Fig. 3F). qRT-PCR analysis on cardiac tissue from different stages of development and disease showed that the *Errα* expression profile resembled that of *Oplah* (Fig. 3G).Under in vitro conditions known to induce OPLAH repression (stretch, hypoxia, and $H_2O_2$), we found that *Errα* expression was reduced, coinciding with *Oplah* depletion (Fig. S9). Overall, these findings suggest that ERRα, and not ERRγ, is involved in the transcriptional regulation of OPLAH in cardiomyocytes.

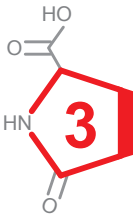


**Cardiac-specific OPLAH overexpression protects mice from IR injury**

To test whether the protective effects of OPLAH in cultured cardiomyoblasts and NRVCs translate into a therapeutic effect, we created OPLAH transgenic (OPLAH-TG) mice with cardiomyocyte-specific hOPLAH overexpression (Fig. 4A). Immunoblotting and qRT-PCR revealed that OPLAH mRNA and protein expression was elevated in the hearts of male OPLAH-TG mice compared to wild-type (WT) littermates (Fig. 4, B to D). In other tissues, including the kidneys, no difference in OPLAH expression was observed between WT and OPLAH-TG mice, confirming that overexpression was confined to the heart. At baseline, the OPLAH-TG mice had comparable body weight, organ weight (right ventricle, left ventricle, atria, kidney, andliver), heart rate, LV ejection fraction, stroke volume, and systolic and diastolic blood pressure to their WT littermates.

To test whether OPLAH-TG mice were protected against oxidative stress–induced cardiac damage, we exposed mice to 60 min of ligation of the anterior descending branch (LAD) of the left coronary artery (ischemia), followed by 4 weeks of reperfusion. OPLAH-TG mice had significantly smaller infarct sizes compared to WT littermates after IR injury, asmeasured by Masson's trichrome staining ($P < 0.05$; Fig. 4E). There was a significant increase in LV weight after IR in the WT mice, an effect that was

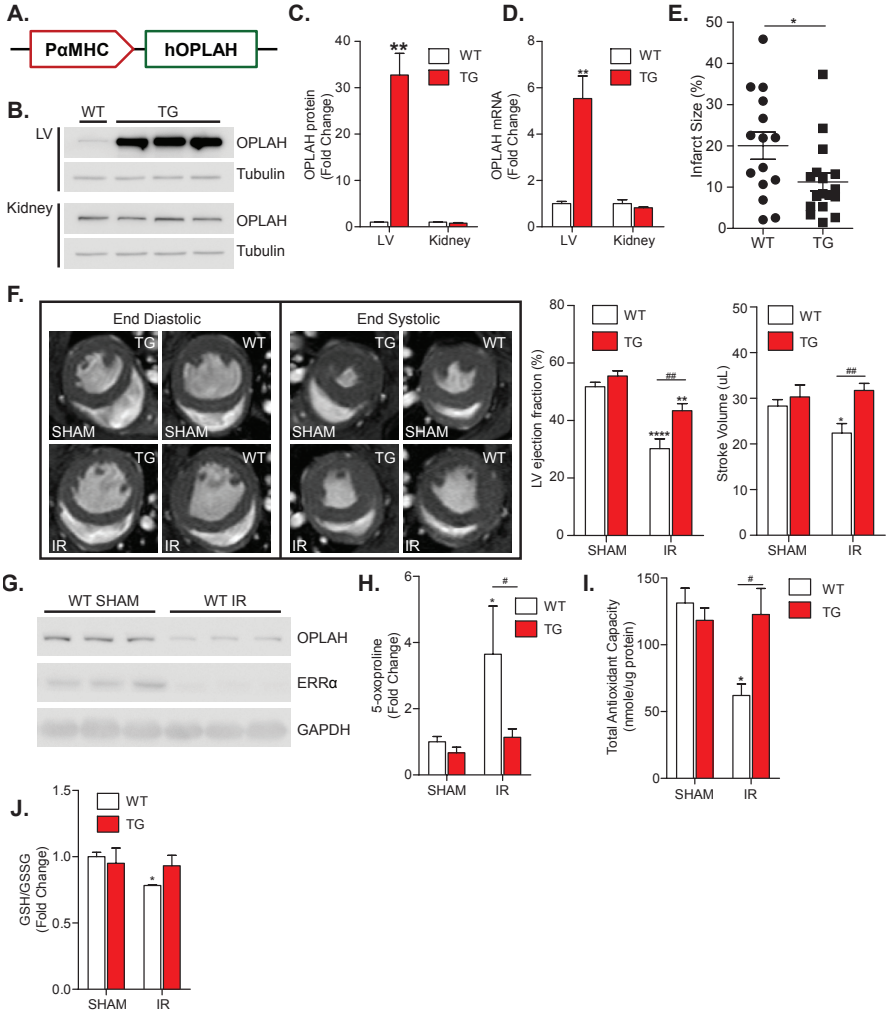


**Fig. 4. OPLAH-TGmice have improved cardiac function after IR injury.**
**(A)** Construct used to develop the OPLAH-TG (TG) mice. (B to D) OPLAH expression in LV and kidney tissue of TG and WT mice (n = 12 and 4, respectively). **(B)** Representative immunoblotting analysis of OPLAH protein. **(C)** Quantified OPLAH protein. **(D)** Quantified OPLAH mRNA. **(E)** Quantification of infarct size (TG IR, n = 17; WT IR, n = 15). **(F)** Representative MRI images of WT and TG mouse hearts, and summary of LV ejection fraction and stroke volume (TG sham, n = 6; TG IR, n = 17; WT sham, n = 15; WT IR, n = 15). **(G)** Representative immunoblotting analysis of OPLAH and ERRα protein expression in the left ventricle of WT sham and IR mice. GAPDH, glyceraldehyde phosphate dehydrogenase. **(H)** 5-Oxoproline concentrations in LV tissue from TG versus WT mice 4 weeks after IR injury (TG sham, n = 9; TG IR, n = 8; WT sham, n = 11; WT IR, n = 7). **(I)** TAC of LV tissue from TG versus WT mice 4 weeks after IR injury (n = 3). **(J)** GSH/GSSG ratio present in LV tissue from TG versus WT mice 4 weeks after IR injury. Data are presented as fold change of microgram GSH/GSSG per microgram protein (TG sham, n = 3; TG IR, n = 4;WT sham, n = 4;WTIR n = 4).Data are presented asmeans ± SEM. *P < 0.05; **P < 0.01; ****P < 0.0001; #P < 0.05; ##P < 0.01, as calculated by Student's t test or one-way ANOVA. "*" indicates significant difference compared to control, whereas "#" denotes differences between groups other than control. n indicates the number of animals.

not present in the TG mice (P < 0.0001; Table S7). The TG mice had reduction in the mRNA expression of fibrotic markers *TIMP-1* and *Col1a1* when compared to the WT mice after IR (Fig. S10). Cardiac magnetic resonance imaging (MRI) and Millar hemodynamics measurements revealed that the TG mice had a higher LV ejection fraction and larger stroke volume after IR when compared to the WT mice (Fig. 4F). Cell size increased after IR; however, no significant differences between WT and TG mice were observed (P = 0.2934; Fig. S11). Cleaved Caspase-3 staining on the left ventricle demonstrated that there was an increase in the number of apoptotic cells; however, the difference between groups was not significant (P = 0.3784; Fig. S12). In WT mice, we observed a reduction in ERRα and OPLAH expression after IR (Fig. 4G), and the decrease in OPLAH in the WT mice resulted in substantially higher 5-oxoproline in cardiac tissue when compared to the OPLAH-TG mice (Fig. 4H). To test whether the observed reduction in 5-oxoproline in the OPLAH-TG mice after IR lowered oxidative stress, we measured the total antioxidant capacity (TAC) and the ratio of reduced glutathione (GSH) to oxidized glutathione (GSSG) in LV tissue. We found a significant decrease in TAC (P < 0.05) and GSH/GSSG ratio (P < 0.05) in the WT mice after IR injury that was not observed in OPLAH-TG mice (Fig. 4, I and J). These data suggest that when murine hearts are exposed to oxidative stress in the form of IR injury in vivo, cardiomyocyte-specific overexpression of OPLAH reduces 5-oxoproline–induced oxidative stress, resulting in reduced infarct size and ultimately leading to improved cardiac function.

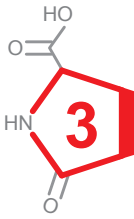


**Cardiac-specific OPLAH overexpression protects mice from permanent MI**

To study the effects of OPLAH overexpression in a more severe form of cardiac injury, we exposed WT and OPLAH-TG mice to permanent MI (Table S8) by ligating the LAD of the left coronary artery. Similar to IR injury, OPLAH-TG mice demonstrated a significant improvement in stroke volume 4 weeks after ligation compared to WT mice (P < 0.01; Fig. 5A). OPLAH-TG mice had significantly smaller infarct sizes (P < 0.05; Fig. 5B) and a reduction in cleaved Caspase-3–positive cells, compared to WT mice after MI (Fig. S12). Furthermore, we also observed a decrease in 5-oxoproline in the OPLAH-TG mice coupled to an improved GSH/GSSG ratio, suggesting a decrease in oxidative stress (Fig. 5, C to E).

**Circulating 5-oxoproline is elevated in patients with HF and predicts outcome**

Because LV tissue 5-oxoproline concentrations were increased in HF animals compared to sham controls, we explored whether this increase could also be found in the plasma of these animals, in hopes of identifying a potential circulating biomarker. In rats with pressure overload–induced HF (REN2) where LV tissue 5-oxoproline was ~20-fold higher than in control rats, circulating 5-oxoproline was also found to be about sixfold higher (Fig. 6, A and B). To determine whether these findings could be extrapolated to the human setting, we measured 5-oxoproline in

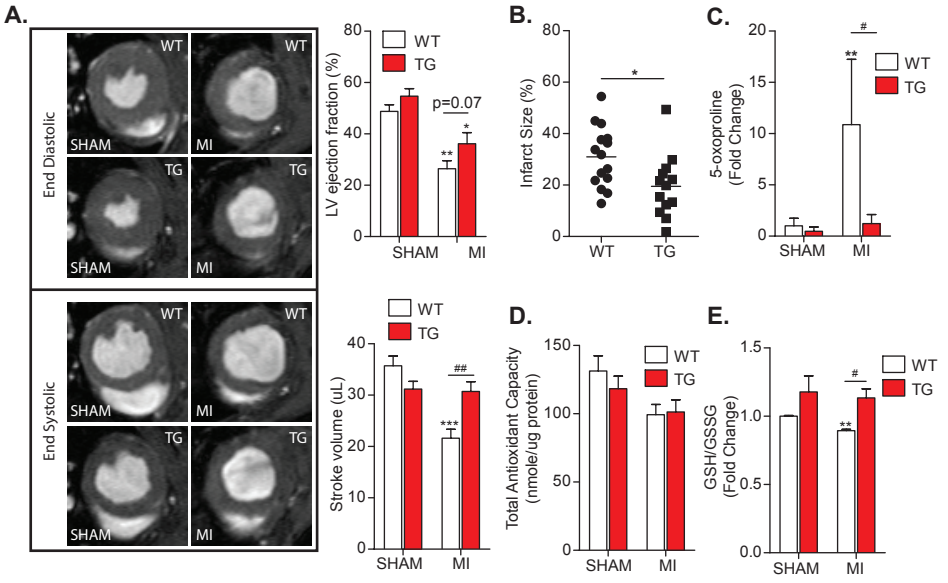


**Fig. 5. OPLAH-TG mice show improved cardiac function after MI.**
**(A)** Representative MRI images of sham and MI hearts of WT and TG mice, and summary of LV ejection fraction and stroke volume (TG sham, n = 6; TG MI, n = 13; WT sham, n=6;WT MI, n=15). **(B)** infarct size (TG MI, n = 13;WT MI, n = 15). **(C)** 5-Oxoproline concentrations (in micromolars per microgram protein) in LV tissue from TG versus WT mice 4 weeks after MI (TG sham, n = 5; TG IR, n = 6;WT sham, n = 5;WT IR, n = 6). **(D)** TAC of LV tissue from TG versus WT mice 4 weeks after MI (n = 3). **(E)** GSH/GSSG ratio present in LV tissue fromTG versus WT mice 4weeks after MI. Data are presented as fold change of microgram GSH/GSSG per microgram protein (n = 3). Data are presented as means ± SEM. * P < 0.05; ** P < 0.01; *** P < 0.001; # P < 0.05; ## P < 0.01, as calculated by Student's t test or one-way ANOVA. "*" indicates significant difference compared to control, whereas "#" denotes differences between groups other than control. n indicates the number of animals.

the plasma of healthy controls (n = 10) and patients with acute HF (n = 10) (24). Plasma 5-oxoproline was increased about fourfold in acute HF patients compared to healthy controls (Fig. 6C).

To further elucidate the potential of 5-oxoproline as a circulating biomarker in clinical HF, we tested the prognostic potential of 5-oxoproline in a cohort of 535 patients who had been hospitalized for acute HF (Table S9) (25). The patients were monitored for 18 months, and the combined primary end point of the study was all-cause mortality and HF hospitalization (26–28). Patients with higher 5-oxoproline had a higher incidence of atrial fibrillation and higher N-terminal pro–brain natriuretic peptide (NT-proBNP) and glutamate (Tables S9 and S10). 5-Oxoproline was associated with known biomarkers for cardiac remodeling, stretch, and oxidative stress, but not with inflammation (Table S11). When looking at the primary end point, we found that higher 5-oxoproline was associated with a worse outcome (Fig. 6D). In multivariable

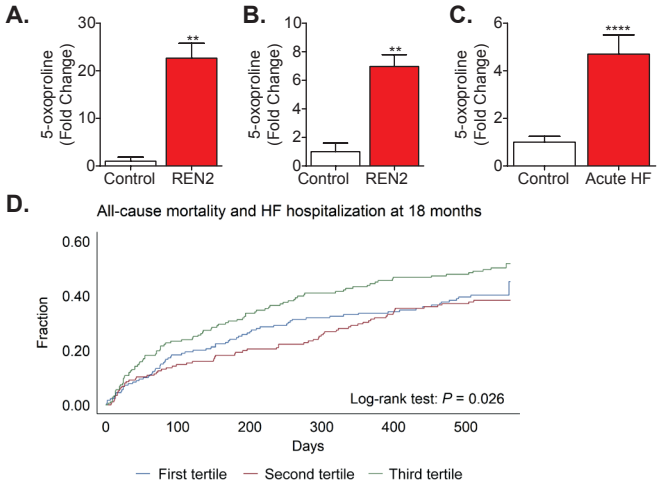


**Fig. 6. Circulating 5-oxoproline in murine and human HF.**
**(A)** 5-Oxoproline concentration in LV tissue of REN2 rats (n = 5) compared to control Sprague Dawley rats (n = 4). **(B)** 5-Oxoproline concentrations in the plasma from control Sprague Dawley rats (n = 4) versus renin overexpression TG Sprague Dawley rats (REN2; n = 5). **(C)** 5-Oxoproline concentration in the human plasma from healthy controls (control; n = 10) and acute HF patients (n = 10). **(D)** Kaplan-Meier plot of all-cause mortality and HF hospitalization at 18 months in COACH HF patients. Patient population is divided into tertiles of plasma 5-oxoproline concentrations (T1, 3.2 to 9.2 mM; T2, 9.3 to 13.2 mM; T3, 13.3 to 35.0 mM). 5-Oxoproline concentrations (in micromolars per microgram protein) are presented as fold change. Data are presented as means ± SEM **P < 0.01; ****P < 0.0001, as calculated by Student's t test. "*" indicates significant difference compared to control. n indicates the number of animals or individual human samples.

analyses corrected for age, sex, renal function, history of atrial fibrillation, and NT-proBNP concentration, the highest tertile of 5-oxoproline remained significantly associated with a higher risk of reaching the primary combined end point compared to risk nadir [hazard ratio (HR), 1.54; 95% confidence interval (CI), 1.09 to 2.17; P = 0.013; Tables S12 and S13] as well as to the lowest two tertiles (HR, 1.42; 95% CI, 1.09 to 1.85; P = 0.009). These data suggest that circulating 5-oxoproline, the substrate of OPLAH, has diagnostic and prognostic potential in patients with HF.

## DISCUSSION

In response to stress, including hypoxia and hypertrophy, cardiac muscle suppresses postnatal gene expression and reactivates fetal genes.This process is mainly characterized by the metabolic switch in energy substrate from fatty acids (postnatal) to carbohydrates (fetal) (2). Using RNA-seq, we identified several known and previously unknown genes involved in this process, which were highly enriched for metabolic (*Hadh* and *MCCC1*) and cardiac disease pathways (*Cacna2d1* and

*Ryr2*). One of the identified genes not previously associated with cardiac disease or development was *Oplah*.We demonstrated that OPLAH has cardioprotective properties and identified 5-oxoproline, the substrate of OPLAH, as a putative oxidative stress HF marker with diagnostic and prognostic potential in the clinical setting.

OPLAH is a gene that encodes for 5-oxoprolinase, an enzyme involved in the γ-glutamyl cycle (5, 6). We identify OPLAH as a novel cardiac gene involved in HF, which is at least, in part, regulated by the PGC-1α/ERRα axis. Both PGC-1α and ERRα are key transcriptional regulators of antioxidant protection genes (23). It has been well established that PGC-1α regulates *ERRα* expression and that the expression of *PGC-1α* is induced in cardiac development and repressed in HF (22, 23). Our data support the interaction between PGC-1α and ERRα by demonstrating that direct inhibition of ERRα activity results in an increase in *PGC-1α* and *ERRα* mRNA, suggesting a compensatory mechanism. Furthermore, the decreased activity of ERRα was shown to reduce OPLAH expression and enhance oxidative stress. These observations are in line with a recent study, which demonstrated by microarray analysis on RNA isolated from ERRα knockout mouse hearts that these mice had significantly increased the expression of *PGC-1α* and reduced *OPLAH* (19).

Here, the consequence of OPLAH depletion in HF is an increase in oxidative stress and 5-oxoproline. Furthermore, exogenous administration of 5-oxoproline to cardiomyocytes also led to increased oxidative stress. This finding is supported by a previous study that identified 5-oxoproline as an inducer of oxidative stress in brain tissue (17, 18). We propose that HF leads to the reduction of PGC-1α, which, as a consequence, results in a decrease in ERRα and antioxidant protection genes, including OPLAH. Because of reduced OPLAH expression, 5-oxoproline cannot be processed into glutamate, and the excessive accumulation of 5-oxoproline leads to increases in oxidative stress, adding further insult to the progression of the disease (Fig. S13). By exposing mice with cardiac-specific OPLAH overexpression to cardiac injury, we demonstrate that these mice have less oxidative stress, lower 5-oxoproline, and reduced fibrosis, resulting in improved cardiac function. Thus, we posit that OPLAH is a potential target for therapeutic intervention in HF.

5-Oxoproline was elevated not only in the myocardium but also in the plasma of animals with HF. This suggests that accumulation of intracellular 5-oxoproline leads to diffusion or active transport of 5-oxoproline out of the cell, a notion supported by the identification of SLC5A8 and SLC16A1 as active transporters of 5-oxoproline in the kidney and brain cells, respectively (29, 30). In HF, circulating 5-oxoproline

was independently associated with patient outcome and associated with known markers for cardiac remodeling, stretch, and oxidative stress, but not with markers for inflammation. These findings, in line with our *in vitro* and *in vivo* work, suggest that 5-oxoproline is an oxidative stress marker with possible diagnostic and prognostic potential. However, it is still uncertain whether the increase in circulating 5-oxoproline in HF is a direct cause of reduced OPLAH in the cardiac tissue or whether 5-oxoproline is also secreted from other organs in response to HF. Besides the heart, OPLAH is also expressed in the kidneys, and hence, cardiac damage leading to renal failure may also result in increased 5-oxoproline production in the kidney. In our experimental setting, we observed that mice overexpressing OPLAH had reduced 5-oxoproline, resulting in an improved cardiac function after cardiac injury. The positive association of increased 5-oxoproline with adverse outcomes in HF patients supports the hypothesis of this study that OPLAH has a cardioprotective effect by reducing 5-oxoproline. However, further work in the human setting is needed to investigate whether reducing 5-oxoproline in patients with HF is beneficial. In addition, the clinical significance of 5-oxoproline as a prognostic biomarker has to be proven in future studies.

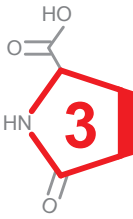


Our translational approach provides insights into the cardiac fetal-like gene program and its role in the failing heart. Here, we characterized *OPLAH*, a novel cardiac gene with protective properties, and its substrate, 5-oxoproline, a putative circulating marker for predicting adverse outcome in patients with HF. Increased efforts in dissecting and modulating the cardiac fetal-like gene program may result in better understanding of genes involved in HF, leading to potential novel diagnostic, prognostic, and therapeutic options in these patients.

## ACKNOWLEDGMENTS

We thank M. Dokter, L. van Genne, and K. van de Kolk for their excellent technical assistance.

# REFERENCES


1. Ponikowski P, Voors AA, Anker SD, Bueno H, Cleland JGF, Coats AJS, Falk V, González-Juanatey JR, Harjola V-P, Jankowska EA, Jessup M, Linde C, Nihoyannopoulos P, Parissis JT, Pieske B, Riley JP, Rosano GMC, Ruilope LM, Ruschitzka F, Rutten FH, Meer P van der, Authors/Task Force Members, Document Reviewers. 2016 ESC Guidelines for the diagnosis and treatment of acute and chronic heart failure. Eur J Heart Fail 2016;18:891–975.
2. Taegtmeyer H, Sen S, Vela D. Return to the fetal gene program: a suggested metabolic link to gene expression in the heart. Ann N Y Acad Sci 2010;1188:191–198.
3. Razeghi P, Young ME, Alcorn JL, Moravec CS, Frazier OH, Taegtmeyer H. Metabolic gene expression in fetal and failing human heart. Circulation 2001;104:2923–2931.
4. Yin Z, Ren J, Guo W. Sarcomeric protein isoform transitions in cardiac muscle: A journey to heart failure. Biochim Biophys Acta - Mol Basis Dis 2015;1852:47–52.
5. Meister A, Anderson ME. Glutathione. Annu Rev Biochem Annual Reviews 4139 El Camino Way, P.O. Box 10139, Palo Alto, CA 94303-0139, USA ; 1983;52:711–760.
6. Liu Y, Hyde AS, Simpson MA, Barycki JJ. Emerging regulatory paradigms in glutathione metabolism. Adv Cancer Res 2014;122:69–101.
7. Sapira V, Cojocaru IM, Socoliuc G, Lilios G, Grigorian M, Craiu E, Cojocaru M. Glutathione reductase levels in patients with unstable angina. Rom J Intern Med = Rev Roum médecine interne 2011;49:197–201.
8. Ruttmann E, Brant LJ, Concin H, Diem G, Rapp K, Ulmer H, Vorarlberg Health Monitoring and Promotion Program Study Group. Gamma-glutamyltransferase as a risk factor for cardiovascular disease mortality: an epidemiological investigation in a cohort of 163,944 Austrian adults. Circulation 2005;112:2130–2137.
9. Adamy C, Mulder P, Khouzami L, Andrieu-abadie N, Defer N, Candiani G, Pavoine C, Caramelle P, Souktani R, Corvoisier P Le, Perier M, Kirsch M, Damy T, Berdeaux A, Levade T, Thuillez C, Hittinger L, Pecker F. Neutral sphingomyelinase inhibition participates to the benefits of N-acetylcysteine treatment in post-myocardial infarction failing heart rats. J Mol Cell Cardiol 2007;43:344–353.
10. Damy T, Kirsch M, Khouzami L, Caramelle P, Corvoisier P Le, Roudot-Thoraval F, Dubois-Randé J-L, Hittinger L, Pavoine C, Pecker F. Glutathione deficiency in cardiac patients is related to the functional status and structural cardiac abnormalities. PLoS One 2009;4:e4871.
11. Watanabe Y, Watanabe K, Kobayashi T, Saito Y, Fujioka D, Nakamura T, Obata J, Kawabata K, Mishina H, Kugiyama K. Chronic depletion of glutathione exacerbates ventricular remodelling and dysfunction in the pressure-overloaded heart. Cardiovasc Res 2013;97:282–292.
12. Forgione MA, Cap A, Liao R, Moldovan NI, Eberhardt RT, Lim CC, Jones J, Goldschmidt-Clermont PJ, Loscalzo J. Heterozygous cellular glutathione peroxidase deficiency in the mouse: abnormalities in vascular and cardiac function and structure. Circulation 2002;106:1154–1158.
13. Taur Y, Frishman WH. The cardiac ryanodine receptor (RyR2) and its role in heart disease. Cardiol Rev 2005;13:142–146.
14. Antzelevitch C, Pollevick GD, Cordeiro JM, Casis O, Sanguinetti MC, Aizawa Y, Guerchicoff A, Pfeiffer R, Oliva A, Wollnik B, Gelber P, Bonaros EP, Burashnikov E, Wu Y, Sargent JD, Schickel S, Oberheiden R, Bhatia A, Hsu L-F, Haïssaguerre M, Schimpf R, Borggrefe M, Wolpert C. Loss-of-function mutations in the cardiac calcium channel underlie a new clinical entity characterized by ST-segment elevation, short QT intervals, and sudden cardiac death. Circulation 2007;115:442–449.
15. El-Armouche A, Ouchi N, Tanaka K, Doros G, Wittköpper K, Schulze T, Eschenhagen T, Walsh K, Sam F. Follistatin-like 1 in chronic systolic heart failure: a marker of left ventricular remodeling. Circ Heart Fail 2011;4:621–627.
16. Villar A V, García R, Llano M, Cobo M, Merino D, Lantero A, Tramullas M, Hurlé JM, Hurlé MA, Nistal JF. BAMBI (BMP and activin membrane-bound inhibitor) protects the murine heart from pressure-overload biomechanical stress by restraining TGF-β signaling. Biochim Biophys Acta 2013;1832:323–335.
17. Pederzolli CD, Sgaravatti AM, Braum CA, Prestes CC, Zorzi GK, Sgarbi MB, Wyse ATS, Wannmacher CMD, Wajner M, Dutra-Filho CS. 5-Oxoproline reduces non-enzymatic antioxidant defenses in vitro in rat brain. Metab Brain Dis 2007;22:51–65.
18. Pederzolli CD, Mescka CP, Zandoná BR, Moura Coelho D de, Sgaravatti AM, Sgarbi MB, Souza Wyse AT de, Duval Wannmacher CM, Wajner M, Vargas CR, Dutra-Filho CS. Acute administration

of 5-oxoproline induces oxidative damage to lipids and proteins and impairs antioxidant defenses in cerebral cortex and cerebellum of young rats. Metab Brain Dis 2010;25:145–154.
19. Dufour CR, Wilson BJ, Huss JM, Kelly DP, Alaynick WA, Downes M, Evans RM, Blanchette M, Giguère V. Genome-wide orchestration of cardiac functions by the orphan nuclear receptors ERRalpha and gamma. Cell Metab 2007;5:345–356.
20. Cunningham KF, Beeson GC, Beeson CC, Baicu CF, Zile MR, McDermott PJ. Estrogen-Related Receptor α (ERRα) is required for adaptive increases in PGC-1 isoform expression during electrically stimulated contraction of adult cardiomyocytes in sustained hypoxic conditions. Int J Cardiol 2015;187:393–400.
21. Coward P, Lee D, Hull M V, Lehmann JM. 4-Hydroxytamoxifen binds to and deactivates the estrogen-related receptor gamma. Proc Natl Acad Sci U S A National Academy of Sciences; 2001;98:8880–8884.
22. Rowe GC, Jiang A, Arany Z. PGC-1 coactivators in cardiac development and disease. Circ Res NIH Public Access; 2010;107:825–838.
23. Huss JM, Torra IP, Staels B, Giguere V, Kelly DP. Estrogen-Related Receptor Directs Peroxisome Proliferator-Activated Receptor Signaling in the Transcriptional Control of Energy Metabolism in Cardiac and Skeletal Muscle. Mol Cell Biol 2004;24:9079–9091.
24. Demissei BG, Valente MAE, Cleland JG, O'Connor CM, Metra M, Ponikowski P, Teerlink JR, Cotter G, Davison B, Givertz MM, Bloomfield DM, Dittrich H, Meer P van der, Veldhuisen DJ van, Hillege HL, Voors AA. Optimizing clinical use of biomarkers in high-risk acute heart failure patients. Eur J Heart Fail 2016;18:269–280.
25. Tromp J, Pol A van der, Klip IJT, Boer RA de, Jaarsma T, Gilst WH van, Voors AA, Veldhuisen DJ van, Meer P van der. Fibrosis marker syndecan-1 and outcome in patients with heart failure with reduced and preserved ejection fraction. Circ Heart Fail Lippincott Williams & Wilkins; 2014;7:457–462.
26. Jaarsma T, Wal MHL Van Der, Hogenhuis J, Lesman I, Luttik M-LA, Veeger NJGM, Veldhuisen DJ Van. Design and methodology of the COACH study: a multicenter randomised Coordinating study evaluating Outcomes of Advising and Counselling in Heart failure. Eur J Heart Fail 2004;6:227–233.
27. Jaarsma T, Wal MHL van der, Lesman-Leegte I, Luttik M-L, Hogenhuis J, Veeger NJ, Sanderman R, Hoes AW, Gilst WH van, Lok DJA, Dunselman PHJM, Tijssen JGP, Hillege HL, Veldhuisen DJ van, Coordinating Study Evaluating Outcomes of Advising and Counseling in Heart Failure (COACH) Investigators. Effect of moderate or intensive disease management program on outcome in patients with heart failure: Coordinating Study Evaluating Outcomes of Advising and Counseling in Heart Failure (COACH). Arch Intern Med 2008;168:316–324.
28. Veldhuisen DJ van, Linssen GCM, Jaarsma T, Gilst WH van, Hoes AW, Tijssen JGP, Paulus WJ, Voors AA, Hillege HL. B-type natriuretic peptide and prognosis in heart failure patients with preserved and reduced ejection fraction. J Am Coll Cardiol 2013;61:1498–1506.
29. Sasaki S, Futagi Y, Kobayashi M, Ogura J, Iseki K. Functional characterization of 5-oxoproline transport via SLC16A1/MCT1. J Biol Chem American Society for Biochemistry and Molecular Biology; 2015;290:2303–2311.
30. Miyauchi S, Gopal E, Babu E, Srinivas SR, Kubo Y, Umapathy NS, Thakkar S V., Ganapathy V, Prasad PD. Sodium-coupled electrogenic transport of pyroglutamate (5-oxoproline) via SLC5A8, a monocarboxylate transporter. Biochim Biophys Acta - Biomembr 2010;1798:1164–1171.
31. Dobin A, Davis CA, Schlesinger F, Drenkow J, Zaleski C, Jha S, Batut P, Chaisson M, Gingeras TR. STAR: ultrafast universal RNA-seq aligner. Bioinformatics 2013;29:15–21.
32. Anders S, Pyl PT, Huber W. HTSeq--a Python framework to work with high-throughput sequencing data. Bioinformatics 2015;31:166–169.
33. Robinson MD, McCarthy DJ, Smyth GK. edgeR: a Bioconductor package for differential expression analysis of digital gene expression data. Bioinformatics 2010;26:139–140.
34. Lu B, Tigchelaar W, Ruifrok WPT, Gilst WH van, Boer RA de, Silljé HHW. DHRS7c, a novel cardiomyocyte-expressed gene that is down-regulated by adrenergic stimulation and in heart failure. Eur J Heart Fail 2012;14:5–13.
35. Ruifrok W-PT, Qian C, Silljé HHW, Goor H van, Veldhuisen DJ van, Gilst WH van, Boer RA de. Heart failure-associated anemia: bone marrow dysfunction and response to erythropoietin. J Mol Med (Berl) 2011;89:377–387.
36. Cannon M V, Silljé HHW, Sijbesma JWA, Vreeswijk-Baudoin I, Ciapaite J, Sluis B van der, Deursen J van, Silva GJJ, Windt LJ de, Gustafsson J-Å, Harst P van der, Gilst WH van, Boer RA de. Cardiac LXRα protects against pathological cardiac hypertrophy and dysfunction by enhancing glucose

uptake and utilization. EMBO Mol Med Wiley-Blackwell; 2015;7:1229–1243.
37. Booij HG, Yu H, Boer RA De, Kolk CWA van de, Sluis B van de, Deursen JM Van, Gilst WH Van, Silljé HHW, Westenbrink BD. Overexpression of A kinase interacting protein 1 attenuates myocardial ischaemia/reperfusion injury but does not influence heart failure development. Cardiovasc Res 2016;111.
38. Meems LMG, Cannon M V., Mahmud H, Voors AA, Gilst WH van, Silljé HHW, Ruifrok WPT, Boer RA de. The vitamin D receptor activator paricalcitol prevents fibrosis and diastolic dysfunction in a murine model of pressure overload. J Steroid Biochem Mol Biol 2012;132:282–289.
39. Schindelin J, Arganda-Carreras I, Frise E, Kaynig V, Longair M, Pietzsch T, Preibisch S, Rueden C, Saalfeld S, Schmid B, Tinevez J-Y, White DJ, Hartenstein V, Eliceiri K, Tomancak P, Cardona A. Fiji: an open-source platform for biological-image analysis. Nat Methods 2012;9:676–682.
40. Eckstein JA, Ammerman GM, Reveles JM, Ackermann BL. Analysis of glutamine, glutamate, pyroglutamate, and GABA in cerebrospinal fluid using ion pairing HPLC with positive electrospray LC/MS/MS. J Neurosci Methods 2008;171:190–196.
41. European Medicines Agency (EMA) - Committee for Medicinal Products for Human Use. Guideline on bioanalytical method validation. London, UK; 2012.
42. US Department of Health and Human Services, Food and Drug Administration - Center for Drug Evaluation and Research C for VM. Guidance for Industry: Bioanalytical Method Validation. Rockville, MD, USA.; 2001.
43. Snijder PM, Boer RA de, Bos EM, Born JC van den, Ruifrok W-PT, Vreeswijk-Baudoin I, Dijk MCRF van, Hillebrands J-L, Leuvenink HGD, Goor H van. Gaseous Hydrogen Sulfide Protects against Myocardial Ischemia-Reperfusion Injury in Mice Partially Independent from Hypometabolism. Salloum FN, ed. PLoS One 2013;8:e63291.
44. Hartman MHT, Vreeswijk-Baudoin I, Groot HE, Kolk KWA van de, Boer RA de, Mateo Leach I, Vliegenthart R, Sillje HHW, Harst P van der. Inhibition of Interleukin-6 Receptor in a Murine Model of Myocardial Ischemia-Reperfusion. González GE, ed. PLoS One 2016;11:e0167195.

# Supplementary Materials

*Supplementary Material and Methods*

**Reagents**

XCT-790 (X4753, Sigma-Aldrich), 4-hydroxytamoxifen (H7904, Sigma-Aldrich), 5-oxoproline (83160, Sigma-Aldrich), $^{13}$C-labeled L-glutamic acid (607851, Sigma-Aldrich), human organ panel (Human Total RNA Master Panel II, Clontech, Cat. No. 636643).

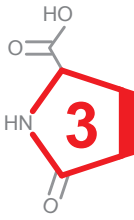


**Cell culture**

Human embryonic stem cell-line HUES9 (Harvard University Embryonic Stem cells, line 9) were obtained from Harvard Stem Cell Institute. The HUES9 human embryonic stem cells (hESC) were cultured on Geltrex coated dishes in Essential 8 medium (E8). Medium of hESC was refreshed daily till cultures reached 85% confluency. At this stage (day 0) cardiac differentiation was induced by replacing E8 medium for RPMI1640/B27 (minus insulin) medium supplemented with 6 μM CHIR99021 (Cayman Chemical). At day 2 of differentiation, the medium was refreshed with RPMI1640/B27 (minus insulin) medium supplemented with Wnt-C59 (R&D Systems). At day 4, medium was replaced with CDM3 medium. Medium was refreshed every other day. Spontaneously contracting cardiomyocytes were observed at day 8. To purify the cardiomyocyte population, medium was replaced for CDM3 medium in which glucose was replaced with lactate at day 12 for 8 days. After purification, stem cell-derived cardiomyocytes were cultured in CDM3 medium containing glucose until experiments were performed.

Neonatal rat ventricle cardiomyocytes (NRVCs) were isolated from the cardiac ventricles of 1- to 3-day-old Sprague-Dawley (SD) pups after decapitation. NRVCs and H9C2 (ATCC, CRL-1446) cells were cultured at 37°C under 5% CO2 in DMEM, supplemented with 10% FCS and 1% penicillin-streptomycin.

Rat aortic smooth muscle cells (R-ASM-580, Lonza) were cultures per manufactures instructions. Mouse Endothelioma cells were cultured on gelatin coated dishes in DMEM medium supplemented with FCS (heat inactivated), Pen/Strep, Glutamine, and sodium pyruvate.

For experiments in which cells were exposed to hypoxia, $H_2O_2$, stretch (1 Hz and 15% elongation), ISO (50 μM), PE (10 μM), XCT-790, 4-hydroxtamoxifen or 5-oxoproline (10 μM), the cells were first starved with serum free media for 24 hrs.

**Subcellular Fractionation**

Cultured NRVCs were lysed in isolation buffer [70 mM sucrose, 190 mM mannitol, 20 mM HEPES, 0.2 mM EDTA, protease inhibitor cocktail (Roche), phosphatase inhibitor cocktail (Sigma-Aldrich), 1 μM sodium orthovanadate, 1 mM PMSF] followed by homogenization with a glass Counde mortar. The homogenate was centrifuged at increasing speeds to separate enriched subcellular fractions. Briefly, 100 μl of the sample was kept as total cell extract, the remainder was centrifuged at 600xg for 10 min at 4$^{o}$C. The pellet produced contained the nuclear fraction and the IF fraction (myofibrils). Supernatant (containing the mitochondrial, ER/membranous, and cytosolic fractions) was transferred to a fresh tube. To separate the nuclear and IF fraction, the pellet was washed with isolation buffer and centrifuged at 600xg for 10 min at 4$^{o}$C. Washing step was repeated twice. Pellet was then resuspended in nuclear extraction buffer (20 mM HEPES, 25% Glycerol, 420 mM NaCl, 1.5 mM $MgCl_2$, and 0.2mM EDTA in $dH_2O$), incubated for 5 min on ice and centrifuged at 600xg for 10 min at 4$^{o}$C. Supernatant contained the nuclear fraction, remaining pellet was washed twice with isolation buffer, and after final centrifugation (600xg for 10 min at 4$^{o}$C), supernatant was discarded. Pellet (containing IF fraction) was resuspended in RIPA buffer with 1% SDS. To separate the mitochondrial fraction from the ER/membranous and cytosolic fractions, supernatant was centrifuged at 5000xg for 15 min at 4$^{o}$C. At this stage the pellet contains the mitochondrial fraction and the supernatant the ER/membranous and cytosolic fractions. The pellet was washed twice with isolation buffer. After final centrifugation supernatant was discarded and pellet resuspended in RIPA buffer with 0.1% SDS. Cytosolic fraction was separated from the ER/membranous fraction by centrifugation at 100,000xg for 1 hr at 4$^{o}$C. Supernatant contained the cytosolic fraction and the remaining pellet contained the ER/membranous fraction. ER/membranous fraction containing pellet was washed twice, and following final centrifugation step resuspended in RIPA buffer with 0.1% SDS. Protein concentrations were measured and processed for western blot.

***In vitro* oxidative stress**

Cells were cultured under hypoxic conditions for 24 hrs, utilizing the BD GasPak EZ Anaerobe Pouch System (per manufactures guidelines). Cells were cultured in medium containing 0-2 mM of $H_2O_2$ for up to 12 hrs. After the cells were incubated with the different culturing conditions oxidative stress was measured (CellROX), RNA or protein was isolated.

**Oxygen saturation and pH measurements**

Measurements for pH, $PCO_2$, $PO_2$, and $sO_2$ within the media of anoxic cultured cells were made using a portable blood gas analyzer (iSTAT Corp). Cultures were taken out of the sealed bag, and the medium sample was transferred to the microchips, quickly sealed and immediately read.

**Cardiomyocyte apoptosis staining**

Apoptosis as a result of experiments in NRVCs was measured by counting the trypan blue positive cells.

**LDH measurements in culture medium**

LDH concentrations in culture medium were determined using an UV assay LDH kit (11822837, Roche Diagnostics).


**CellROX:**

Oxidative stress was measured by means of CellROX Orange Reagent (Thermo Fisher Scientific) per manufacturer's instructions. Briefly, cells were cultured in black clear-bottom 96-well plates. A day before preforming the assay, cells were switched from 10% FCS medium to serum free medium. 2 hours prior to performing the CellROX assay, medium was refreshed with phenol red-free medium without FCS. At the time of the experiment, 25 µL CellROX mix (25 µl phenol red-free medium, 1:250 CellROX Orange Reagent, and 1:50 HEPES) was added to each well. Plates were measured using the Synergy H1 Multi-Mode Reader with Ex/Em of 540/570 nm once every minute for 2 hours. Values are displayed as Area under the curve (A.U.) corrected for microgram protein. To measure oxidative stress in stretched NRVCs, control and stretched NRVCs were loaded with 5 µM CellROX Orange in culture medium and stained in the dark for 30 min at 37°C. Stained cells were washed once with PBS, dissociated with TrypLE and suspended in PBS. Cells were centrifuged for 5 minutes at 2000x g and resuspended in 600 µl of PBS. 100 µl of cell suspension were transferred to a black 96 well plate and analyzed immediately using the Synergy H1 Multi-Mode Reader with Ex/Em of 540/570 nm. The signal intensity was corrected for the amount of cells as counted manually with a Fuchs-Rosenthal hemocytometer.

**Total Antioxidant Capacity**

The antioxidant capacity of tissue samples was measured by means of the Total Antioxidant Capacity Assay kit (ab65329, Abcam) per manufactures instructions. Briefly, snap frozen LV tissue was homogenized in ice-cold RIPA (50 mM Tris pH 8.0, 1% nonidet P40, 0.5% deoxycholate, 0.1% SDS, 150 mM NaCl), followed by centrifugation at 12,000 rcf for 10 min at 4°C. Supernatant was collected and assayed.

**GSH/GSSG measurements**

Snap frozen LV tissue was homogenized in 100 uL ice cold Glutathione Assay Buffer. 60 uL of the homogenate was stabilized by addition of 20 uL PCA (Perchloric Acid, 6N). The remaining 40 uL was used for protein quantification. The PCA stabilized samples were centrifuged 13,000 rcf for 2 min at 4°C, and the glutathione containing

supernatant was collected and assayed.

**Quantitative real time PCR:**
Total RNA from cells and tissues were isolated by the TRIzol RNA isolation protocol. QuantiTect RT kit (Qiagen) was then used to make cDNA from the RNA samples, following manufacturer's instructions.

Relative gene expression was determined by quantitative real-time PCR (qRT-PCR) on a BioRad CFX384 real time system using ABsolute QPCR SYBR Green mix (Thermo Fisher Scientific). Gene expression was determined by correcting for reference gene values (36B4), and the calculated values were expressed relative to the control group per experiment.

**Western Blotting:**
Cells and tissues were homogenized in ice-cold RIPA (50 mM Tris pH 8.0, 1% nonidet P40, 0.5% deoxycholate, 0.1% SDS, 150 mM NaCl) containing phosphatase inhibitor cocktail 3 (Sigma-Aldrich), protease inhibitor (Roche Diagnostics), 1 mM phenylmethylsulfonyl fluoride (PMSF; Roche Diagnostics), and 15 mM NaVanadate. Protein concentrations were determined with a DC protein assay kit (Bio-Rad).

Equal amounts of protein were loaded on 10% polycrylamide gels. After electrophoresis, the gels were blotted onto PVDF membranes. Membranes were then incubated overnight at 4$^{o}$C with the primary antibody, followed by 1h incubation at room temperature with secondary antibody. Detection was performed by ECL and analyzed with densitometry (ImageQuant LAS4000; GE Healthcare Europe).

**Rodent models of heart failure**
Permanent MI was performed by means of ligation of the LAD of the left coronary artery. MI induction in rats (permit number: DEC6176) was performed on 10 week old male SD rats obtained from Harlan. Three SD rats underwent surgical induction of MI (MI group), and three SD rats underwent the same procedure without the ligation of the left coronary artery (sham group). For MI induction in mice (permit number: DEC1583-2), a total of 54 mice, 26 TG and 26 WT littermates, were included in the permanent MI study. All mice were 14-20 weeks of age and 35-40 g of body weight. Both TG and WT mice were randomized into the sham operated group (n = 6) and the MI group (n = 20). The animals were followed for 10 weeks (rats) or 4 weeks (mice).

IR injury model in C57BL/6 mice (permit number: DEC6603) was performed by ligation of the LAD of the left coronary artery for 45 min, followed by reperfusion for 4 weeks. Mice were obtained from Harlan and upon initiation of the experiment the

average weight of the animals was 25g. Five mice were included in the IR injury group and three mice underwent the same procedure without the induction of IR (sham group). For the induction of IR injury in the OPLAH overexpression mice, a total of 89 mice, 38 TG and 51 WT littermates, were included (permit number: DEC6632). All mice were 14-20 weeks of age and 35-40 g of body weight. Both TG and WT mice were randomized into two groups, the sham operated group and the IR group. The IR group (WT n = 25, TG n = 24) underwent ligation of the LAD of the left coronary artery for 60 min, followed by reperfusion for 4 weeks. The sham operated group (WT n = 26, TG n = 14) underwent the same procedure without induction of ischemia.

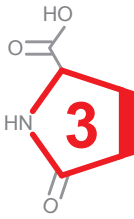


Prior to sacrifice an echocardiogram (rats) or cardiac MRI (mice) was performed, followed by hemodynamic measurements. At sacrifice, blood was collected and organs were weighted and collected for histology and molecular analysis. Animals were excluded from the studies based on the following criteria: death due to procedures (MI or IR induction, MRI, or hemodynamic measurements).

**Cardiac MRI measurements**

Mice were anesthetized with isoflurane (2%) and imaged in a vertical 9.4-T, 89-mm bore size magnet equipped with 1500 mT/m gradients and connected to an advanced 400 MR system (Bruker Biospin) using a quadrature-driven birdcage coil with an inner diameter of 3 cm.

Respiration and ECG were monitored by ECG Trigger Unit (RAPID biomedical GmBH). Heart rate was maintained between 400-600 bpm and respiration rate between 20-60 breaths per minute. ParaVison 4.0 and IntraGate software (Bruker Biospin GmH) were used for cine MR acquisition and reconstruction. After orthogonal scout imaging, short axis (oriented perpendicular to the septum) cardiac cine MR images were acquired. To cover the entire heart from apex to base, 7 slices (sham) and 8-9 slices (IR) were needed. The images were reconstructed and for all mice, dedicated, semi-automatic contour detection software (QMass, version MR 6.1.5, Medis Medical Imaging Systems) was used for the determination of the LV end-diastolic volume, LV end-systolic volume, stroke volume, and ejection fraction. The investigators were blinded to experimental settings during data analysis.

**Hemodynamic measurements**

For mice a 1.2 French electrode with 4.5 spacing (Transonic Scisense Inc) and for rats a 1.4 French electrode (Millar Instr. Inc.) was used. Analyses were performed offline with LabChart7 software (version 7.2, ADinstruments). After hemodynamic measurements, mice and rats were sacrificed by excision of the heart and tissues and tibia were collected. The investigators were blinded to experimental settings

during data analysis.

**Histology**

Masson's trichrome straining was performed to analyze collagen deposition. To quantify fibrosis, whole ventricle slice pictures were photographed using a Hamamatsu microscope, and fibrotic area was determined with Aperio's ImageScope software. Areas of fibrosis were calculated as percentages of total area of the left ventricle. To quantify the infarct size, area of infarct were calculated as percentages of total area of the left ventricle. For cardiomyocyte size, FITC-labeled wheat germ agglutinin (WGA) staining was performed. For quantification Fiji (47) was used, briefly five randomly selected fields from whole-stained WGA-FITC LV sections imaged ad 20x magnification were used to measure cross-sectional diameter from approximately 30 cells per mouse heart, and calculated as area. To quantify the amount of apoptotic cells, cleaved Caspase-3 staining was performed. Whole ventricle slice pictures were photographed using a Hamamatsu microscope, positive cleaved Caspase-3 and negative nuclei were counted using Fiji (47). Briefly 10-20 randomly selected fields from the whole-stained LV cross-section imaged at 20x magnification were used for counting positive cleaved Caspase-3 and negative nuclei.

**Internal standard preparation ($^{13}$C-5-oxoproline and L-glutamic acid) and validation of the analytical method:**

5-Oxoproline internal standard (IS) was prepared from $^{13}$C-labeled L-glutamic acid. 250 mg L-glutamic acid were dissolved in 0.1N HCl and heated at 80$^{o}$C for 72hrs, to convert $^{13}$C-L-glutamic acid into $^{13}$C-5-oxoproline, as previously described (48). The solution was placed under a nitrogen gas stream to remove the HCl and the product re-dissolved in 50 mL water. This method resulted in a mixed internal standard of $^{13}$C-5-oxoproline and $^{13}$C-L-glutamic acid.

For validation purposes 5-oxoproline and L-glutamic acid (primary standards) were weighed, dissolved in PBS containing 2% BSA and mixed to obtain a single stock solution with a concentration of 200 µM per analyte. The stock solution was diluted with PBS containing 2% BSA to obtain ten calibration points with concentrations of the analytes ranging from 0.12 to 200 µM. These calibration points were subjected to the same sample preparation procedure as for plasma samples (see next section). After the extraction procedure, 10 calibration points were obtained with final concentrations ranging from 0.03 to 50 µM. Calibration curves were constructed based on the peak area ratios of unlabeled metabolites to their corresponding $^{13}$C-labeled standards.

Following international guidelines, method validation was performed by evaluating the following parameters: intra-day variability (repeatability), inter-day variability (intermediate precision), lower limit of quantification (LLOQ), linearity and accuracy.

Repeatability was assessed by testing 3 independently prepared plasma samples that were extracted and measured 3 times in one batch. Three calibration curves were prepared and measured on three different days to assess intermediate precision and accuracy. The lower limit of quantification (LLOQ) was set to the lowest point on the calibration curve where the analyte responses were at least 5-times higher than a blank and where the coefficient of variation (CV) was less than 20% (Fig. S8, Tables S17-S18).

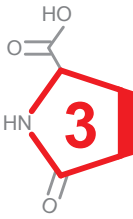


**LC-MS of 5-oxoproline and L-glutamic acid:**

5-Oxoproline and L-glutamic acid were separated in the HILIC mode using a Luna NH2 column (3 µm, 100 × 2 mm; Phenomenex) on an Agilent 1290 Infinity LC system. Mobile phases consisted of a mixture of 5 mM ammonium acetate and 0.1% ammonium hydroxide in water (eluent A) and acetonitrile (eluent B). Linear gradient elution went from 30% eluent A to 99% eluent A in 8 min, followed by isocratic elution at 99% eluent A until 14 min. A conditioning cycle of 6 min with the initial proportions of eluents A and B was performed prior to the next analysis. The column temperature was set at 25°C, the flow rate was 0.25 mL/min, and the injection volume per sample was 10 µL.

Mass spectrometry (MS) detection was performed using an Agilent 6410 triple quadrupole system. The analytes were detected by positive electrospray ionization (ESI+) in the Multiple Reaction Monitoring (MRM) mode. The optimized MS source parameters were as following: ionspray voltage: +1500V, drying gas flow ($N_2$): 6 L/min, drying gas temperature 300°C, and nebulizer pressure: 15 psi. To obtain adequate selectivity and sensitivity, the mass spectrometer was set to unit resolution and the electron multiplier was set to 400 V. The run was divided into two segments looking for the MS/MS transitions 130/84 for 5-oxoproline, 135/88 for $^{13}$C-labeled 5-oxoproline (internal standard), 148/84 for L-glutamic acid and 153/88 for $^{13}$C-labeled L-glutamic acid (internal standard). The fragmentor and collision energy were optimized to 100 V and 9 V for 5-oxoproline; and 75 V and 13 V for L-glutamic acid, respectively. The dwell time for each transition was 100 ms. Separation (UPLC) and detection (MS) systems were controlled by Agilent MassHunter Workstation software.

*Supplementary Figures*

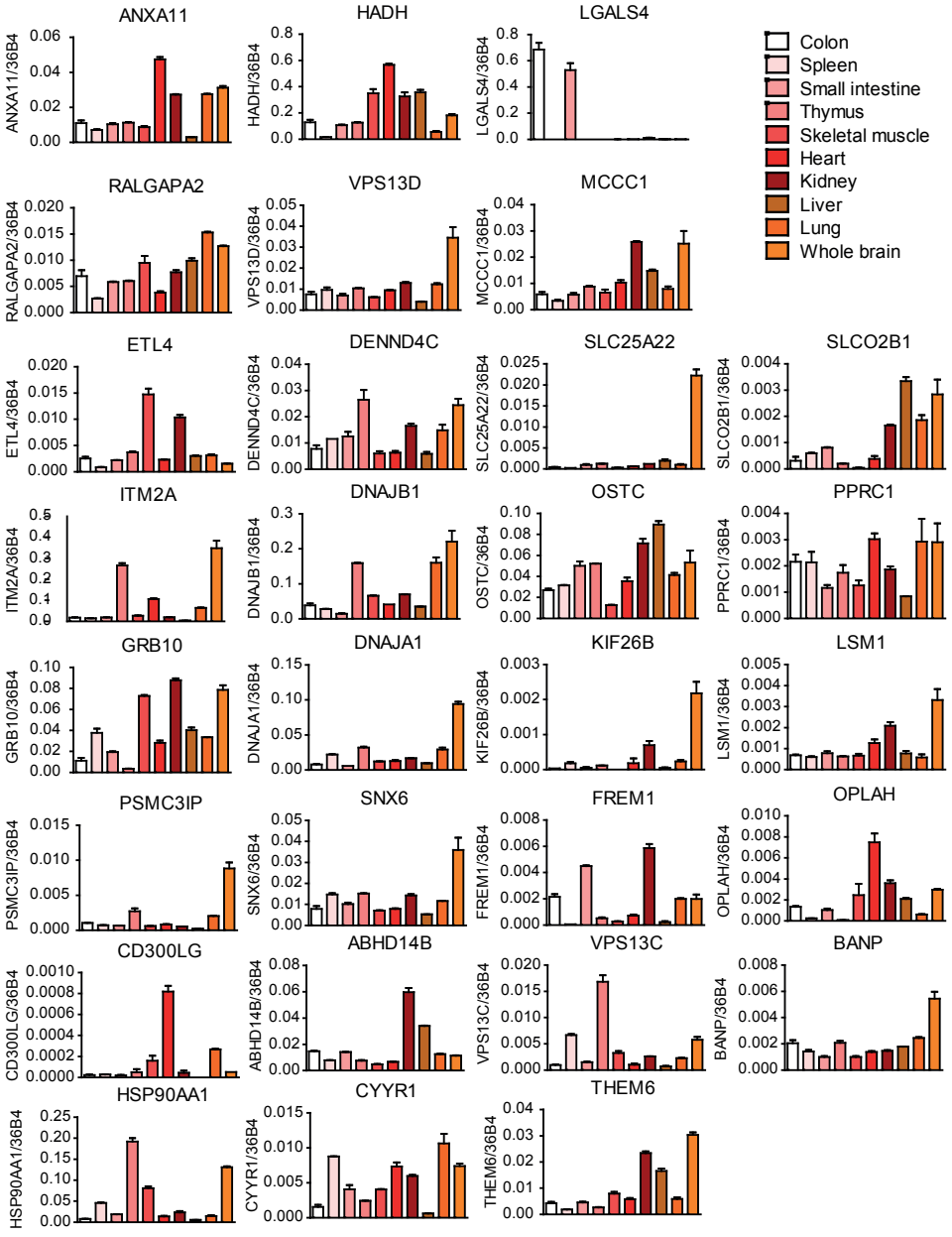


**Fig. S1. Top 29 novel cardiac fetal genes mRNA expression profiles across a human organ panel.** All data is represented as gene expression relative to 36B4.

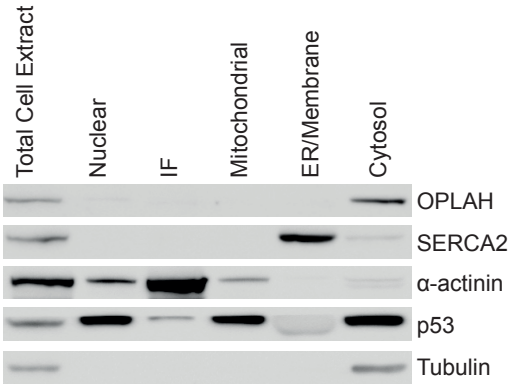


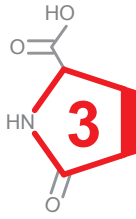


**Fig. S2. OPLAH is localized in the cytosol of cardiomyocytes.**
Cultured NRVCs were utilized for cellular fractionation. SERCA2 was used as marker for the ER/Membrane fraction, α-actinin for the myofibril fraction, p53 for the nuclear fraction (since p53 is a shuttle protein, it was also detected in the mitochondrial and cytoplasmic fraction), Tubulin for the cytoplasmic fraction, and EXOG for the mitochondrial fraction. Two additional cellular fractionation experiments confirmed these results.

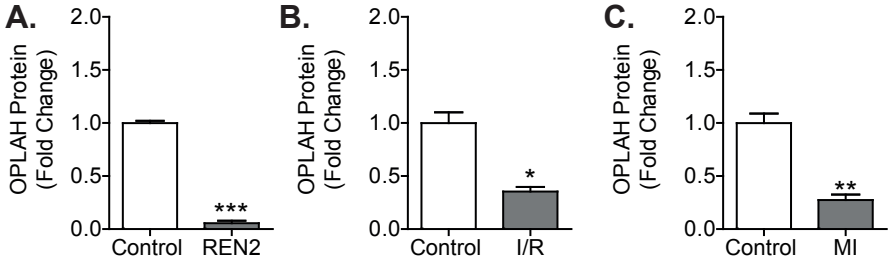


**Fig. S3. OPLAH protein expression in HF animal models.**
**A.** Quantified OPLAH expression in Sprague Dawley rats (control, n = 4) versus Renin over-expression transgenic Sprague Dawley rats (REN2, n = 5). **B.** Quantified OPLAH expression in sham (Control, n = 3) versus ischemia/reperfusion (IR, n = 5) C57BL/6 mice. **C.** Quantified OPLAH expression in sham (Control, n = 3) versus myocardial infarction (MI, n = 3) Sprague Dawley rats. Data are presented as means ± SEM *, P < 0.05; **, P < 0.01; ***, P < 0.001, as calculated by Student's t test. "*" indicates significant difference compared to control. n indicates the number of animals.

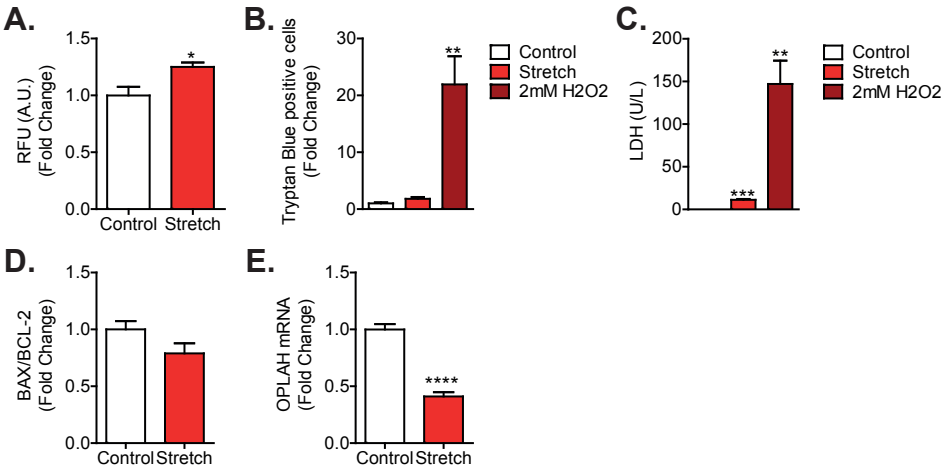


**Fig. S4. Mechanical stretch results in oxidative stress and OPLAH depletion in NRVCs.**
**A.** CellROX analysis of NRVCs exposed to 24 hourse of stretch (n = 24) **B.** Trypan blue positive NRVCs following 24 hours of stretch (n = 4), as a positive control NRVCs were stimulated with 2 mM $H_2O_2$ (n = 2). **C.** LDH measurement of NRVCs exposed to 24 hours of stretch (n = 6), as a positive control NRVCs were stimulated with 2 mM $H_2O_2$ (n = 3). **D.** The ratio of BAX and BCL-2 expression in NRVCs exposed to 24 hours of stretch (Control n = 6, Stretch n = 16). **E.** OPLAH mRNA in NRVCs exposed to 24 hours of stretch (Control n = 6, Stretch n = 16). CellROX data are presented as fold change of RFU (A.U.) per microgram protein. Data are presented as means ± SEM *, $P < 0.05$; **, $P < 0.01$; ***, $P < 0.001$; ****, $P < 0.0001$, as calculated by a Student's t test. "*" indicates significant difference compared to control. n indicates the number of biological replicates of cell experiments.

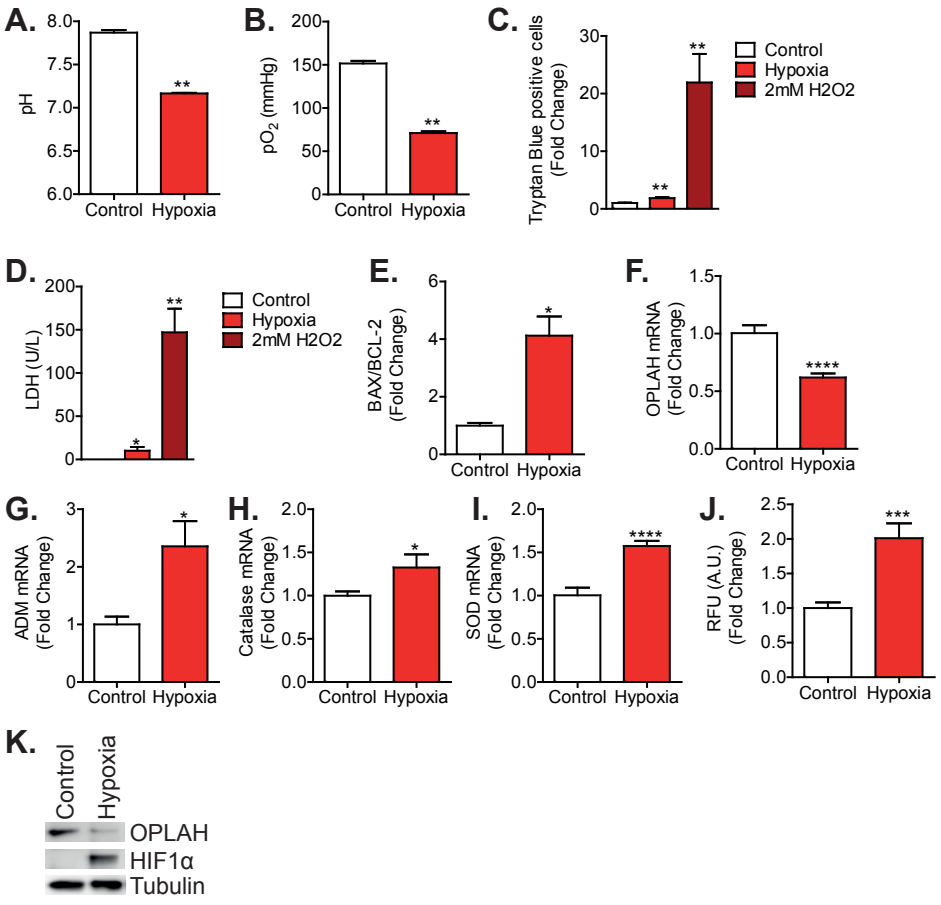


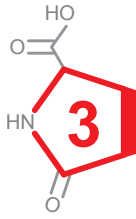


**Fig. S5. Hypoxia induces oxidative stress and OPLAH depletion in NRVCs.**
NRVCs exposed to 24 hours of hypoxia compared to controls. **A.** pH measurements of culture media (hypoxia n = 8, controls n = 4). **B.** $PO_2$ measurements of culture media (hypoxia n = 8, controls n = 4). **C.** Trytan blue positive cells (hypoxia n = 8, controls n = 4), NRVCs exposed to 2 mM $H_2O_2$ were used as positive control (n = 2) **D.** LDH release measured in culture medium (hypoxia n = 8, controls n = 4), NRVCs exposed to 2 mM $H_2O_2$ were used as positive control (n = 3). **E.** The ratio of BAX and BCL-2 expression (hypoxia n = 14, controls n = 8). **F.** OPLAH mRNA expression (hypoxia n = 32, controls n = 30). **G.** ADM mRNA expression (hypoxia n = 16, controls n = 15). **H.** Catalase mRNA expression (hypoxia n = 32, controls n = 30). **I.** SOD mRNA expression (hypoxia n = 32, controls n = 30). **J.** CellROX analysis (hypoxia n = 16, controls n = 8). **K.** Representative immunoblot of NRVCs exposed to 24hrs of hypoxic culturing conditions. CellROX data are presented as fold change of RFU (A.U.) per microgram protein. Data are presented as means ± SEM *, $P < 0.05$; **, $P < 0.01$; ***, $P < 0.001$; ****, $P < 0.0001$, as calculated by Student's t test. "*" indicates significant difference compared to control. n indicates the number of biological replicates of cell experiments.

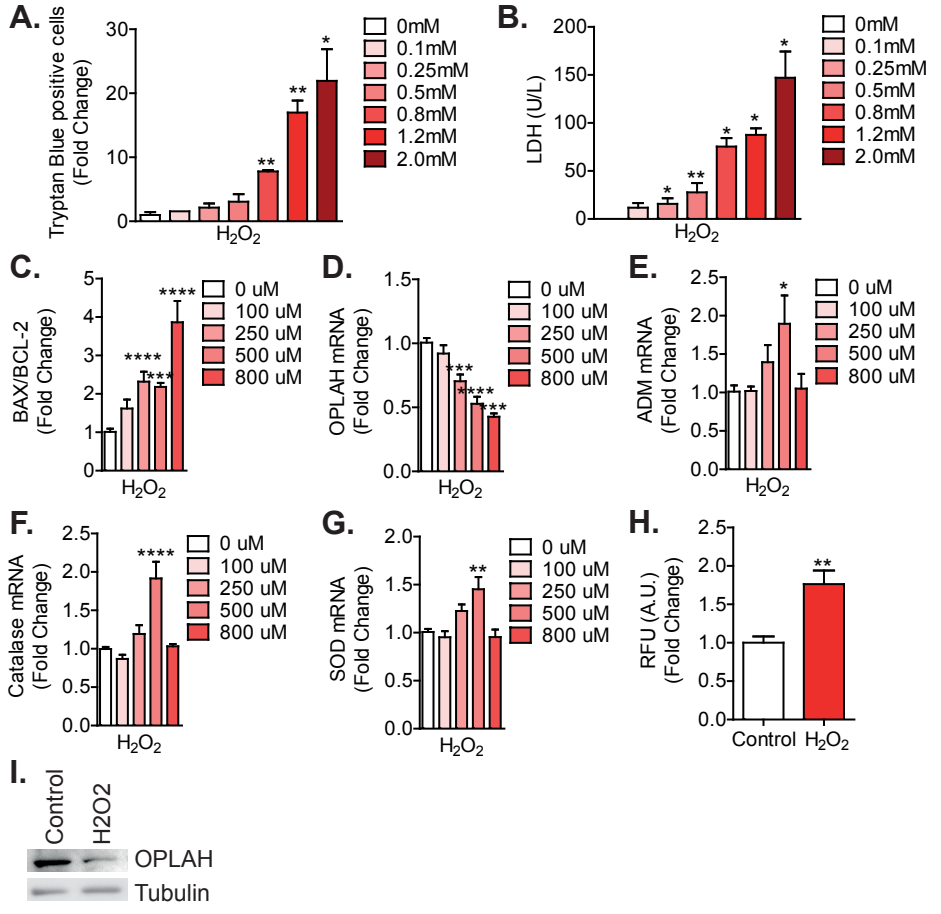


**Fig. S6. $H_2O_2$ induces oxidative stress and OPLAH depletion in NRVCs.**
NRVCs exposed to 12hrs of 0-2 mM $H_2O_2$ compared to controls. **A.** Trypan blue positive cells following exposure of NRVCs to different concentration of $H_2O_2$ (0 mM, n = 3; 0.1 mM, n = 1; 0.25 mM, n = 3; 0.5 mM, n = 2; 0.8 mM, n = 2; 1.2 mM, n = 2; 2 mM, n = 2). **B.** LDH release measured in culture medium (0 mM, n = 4; 0.1 mM, n = 4; 0.25 mM, n = 11; 0.5 mM, n = 11; 0.8 mM, n = 3; 1.2 mM, n = 3; 2 mM, n = 3). **C.** The ratio of BAX and BCL-2 expression in NRVCs exposed to 0 (n = 12), 100 (n = 8), 250 (n = 12), 500 (n = 10), and 800 (n = 4) μM $H_2O_2$. **D.** OPLAH mRNA expression in NRVCs exposed to 0 (n = 18), 100 (n = 20), 250 (n = 24), 500 (n = 16), and 800 (n = 4) μM $H_2O_2$. **E.** ADM mRNA expression in NRVCs exposed to 0 (n = 11), 100 (n = 8), 250 (n = 12), 500 (n = 10), and 800 (n = 4) μM $H_2O_2$. **F.** Catalase mRNA expression in NRVCs exposed to 0 (n = 12), 100 (n = 8), 250 (n = 12), 500 (n = 10), and 800 (n = 4) μM $H_2O_2$. **G.** SOD mRNA expression in NRVCs exposed to 0 (n = 12), 100 (n = 8), 250 (n = 30), 500 (n = 10), and 800 (n = 4) μM $H_2O_2$. **H.** CellROX analysis (control, n = 8; 500 μM $H_2O_2$ n = 8). **I.** Representative immunoblot of NRVCs exposed to 500 μM of $H_2O_2$. CellROX data are presented as fold change of RFU (A.U.) per microgram protein. Data are presented as means ± SEM *, P < 0.05; **, P < 0.01; ***, P < 0.001; ****, P < 0.0001, as calculated by Student's t test or one-way ANOVA. "*" indicates significant difference compared to control. n indicates the number of biological replicates of cell experiments.

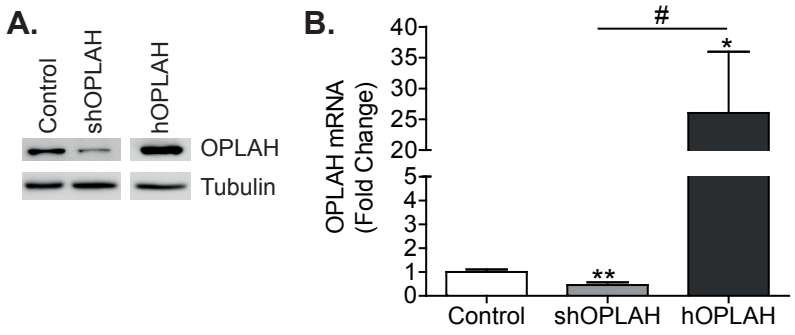


**Fig. S7. OPLAH short-hairpin and overexpression constructs in NRVCs.**
NRVCs infected with either the control, short-hairpin OPLAH (shOPLAH), or human OPLAH overexpression (hOPLAH) constructs. **A.** Representative immunoblotting analysis of one experiment. **B.** qRT-PCR results of OPLAH expression (Control n = 18, shOPLAH n = 16, hOPLAH n = 9). Data are presented as means ± SEM * or #, P < 0.05; **, P < 0.01, as calculated by one-way ANOVA. "*" indicates significant difference compared to control, whereas "#" denotes differences between groups other than control. n indicates the number of biological replicates of cell experiments.

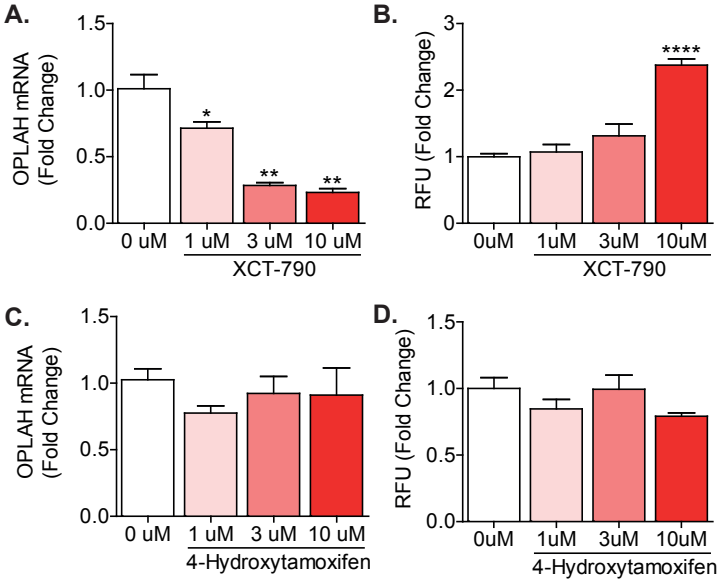


**Fig. S8. ERRα is involved in the regulation of OPLAH in NRVCs.**
**A.** OPLAH expression in NRVCs exposed to increasing concentration of XCT-790 (0 μM, n = 4; 1-10 μM, n = 6). **B.** CellROX analysis of NRVCs exposed to increasing concentrations of XCT-790 (n = 6). **C.** OPLAH expression in NRVCs exposed to increasing concentration of 4-hydroxytamoxifen ((0 μM, n = 4; 1-10 μM, n = 6). **D.** CellROX analysis of NRVCs exposed to increasing concentrations of 4-hydroxytamoxifen (n = 6). CellROX data are presented as fold change of RFU (A.U.) per microgram protein. Data are presented as means ± SEM *, P < 0.05; **, P < 0.01; ****, P < 0.0001, as calculated by Student's t test or one-way ANOVA. "*" indicates significant difference compared to control. n indicates the number of biological replicates of cell experiments.

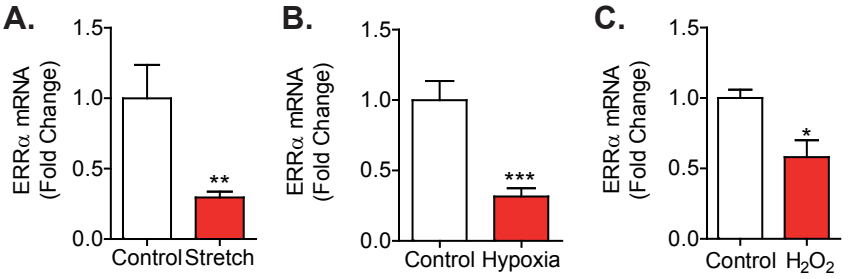


**Fig. S9. ERRα expression in NRVCs exposed to stretch, hypoxia, or $H_2O_2$.**
**A.** ERRα mRNA expression in NRVCs exposed 24 hours stretch (n = 17) compared to control (n = 10). **B.** ERRα mRNA expression in NRVCs exposed 24 hours hypoxia (n = 19) compared to control (n = 15). **C.** ERRα mRNA expression in NRVCs exposed 12 hours of 500 μM $H_2O_2$ (n = 9) compared to control (n = 4). Data are presented as means ± SEM *, P < 0.05; **, P > 0.01; ***, P > 0.001, as calculated by Student's t test. "*" indicates significant difference compared to control. n indicates the number of biological replicates of cell experiments.

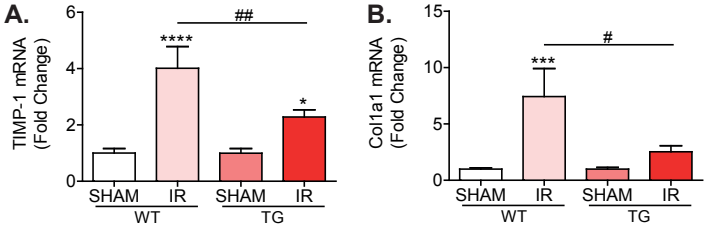


**Fig. S10. OPLAH-TG mice have reduced fibrosis compared to WT mice after IR injury.**
**A.** TIMP-1 mRNA expression (TG sham n = 11; TG IR n = 9; WT sham n = 17; WT IR n = 8). **B.** Col1a1 mRNA expression (TG sham n = 11; TG IR n = 10; WT sham n = 17; WT IR n = 10). Data are presented as means ± SEM * or #, P < 0.05; ** or ##, P < 0.01; ***, P < 0.001; ****, P < 0.0001, as calculated by one-way ANOVA (multiple groups) or Student's t test (two groups). "*" indicates significant difference compared to control, whereas "#" denotes differences between groups other than control. n indicates the number of animals.

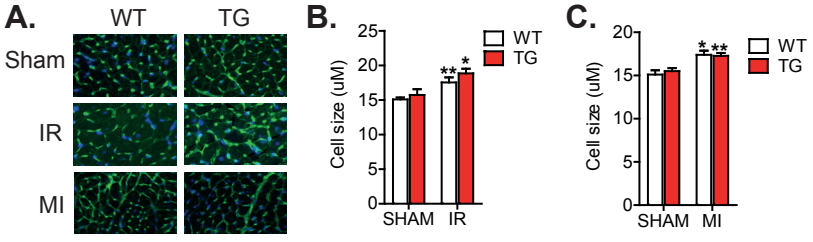


**Fig. S11. OPLAH-TG mice show no difference in LV hypertrophy compared to WT mice after IR injury or after MI.**
**A.** Representative image of WGA stainings on left ventricular (LV) slices of the different groups. **B.** Quantified cell size of the WGA stained slices from the IR study (TG sham n = 7; TG IR n = 14; WT sham n = 17; WT IR n = 9). **C.** Quantified cell size of the WGA stained slices from the MI study (TG sham n = 6; TG MI n = 13; WT sham n = 6; WT MI n = 15). Data are presented as means ± SEM *, P < 0.05; **, P < 0.01, as calculated by one-way ANOVA. "*" indicates significant difference compared to control. n indicates the number of animals.

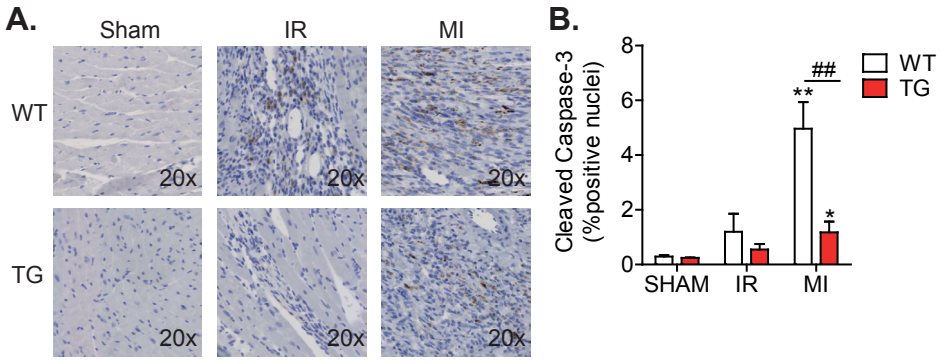


**Fig. S12. OPLAH-TG mice have reduced cleaved Caspase-3–positive cells in the left ventricle after MI.**
**A.** Representative images of cleaved Caspase-3 staining on left ventricular (LV) slices of the different groups. **B.** Quantified cleaved Caspase-3-positive cells from the different groups (n = 5). Data are presented as means ± SEM *, P < 0.05; ##, P < 0.01, as calculated by one-way ANOVA. "*" indicates significant difference compared to control, whereas "#" denotes differences between groups other than control. n indicates the number of animals.

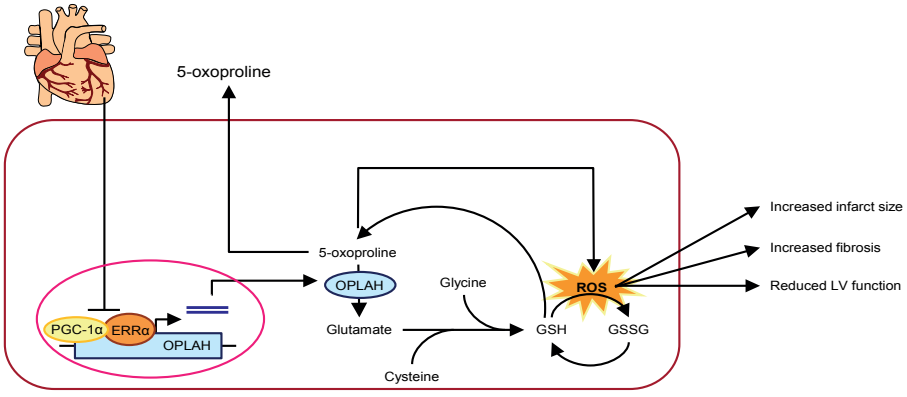


**Fig. S13. Schematic of OPLAH regulation in the cardiomyocyte.**
Under physiological conditions, PGC-1α co-activates the expression of OPLAH together with ERRα by binding to the OPLAH promoter. OPLAH mRNA is then translocated to the cytoplasm where it is translated into protein. OPLAH protein functions by converting 5-oxoproline, a degradation product of glutathione (GSH), to glutamate. Glutamate, cysteine and glycine are then utilized for the formation of de novo GSH. GSH is utilized by glutathione peroxidase to reduce reactive oxygen species (ROS), forming oxidized glutathione (GSSG). GSSG can be reduced to GSH by glutathione reductase. Upon induction of cardiac damage, PGC-1α and ERRα are inhibited, resulting in a reduction in OPLAH expression. This leads to an accumulation of 5-oxoproline, which in turn stimulates ROS production. The increase in ROS leads to the progression of HF, by increasing infarct size and fibrosis, eventually leading to a decreased left ventricular (LV) function. The excessive accumulation of intracellular 5-oxoproline also results in the transport of this metabolite into the extracellular milieu.

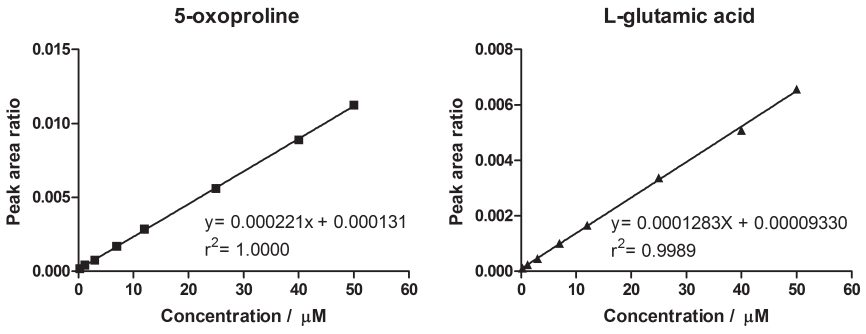


**Fig. S14. Calibration curves for LC-MS ISs $^{13}$C-5-oxoproline and L-glutamic acid.**
**A.** Calibration curve for $^{13}$C-5-oxoproline. **B.** Calibration curve for $^{13}$C-5-L-glutamic acid.

## *Supplementary Tables*

**Table S1.** Significantly up-regulated genes during murine cardiac development.

**Table S2.** Significantly down-regulated genes during murine cardiac development.

**Table S3.** Top cardiac fetal reprogramming genes.

**Table S19.** Individual subject level data for experiments with n < 20.

(available at *www.sciencetranslationalmedicine.org/cgi/content/full/9/415/eaam8574/DC1*)

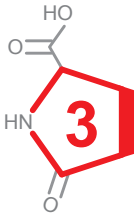


**Table 1. Characteristics of renin overexpression rats (REN2) and Sprague Dawley rats.**

| Variable | SD (N=4) | REN2 (N=5) | Pvalue |
|---|---|---|---|
| Body weight, g | **375.3 ± 13.6** | **312.5 ± 22.4** | **0.001** *** |
| Organ weight (body weight corrected), mg/g | | | |
| Left Ventricle | **2.3 ± 0.2** | **3.7 ± 0.4** | **0.001** *** |
| Kidney | **6.9 ± 0.2** | **8.9 ± 0.7** | **0.001** *** |
| Liver | **33.7 ± 1.1** | **43.8 ± 4.3** | **0.001** ** |
| | | | |
| Hemodynamic measurements | | | |
| End systolic pressure (mmHg) | **122.9 ± 13.7** | **98.6 ± 14.4** | **0.024** * |
| End diastolyc pressure (mmHg) | 7.7 ± 1.4 | 9.8 ± 2.3 | 0.145 |
| Heart rate (BPM) | 317.5 ± 31.9 | 321.8 ± 30.2 | 0.829 |
| Left Ventricular ejection fraction (%) | **81.0 ± 3.0** | **68.7 ± 5.6** | **0.003** ** |
| Stroke volume (mL) | **426.0 ± 41.0** | **265.0 ± 62.4** | **0.003** ** |

* = p<0.05

** = p<0.01

*** = p<0.001

**Table 2. Characteristics of WT mice after IR injury.**

| Variable | Sham (N=3) | IR (N=5) | Pvalue |
|---|---|---|---|
| Body weight (tibia corrected), g/cm | 14.7 ± 0.1 | 15.7 ± 0.1 | 0.124 |
| Organ weight (tibia corrected), mg/cm | | | |
| Atria | **4.0 ± 0.2** | **5.3 ± 0.1** | **0.025*** |
| Right Ventricle | 14.5 ± 1.4 | 16.1 ± 2.3 | 0.391 |
| Left Ventricle | **63.1 ± 1.7** | **77.2 ± 7.2** | **0.032*** |
| Kidney | 210.1 ± 6.7 | 202.3 ± 5.2 | 0.163 |
| Liver | 795.5 ± 7.5 | 772.9 ± 35.5 | 0.381 |
| | | | |
| Hemodynamic measurements | | | |
| End systolic pressure (mmHg) | 96.3 ± 6.8 | 104.6 ± 12.2 | 0.384 |
| End diastolyc pressure (mmHg) | **8.5 ± 1.7** | **12.5 ± 2.0** | **0.046*** |
| Heart rate (BPM) | 534.8 ± 44.9 | 512.3 ± 11.5 | 0.392 |
| Left Ventricular ejection fraction (%) | **50.9 ± 0.1** | **33.0 ± 0.1** | **0.004**** |
| Stroke volume (µL) | 24.0 ± 0.8 | 23.4 ± 2.6 | 0.784 |

* = p<0.05

** = p<0.01

**Table 3. Characteristics of Sprague Dawley rats after MI.**

| Variable | Sham (N=3) | MI (N=3) | Pvalue |
|---|---|---|---|
| Body weight, g | 428 ± 26.3 | 402.3 ± 27.0 | 0.390 |
| Organ weight (body weight corrected), mg/g | | | |
| Atria | 0.07 ± 0.02 | 0.06 ± 0.02 | 0.687 |
| Right Ventricle | 0.18 ± 0.03 | 0.15 ± 0.05 | 0.621 |
| Left Ventricle | 1.09 ± 0.12 | 0.97 ± 0.04 | 0.361 |
| Kidney | 1.42 ± 0.14 | 1.37 ± 0.12 | 0.718 |
| Spleen | 0.77 ± 0.06 | 0.86 ± 0.08 | 0.259 |
| | | | |
| Hemodynamic measurements | | | |
| End systolic pressure (mmHg) | **118.2 ± 1.6** | **102.5 ± 4.1** | **0.007**** |
| End diastolyc pressure (mmHg) | 8.44 ± 1.6 | 9.19 ± 1.8 | 0.776 |
| Heart rate (BPM) | 342.9 ± 15.4 | 346.0 ± 15.5 | 0.851 |
| Left Ventricular ejection fraction (%) | **83.3 ± 5.1** | **43.0 ± 9.7** | **0.007**** |

** = p<0.01

**Table 4. Characteristics of OPLAH overexpression (TG) and WT mice at baseline (sham) and after IR injury.**

| | WT | | TG | |
|---|---|---|---|---|
| **Variable** | **Sham (N=20)** | **IR (N=17)** | **SHAM (N=7)** | **IR (N=17)** |
| Body weight (tibia corrected), g/cm | 18.5 ± 2.2 | 18.2 ± 1.6 | 18.5 ± 0.9 | 17.3 ± 1.5 |
| Organ weight (tibia corrected), mg/cm | | | | |
| Atria | 4.1 ± 1.3 | **5.1 ± 0.8 *** | **5.4 ± 1.2 #** | **5.9 ± 1.2 *** |
| Right Ventricle | 15.5 ± 2.5 | 16.3 ± 1.6 | 17.1 ± 3.5 | 18.0 ± 4.7 |
| Left Ventricle | 66.7 ± 7.0 | **76.5 ± 6.6 ****** | **74.7 ± 7.0 #** | 73.5 ± 9.5 |
| Kidney | 260.8 ± 30.0 | 261.7 ± 32.5 | 255.6 ± 32.7 | 250.3 ± 32.5 |
| Liver | 918.6 ± 144.4 | 910.8 ± 74.5 | 917.0 ± 66.6 | **832.5 ± 80.3 #** |
| | | | | |
| Hemodynamic measurements | | | | |
| LV End systolic pressure (mmHg) | 100.0 ± 10.8 | 100.0 ± 11.2 | 106.5 ± 2.6 | 96.5 ± 8.7 # |
| LV End diastolyc pressure (mmHg) | 9.0 ± 7.2 | **15.5 ± 4.7 **** | 11.2 ± 4.4 | 13.9 ± 4.4 |
| Heart rate (BPM) | 479.4 ± 43.6 | 488.4 ± 43.0 | 512.0 ± 44.8 | 487.7 ± 40.8 |
| LV ejection fraction (%) | 52.2 ± 5.1 | **30.2 ± 13.1 ***** | 57.6 ± 6.9 | **43.4 ± 9.9 **, #** |
| LV End systolic volume (µL) | 28.7 ± 7.5 | **56.6 ± 31.1 ****** | **22.2 ± 4.9 #** | **45.6 ± 22.8 **** |
| LV End diastolyc volume (µL) | 57.0 ± 11.2 | **78.9 ± 33.0 **** | 52.5 ± 9.2 | **77.3 ± 25.7 *** |
| Stroke volume (µL) | 28.3 ± 6.1 | **22.4 ± 8.1 *** | 30.3 ± 6.9 | **31.7 ± 6.2 ##** |

* = p>0.05 Sham VS IR

** = p>0.01 Sham VS IR

*** = p>0.001 Sham VS IR

**** = p>0.0001 Sham VS IR

# = p>0.05 WT VS TG

## = p>0.01 WT VS TG

**Table 5. Characteristics of OPLAH overexpression (TG) and WT mice at baseline (sham) and after MI.**

| | WT | | TG | |
|---|---|---|---|---|
| **Variable** | **Sham (N=6)** | **MI (N=15)** | **SHAM (N=6)** | **MI (N=13)** |
| Body weight (tibia corrected), g/cm | 17.5 ± 1.9 | 17.6 ± 0.9 | 17.9 ± 2.2 | 16.4 ± 2.1 |
| Organ weight (tibia corrected), mg/cm | | | | |
| Atria | 4.4 ± 1.2 | **7.4 ± 1.8 **** | 5.2 ± 0.5 | 6.2 ± 2.0 |
| Right Ventricle | 16.8 ± 1.5 | 15.5 ± 1.6 | 15.9 ± 2.5 | 16.4 ± 2.3 |
| Left Ventricle | 67.6 ± 8.0 | **77.5 ± 9.3 *** | 74.4 ± 6.4 | 78.0 ± 11.8 |
| Kidney | 226.6 ± 21.4 | 231.6 ± 23.4 | 218.6 ± 17.3 | 214.1 ± 30.3 |
| Liver | 914.1 ± 109.4 | 854.4 ± 92.9 | 939.0 ± 113.7 | **798.8 ± 86.8 **** |
| | | | | |
| Hemodynamic measurements | | | | |
| LV End systolic pressure (mmHg) | 105.2 ± 6.8 | **90.9 ± 14.6 *** | **116.1 ± 7.6 #** | **95.7 ± 9.0 ***** |
| LV End diastolyc pressure (mmHg) | 10.2 ± 2.7 | **15.6 ± 4.9 *** | 10.6 ± 6.1 | **18.2 ± 7.2 *** |
| Heart rate (BPM) | 475.5 ± 61.4 | 515.4 ± 55.4 | 517.5 ± 52.3 | 503.9 ± 32.4 |
| LV ejection fraction (%) | 48.8 ± 6.3 | **26.4 ± 12.1 **** | 54.7 ± 7.2 | **36.2 ± 15.5 *** |
| LV End systolic volume (µL) | 37.9 ± 7.9 | **74.0 ± 39.3 *** | 26.9 ± 9.7 | **71.5 ± 50.2 *** |
| LV End diastolyc volume (µL) | 73.6 ± 8.9 | 95.6 ± 34.9 | **58.1 ± 11.2 #** | 102.3 ± 53.9 |
| Stroke volume (µL) | 35.7 ± 4.7 | **21.6 ± 6.7 ***** | 31.2 ± 3.7 | **30.7 ± 6.8 ##** |

* = p>0.05 Sham VS MI

** = p>0.01 Sham VS MI

*** = p>0.001 Sham VS MI

# = p>0.05 WT VS TG

**Table 6. Baseline characteristics of all 535 patients compared to total COACH cohort (n = 1023).**

| | No 5-oxoproline measurements | 5-oxoproline measurements | |
|---|---|---|---|
| **Demographics** | 488 | 535 | p-value |
| Age (years) | 70.2 (12.0) | 71.3 (10.9) | 0.130 |
| Female sex n(%) | 176 (36.1%) | 208 (38.9%) | 0.350 |
| NYHA n(%) | | | **0.003** |
| II | 269 (56.5%) | 244 (45.9%) | |
| III | 191 (40.1%) | 270 (50.8%) | |
| IV | 16 (3.4%) | 18 (3.4%) | |
| Previous HF hospitalization n(%) | 150 (30.7%) | 184 (34.4%) | 0.210 |
| BMI | 26.8 (5.0) | 27.1 (5.5) | 0.330 |
| Systolic BP (mmHg) | 118.5 (21.0) | 118.2 (21.0) | 0.850 |
| Diastolic BP (mmHg) | 68.1 (11.7) | 68.6 (12.3) | 0.520 |
| eGFR | 57.1 (22.1) | 53.4 (20.0) | **0.005** |
| Heart rate (bpm) | 74.9 (13.7) | 74.3 (13.1) | 0.450 |
| **Previous medical history** n(%) | | | |
| Myocardial infarction | 217 (44.5%) | 219 (40.9%) | 0.250 |
| Hypertension | 207 (42.4%) | 232 (43.4%) | 0.760 |
| Diabetes mellitus | 123 (25.2%) | 166 (31.0%) | **0.039** |
| COPD | 122 (25.0%) | 146 (27.3%) | 0.410 |
| Atrial fibrillation/Flutter | 207 (42.4%) | 244 (45.6%) | 0.300 |
| **Medication** n(%) | | | |
| Ace-inhibitors | 359 (73.6%) | 385 (72.0%) | 0.570 |
| MRA | 267 (54.7%) | 286 (53.5%) | 0.690 |
| Beta blockers | 323 (66.2%) | 354 (66.2%) | 0.990 |
| Diuretics | 470 (96.3%) | 510 (95.3%) | 0.430 |
| Statins | 183 (37.5%) | 205 (38.3%) | 0.790 |
| Glycosides | 141 (28.9%) | 168 (31.4%) | 0.380 |
| **Laboratory** | | | |
| NT-proBNP | 2227.0 (1132.0, 5495.0) | 2534.4 (1314.0, 5548.0) | 0.280 |
| Sodium (mmEq/L) | 140.0 (137.0, 142.0) | 139.0 (136.0, 142.0) | 0.059 |
| Potassium (mmEq/L) | 4.1 (3.8, 4.5) | 4.2 (3.9, 4.6) | 0.018 |

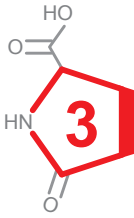

**Table 7. Baseline characteristics of all 535 patients at discharge, divided into tertiles of 5-oxoproline (in micromolars).**

| | 1st tertile (N=179) | 2nd tertile (N= 178) | 3rd tertile (N= 178) | |
|---|---|---|---|---|
| **Demographics** | 3.2-9.2 µM | 9.3-13.2 µM | 13.3-35.0 µM | **p-value** |
| Age (years) | 72.0 (11.0) | 70.9 (10.8) | 71.1 (10.9) | 0.600 |
| Female sex n(%) | 80 (44.7%) | 60 (33.7%) | 68 (38.2%) | 0.100 |
| NYHA n(%) | | | | 0.310 |
| II | 92 (51.4%) | 77 (43.3%) | 75 (42.9%) | |
| III | 81 (45.3%) | 93 (52.2%) | 96 (54.9%) | |
| IV | 6 (3.4%) | 8 (4.5%) | 4 (2.3%) | |
| Previous HF hospitalization n(%) | 59 (33.0%) | 60 (33.7%) | 65 (36.5%) | 0.760 |
| BMI | 27.4 (5.1) | 26.8 (5.0) | 27.2 (6.2) | 0.530 |
| Systolic BP (mmHg) | 117.7 (20.4) | 119.2 (20.7) | 117.8 (22.2) | 0.740 |
| Diastolic BP (mmHg) | 67.7 (11.8) | 69.8 (12.7) | 68.3 (12.4) | 0.250 |
| eGFR | 55.1 (19.3) | 52.8 (21.4) | 52.3 (19.2) | 0.370 |
| eGFR <60 n(%) | 68 (38.6%) | 66 (37.7%) | 66 (37.9%) | 0.980 |
| Heart rate (bmp) | 74.8 (13.1) | 74.3 (12.1) | 73.8 (14.1) | 0.770 |
| **Previous medical history** n(%) | | | | |
| Myocardial infarction | 67 (37.4%) | 74 (41.6%) | 78 (43.8%) | 0.460 |
| Hypertension | 75 (41.9%) | 78 (43.8%) | 79 (44.4%) | 0.880 |
| Diabetes mellitus | 57 (31.8%) | 55 (30.9%) | 54 (30.3%) | 0.950 |
| COPD | 47 (26.3%) | 53 (29.8%) | 46 (25.8%) | 0.660 |
| Atrial fibrillation/Flutter | 68 (38.0%) | 78 (43.8%) | 98 (55.1%) | 0.004 |
| **Medication** n(%) | | | | |
| Ace-inhibitors | 134 (74.9%) | 123 (69.1%) | 128 (71.9%) | 0.480 |
| MRA | 98 (54.7%) | 101 (56.7%) | 87 (48.9%) | 0.300 |
| Beta blockers | 112 (62.6%) | 117 (65.7%) | 125 (70.2%) | 0.310 |
| Diuretics | 171 (95.5%) | 169 (94.9%) | 170 (95.5%) | 0.960 |
| Statins | 62 (34.6%) | 77 (43.3%) | 66 (37.1%) | 0.230 |
| Glycosides | 56 (31.3%) | 52 (29.2%) | 60 (33.7%) | 0.660 |
| **Laboratory** | | | | |
| NT-proBNP | 2248.0 (1203.6, 4430.3) | 2386.0 (1092.2, 5721.0) | 3414.6 (1742.4, 7599.8) | 0.002 |
| Sodium (mmEq/L) | 140.0 (136.0, 142.0) | 138.5 (136.0, 141.0) | 139.0 (136.0, 141.0) | 0.034 |
| Potassium (mmEq/L) | 4.2 (3.8, 4.6) | 4.2 (3.8, 4.6) | 4.3 (3.9, 4.6) | 0.870 |
| Glutamate | 25.1 (18.8, 33.0) | 27.8 (21.2, 40.9) | 32.3 (22.3, 48.2) | <0.001 |

**Table 8. Regression analyses of 5-oxoproline association with HF biomarkers.**

| | Univariable | | Multivariable* | |
|---|---|---|---|---|
| | Beta | p-value | Beta | p-value |
| CRP | -0.006 | 0.898 | | |
| IL6 | 0.017 | 0.713 | | |
| GDF15 | 0.146 | **0.001** | 0.096 | 0.065 |
| TNF-a | 0.084 | 0.081 | | |
| MPO | 0.194 | **<0.001** | 0.164 | **<0.001** |
| Galectin-3 | 0.145 | **0.001** | 0.15 | **0.004** |
| ST2 | 0.136 | **0.002** | 0.116 | **0.008** |
| NT-proBNP | 0.146 | **0.001** | 0.126 | **0.006** |

*Corrected for age, sex, eGFR and history of atrial fibrillation.

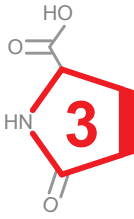


**Table 9. Regression analyses of multivariable model corrected for univariable associations.**

| | Univariable | | Multivariable | |
|---|---|---|---|---|
| 5-oxoproline (doubling) | Beta | p-value | Beta | p-value |
| Age | -0.047 | 0.272 | | |
| Sex | -0.063 | 0.145 | | |
| eGFR | -0.091 | **0.038** | -0.049 | 0.271 |
| Atrial fibrillation | 0.153 | **<0.001** | 0.113 | **0.009** |
| NT-proBNP | 0.146 | **0.001** | 0.129 | **0.004** |
| Glutamate | 0.272 | **<0.001** | 0.251 | **<0.001** |

Multivariable model: corrected for univariable associations

**Table 10. Survival analyses.**

| | **1st tertile** | **2nd tertile** | **3rd tertile** |
|---|---|---|---|
| | HR (95%CI) p-value | | HR (95%CI) p-value |
| Univariable | 1.13 (0.81-1.58) 0.456 | 1.0 (ref) | 1.52 (1.10-2.08) 0.010 |
| Model 1 | 1.14 (0.82-1.59) 0.447 | 1.0 (ref) | 1.54 (1.12-2.12) 0.008 |
| Model 2 | 1.21 (0.86-1.70) 0.267 | 1.0 (ref) | 1.51 (1.09-2.09) 0.012 |
| Model 3 | 1.38 (0.97-1.98) 0.074 | 1.0 (ref) | 1.54 (1.09-2.17) 0.013 |

Model 1: Age & sex

Model 2: Model 1 + atrial fibrillation and renal dysfunction

Model 3: Model 2 + NT-proBNP & glutamate

**Table 11. OPLAH-specific shRNA–targeting oligonucleotides and cloning primers for human OPLAH overexpression.**

| | | |
|---|---|---|
| **Short-hairpin** | | |
| shOPLAH1 | Sense | GATCCCGCTAGACACCAGTCGCATTTTCAAGAGAAATGCGACTGGTGTC-TAGCTTTTTGGAAA |
| | Antisense | AGCTTTTCCAAAAAGCTAGACACCAGTCGCATTTCTCTTGAA AATGCGACTG-GTGTCTAGCGG |
| shOPLAH2 | Sense | GATCCCCCGCTATGCTGGAGAATTTTTCAAGAGAAAATTCTCCAGCATAGCG-GTTTTTGGAAA |
| | Antisense | AGCTTTTCCAAAAACCGCTATGCTGGAGAATTTTCTCTTGAA AAATTCTCCAG-CATAGCGGGG |
| shOPLAH3 | Sense | GATCCCGTCCTAGTATGGCAGATACTTCAAGAGAGTATCTGCCATACTAGGACT-TTTTGGAAA |
| | Antisense | AGCTTTTCCAAAAAGTCCTAGTATGGCAGATACTCTCTTGAAGTATCTGCCA-TACTAGGACGG |
| shOPLAH4 | Sense | GATCCCTGGGAGAGCTGATCGGACATTCAAGAGATGTCCGATCAGCTCTCC-CATTTTTGGAAA |
| | Antisense | AGCTTTTCCAAAAATGGGAGAGCTGATCGGACATCTCTTGAATGTCCGAT-CAGCTCTCCCAGG |
| **Cloning** | | |
| human OPLAH | Forward (5'- 3') | GAAGTCGACACCATGGGCAGCCCCGAGGGCCGC (sal1) |
| | Reverse (5'- 3') | GACAAGCTTTCACACGGCCTCCTGGGCCCGG (hindIII) |

**Table 12. List of primers used in this study.**

| Transcript | Forward primer (5' - 3') | Reverse primer (5' - 3') |
|---|---|---|
| *OPLAH* (mouse/rat) | TCCGAGAGCTGGTCTTTC | ATTCACTGTGCGCCCATC |
| *OPLAH* (human) | GAGCTGCTCTTTCGTGAGG | GCGGATCAGCAGGTTTAGG |
| *ANXA11* (human) | GTGGGTGAAGCACCGTGT | TCACCAGATGCACAGGCTAC |
| *HadH* (human) | TGTCATGAAACTTGTGGAGGTC | TGCTTTCCTAGGGCTTTGC |
| *Lgals4* (human) | TTCATAGTCCTGGCTGAGCAC | CGGTGCCCGTACTCATAGA |
| *CYYR1* (human) | TCACATCAACACCGTCTCCT | TATTCCATCTCGTGGTCGTG |
| *Cd300lg* (human) | AAGGCAAAAGCTCAGCAAAC | CTGTCTTCCCCTGCTTGG |
| *RALGAPA2* (human) | GCCAAAGGATAAACAAATAAAGGA | AGCTACCATGAGCGTCCTAAA |
| *Vps13d* (human) | GCCAGGAGCATGGAGAGTC | TCAAAAGAGCAGATGCAAACA |
| *MCCC1* (human) | TGCATGTAGATATGGCAGATGA | TTGGCCACTTGAATGATTTTC |
| *THEM6* (human | TGGAGACACCAGGCTACTAGG | AGCTGTAAGGTGAGGCATTAGG |
| *ABHD14B* (human) | TCCTGTGGAGGGTAATCCAT | CAGGGGAAGGAGTGAAAGC |
| *Etl4* (human) | CTCCGATTTCAAGAACTGATGA | CACTGATTGTATTTTCGAGCTGTT |
| *DENND4C* (human) | AGCGATTGACATGACTCCAA | TTTCCATCTCAAGCTGTGTCA |
| *SLC25A22* (human) | TCTCTACAAGGGACTCGGGG | GCTGGTTCAGGTTGGCAAAG |
| *SLCO2B1* (human) | CCTGTCCCAGGTATGCTTGT | GGAGGCTGTGATGGAAAACT |
| *Vps13c* (human) | CGACCCTGGAAGGATTATACC | GGATTTTTCTTCTTTTACAGCATCA |
| *ITM2A* (human) | ATCCTGCAAATTCCCTTCGT | TCATCCTCACGAATGTCAGC |
| *DNAJB1* (human) | TTCTGTATTTGTCTCCCATGTCTT | CAATTTGAGATGGCCAAAGAG |
| *OSTC* (human) | GGAAGCGTATTGAAGCTTGG | AAGAAAATGCCACTCAACATCA |
| *PPRC1* (human) | TGACAGCTTGGCTGTAGGAA | GGGCTTGTAACCGGTCTAGG |
| *BANP* (human) | CCTTCAGAGCCGATGATGAG | GTGGATCTGCACCTGCTGT |
| *GRB10* (human) | TGGACTTAAACGACGATTTGC | TTCAACTTTCCGCTGGATCT |
| *DNAJA1* (human) | AGAACGCTCGGTGAGAGG | GACCCCCAAAACATCGTAGTAA |
| *KIF26B* (human) | GCCCTGATTGTATCCCTCGC | GGTTGGGGTCGCTGGTTTAT |
| *LSM1* (human) | ACGTGTTACAGGAAGTGGGTAAG | CGACCGAGACCAGCACTT |
| *HSP90AA1* (human) | ACCAAAGAAGGCCTGGAACT | GTCTTTCATGATTTTGCAGAGGT |
| *PSMC3IP* (human) | TCACTGCTAAGGTGCAGAGC | CAGGGCACTAGATAATTCCTTGA |
| *SNX6* (human) | TCGGACAGAGGCAGGTTAGT | ATCCGGGAAACCACAACAG |
| *FREM1* (human) | TGGTGGACAGCATACCAAAA | AGCATGCTGAGTGAATGACCT |
| *ERRα* (mouse/rat) | CTCAGCTCTCTACCCAAACGC | CCGCTTGGTGATCTCACACTC |
| *ERRα* (human) | CTCAGCTCCCTGCCCAAGCGC | CCGCTTGGTGATCTCACACTC |

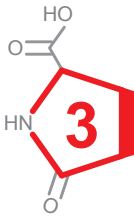

**Table 12. (continued)**

| Transcript | Forward primer (5' - 3') | Reverse primer (5' - 3') |
|---|---|---|
| *PGC1-α* (mouse) | CAGTCCTTCCTCCATGCCTG | GGGTTTGTTCTGATCCTGTGG |
| *PGC1-α* (rat) | AAAGGGCCAAGCAGAGAGA | GTAAATCACACGGCGCTCTT |
| *PGC1-α* (human) | AGAGGGCCAAGCAAAGGGA | ATAAATCACACGGCGCTCTT |
| *Catalase* (rat) | GCAGATACCTGTGAACTGTC | GTAGAATGTCCGCACCTGAG |
| *SOD* (rat) | TGGCTTGGCTTCAATAAGGA | AAGGTAGTAAGCGTGCTCCCACAC |
| *ADM* (rat) | GCAGTCAGTCTTGGACTTTG | CAATAACATCAGGGCGATGG |
| *Bax* (rat) | CATCATGGGCTGGACACTGG | GTCCCGAAGTAGGAGAGGAG |
| *BCL-2* (rat) | CGCGACTTTGCAGAGATG | CACCGAACTCAAAGAAGG |
| *Timp-1* (rat) | AGAGCCTCTGTGGATATGTC | CTCAGAATTATGCCAGGGAAC |
| *Col1a1* (rat) | ACAGCGTAGCCTACATGG | AAGTTCCGGTGTGACTCG |
| *36B4* (mouse) | AAGCGCGTCCTGGCATTGTC | GCAGCCGCAAATGCAGATGG |
| *36B4* (rat) | GTTGCCTCAGTGCCTCACTC | GCAGCCGCAAATGCAGATGG |
| *36B4* (human) | AACGGGTACAAACGAGTC | AGATGGATCAGCCAAGAAG |

**Table 13. List of antibodies used in this study.**

| Antigen | Cat. No. | Supplier |
|---|---|---|
| OPLAH | sc-271807 | Santa Cruz Biotechnology Inc. |
| α-tubulin | t5168 | Sigma-Aldrich |
| ERRα | ab76228 | Abcam |
| GAPDH | 10R-G109A | Fitzgerald |
| α-actinin | a7811 | Sigma-Aldrich |
| HIF1α | 10006421 | Cayman Chemical |
| SERCA2 | ab2861 | Abcam |
| p53 | BD554166 | BD Biosciences |
| EXOG | 21523-1-AP | Protein Tech |
| Cleaved Caspase-3 | 9664 | Cell Signaling |
| Vimentin | v5255 | Sigma-Aldrich |
| α-smooth muscle actin | ab5694 | Abcam |
| OCT-3/4 | SC-17743 | Santa Cruz Biotechnology Inc. |

**Table 14. Accuracy and precision results for 5-oxoproline.**

| **Nominal concentration** | (µM) | 50 | 40 | 25 | 12 | 7 | 3 | 1.2 | 0.3 |
|---|---|---|---|---|---|---|---|---|---|
| **Calculated response** | (µM) | 50,3 | 39,6 | 24,7 | 12,4 | 7,09 | 2,84 | 1,29 | 0,19 |
| **CV** | (%) | 1,3 | 0,3 | 1,2 | 0,8 | 2,2 | 4,8 | 1,6 | 72,6 |
| **Bias** | (%) | 0,6 | -0,9 | -1,0 | 3,0 | 1,4 | -5,2 | 7,5 | -36,4 |
| **Accuracy** | (%) | 100,6 | 99,1 | 99,0 | 103,0 | 101,4 | 94,8 | 107,5 | 63,6 |

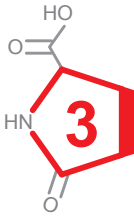


**Table 15. Accuracy and precision results for L-glutamic acid.**

| **Nominal concentration** | (µM) | 50 | 40 | 25 | 12 | 7 | 3 | 1.2 | 0.3 |
|---|---|---|---|---|---|---|---|---|---|
| **Calculated response** | (µM) | 50,5 | 38,9 | 25,5 | 12,2 | 7,14 | 2,90 | 1,10 | 0,14 |
| **CV** | (%) | 2,3 | 1,0 | 1,0 | 0,4 | 0,4 | 4,8 | 4,1 | 15,2 |
| **Bias** | (%) | 1,0 | -2,7 | 2,2 | 1,9 | 1,9 | -3,4 | -8,6 | -51,8 |
| **Accuracy** | (%) | 101,0 | 97,3 | 102,2 | 101,9 | 101,9 | 96,6 | 91,4 | 48,2 |

# Chapter 4

## OPLAH ablation leads to accumulation of 5-oxoproline, oxidative stress, fibrosis and elevated fillings pressures in a murine model for heart failure with a preserved ejection fraction

Atze van der Pol[1], Andres Gil[2], Jasper Tromp[1,3], Herman H.W. Silljé[1], Dirk J. van Veldhuisen[1], Adriaan A. Voors[1], Elke S. Hoendermis[1], Niels Grote Beverborg[1], Elisabeth-Maria Schouten[1], Rudolf A. de Boer[1], Rainer Bischoff[2], Peter van der Meer[1]

[1]Department of Cardiology, University Medical Center Groningen, University of Groningen
[2]Department of Pharmacy, Analytical Biochemistry, University of Groningen
[3]National Heart Centre Singapore

*Under review at Cardiovascular Research*

## Abstract

**Aims**: The prevalence of heart failure with a preserved ejection fraction (HFpEF) is increasing, but therapeutic options are limited. Oxidative stress is suggested to play an important role in the pathophysiology of HFpEF. However, whether oxidative stress is a bystander due to comorbidities or causative in itself remains unknown. Recent results have shown that depletion of 5-oxoprolinase (OPLAH) leads to 5-oxoproline accumulation, which is an important mediator of oxidative stress in the heart. We hypothesize that oxidative stress induced by elevated levels of 5-oxoproline leads to the onset of a murine HFpEF-like phenotype.

**Methods and Results**: Oplah full body knock-out (KO) mice had higher 5-oxoproline levels coupled to increased oxidative stress. Compared to wild-type littermates (WT), KO mice had increased cardiac and renal fibrosis with concurrent elevated left ventricular filling pressures, impaired LV relaxation, yet a normal left ventricular ejection fraction (LVEF). Following the induction of cardiac ischemia/reperfusion (IR) injury, 52.4% of the KO mice died compared to, only 15.4% of the WT mice ($p<0.03$). Furthermore, KO mice showed a significantly increased atrial, ventricular, kidney, and liver weights compared to WT mice ($P<0.05$ for all). Cardiac and renal fibrosis were more pronounced following cardiac IR injury in the KO mice and these mice developed proteinuria post IR injury. To further address the link between 5-oxoproline and HFpEF, 5-oxoproline was measured in the plasma of HFpEF patients. Compared to healthy controls (3.8 ± 0.6 μM), 5-oxoproline levels were significantly elevated in HFpEF patients (6.8 ± 1.9 μM, $P<0.0001$). Furthermore, levels of 5-oxoproline were independently associated with more concentric remodeling on echocardiography.

**Conclusions**: Oxidative stress induced by 5-oxoproline results in a murine phenotype reminiscent of the clinical manifestation of HFpEF without the need for surgical or pharmacological interference. Better understanding the role of oxidative stress in HFpEF may potentially lead to novel therapeutic options.

## Introduction:

Heart failure (HF) is associated with high mortality and morbidity (1). While treatment possibilities for patients with HF and a reduced ejection fraction (HFrEF) have considerably improved outcomes, this has not been the case for HF patients with a preserved ejection fraction (HFpEF) (2). The incidence of HFpEF has increased rapidly during the past decades and is becoming the dominant form of HF (2). Typical features of HFpEF include elevated LV filling pressures, impaired relaxation and structural abnormalities (i.e. left ventricular concentric remodeling). Unfortunately, the underlying pathophysiology of HFpEF remains poorly understood. To increase our understanding of the pathophysiology of HFpEF, several animal models have been developed that recapitulate some, but not all the characteristics described in HFpEF patients (3,4). As a result these animal models are limited in their use in developing therapeutic strategies specifically targeting HFpEF. Therefore, it is essential to unravel the underlying cardiac pathophysiology leading to the onset of HFpEF, by developing novel animal models, which could lead to therapies directed towards HFpEF (4).

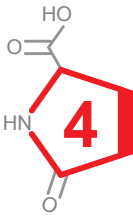


In recent years it has been suggested that oxidative stress, resulting from an increased systemic proinflammatory state, plays a role in the onset and progression of HFpEF (5). Oxidative stress is defined as an imbalance between the production of reactive oxygen species (ROS) and the endogenous antioxidant defense mechanisms (the so called “redox state”). Under physiological conditions, small quantities of ROS are produced intracellularly, which function in cell signaling, and can be readily reduced by the antioxidant defense system. However under pathophysiological conditions, the production of ROS exceeds the buffering capacity of the antioxidant defense system, resulting in cell damage and death. The major source of antioxidants in mammalian cells are glutathione (GSH), which is formed by the γ-Glutamyl cycle and thioredoxin (Trx) (6–8). Trx are small redox proteins that exert its antioxidant function primarily through peroxiredoxins (Prx), which utilizes Trx to reduce peroxides (i.e. $H_2O_2$). This reaction results in the formation of oxidized Trx, which can then be recycles by thioredoxin reductase (TrxR). Similarly, GSH is utilized by GSH peroxidase (GPx) to reduce $H_2O_2$, producing oxidized GSH (GSSG) in the process. GSSG is then recycled by GSH reductase (GR) (9). Recent studies have established an important role of the Trx antioxidant system in HF (10,11). GSH has also been implicated in cardiovascular diseases, however, only recently have the enzymes of the GSH synthesis and salvage pathways been implicated in HF (12–18).

One such enzyme is 5-oxoprolinase (OPLAH), that is responsible for converting 5-oxoproline, a degradation product of glutathione, into glutamate (6,19). 5-Oxoproline

has been shown to induce oxidative stress in rat brain tissue, rat cardiomyocytes, and human embryonic derived cardiomyocytes (16,20,21). Furthermore, OPLAH expression is reduced in both rodent models of HFrEF and in the clinical setting (16,22). This reduction of OPLAH expression is coupled to an increase in circulating 5-oxoproline, which is associated with a poor outcome in patients with HF (16). In a murine model for myocardial infarction, it was observed that OPLAH has a cardio-protective effect by reducing 5-oxoproline, oxidative stress, and improving cardiac function (16). These findings demonstrate that OPLAH and 5-oxoproline are highly involved in oxidative stress and HF, and could suggest a novel therapeutic target for HF. Based on these observations and the recent implication of oxidative stress in the development of HFpEF, we hypothesized that OPLAH knock-out (KO) mice would develop a cardiac phenotype reminiscent of clinical HFpEF. Furthermore, we were interested in identifying whether OPLAH KO mice would be more susceptible to cardiac injury.

## Methods

### Generation of Oplah knock-out mice

*Oplah* knock-out mice, Oplah$^{tm1a(KOMP)Wtsi}$ (here after referred to as KO) mice were generated as part of the European Conditional Mouse Mutagenesis Program and Knockout Mouse Project projects and the Sanger Mouse Genetics Projects (EUCOMM/KOMP-CSD) (23). Mice were generated from embryonic stem cell clone EPD0244_4_F09 and backcrossed to C57L/6 background. Genotype analysis was performed by PCR on isolated genomic DNA as previously described (25). All animal protocols were approved by the Animal Ethical Committee of the University of Groningen (permit number: DEC6632). The animal experiments were performed conform the ARRIVE guidelines (25).

### Cardiac ischemia/reperfusion injury in Oplah knock-out mice

Animal protocol was approved by the Animal Ethical Committee of the University of Groningen (permit number: DEC6632). The animal experiments were performed conform the ARRIVE guidelines. A total of 103 male mice, 37 knock-out (KO), 38 heterozygous (HET) and 28 wild-type (WT), were included in the ischemia/reperfusion (IR) study. All mice were 14-20 weeks of age and 35-40 g of body weight. The KO, HET and WT mice were randomized into two groups, the SHAM operated group and the IR group. Animals were anesthetized with isoflurane and medical oxygen, followed by the administration of 5mg/kg of carprofen. The IR group (WT n = 13, HET n = 16, and KO n = 21) underwent ligation of the left anterior descending branch (LAD) of the left coronary artery for 60 min, followed by reperfusion for 4 weeks. The ligation of the LAD was placed by the surgeon to achieve a ±30% area

at risk of the LV. The SHAM operated group (WT n = 15, HET n = 22 and KO n = 16) underwent the same procedure without induction of ischemia. The surgeon was blinded to which animal was KO, HET or WT. After 4 weeks animals were placed in the MRI followed by hemodynamic measurements and animals were sacrificed. At sacrifice, blood was collected and organs were weighed and collected for histology and molecular analysis.

**Cardiac MRI measurements**

Cardiac MRI was performed as described previously (16,26). Mice were anesthetized with isoflurane (2%) and imaged in a vertical 9.4-T, 89-mm bore size magnet equipped with 1500 mT/m gradients and connected to an advanced 400 MR system (Bruker Biospin) using a quadrature-driven birdcage coil with an inner diameter of 3 cm. Respiration and ECG were monitored by ECG Trigger Unit (RAPID biomedical GmBH). Heart rate was maintained between 400-600 bpm and respiration rate between 20-60 breaths per minute. ParaVison 4.0 and IntraGate software (Bruker Biospin GmH) were used for cine MR acquisition and reconstruction. After orthogonal scout imaging, short axis (oriented perpendicular to the septum) cardiac cine MR images were acquired. To cover the entire heart from apex to base, 7 slices (sham) and 8-9 slices (IR) were needed. The images were reconstructed and for all mice, dedicated, semi-automatic contour detection software (QMass, version MR 6.1.5, Medis Medical Imaging Systems) was used for the determination of the LV end-diastolic volume, LV end-systolic volume, stroke volume, and ejection fraction. The investigators were blinded to experimental settings during data analysis.

**Hemodynamic measurements**

Heart rate and pressures of aorta and LV were measured after 4 weeks using the Scisense Advantage PV measurement system with a PV catheter, as previously described (16). A 1.2 French electrode with 4.5 spacing (Transonic Scisense Inc) was used. Analyses were performed offline with LabChart7 software (version 7.2, ADinstruments). After hemodynamic measurements, mice were sacrificed by excision of the heart and tissues and tibia were collected. The investigators were blinded to experimental settings during data analysis.

**Electrocardiography**

A total of 23 mice, 18 KO and 5 WT, were utilized to perform electrocardiography (ECG) measurements. All mice were 14-20 weeks of age and 35-40 g of body weight. Animals were anesthetized with isoflurane and medical oxygen, followed by the administration of 5mg/kg of carprofen. At this point 1 min baseline ECG recording was made of each animal. For ECG measurements, subcutaneous recording electrodes were placed, one in the right armpit and the other in the left groin (Lead II). Following the baseline measurements, the electrodes were removed and a ligation of the was

placed on the LAD. After which electrodes were again placed and a 45 min ECG recording was performed. At the end of the 45 min ischemic ECG recording, the animals were terminated by excision of the heart.

**Histology**

For immunohistochemical analysis, hearts were fixed overnight with 10% neutral-buffered formalin at 4°C. After fixation, samples were subjected to a dehydration series, embedded in paraffin and cut into 4 µM sections. Masson trichrome straining was performed to analyze collagen deposition. To quantify fibrosis, whole ventricle slice pictures were photographed using Hamamatsu microscope, and fibrotic area was determined with Aperio's ImageScope software. Areas of fibrosis were calculated as percentages of total area of the left ventricle. To quantify the infarct size, area of infarct were calculated as percentages of total area of the left ventricle. To quantify the non-infract fibrosis, fibrosis was calculated as a percentage of the total area opposite of the infarct. For cardiomyocyte size, FITC-labeled wheat germ agglutinin (WGA) staining was performed. For quantification Fiji (27) was used, briefly five randomly selected fields from whole-stained WGA-FITC LV sections imaged ad 20x magnification were used to measure cross-sectional diameter from approximately 30 cells per mouse heart, and calculated as area. The investigators were blinded to experimental settings during data analysis.

**Urine measurements**

Urine from mice was collected following excision of the heart directly from the bladder. To assess the total urinary protein, urea and creatinine 25 µl of urine was diluted with 225 µl MilliQ (1:10 dilution). For determining the total protein the UV assay U/CSF Protein kit (Roche Diagnostics) was used. For urea measurements the UV assay UREA/UN kit (Roche Diagnostics) was used. For creatinine measurements the UV assay CREA plus (Roche Diagnostics) was used.

**Total Antioxidant Capacity**

The antioxidant capacity of tissue samples was measured by means of the Total Antioxidant Capacity Assay kit (ab65329, Abcam) per manufactures instructions. Briefly, snap frozen LV tissue was homogenized in ice-cold RIPA (50 mM Tris pH 8.0, 1% nonidet P40, 0.5% deoxycholate, 0.1% SDS, 150 mM NaCl), followed by centrifugation at 12,000 rcf for 10 min at 4°C. Supernatant was collected and assayed.

**Quantitative real time PCR**

Total RNA from tissues were isolated by the TRIzol RNA isolation protocol. QuantiTect RT kit (Qiagen) was then used to make cDNA from the RNA samples, following manufacturer's instructions.

Relative gene expression was determined by quantitative real-time PCR (qRT-PCR) on a BioRad CFX384 real time system using ABsolute QPCR SYBR Green mix (Thermo Scientific). Gene expression was determined by correcting for reference gene values (36B4), and the calculated values were expressed relative to the control group per experiment. Primer sequences can be found in Table S1.

**Western Blotting**

Tissues were homogenized in ice-cold RIPA (50 mM Tris pH 8.0, 1% nonidet P40, 0.5% deoxycholate, 0.1% SDS, 150 mM NaCl) containing phosphatase inhibitor cocktail 3 (Sigma-Aldrich), protease inhibitor (Roche Diagnostics), 1 mM phenylmethylsulfonyl fluoride (PMSF; Roche Diagnostics), and 15 mM NaVanadate. Protein concentrations were determined with a DC protein assay kit (Bio-Rad).

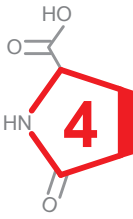


Equal amounts of protein were loaded on 10% polycrylamide gels. After electrophoresis, the gels were blotted onto PVDF membranes. Membranes were then incubated overnight at 4°C with the primary antibody, followed by 1h incubation at room temperature with secondary antibody. Detection was performed by ECL and analyzed with densitometry (ImageQuant LAS4000; GE Healthcare Europe). Antibodies used are described in Table S2.

For the detection of oxidized proteins we utilized the Oxidized Protein Western Blot Kit (Abcam). Tissue samples were homogenized and processed as per manufacturer's instructions. Protein concentrations were measured using the Bradford Protein Assay (Bio-Rad). Briefly, equal amounts of protein were derivatized using 2, 4 dinitrophenyl hydrazine (DNPH) for 15 min at room temperature and then neutralized. The samples were then loaded on a 10% polyacrylamide gels and DNP conjugated proteins were detected by western blotting using primary DNP antibody and HRP conjugated secondary antibody.

**Healthy control patient population and study design**

As a control group, healthy individuals, included as control population for a previously published study, were used (28). Subjects scheduled for total hip or knee replacement surgery at the University Medical Center Groningen, Groningen, The Netherlands were eligible. Exclusion criteria included the presence of previously diagnosed cardiovascular disease, diabetes mellitus or more than one of the following cardiovascular risk factors: hypertension, smoking, hypercholesterolemia, obesity and physical inactivity. Laboratory measurements were made in venous blood stored at -80°C which was never thawed before assaying. The study protocol was approved by the local ethics committee and the study was conducted in accordance with the Declaration of Helsinki. All subjects gave written informed consent prior to any study-related procedures.

**Patient population and study design**

The methods and primary results of this study have been reported elsewhere (29–31). Briefly, 52 patients with symptomatic HFpEF and pulmonary hypertension were randomly assigned to either the treatment group (sildenafil 60 mg t.i.d. three times daily) or the placebo group. Eligible patients were male or female, with HFpEF (left ventricular ejection fraction [LVEF] ≥ 45% and New York Heart Association [NYHA] functional class II-IV) and pulmonary hypertension (mean PAP>25mmHg and mean PAWP>15mmHg), which was invasively diagnosed by right-sided cardiac catheterization and two-dimensional echocardiography. The primary objective was to evaluate the effect of 12-week treatment with sildenafil compared to placebo on invasively measure mean pulmonary artery pressure (PAP) in patients with HFpEF and pulmonary hypertension. The secondary objectives were to assess the effects of sildenafil on pulmonary artery wedge pressure (PAWP), cardiac output, and exercise capacity, as measured by cardiopulmonary exercise testing. Overall, results from this study were neutral (29–31).

At baseline patients underwent physical examination, right-sided catheterization, two-dimensional echocardiography, laboratory assessments, and an exercise capacity test, and started with sildenafil or placebo, as previously described (29–31). After 2 weeks patients were titrated to sildenafil or placebo 60 mg t.i.d. The same medical assessment was performed after 12 weeks of treatment, as previously described (29–31). The randomized clinical trial conformed to the Declaration of Helsinki and the Medical Research Involving Human Subjects Act, and was approved by the institutional review board and local Ethics Committee. All patients provided written informed consent. This trial is registered at Clinicaltrails.gov, number NCT01726049.

In this study 51 patient plasma samples at baseline were analyzed, from the 52 previously described, of the remaining patient no plasma was available for 5-oxoproline measurements and was excluded from this analysis. Since sildenafil was found to have no effects on the primary or secondary objectives of the trial, we pooled the patient population to assess the effects of plasma 5-oxoproline levels in the total population on cardiac structure and function.

**LC-MS measurements**

5-oxoproline internal standard was prepared from $^{13}C$-labeled L-glutamic acid as previously described (16). Oxidized glutathione (GSSG) was prepared by a controlled oxidation of $^{13}C$, $^{15}N$-labeled GSH. Briefly, 10 mg of $^{13}C$, $^{15}N$-labeled GSH were dissolved in 1 mL water. Half of the solution (0.5 mL) was mixed with of 0.5 mg NaI (final concentration 6.7 mM) and 1 µL 30% $H_2O_2$. The mixture was heated at 25°C for 60 min to allow oxidation. Excess $H_2O_2$ was eliminated by increasing the temperature of the mixture to 65°C for 5 min as previously described (32).

For 5-oxoproline measurements were performed on plasma samples from the patients and urine, plasma, and tissue samples from mice,. The sample preparation was performed as previously published (16), with some minor modifications. Briefly, 25 µL sample (urine or plasma) and ±1 mg of powdered tissue was mixed with 200 µL of the extraction solution (0.5 µL IS 5-oxoproline in 75% methanol). Samples were vortex mixed and centrifuged for 10 min at 20,000g. Supernatant was dried under a stream of nitrogen gas at room temperature, followed by resuspension in 100 µL of water. At this stage, samples were stored at -80°C until LC-MS measurements were performed. LC-MS measurements of 5-oxoproline were performed as previously described (16).

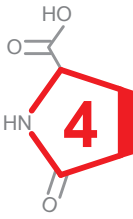


For GSH and GSSG measurements were performed on tissue samples of mice. Murine tissues (cardiac or renal) were prepared by adding 200 µL of cold (-20°C) extraction solution [0.5 µL isotopically-labeled internal standard of GSH and GSSG (ratio of 2:1) and 1.25 mg of N-ethylmaleimide (NEM) in 75% methanol] to ±1 mg of powdered tissue. The mixture was then sonicated for 5 min, followed by incubation for 45 min in a thermomixer at room temperature and 900 rpm to allow derivatization of GSH to GSH-NEM. Samples were centrifuged at 4°C and 20800g for 20 min. The supernatant was collected and dried under a stream of nitrogen at room temperature, followed by resuspension in 100 µL water. At this stage, samples were stored at -80°C until LC-MS measurements were performed. GSH-NEM and GSSG were separated in reverse phase mode on an Acquity HSS T3 column (1.8 µm, 100 × 2.1 mm; Waters) using a 1290 Infinity LC system (Agilent). Formic acid ( 0.1%) in water was used as eluent A and methanol as eluent B. The following gradient was applied: 0 min – 100%A, 2.5 min – 100%A, 5 min – 95%A, 6 min – 15%A, 8 min – 15%A and 10 min – 100%A. The column temperature was set at 30°C, the flow rate was 0.3 mL/min, and the injection volume was 10 µL.

Mass spectrometry detection was performed using a 6410 Triple Quadrupole MS system (Agilent) by positive electrospray ionization (ESI+) in the Multiple Reaction Monitoring (MRM) mode. The optimized MS source parameters were: ionspray voltage: +1500V, drying gas flow (N2): 6 L/min, drying gas temperature 300°C, nebulizer pressure: 15 psi. The quadrupole mass analyzer was set to unit resolution and the electron multiplier to 2400 V. The run was divided into 2 segments with MS/MS transitions 433/304 for GSH-NEM, 436/307 for $^{13}C$, $^{15}N$-labeled GSH-NEM (IS), and 613/355 for GSSG, 619/361 for $^{13}C$, $^{15}N$-labeled GSSG (IS). Fragmentor and collision energies were optimized to 125 V and 9 V for GSH-NEM and 200 V and 21 V for GSSG, respectively. The dwell time for each transition was 100 ms. The LC-MS system was controlled by MassHunter Workstation software (Agilent).

For tissue samples, pellets formed after centrifugation were homogenized in 200 µL ice-cold RIPA buffer (50 mM Tris pH 8.0, 1% Nonidet P40, 0.5% deoxycholate, 0.1% SDS, 150 mM NaCl). Protein concentrations were determined with the Pierce BCA Protein Assay Kit (ThermoFisher Scientific), following the manufacturer's instructions. Tissue concentrations of 5-oxoproline, GSH, and GSSG were normalized to tissue protein concentrations.

**Statistical analysis**

All animal experimental data is represented as mean values ± standard error of the mean (SEM). To compare the difference between two groups, the Student's t-test was performed. Comparison between more than two groups were done using one-way analysis of variance (ANOVA) with post hoc Bonferroni test. P-values of $< 0.05$ were considered statistically significant. All analyses were done using GraphPad Prism software V5.04 (GraphPad software, Inc, La Jolla, CA, USA). For the animal experiments, we chose the sample sizes for all the groups based on the feasibility and prior knowledge of statistical power from previously published experiments (16). With small sample sizes we did not apply statistical tests for normality or equality of variances.

Patients from the sildenafil study were divided according to low (below median) and high (above median) levels of 5-oxoproline. To compare clinical characteristics and echocardiographic parameters between patients with low and high levels of 5-oxoproline, the Student's t-test, Mann-Whitney-U test or the chi-2 test was used depending on the nature of the variable. To test for the association between concentric remodeling and 5-oxoprolinase, logistic regression was used with concentric remodeling as the dependent variable. We then subsequently corrected for clinically relevant confounders including age, sex, renal function, BMI, systolic blood pressure and levels of NT-proBNP. All tests were performed 2 sided, and a P value $< 0.05$ was considered statistically significant. All statistical analyses were performed using STATA version 14.2 (StataCorp LP, College station, Texas, USA).

## Results

**OPLAH knock-out mice have increased levels of 5-oxoproline**

To study the effects of OPLAH depletion *in vivo*, we generated *Oplah* knock-out mice, Oplah$^{tm1a(KOMP)Wtsi}$ (here after referred to as KO) mice (23). Heterozygous (HET) male mice were mated with HET female mice resulting on average in a nest size of 7.8 pups with the mendelian distribution of 32.5% KO, 45.5% HET, and 22.0% wild-type (WT) mice. On mRNA and protein level the expression of OPLAH was ~50% reduced in the HET mice, relative to the expression in the WT littermates

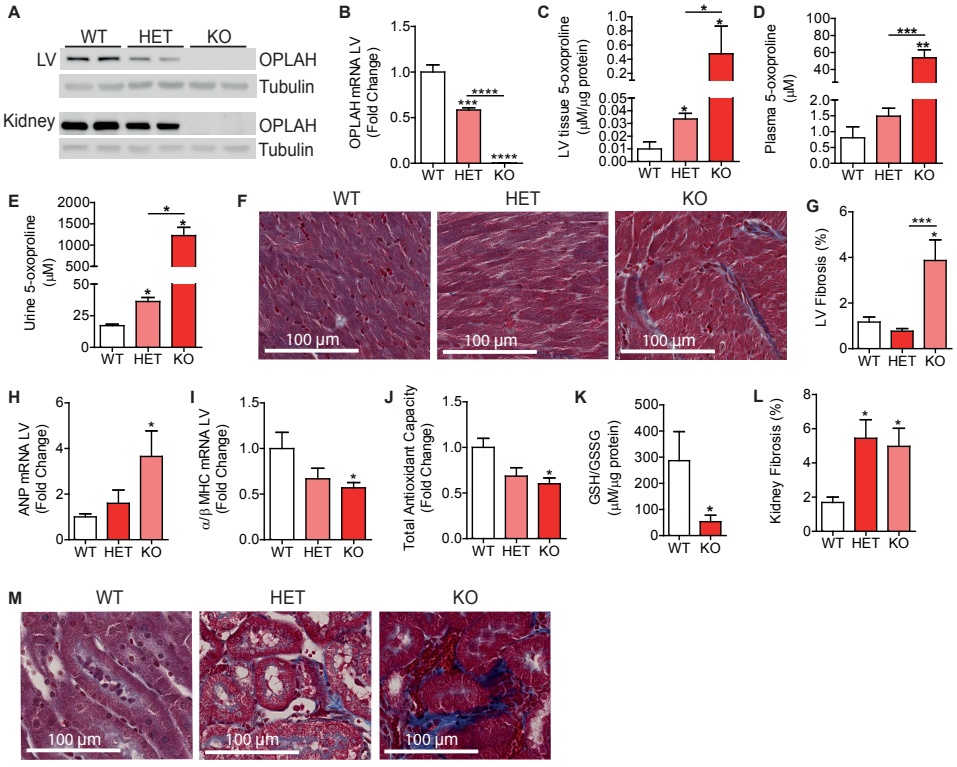


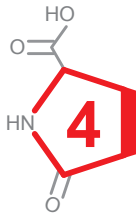


**Fig. 1. Baseline characterization of the Oplah knock-out mice.**
**A.** Representative immunoblotting analysis of OPLAH expression in the left ventricle (LV) and kidney of wild-type mice (WT), heterozygous mice (HET), and full body Oplah knock-out mice (KO). **B.** qRT-PCR mRNA expression of OPLAH in the LV of WT (n = 6), HET (n = 7), and KO (n = 5) mice. **C.** LV tissue 5-oxoproline of WT (n = 5), HET (n = 7), and KO (n = 5) mice. **D.** Plasma 5-oxoproline of WT (n = 5), HET (n = 9), and KO (n = 5) mice. **E.** Urine 5-oxoproline of WT, HET, and KO (n = 4) mice. **F.** Representative LV tissue sections with Masson's trichrome of WT, HET and KO mice. **G.** Percent LV fibrosis in WT (n = 6), HET (n = 9) and KO (n = 5) mice. **H.** qRT-PCR mRNA expression of ANP in the LV of WT (n = 5), HET (n = 7) and KO (n = 5) mice. **I.** qRT-PCR mRNA expression of α/β-MHC ratio in the LV of WT (n = 6), HET (n = 7) and KO (n = 5) mice. **J.** LV tissue total antioxidant capacity of WT (n = 4), HET (n = 3) and KO (n = 4) mice. **K.** Ratio of reduced glutathione (GSH) to oxidized glutathione (GSSG) in WT (n = 3) and KO (n = 5) mice. **L.** Percent kidney fibrosis in WT (n = 6), HET (n = 9) and KO (n = 5) mice. **M.** Representative kidney tissue sections with Masson's trichrome staining of WT, HET and KO mice. Data are presented as means ± SEM *, P < 0.05; **, P < 0.01; ***, P < 0.001; ****, P < 0.0001, as calculated by one-way analysis of variance (ANOVA) and Student's T-test.

and absent in the KO mice (Fig. 1A-1B). Since OPLAH is an enzyme involved in converting 5-oxoproline to glutamate, we measured the concentration of left ventricular (LV) tissue, plasma and urine 5-oxoproline in these mice. 5-Oxoproline levels in all samples were significantly elevated in the KO mice, compared to the WT mice (Fig. 1C-1E). HET mice demonstrated a significant increase in LV tissue and urine 5-oxoproline, and a mild non-significant increase in 5-oxoproline levels in the plasma, compared to the WT mice. These findings suggest that a single functional

**Table 1. Phenotypic characterization of wild-type (WT), heterozygous (HET), and knock-out (KO) mice.**

| | WT | HET | KO |
|---|---|---|---|
| **Variable** | **n = 6** | **n = 9** | **n = 5** |
| Body weight (tibia corrected), g/cm | 17.6 ± 2.5 | 17.6 ± 2.9 | 18.5 ± 4.7 |
| Organ weight (tibia corrected), mg/cm | | | |
| Atria | 3.3 ± 0.4 | 4.2 ± 0.8* | 4.1 ± 0.3* |
| Right Ventricle | 14.6 ± 1.2 | 14.2 ± 1.9 | 14.1 ± 1.7 |
| Left Ventricle | 61.8 ± 5.5 | 62.8 ± 9.0 | 64.9 ± 8.4 |
| Kidney | 248.1 ± 29.3 | 239.8 ± 29.0 | 267.2 ± 38.6 |
| Liver | 822.8 ± 105.1 | 821.7 ± 119.6 | 860.1 ± 226.3 |
| Hemodynamic measurements | | | |
| Systolic blood pressure (mmHg) | 99.6 ± 8.9 | 99.2 ± 6.9 | 103.7 ± 8.8 |
| Diastolic blood pressure (mmHg) | 67.1 ± 6.8 | 66.5 ± 6.3 | 61.1 ± 6.6 |
| LV End systolic pressure (mmHg) | 88.9 ± 10.5 | 88.2 ± 13.8 | 92.6 ± 12.1 |
| LV End diastolic pressure (mmHg) | 5.8 ± 2.9 | 8.4 ± 4.2 | 11.3 ± 4.6* |
| Tau (ms) | 6.8 ± 0.8 | 7.29 ± 1.0 | 8.5 ± 1.2* |
| dP/dT max (mmHg/s) | 8493.4 ± 1331.1 | 8023.6 ± 1241.9 | 7676.5 ± 982.5 |
| dP/dT min (mmHg/s) | -7624.8 ± 1115.7 | -7162.5 ± 1397.4 | -6624.1 ± 1358.6 |
| Heart rate (BPM) | 450.9 ± 23.5 | 427.0 ± 56.5 | 455.6 ± 63.5 |
| LV ejection fraction (%) | 53.2 ± 2.6 | 55.3 ± 8.8 | 54.8 ± 2.9 |
| LV End systolic volume (µL) | 24.6 ± 5.5 | 23.6 ± 8.6 | 21.3 ± 1.5 |
| LV End diastolic volume (µL) | 52.8 ± 11.4 | 51.6 ± 11.9 | 50.1 ± 5.9 |
| Stroke volume (µL) | 28.2 ± 6.3 | 27.9 ± 5.6 | 28.9 ± 4.9 |

* = P > 0.05 WT VS KO or HET

*Oplah* gene is sufficient to some extend maintain the homeostasis of 5-oxoproline.

**Oplah knock-out mice develop a HFpEF phenotype**

Next, we were interested in characterizing if the reduction in OPLAH, and therefore an increase in 5-oxoproline, resulted in a cardiac phenotype. At 20 weeks of age we performed cardiac MRI, hemodynamic measurements and histological analysis on the KO, HET and WT mice. With exception to an increase in atria weight in the KO and HET mice, organ weights were similar to those of the WT littermates (Table 1). Interestingly, in terms of hemodynamic measurements we observed that the KO mice had significantly increased LV end diastolic pressures (LVEDP) [11.3 ± 4.6 mmHg (KO) vs 5.8 ± 2.9 mmHg (WT), P = 0.047] and an increase in the isovolumic relaxation constant (Tau) [8.5 ± 1.2 ms (KO) vs 6.8 ± 0.8 ms (WT), P = 0.037],

with a preserved LV ejection fraction (LVEF) (Table 1). The HET mice demonstrated a similar trend, however these were significantly different from the WT littermates [LVEDP = 8.4 ± 4.2 mmHg (HET) vs 5.8 ± 2.9 mmHg (WT), P = 0.093, Tau = 7.3 ± 1.0 ms (HET) vs 6.8 ± 0.8 ms (WT), P = 0.368]. Histological analysis revealed that the KO mice had increased LV fibrosis, which was coupled to an increase in atrial natriuretic peptide (*Anp*) expression and reduction in α/β myosin heavy chain (MHC) ratio (both of which are markers for increased cardiac injury) (Fig. 1F-1I). The HET mice did not demonstrate an increase in LV fibrosis, nor did they display a significant increase in *Anp* or reduction in α/β MHC ratio. To determine whether the cardiac phenotype was a result of an increase in oxidative stress, we assessed the total antioxidant capacity (TAC) in these mice. The KO mice were found to have a significantly reduced TAC, while the HET demonstrate a non-significant reduction, when compared to the WT littermates (Fig. 1J). It was previously also reported that 5-oxoproline could induce protein oxidation in rat brain tissue (20,21). To test whether this was also the case in these mice, we measured the total protein carbonylation, a well-known marker for oxidative stress and protein oxidation, in the LV of these animals (Fig. S1). The KO mice were found to have a significant increase in total protein carbonyl content, while the HET animals had a mild non-significant increase, when compared to the WT littermates. To further assess the levels of oxidative stress in the KO mice, we measured the reduced to oxidized glutathione (GSH/GSSG) ratio, a well-established indicator for oxidative stress, by means of LC-MS (Fig. 1K). The KO mice were found to have a significant reduction in the GSH/GSSG. These observations are in line with previous reports showing that 5-oxoproline is an oxidative stress inducing agent (16,20,21). Surprisingly, both the KO and HET mice were found to have significantly elevated kidney fibrosis (Fig. 1L-M). Combined these findings demonstrate that the ablation of OPLAH, resulting in increased 5-oxoproline levels, leads to oxidative stress, cardiac fibrosis, atrial enlargement, impaired LV relaxation, increased LV filling pressures, and renal fibrosis with a preserved LVEF. These observations are similar to those observed in patients with HFpEF (33), suggesting a possible link between the OPLAH/5-oxoproline axis and the onset of HFpEF.

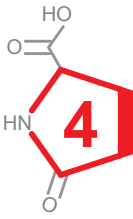


**Oplah knock-out mice are more susceptible to cardiac ischemia/reperfusion injury**

Following the baseline characterization of the KO mice, we hypothesized that these mice would be more susceptible to cardiac events. Therefore, we performed cardiac ischemia/reperfusion (IR), were the mice underwent 60 min of ischemia followed by 4 weeks of reperfusion. Upon the induction of IR injury there was a dramatic incidence of sudden death in both the KO and HET mice, an effect not observed in the WT littermates [survival rate 47.6%, 68.8% and 84.6%, respectively (Fig. 2A)]. To assess why this significant incidence of sudden death occurred in the KO mice, when compared to the WT mice (P = 0.03), we performed ECG measurement during

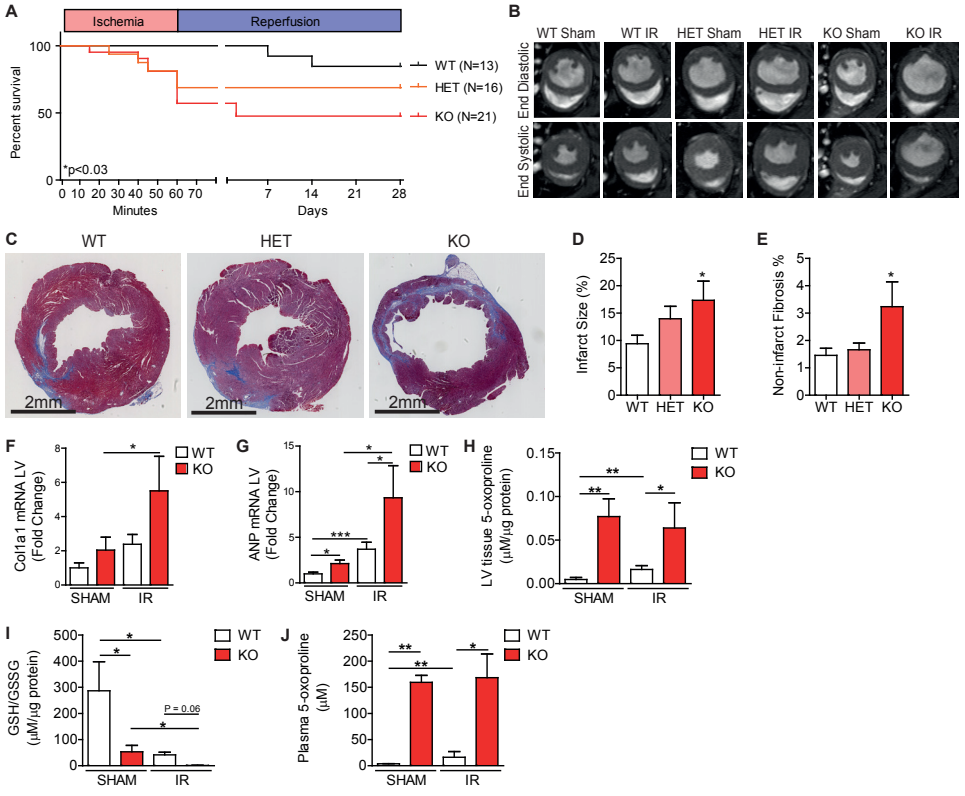


**Fig. 2. Oplah knock-out mice are more susceptible to cardiac ischemia/reperfusion (IR) injury.** **A.** Survival data of wild-type (WT, n = 13), heterozygous (HET, n = 16) and Oplah knock-out (KO, n = 21) mice following the implementation of IR injury. **B.** Representative cardiac MRI images of WT, HET and KO mice hearts. **C.** Representative LV tissue sections with Masson's trichrome staining of WT, HET and KO mice with cardiac IR injury. **D-E.** Quantified LV infarct size (**D**) and non-infarct fibrosis (**E**) of WT (n = 11), HET (n = 8) and KO (n = 8) post-IR injury. **F.** qRT-PCR analysis of LV mRNA for Collagen type 1, alpha 1 (*Col1a1*) (WT SHAM n = 15, WT IR n = 11, KO SHAM n = 14, KO IR n = 10). **G.** qRT-PCR analysis of LV mRNA for Atrial natriuretic peptide (*Anp*) (WT SHAM n = 15, WT IR n = 11, KO SHAM n = 14, KO IR n = 10). **H.** LV tissue 5-oxoproline levels (WT SHAM n = 11, WT IR n = 11, KO SHAM n = 6, KO IR n = 4). **I.** Ratio of reduced glutathione (GSH) to oxidized glutathione (GSSG) in LV tissue (WT SHAM n = 3, WT IR n = 4, KO SHAM n = 5, KO IR n = 3). **J.** Plasma 5-oxoproline levels (WT SHAM n = 11, WT IR n = 11, KO SHAM n = 6, KO IR n = 3). Data are presented as means ± SEM *, P < 0.05; **, P < 0.01; ***, P < 0.001, as calculated by one-way analysis of variance (ANOVA) and Student's T-test. In (A) as calculated by Log-rank (Mantel-Cox) Test.

the ischemic phase. We found no incidence of ventricular tachycardia or ventricular fibrillation (Figure S2A). Furthermore, we also did not observe cardiac tamponade (also known as cardiac rupture or free wall rupture) in the KO mice that perished during the procedure. (Figure S2B-S2D). The KO animals that did die had an ECG with a dying heart pattern, characterized by an extreme bradycardia, widening of the QRS complexes and a decrease in R amplitude, leading to asystole. The KO mice that survived the procedure, seemed to have similar cardiac electrical activity as the

WT littermates. The incidence of sudden death in the KO mice is not a result from tachyarrhythmias, but rather of a dying heart

**Oplah knock-out mice have more cardiac and renal damage following cardiac ischemia/reperfusion injury**

To assess what the effect of IR injury were on the surviving KO mice, cardiac MRI and PV-loop analysis were performed 4 weeks after the induction of IR. The surviving KO mice had a substantially worsened cardiac function post-IR, compared to the HET and WT mice, as measured by LVEF and stroke volume (Fig. 2B and Table 2). Furthermore, we observed a significant enlargement of the atria, LV, kidney, and liver of the KO mice exposed to IR-injury (Table 2). Histological analysis of the LV demonstrated that the KO mice had significantly larger infarct sizes compared to WT [17.3 ± 9.9% vs 10.4 ± 5.2%, respectively, p=0.043 (Fig. 2C-2D)], coupled to an increase in non-infarcted fibrosis [3.2 ± 2.6% vs 1.2 ± 0.9%, respectively, P = 0.045 (Fig. 2E)]. Following IR injury, the KO mice were also found to have a significant increase in cell size, as measured by means of FITC-labeled WGA staining, an effect not observed in the WT or HET mice (Fig. S3). The effects of IR injury on the HET mice were comparable to those observed in the WT mice, with no significant differences in terms of cardiac function, infarct size and organ weights (Fig. 2C-2E and Table 2).

To further characterize the increase in cardiac fibrosis observed in the KO mice, we measured the expression of several fibrosis markers; collagen type 1 (*Col1a1*), collagen type 3 (*Col1a3*), TIMP metallopeptidase inhibitor 1 (*Timp-1*), matrix metalloproteinase 2 (*Mmp-2*), matrix metalloproteinase 9 (*Mmp-9*), Galectin-3 (*Gal-3*), Procollagen C-endopeptidase enhancer 1 (*Pcolce*), and interleukin 1 receptor-like 1 (*Il1rl1*, also known as *St2*) in cardiac tissue. The KO mice were found to have a significant increase in *Col1a1*, *Col1a3*, *Gal-3*, *Pcolce*, and *Il1rl1*, when compared to the WT mice post-IR injury (Fig. 2F and Fig. S4A-D). Interestingly, the KO mice also had an increase in *Timp-1*/*Mmp-2* and *Timp-1*/*Mmp-9* ratios (Fig. S4E-S4I). These findings suggest that within the KO mice there is a shift from fibrosis breakdown to production. Furthermore, the KO mice also demonstrated an increased Anp expression levels when compared to the WT littermates (Fig. 2G). Besides the evident increase in cardiac fibrosis, we also observed that the KO mice had a substantial increase in LV tissue 5-oxoproline levels, coupled to an increase in oxidative stress as measured by means of the GSH/GSSG ratio (Fig. 2H-2I). Furthermore, the plasma 5-oxoproline levels were also elevated in the KO mice (Fig. 2J). Interestingly, in both the cardiac tissue and plasma we observed an increase in 5-oxoproline levels in the WT mice following IR injury, which coincides with an increase in cardiac tissue oxidative stress (Fig. 2H-2J).

**Table 2. Characteristics of wild-type (WT), heterozygous (HET) and knock-out (KO) mice at baseline (Sham) and post-ischemia/reperfusion (IR) injury.**

| | WT | | HET | | KO | |
|---|---|---|---|---|---|---|
| **Variable** | **Sham (n = 15)** | **IR (n = 11)** | **Sham (n = 22)** | **IR (n = 11)** | **SHAM (n = 16)** | **IR (n = 10)** |
| Body weight (tibia corrected), g/cm | 17.7 ± 2.2 | 17.6 ± 1.1 | 18.4 ± 2.7 | 19.2 ± 1.5 | 18.1 ± 2.9 | 18.6 ± 1.3 |
| Organ weight (tibia corrected), mg/cm | | | | | | |
| Atria | 3.5 ± 0.6 | 4.4 ± 0.6* | 4.1 ± 0.8# | 3.6 ± 0.7 | 4.2 ± 0.9# | 5.5 ± 0.9**,# |
| Right Ventricle | 13.8 ± 1.5 | 15.4 ± 1.2* | 14.2 ± 1.9 | 15.5 ± 3.3 | 14.4 ± 1.9 | 16.4 ± 2.3* |
| Left Ventricle | 61.3 ± 5.4 | 72.0 ± 3.9**** | 64.9 ± 3.9 | 68.4 ± 5.8 | 64.6 ± 6.2 | 83.0 ± 11.0****,# |
| Kidney | 239.5 ± 30.4 | 241.8 ± 16.7 | 247.0 ± 34.3 | 266.6 ± 24.8* | 244.8 ± 29.3 | 284.7 ± 29.3*,# |
| Liver | 850.2 ± 105.3 | 857.2 ± 32.5 | 873.4 ± 137.0 | 922.5 ± 89.9 | 868.0 ± 134.3 | 1059.8 ± 137.9**,## |
| Hemodynamic measurements | | | | | | |
| Systolic blood pressure (mmHg) | 99.0 ± 9.6 | 97.1 ± 10.3 | 100.7 ± 6.3 | 103.9 ± 9.0 | 99.7 ± 12.6 | 98.2 ± 5.2 |
| Diastolic blood pressure (mmHg) | 65.8 ± 5.9 | 66.1 ± 9.4 | 65.9 ± 5.3 | 67.5 ± 8.4 | 60.8 ± 13.9 | 65.8 ± 5.3 |
| LV End systolic pressure (mmHg) | 94.4 ± 10.2 | 97.9 ± 9.5 | 93.7 ± 11.5 | 91.9 ± 13.9 | 92.4 ± 15.2 | 94.8 ± 6.3 |
| LV End diastolic pressure (mmHg) | 5.5 ± 3.8 | 15.9 ± 4.3**** | 9.6 ± 5.1# | 14.8 ± 5.9* | 9.3 ± 3.4# | 16.2 ± 2.3**** |
| Tau (ms) | 7.1 ± 1.4 | 10.4 ± 2.8*** | 7.6 ± 1.6 | 9.1 ± 2.0* | 8.5 ± 1.2# | 9.3 ± 2.2 |
| dP/dT max (mmHg/s) | 8210.4 ± 1297.0 | 7046.5 ± 1418.5 | 7837.8 ± 1140.8 | 7494.9 ± 1247.9 | 7287.4 ± 967.9 | 6983.8 ± 956.7 |
| dP/dT min (mmHg/s) | -7543.6 ± 1520.1 | -5473.3 ± 1172.2 ** | -7097.9 ± 1343.9 | -6018.7 ± 1427.4 | -6419.3 ± 1071.6 | -5811.1 ± 978.7 |
| Heart rate (BPM) | 454.3 ± 27.5 | 477.2 ± 41.7 | 433.6 ± 53.0 | 462.9 ± 44.5 | 463.3 ± 54.0 | 488.2 ± 47.0 |
| LV ejection fraction (%) | 49.2 ± 5.6 | 42.0 ± 7.4* | 54.7 ± 7.9 | 42.7 ± 11.7** | 51.7 ± 8.9 | 33.9 ± 8.4**,# |
| LV End systolic volume (µL) | 27.6 ± 6.9 | 38.8 ± 12.9* | 24.4 ± 7.4 | 39.6 ± 18.9* | 26.4 ± 10.2 | 44.1 ± 19.3* |
| LV End diastolic volume (µL) | 54.0 ± 9.9 | 66.1 ± 16.4* | 53.0 ± 9.8 | 66.8 ± 18.3* | 53.3 ± 12.2 | 66.1 ± 20.4 |
| Stroke volume (µL) | 26.4 ± 4.8 | 27.3 ± 5.7 | 28.6 ± 4.7 | 27.2 ± 4.2 | 27.0 ± 4.9 | 21.9 ± 1.9*,# |

* = p>0.05 Sham VS IR

** = p>0.01 Sham VS IR

*** = p>0.001 Sham VS IR

**** = p>0.0001 Sham VS IR

# = p>0.05 WT VS KO or HET

## = p>0.01 WT VS KO or HET

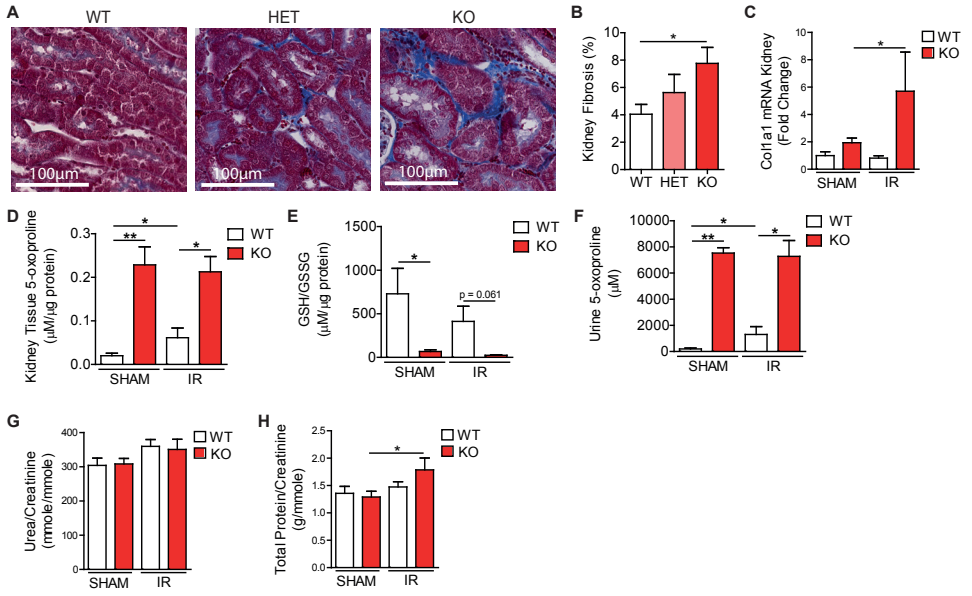


**Fig. 3. Oplah knock-out mice develop increased renal damage following cardiac ischemia/reperfusion (IR) injury.**
**A.** Representative kidney tissue sections with Masson's trichrome staining of WT, HET and KO mice with cardiac IR injury. **B.** Quantification of percent kidney fibrosis (WT n = 11, HET n = 11, KO n = 8). **C.** qRT-PCR analysis of kidney mRNA for Collagen type 3, alpha 1 (*Col3a1*) (WT SHAM n = 10, WT IR n = 9, KO SHAM n = 15, KO IR n = 10). **D.** Kidney tissue 5-oxoproline (WT SHAM n = 11, WT IR n = 11, KO SHAM n = 6, KO IR n = 3). **E.** Ratio of reduced glutathione (GSH) to oxidized glutathione (GSSG) in kidney tissue (WT SHAM n = 3, WT IR n = 11, KO SHAM n = 4, KO IR n = 3). **F.** Urine 5-oxoproline (WT SHAM n = 11, WT IR n = 11, KO SHAM n = 6, KO IR n = 3). **G.** Urinary urea to creatinine ratio (WT SHAM n = 11, WT IR n = 10, KO SHAM n = 9, KO IR n = 7). **H.** Urinary total protein to creatinine ratio (WT SHAM n = 11, WT IR n = 10, KO SHAM n = 9, KO IR n = 7). Data are presented as means ± SEM *, P < 0.05; **, P < 0.01, as calculated by one-way analysis of variance (ANOVA) and Student's T-test.

Since at baseline we observed that the KO and HET mice had an increase in renal fibrosis, we also assessed renal fibrosis following IR injury in these mice. We observed that the KO mice had a significant increase in renal fibrosis compared to the WT littermates, while the HET only demonstrate a mild non-significant increase (Fig. 3A-3B).The kidneys of the KO mice were also found to have increased expression of fibrotic markers *Col1a1* and an increase in the *Timp-1*/*Mmp-2* and *Timp-1*/*Mmp-9* (Fig. 3C and Fig. S5A-S5E). Furthermore, we also found the kidneys of the KO mice to have increased expression of *Il1rl1*, when compared to the WT mice (Fig. S4F). These findings suggest that similar to the heart, in the kidneys there also seems to be a switch towards increased fibrosis deposition. Interestingly, we also observed an increase in renal 5-oxoproline levels and oxidative stress (Fig. 3D-3E). To further characterize the effect OPLAH depletion has on kidney function, we measured the 5-oxoproline levels, urea/creatinine and total protein/creatinine ratios in the urine of

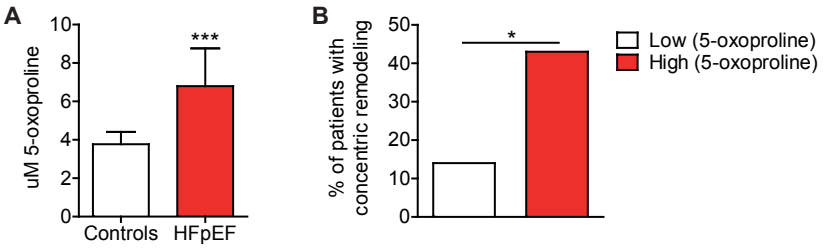


**Fig. 4. 5-oxoproline in patients with HFpEF.**
**A.** 5-oxoproline concentrations in healthy controls (controls, n = 6) compared to patients with HFpEF (n = 51). **B.** Percentage of HFpEF patients with left ventricular concentric remodeling according to levels of 5-oxoproline above (High, 6.7 – 12.8 μM, n = 25) and below (Low, 3.7 – 6.7 μM, n = 26) the median. In (**A**) data are presented as means ± SEM ***, P < 0.001, as calculated by Student's t test. In (**B**) data are presented as percentages *, P < 0.05, as calculated by Student's t test.

our mice (Fig. 3F-3H). 5-Oxoproline levels were found to be significantly elevated in the urine of the KO mice, and the WT mice demonstrated an increase in urine 5-oxoproline following IR injury. No significant differences were observed in the urea/creatinine ratio between the KO and WT mice . However, the KO mice were found to have an increase in total protein/creatinine ratio following cardiac IR injury compared to WT. Combined these findings suggest that mice lacking OPLAH, are not only more susceptible to cardiac injury when challenged with IR, but also to renal injury.

**5-oxoproline in plasma of HFpEF patients**

Plasma 5-oxoproline was measured in 6 healthy controls (Table S3) and in a cohort of 51 HFpEF patients (Table S4). We found plasma 5-oxoproline levels to be ±2-fold higher in the HFpEF patients compared to healthy controls (6.8 ± 1.9 μM vs 3.8 ± 0.6 μM, respectively, P = 0.0001) (Fig. 4A). To further address the involvement of 5-oxoproline within the patient HFpEF patient cohort, we compared clinical charateristics and echocardiographic parameters between patients with high (above the median) and low (below the median) levels of 5-oxoproline. The data on echocardiography measurements of the HFpEF patient cohort are presented in Table 3. Within this cohort of HFpEF patients we observed equal levels of plasma 5-oxoproline in men and women (p = 0.273). Overall, patients with high 5-oxoproline levels had almost double the prevalence of concentric remodeling (14% vs. 43%, p= 0.040, Fig. 3B). When additionally correcting for age, sex, BMI and levels of NT-proBNP, levels of 5-oxoprolinase remained independently associated with more concentric remodeling (Odds ratio:1.55; 95%CI 1.03-2.33; p=0.038). This observations suggests that OPLAH and 5-oxoproline are not only involved in HFpEF in the murine setting, but also in the clinical manifestation of the disease.

**Table 3. Echocardiographic characteristics by 5-oxoproline concentration**

| | 5-oxoproline (3.7 - 6.7 µM) | 5-oxoproline (6.7 - 12.8 µM) | |
|---|---|---|---|
| **Factor** | **n = 26** | **n = 25** | **P value** |
| Left ventricular ejection fraction, % | 60.0 (55.0, 60.0) | 60.0 (60.0, 60.0) | 0.47 |
| Left ventricular end diastolic diameter, mm | 48.0 (44.0, 52.0) | 46.0 (43.0, 51.0) | 0.69 |
| Left ventricular posterior wall thickness, mm | 9.0 (8.0, 9.0) | 10.0 (9.0, 11.0) | 0.020 |
| Intraventricular septum thickness, mm | 11.0 (9.0, 12.0) | 11.0 (9.5, 12.0) | 0.39 |
| e' lateral, cm/s | 8.3 (5.9, 9.7) | 8.5 (7.2, 13.7) | 0.20 |
| E/e' ratio | 13.4 (11.1, 20.3) | 11.8 (10.0, 16.6) | 0.24 |
| Isovolumetric relaxation time, ms | 89.0 (74.0, 94.0) | 77.0 (69.0, 89.0) | 0.26 |
| TAPSE, mm | 19.0 (17.0, 22.0) | 18.0 (16.0, 21.0) | 0.39 |
| Concentric remodeling, % | 14 | 43 | 0.04 |

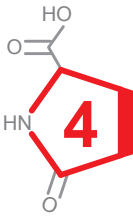


## Discussion

HF is one the most challenging health problems of the developed world, with a five year survival rate of less than 50% (2). Nearly half of all patients with HF symptoms, have a preserved ejection fraction which is characterized by renal damage, cardiac stiffening, increased oxidative stress, and atrial enlargement (2,33). Due to the fact that HFpEF patients generally are afflicted with multiple comorbidities [including obesity, hypertension, renal disease, atrial fibrillation, metabolic syndrome, and diabetes mellitus (33)], it is difficult to discern the underlying cardiac pathophysiology leading to the disease. Therefore it is essential to develop novel animal models to help uncover the pathophysiological pathways implicated in this disease (4).

In the field of cardiovascular research most of the HF animal models currently employed are representative of HFrEF, although several models have been proposed that mimic HFpEF. Most of these animal models currently available attempt to reproduce the typical causes of diastolic dysfunction in HFpEF, namely ageing [i.e. FVB/N mice (34)], diabetes mellitus [i.e. db/db mice (35) and ob/ob mice (36)] and hypertension [i.e. aortic constriction (37) and DOCA-Salt mice (38)]. However, these animal models are unable to recapitulate all the features present in the human disease. Furthermore, in most cases these animal models eventually lead to the development of HFrEF (3), whereas in the clinical setting patients diagnosed with HFpEF only transitions into HFrEF with an additional cardiac event (i.e. myocardial infarction, coronary artery disease) (39–41). As such these animal models have limitations for preclinical evaluation of potentially novel therapeutic strategies.

One of the proposed pathophysiological pathways implicated in HFpEF is an increase in oxidative stress (33,42,43). The increase in ROS production has been shown to induce a hypophosphorylation of titin, leading to increased resting tension of cardiomyocytes (a characteristic of increased myocardial passive stiffness) (44-46). Excess ROS production also results in inflammation and cardiomyocyte stress (44,45). Furthermore, ROS has been shown to increase collagen deposition leading to fibrosis (5). These observations suggest that oxidative stress may play an important role in the onset of HFpEF.

The involvement of OPLAH in the heart, and in particular in HF, has only recently been described (16). OPLAH is an enzyme involved in the γ-Glutamyl cycle, where it is responsible for the conversion of 5-oxoproline, a degradation product of Glutathione, back into glutamate (6,19). Previous studies have demonstrated that 5-oxoproline is an oxidative stress inducing agent, thus OPLAH has an antioxidant function by removing this metabolite (16,20,21). In this study we further characterized the role of OPLAH and its substrate 5-oxoproline in HF, with a specific focus on HFpEF. At baseline OPLAH ablation in mice resulted in increased 5-oxoproline, oxidative stress, atrial enlargement, fibrosis, ventricular filling pressures, and impaired LV relaxation coupled to a preserved LV ejection fraction. Interestingly, at baseline the *Oplah* KO mice did not only develop a cardiac phenotype, but we also observed an increase in renal fibrosis, suggesting the increase in 5-oxorpoline was resulting in renal damage. This is of particular interest, since one of the well characterized non-cardiac comorbidities of patients with HFpEF is renal failure (2). Furthermore, we also found that both the heart and the kidneys of the KO mice had higher expression of *St2*, a known marker for inflammation and fibrosis, with a strong link to clinical HFpEF (47–49). Interestingly, when challenged, these mice were found to be more susceptible to cardiac damage and sudden death, following cardiac IR injury. This observation is in line with the observations that HFpEF patients exposed to a cardiac event have an increase incidence of sudden death (39–41). Furthermore, genetic disruption of *Oplah* not only lead to an increase in cardiac damage, but we also observed that the *Oplah* KO mice developed proteinuria following IR injury. Taken together the observed cardiac and renal phenotype in the *Oplah* KO mice, suggests that complete disruption of *Oplah* leads to changes resembling clinical HFpEF (Table S5). Combined with previous findings, that OPLAH overexpression has a cardio protective effect (16), suggest future efforts should be made in identifying compounds with the capacity to indue OPLAH expression or activity. This could lead to novel therapeutic strategies for HF patients, and more interestingly for HFpEF patients.

To further establish the link between our *Oplah* KO mice and HFpEF, we measured

the levels of circulating 5-oxoproline in a cohort of HFpEF patients. We found 5-oxoproline to be significantly elevated in HFpEF patients, when compared to healthy controls. Furthermore, higher levels of circulating 5-oxoproline were found to independently associate with more concentric remodeling, a hallmark of HFpEF.

Although our proposed murine model for HFpEF strongly mimics the development of this disease in the human setting, there remain several limitations to this model. The main limitation is that in this model HFpEF is developed as a result of direct genetic manipulation. Thus, it is uncertain whether the pathophysiological pathway, implicating OPLAH and 5-oxoproline, is also involved in the onset of HFpEF in humans. Rather one could also speculate that the effects we observe in the *Oplah* KO mice are a result of the severe oxidative stress, due to accumulation of the oxidative stress inducing agent 5-oxoproline. Another limitation is that following the induction of IR injury, there was a drastic incidence of sudden death in the *Oplah* KO mice, therefore any analysis performed on the surviving KO mice is an underestimation of severity of cardiac injury on these mice. Furthermore, the surviving mice transitioned into a HFrEF phenotype, with reduce LV ejection fraction. These observation are in line with previous clinical studies which found that following a cardiac event, HFpEF patients would transition into HFrEF and had an increased incidence of sudden death (39–41). Therefore, it would be of interest to perform an RNA sequencing analysis on these animals to maybe shed some new light on possible pathophysiological pathways involved in the onset of HFpEF in these animals at baseline and how this shifts to a HFrEF phenotype following IR injury. Additionally, circulating 5-oxoproline was measured in a very specific cohort of HFpEF patients with pulmonary hypertension, and therefore it is uncertain to which extent findings of this patient cohort can be extrapolated to other patients with HFpEF. Furthermore, the sample size was rather small, inhibiting us from performing more extensive analyses.

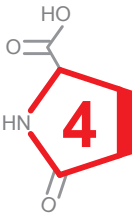


## Acknowledgments

We thank Martin Dokter and Kees van de Kolk for their excellent technical assistance.

# References


1. Owens AT, Brozena SC, Jessup M. New Management Strategies in Heart Failure. Circ Res American Heart Association, Inc.; 2016;118:480–495.
2. Ponikowski P, Voors AA, Anker SD, Bueno H, Cleland JGF, Coats AJS, Falk V, González-Juanatey JR, Harjola V-P, Jankowska EA, Jessup M, Linde C, Nihoyannopoulos P, Parissis JT, Pieske B, Riley JP, Rosano GMC, Ruilope LM, Ruschitzka F, Rutten FH, Meer P van der, Authors/Task Force Members, Document Reviewers. 2016 ESC Guidelines for the diagnosis and treatment of acute and chronic heart failure. Eur J Heart Fail 2016;18:891–975.
3. Conceição G, Heinonen I, Lourenço AP, Duncker DJ, Falcão-Pires I. Animal models of heart failure with preserved ejection fraction. Netherlands Hear J Bohn Stafleu van Loghum; 2016;24:275–286.
4. Roh J, Houstis N, Rosenzweig A. Why Don't We Have Proven Treatments for HFpEF? Circ Res American Heart Association, Inc.; 2017;120:1243–1245.
5. Paulus WJ, Tschöpe C. A Novel Paradigm for Heart Failure With Preserved Ejection Fraction. J Am Coll Cardiol 2013;62:263–271.
6. Liu Y, Hyde AS, Simpson MA, Barycki JJ. Emerging regulatory paradigms in glutathione metabolism. Adv Cancer Res 2014;122:69–101.
7. Stanley BA, Sivakumaran V, Shi S, McDonald I, Lloyd D, Watson WH, Aon MA, Paolocci N. Thioredoxin reductase-2 is essential for keeping low levels of H(2)O(2) emission from isolated heart mitochondria. J Biol Chem American Society for Biochemistry and Molecular Biology; 2011;286:33669–33677.
8. Aon MA, Stanley BA, Sivakumaran V, Kembro JM, O'Rourke B, Paolocci N, Cortassa S. Glutathione/thioredoxin systems modulate mitochondrial H2O2 emission: an experimental-computational study. J Gen Physiol The Rockefeller University Press; 2012;139:479–491.
9. Hoshino Y, Shioji K, Nakamura H, Masutani H, Yodoi J. From Oxygen Sensing to Heart Failure: Role of Thioredoxin. Antioxid Redox Signal Mary Ann Liebert, Inc. 2 Madison Avenue Larchmont, NY 10538 USA ; 2007;9:689–699.
10. Chen C, Chen H, Zhou HJ, Ji W, Min W. Mechanistic Role of Thioredoxin 2 in Heart Failure. Advances in experimental medicine and biology 2017. p. 265–276.
11. Whayne TF, Parinandi N, Maulik N. Thioredoxins in cardiovascular disease. Can J Physiol Pharmacol 2015;93:903–911.
12. Kobayashi T, Watanabe Y, Saito Y, Fujioka D, Nakamura T, Obata J, Kitta Y, Yano T, Kawabata K, Watanabe K, Mishina H, Ito S, Kugiyama K. Mice lacking the glutamate-cysteine ligase modifier subunit are susceptible to myocardial ischaemia-reperfusion injury. Cardiovasc Res 2010;85:785–795.
13. Nakamura S, Kugiyama K, Sugiyama S, Miyamoto S, Koide S, Fukushima H, Honda O, Yoshimura M, Ogawa H. Polymorphism in the 5'-flanking region of human glutamate-cysteine ligase modifier subunit gene is associated with myocardial infarction. Circulation 2002;105:2968–2973.
14. Shiomi T, Tsutsui H, Matsusaka H, Murakami K, Hayashidani S, Ikeuchi M, Wen J, Kubota T, Utsumi H, Takeshita A. Overexpression of glutathione peroxidase prevents left ventricular remodeling and failure after myocardial infarction in mice. Circulation 2004;109:544–549.
15. Zhang Y, Handy DE, Loscalzo J. Adenosine-dependent induction of glutathione peroxidase 1 in human primary endothelial cells and protection against oxidative stress. Circ Res American Heart Association, Inc.; 2005;96:831–837.
16. Pol A van der, Gil A, Silljé HHW, Tromp J, Ovchinnikova ES, Vreeswijk-Baudoin I, Hoes M, Domian IJ, Sluis B van de, Deursen JM van, Voors AA, Veldhuisen DJ van, Gilst WH van, Berezikov E, Harst P van der, Boer RA de, Bischoff R, Meer P van der. Accumulation of 5-oxoproline in myocardial dysfunction and the protective effects of OPLAH. Sci Transl Med 2017;9:eaam8574.
17. Galasso G, Schiekofer S, Sato K, Shibata R, Handy DE, Ouchi N, Leopold JA, Loscalzo J, Walsh K. Impaired angiogenesis in glutathione peroxidase-1-deficient mice is associated with endothelial progenitor cell dysfunction. Circ Res American Heart Association, Inc.; 2006;98:254–261.
18. Damy T, Kirsch M, Khouzami L, Caramelle P, Corvoisier P Le, Roudot-Thoraval F, Dubois-Randé J-L, Hittinger L, Pavoine C, Pecker F. Glutathione deficiency in cardiac patients is related to the functional status and structural cardiac abnormalities. PLoS One 2009;4:e4871.
19. Meister A, Anderson ME. Glutathione. Annu Rev Biochem Annual Reviews 4139 El Camino Way, P.O. Box 10139, Palo Alto, CA 94303-0139, USA ; 1983;52:711–760.
20. Pederzolli CD, Sgaravatti AM, Braum CA, Prestes CC, Zorzi GK, Sgarbi MB, Wyse ATS, Wannmacher

CMD, Wajner M, Dutra-Filho CS. 5-Oxoproline reduces non-enzymatic antioxidant defenses in vitro in rat brain. Metab Brain Dis 2007;22:51–65.
21. Pederzolli CD, Mescka CP, Zandoná BR, Moura Coelho D de, Sgaravatti AM, Sgarbi MB, Souza Wyse AT de, Duval Wannmacher CM, Wajner M, Vargas CR, Dutra-Filho CS. Acute administration of 5-oxoproline induces oxidative damage to lipids and proteins and impairs antioxidant defenses in cerebral cortex and cerebellum of young rats. Metab Brain Dis 2010;25:145–154.
22. Yang K-C, Yamada KA, Patel AY, Topkara VK, George I, Cheema FH, Ewald GA, Mann DL, Nerbonne JM. Deep RNA sequencing reveals dynamic regulation of myocardial noncoding RNAs in failing human heart and remodeling with mechanical circulatory support. Circulation 2014;129:1009–1021.
23. Skarnes WC, Rosen B, West AP, Koutsourakis M, Bushell W, Iyer V, Mujica AO, Thomas M, Harrow J, Cox T, Jackson D, Severin J, Biggs P, Fu J, Nefedov M, Jong PJ de, Stewart AF, Bradley A. A conditional knockout resource for the genome-wide study of mouse gene function. Nature Nature Research; 2011;474:337–342.
24. Ryder E, Gleeson D, Sethi D, Vyas S, Miklejewska E, Dalvi P, Habib B, Cook R, Hardy M, Jhaveri K, Bottomley J, Wardle-Jones H, Bussell JN, Houghton R, Salisbury J, Skarnes WC, Ramirez-Solis R, Ramirez-Solis R. Molecular Characterization of Mutant Mouse Strains Generated from the EUCOMM/KOMP-CSD ES Cell Resource. Mamm Genome Springer US; 2013;24:286–294.
25. Karp NA, Meehan TF, Morgan H, Mason JC, Blake A, Kurbatova N, Smedley D, Jacobsen J, Mott RF, Iyer V, Matthews P, Melvin DG, Wells S, Flenniken AM, Masuya H, Wakana S, White JK, Lloyd KCK, Reynolds CL, Paylor R, West DB, Svenson KL, Chesler EJ, Angelis MH de, Tocchini-Valentini GP, Sorg T, Herault Y, Parkinson H, Mallon A-M, Brown SDM. Applying the ARRIVE Guidelines to an In Vivo Database. PLOS Biol 2015;13:e1002151.
26. Booij HG, Yu H, Boer RA De, Kolk CWA van de, Sluis B van de, Deursen JM Van, Gilst WH Van, Silljé HHW, Westenbrink BD. Overexpression of A kinase interacting protein 1 attenuates myocardial ischaemia/reperfusion injury but does not influence heart failure development. Cardiovasc Res 2016;111.
27. Schindelin J, Arganda-Carreras I, Frise E, Kaynig V, Longair M, Pietzsch T, Preibisch S, Rueden C, Saalfeld S, Schmid B, Tinevez J-Y, White DJ, Hartenstein V, Eliceiri K, Tomancak P, Cardona A. Fiji: an open-source platform for biological-image analysis. Nat Methods 2012;9:676–682.
28. Grote Beverborg N, Klip IjT, Meijers WC, Voors AA, Vegter EL, Wal HH van der, Swinkels DW, Pelt J van, Mulder AB, Bulstra SK, Vellenga E, Mariani MA, Boer RA de, Veldhuisen DJ van, Meer P van der. Definition of Iron Deficiency Based on the Gold Standard of Bone Marrow Iron Staining in Heart Failure Patients. Circ Heart Fail 2018;11:e004519.
29. Hoendermis ES, Liu LCY, Hummel YM, Meer P van der, Boer RA de, Berger RMF, Veldhuisen DJ van, Voors AA. Effects of sildenafil on invasive haemodynamics and exercise capacity in heart failure patients with preserved ejection fraction and pulmonary hypertension: a randomized controlled trial. Eur Heart J 2015;36:2565–2573.
30. Liu LCY, Hummel YM, Meer P van der, Berger RMF, Damman K, Veldhuisen DJ van, Voors AA, Hoendermis ES. Effects of sildenafil on cardiac structure and function, cardiopulmonary exercise testing and health-related quality of life measures in heart failure patients with preserved ejection fraction and pulmonary hypertension. Eur J Heart Fail 2017;19:116–125.
31. Lam CSP, Rienstra M, Tay WT, Liu LCY, Hummel YM, Meer P van der, Boer RA de, Gelder IC Van, Veldhuisen DJ van, Voors AA, Hoendermis ES. Atrial Fibrillation in Heart Failure With Preserved Ejection Fraction: Association With Exercise Capacity, Left Ventricular Filling Pressures, Natriuretic Peptides, and Left Atrial Volume. JACC Heart Fail 2017;5:92–98.
32. Haberhauer-Troyer C, Delic M, Gasser B, Mattanovich D, Hann S, Koellensperger G. Accurate quantification of the redox-sensitive GSH/GSSG ratios in the yeast Pichia pastoris by HILIC-MS/MS. Anal Bioanal Chem 2013;405:2031–2039.
33. Sharma K, Kass DA. Heart Failure With Preserved Ejection Fraction: Mechanisms, Clinical Features, and Therapies. Circ Res 2014;115:79–96.
34. Koch SE, Haworth KJ, Robbins N, Smith MA, Lather N, Anjak A, Jiang M, Varma P, Jones WK, Rubinstein J. Age- and gender-related changes in ventricular performance in wild-type FVB/N mice as evaluated by conventional and vector velocity echocardiography imaging: a retrospective study. Ultrasound Med Biol 2013;39:2034–2043.
35. Mori J, Patel VB, Abo Alrob O, Basu R, Altamimi T, Desaulniers J, Wagg CS, Kassiri Z, Lopaschuk GD, Oudit GY. Angiotensin 1-7 ameliorates diabetic cardiomyopathy and diastolic dysfunction in db/db mice by reducing lipotoxicity and inflammation. Circ Heart Fail 2014;7:327–339.

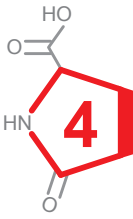

36. Bergh A Van den, Vanderper A, Vangheluwe P, Desjardins F, Nevelsteen I, Verreth W, Wuytack F, Holvoet P, Flameng W, Balligand J-L, Herijgers P. Dyslipidaemia in type II diabetic mice does not aggravate contractile impairment but increases ventricular stiffness. Cardiovasc Res Oxford University Press; 2008;77:371–379.
37. Litwin SE, Katz SE, Weinberg EO, Lorell BH, Aurigemma GP, Douglas PS. Serial echocardiographic-Doppler assessment of left ventricular geometry and function in rats with pressure-overload hypertrophy. Chronic angiotensin-converting enzyme inhibition attenuates the transition to heart failure. Circulation 1995;91:2642–2654.
38. Lovelock JD, Monasky MM, Jeong E-M, Lardin HA, Liu H, Patel BG, Taglieri DM, Gu L, Kumar P, Pokhrel N, Zeng D, Belardinelli L, Sorescu D, Solaro RJ, Dudley SC. Ranolazine improves cardiac diastolic dysfunction through modulation of myofilament calcium sensitivity. Circ Res 2012;110:841–850.
39. Clarke CL, Grunwald GK, Allen LA, Barón AE, Peterson PN, Brand DW, Magid DJ, Masoudi FA. Natural history of left ventricular ejection fraction in patients with heart failure. Circ Cardiovasc Qual Outcomes 2013;6:680–686.
40. Hwang SJ, Melenovsky V, Borlaug BA. Implications of coronary artery disease in heart failure with preserved ejection fraction. J Am Coll Cardiol 2014;63:2817–2827.
41. Dunlay SM, Roger VL, Weston SA, Jiang R, Redfield MM. Longitudinal Changes in Ejection Fraction in Heart Failure Patients With Preserved and Reduced Ejection Fraction. Circ Hear Fail 2012;5:720–726.
42. Heerebeek L van, Hamdani N, Falcão-Pires I, Leite-Moreira AF, Begieneman MP, Bronzwaer JG, Velden J van der, Stienen GJ, Laarman GJ, Somsen A, Verheugt FW, Niessen HW, Paulus WJ. Increased nitrosative/oxidative stress lowers myocardial protein kinase G activity in heart failure with preserved ejection fraction. BMC Pharmacol Toxicol BioMed Central; 2013;14:O2.
43. Franssen C, Chen S, Hamdani N, Paulus WJ. From comorbidities to heart failure with preserved ejection fraction: a story of oxidative stress. Heart 2016;102:320–330.
44. Bishu K, Hamdani N, Mohammed SF, Kruger M, Ohtani T, Ogut O, Brozovich F V, Burnett JC, Linke WA, Redfield MM. Sildenafil and B-type natriuretic peptide acutely phosphorylate titin and improve diastolic distensibility in vivo. Circulation 2011;124:2882–2891.
45. Krüger M, Kötter S, Grützner A, Lang P, Andresen C, Redfield MM, Butt E, Remedios CG dos, Linke WA. Protein kinase G modulates human myocardial passive stiffness by phosphorylation of the titin springs. Circ Res 2009;104:87–94.
46. Bull M, Methawasin M, Strom J, Nair P, Hutchinson K, Granzier H. Alternative Splicing of Titin Restores Diastolic Function in an HFpEF-Like Genetic Murine Model (TtnΔIAjxn). Circ Res American Heart Association, Inc.; 2016;119:764–772.
47. Weinberg EO, Shimpo M, Keulenaer GW De, MacGillivray C, Tominaga S, Solomon SD, Rouleau J-L, Lee RT. Expression and regulation of ST2, an interleukin-1 receptor family member, in cardiomyocytes and myocardial infarction. Circulation American Heart Association, Inc.; 2002;106:2961–2966.
48. AbouEzzeddine OF, McKie PM, Dunlay SM, Stevens SR, Felker GM, Borlaug BA, Chen HH, Tracy RP, Braunwald E, Redfield MM. Suppression of Tumorigenicity 2 in Heart Failure With Preserved Ejection Fraction. J Am Heart Assoc American Heart Association, Inc.; 2017;6:e004382.
49. Dieplinger B, Mueller T. Soluble ST2 in heart failure. Clin Chim Acta Elsevier; 2015;443:57–70.

# Supplementary Materials

## *Supplementary Figures*

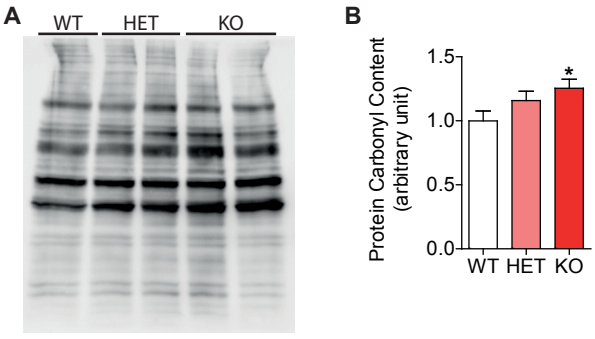


**Fig. S1. Oplah knock-out mice have more left ventricular protein oxidation.**
**A.** Representative immunoblot analysis of DNP (2,4 dinitophenyl hydrazine) derivatized oxidized proteins (total protein carbonyl content) in the left ventricles of Oplah knock-out (KO), heterozygous (HET), and wild-type littermates (WT). **B.** Quantified levels of the total protein carbonyl content in the KO (n =7 ), HET (n = 8) and WT (n = 6) mice. Levels were calculated as fold-change relative to WT levels. Data are presented as means ± SEM *, P < 0.05, as calculated Student's T-test.

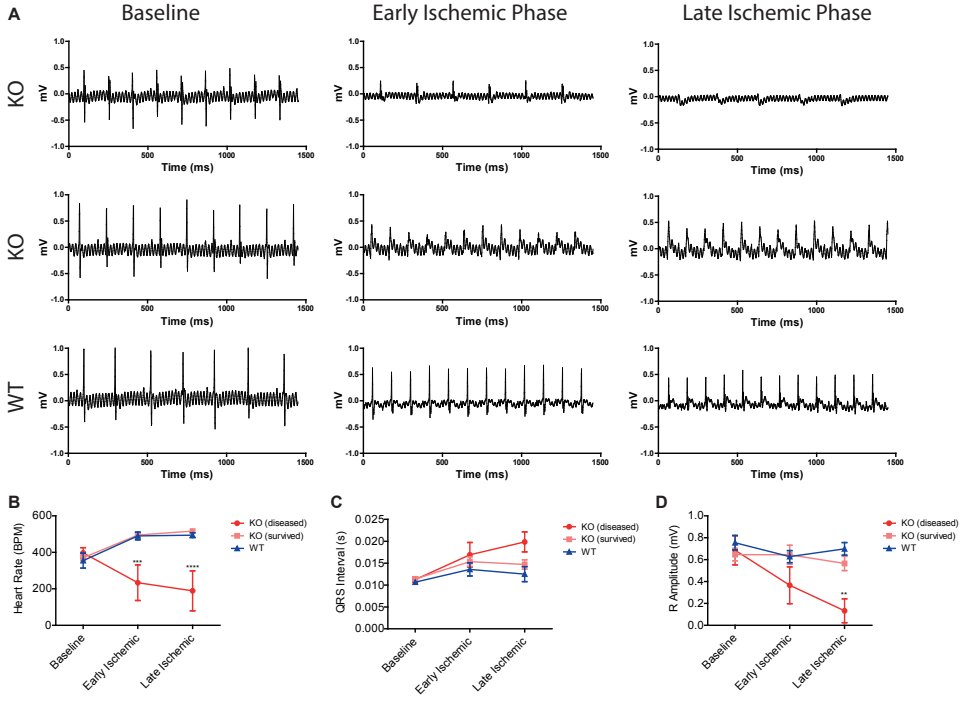


**Fig. S2. Oplah knock-out mice are more prone to sudden death following ischemic injury.**
**A.** Representative electrocardiography (ECG) images of Oplah knock-out (KO) and wild-type littermates (WT) at baseline, within the first 15 min following ischemic injury (early ischemic phase), and in the final 15 min following ischemic injury (late ischemic phase). (**TOP**) ECG of KO mice that exhibited sudden death. (**MIDDLE**) ECG of KO mice that survived ischemic injury. (**BOTTOM**) ECG of WT mice. **B-D.** ECG analysis of heart rate (**B**), QRS interval (**C**) and R amplitude (**D**) of the KO animals that died during the procedure (n = 4), KO animals that survived the procedure (n = 14), and WT mice (n = 5). Data are presented as means ± SEM **, P < 0.01; ***, P < 0.001; ****, P < 0.0001 as calculated by two-way analysis of variance (ANOVA).

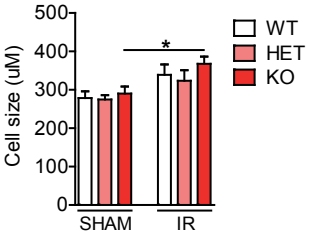


**Fig. S3. Oplah KO mice have increased left ventricular hypertrophy post cardiac ischemia/reperfusion (IR) injury.**
Quantified cell size of the WGA stained slices from the IR study (WT sham n = 12, WT IR n = 5, KO sham n = 11, KO IR n = 5). Data are presented as means ± SEM *, P < 0.05, as calculated Student's T-test.

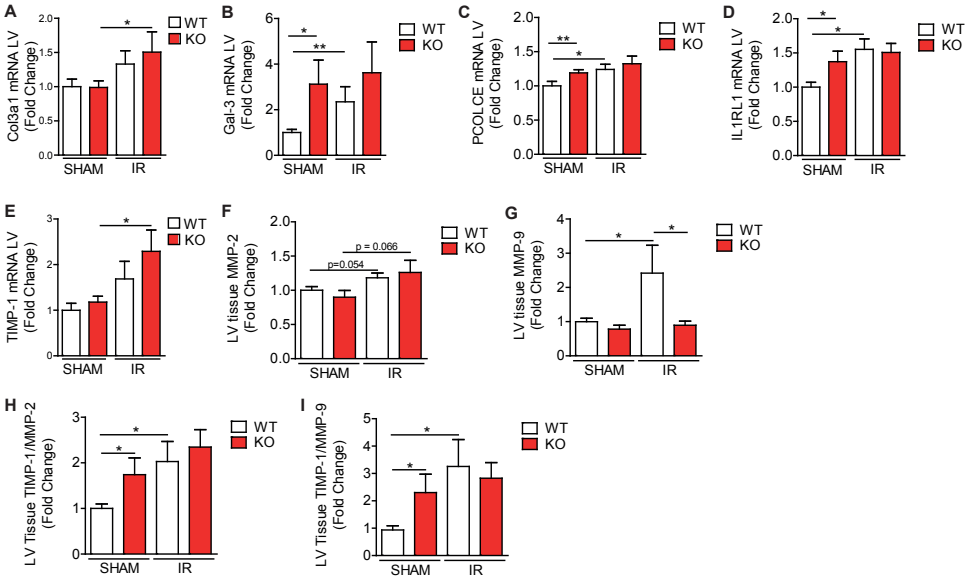


**Fig. S4. Oplah knock-out mice have more cardiac fibrosis following cardiac ischemia/reperfusion (IR) injury.**
**A-G.** qRT-PCR analysis of LV mRNA (WT SHAM n = 15, WT IR n = 11, KO SHAM n = 14, KO IR n = 10), for (**A**) Collagen type 3, alpha 1 (*Col3a1*), (**B**) Galectin-3 (*Gal-3*), (**C**) Procollagen C-endopeptidase enhancer 1 (*Pcolce*), (**D**) Interleukin 1 receptor-like 1 (*Il1rl1*, also known as *St2*), (**E**) TIMP metallopeptidase inhibitor 1 (*Timp-1*), (**F**) matrix metallopeptidase 2 (*Mmp-2*), and (**G**) matrix metallopeptidase 9 (*Mmp-9*). **H-I.** The ratio between *Timp-1* and *Mmp-2* (**H**) and *Mmp-9* (**I**). Data are presented as means ± SEM *, P < 0.05; **, P < 0.01 as calculated by one-way analysis of variance (ANOVA).

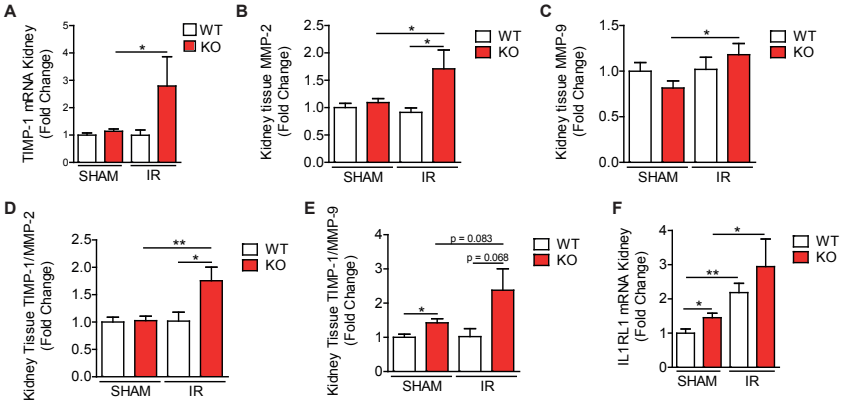


**Fig. S5. Oplah knock-out mice have more renal fibrosis following cardiac ischemia/reperfusion (IR) injury.**
**A-C.** qRT-PCR analysis of kidney mRNA (WT SHAM n = 10, WT IR n = 9, KO SHAM n = 15, KO IR n = 10), for (**A**) TIMP metallopeptidase inhibitor 1 (*Timp-1*), (**B**) matrix metallopeptidase 2 (*Mmp-2*), and (**C**) matrix metallopeptidase 9 (*Mmp-9*). **D-E.** The ratio between *Timp-1* and *Mmp-2* (**D**) and *Mmp-9* (**E**). **F.** qRT-PCR analysis of kidney mRNA for Interleukin 1 receptor-like 1 (*Il1rl1*, also known as *St2*). Data are presented as means ± SEM *, P < 0.05; **, P < 0.01 as calculated by one-way analysis of variance (ANOVA).

## *Supplementary Tables*

**Table S1. Primer sequences used in this study.**

| Transcript | Forward primer (5' - 3') | Reverse primer (5' - 3') |
|---|---|---|
| *OPLAH* (mouse/rat) | TCCGAGAGCTGGTCTTTC | ATTCACTGTGCGCCCATC |
| *Timp-1* (mouse) | CTGCTCAGCAAGAGCTTTC | CTCCAGTTTGCAAGGGATAG |
| *Mmp-2* (mouse) | CCCTGATGTCCAGCAAGTAG | GGAGTCTGCGATGAGCTTAG |
| *Mmp-9* (mouse) | TCCCAGACGTGGGTCGATTC | GTCTCGCGGCAAGTCTTCAG |
| *Col1a1* (mouse) | TTCTCCTGGCAAAGACGGAC | CCATCGGTCATGCTCTCTCC |
| *Col3a1* (mouse) | GCGATTCAAGGCTGAAG | GGGTGCGATATCTATGATGG |
| *ANP* (mouse) | ATGGGCTCCTTCTCCATCAC | TCTACCGGCATCTTCTCCTC |
| *α-MHC* (mouse) | GTTAACCAGAGTTTGAGTGACA | CCTTCTCTGACTTTCGGAGGTACT |
| β-*MHC* (mouse) | ATGTGCCGGACCTTGGAAG | CCTCGGGTTAGCTGAGAGATCA |
| *Gal-3* (mouse) | TATCCTGCTGCTGGCCCTTATG | GTTTGCGTTGGGTTTCACTG |
| *PCOLCE* (mouse) | TCAGTCTCCTTGGTGTCTAC | CTGACCCATCAGCAGATAAC |
| *sST2* (mouse) | GCCAGAGTTGTGACTCATAG | CCCGGAGTAACACCATTATC |
| *Catalase* (mouse) | TTTTGCCTACCCGGACACTC | GGGGTAATAGTTGGGGGCAC |
| *36B4* (mouse) | AAGCGCGTCCTGGCATTGTC | GCAGCCGCAAATGCAGATGG |

**Table S2. List of antibodies used in this study**

| Antigen | Cat. No. | Supplier |
|---|---|---|
| OPLAH | sc-271807 | Santa Cruz Biotechnology Inc. |
| α-tubulin | t5168 | Sigma-Aldrich |

**Table S3. Clinical characteristics of healthy control patient population**

| Demographics | n = 6 |
|---|---|
| Age (years) | 61.3 ± 7.0 |
| Female sex n (%) | 3 (50%) |
| BMI | 26.1 ± 3.6 |
| Systolic BP (mmHg) | 136.8 ± 16.9 |
| Medical History | |
| History of hypertension | 1 (17%) |
| History of hypercholesterolemia | 0 (0%) |
| History of diabetes mellitus | 0 (0%) |
| Laboratory values | |
| NT-proNP, pg/ml | 55.00 (32.00, 63.00) |

**Table S4. Clinical characteristics of HFpEF patients by 5-oxoproline concentrations**

| | 5-oxoproline (3.7 - 6.7 µM) | 5-oxoproline (6.7 - 12.8 µM) | |
|---|---|---|---|
| **Demographics** | **n = 26** | **n = 25** | **P value** |
| Age (years) | 74.3 (10.8) | 74.3 (8.6) | 0.99 |
| Female sex n (%) | 20 (77%) | 16 (64%) | 0.31 |
| NYHA n (%) | | | |
| II | 7 (27%) | 4 (16%) | 0.34 |
| III | 19 (73%) | 21 (84%) | |
| BMI | 31.0 (7.7) | 27.4 (4.2) | 0.044 |
| Systolic BP (mmHg) | 140.0 (15.5) | 143.1 (10.8) | 0.41 |
| Diastolic BP (mmHg) | 72.8 (8.1) | 75.9 (6.9) | 0.15 |
| Heart rate (bmp) | 69.7 (8.9) | 72.5 (12.2) | 0.35 |
| Comoridities % | | | |
| History of myocardial infarction | 1 (4%) | 1 (4%) | 0.98 |
| History of hypertension | 22 (85%) | 24 (96%) | 0.17 |
| History of atrial fibrilation | 16 (94%) | 16 (89%) | 0.58 |
| History of hypercholesterolemia | 13 (50%) | 13 (52%) | 0.89 |
| History of diabetes mellitus | 9 (35%) | 8 (32%) | 0.84 |
| Laboratory values | | | |
| Creatinine, µmol/l | 82.0 (63.0, 112.0) | 94.0 (77.0, 122.0) | 0.16 |
| NT-proNP, pg/ml | 989.0 (403.0, 1681.0) | 1087.0 (747.0, 1945.0) | 0.26 |

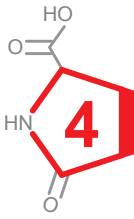

**Table S5. Characteristics of Oplah KO mice compared to the clinical criteria for the diagnosis of HFpEF.**

| Clinical criteria for diagnosis of HFpEF | OPLAH KO mice |
|---|---|
| The presence of symptoms of HF | |
| Breathlessness, elevated jugular venous pressure, fatigue, etc. | N/A |
| A 'preserved' EF (LVEF ≥ 50%) | Preserved LVEF<br>WT = 53.2 ± 2.6%<br>HET = 55.3 ± 8.8%<br>KO = 54.8 ± 2.9% |
| Elevated levels of NPs | Increased ANP expression<br>(Fold change relative to WT)<br>WT = 1.0 ± 0.3<br>HET = 1.6 ± 1.4<br>KO = 3.6 ± 2.2 |
| Objective evidence of other cardaic functional and structural alterations underlying HF | |
| Left atrial volume index (LAVI) > 34 mL/$m^2$ | Increased atria weight<br>WT = 3.3 ± 0.4 mg/cm<br>HET = 4.2 ± 0.8 mg/cm<br>KO = 4.1 ± 0.3 mg/cm |
| Left ventricular mass index (LVMI) ≥ 115 g/$m^2$ (males) or ≥95 g/$m^2$ (females) | |
| Diastolic dysfunction | Impaired LV relaxation (Tau)<br>WT = 6.8 ± 0.8 ms<br>HET = 7.29 ± 1.0 ms<br>KO = 8.5 ± 1.2 ms |
| Elevated LV filling pressures | |
| Pulmonary capillary wedge pressure (PCWP) ≥ 15 mmHg | |
| Left ventricular end diastolic pressure (LVEDP) ≥ 16 mmHg | Increased LVEDP<br>WT = 5.8 ± 2.9 mmHg<br>HET = 8.4 ± 4.2 mmHg<br>KO = 11.3 ± 4.6 mmHg |
| Increased LV wall thickness | |
| Increased left atrial size | |
| Concomitant cardiovascular diseases (i.e. atrial fibrillation, hypertension, ect.) | |
| Concomitant non-cardiovascular diseases (i.e. kidney disease, diabetes, ect.) | Kidney damage/fibrosis<br>WT = 1.7 ± 0.7%<br>HET = 6.5 ± 3.1%<br>KO = 5.0 ± 2.1% |

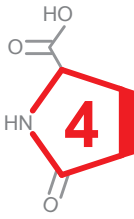
HO
O
HN
4
O

# Chapter 5

## LC-MS analysis of key components of the γ-Glutamyl cycle in tissues and body fluids from mice with Myocardial Infarction

Andres Gil[1], Atze van der Pol[2], Peter van der Meer[2], Rainer Bischoff[1]

[1]Department of Pharmacy, Analytical Biochemistry, University of Groningen
[2]Department of Cardiology, University Medical Center Groningen, University of Groningen

*Under review at the Journal of Pharmaceutical and Biomedical Analysis*

## Abstract

**Background**: Oxidative stress is suggested to play an important role in several pathophysiologic conditions. A recent study showed that decreasing 5-oxoproline levels, an important mediator of oxidative stress, by over-expressing 5-oxoprolinase (OPLAH), improves cardiac function post-myocardial infarction in mice. The aim of the current study is to gain a better understanding of the role of the γ-glutamyl cycle in a mouse model of myocardial infarction by establishing quantitative relationships between key components (5-oxoproline, L-glutamate, GSH and GSSG).

**Methods**: We developed and validated an LC-MS method to quantify 5-oxoproline, L-glutamate, GSH and GSSG in different biological samples (heart, kidney and liver tissue, as well as plasma and urine) of mice with and without myocardial infarction.

**Results**: 5-Oxoproline levels were elevated in all biological samples from mice with myocardial infarction relative to healthy controls and the ratio of GSH/GSSG was significantly decreased in cardiac tissue of mice with myocardial infarction, while this was not the case in the other tissues/body fluids. This emphasizes the role of 5-oxoproline as an inducer of oxidative stress related to myocardial infarction and as a possible biomarker.

**Conclusions**: An increase in the level of 5-oxoproline is associated with a decrease in the GSH/GSSG ratio, a well-established marker for oxidative stress, in cardiac tissue post-myocardial infarction. This suggests that 5-oxoproline may serve as an easily measurable marker for oxidative stress resulting from cardiac injury. Our findings show further that liver and kidneys have more capacity to cope with oxidative stress conditions in comparison to the heart, since the GSH/GSSG ratio is not affected in these organs despite a significant increase in 5-oxoproline.

## Introduction

Oxidative stress is defined as the imbalance between the production of reactive oxygen species (ROS), and the capacity of the endogenous antioxidant defense system to deal with ROS (1). Under physiological conditions, small quantities of ROS, which function in cell signaling, and can be readily neutralized by the antioxidant defense system, are produced intracellularly. However, under pathophysiological conditions, the production of ROS may exceed the buffering capacity of the antioxidant defense system, resulting in cell damage and ultimately cell death. This imbalance in redox state has been implicated in the onset and progression of several diseases, including cardiovascular disease (1,2).

The major source of antioxidants in mammalian cells is glutathione (GSH), which is formed by the γ-glutamyl cycle (Fig. 1). Although the enzymes and metabolites of the γ-glutamyl cycle have been characterized extensively, they have only recently been implicated in the pathophysiology of heart failure (3). One such enzyme, 5-oxoprolinase (OPLAH), is responsible for converting 5-oxoproline, a degradation product of GSH, into L-glutamate (4,5). 5-Oxoproline has been shown to induce oxidative stress in rat brain tissue, rat cardiomyocytes, and human embryonic stem-cell-derived cardiomyocytes (3,6,7). Furthermore, decreasing the level of 5-oxoproline by over-expressing OPLAH in mice has been shown to improve cardiac function post cardiac injury (3). These observations suggest a major role of the γ-glutamyl cycle in heart failure.

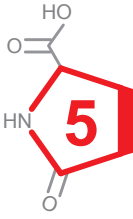


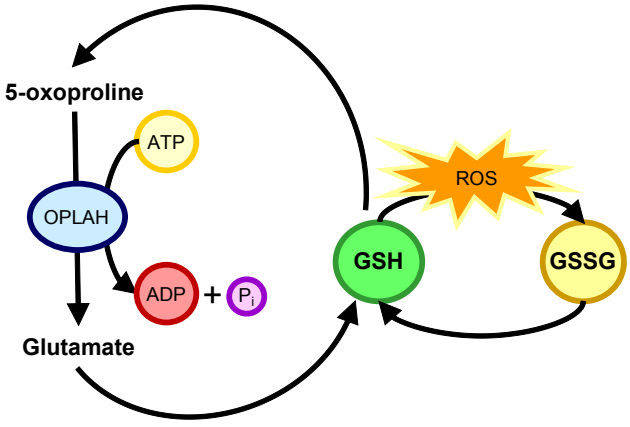


**Fig. 1. Schematic representaion of the γ-glutamyl cycle.**
5-oxoproline, a degradation product of glutathione (GSH), is transformed into L-glutamate via 5-oxoprolinase (OPLAH) activity. The produced L-glutamate is reused to produce *de novo* GSH. GSH can then be utilized as an antioxidant, producing oxidize glutathione (GSSG) in the process.

To obtain a better understanding of the γ-glutamyl cycle and its involvement in heart failure, it is essential to decipher how the different metabolites change under physiological and pathophysiological conditions. To date, numerous analytical methods have been established to separately quantify key metabolites of the γ-glutamyl cycle; 5-oxoproline, L-glutamate, GSH and GSSG (oxidized GSH) (8–13). Here we report the development and validation of an LC-MS method for the simultaneous quantitative determination of 5-oxoproline, L-glutamate, GSH (derivatized with NEM) and GSSG in different biological samples (heart, kidney and liver tissue, as well as plasma and urine) of mice with and without myocardial infarction (MI). From a methodological point of view, we show that certain matrices may lead to interferences that must be taken into account. From a disease mechanism point of view, we show that the failing heart has rather limited anti-oxidant capacity as compared to kidney and liver, which makes it particularly vulnerable to ROS.

## Materials and methods

### Solvents, chemicals and standards

All chemicals used were analytical grade or of the highest purity commercially available. Methanol (MeOH, HPLC SupraGradient grade) was purchased from Biosolve (Valkenswaard, The Netherlands). Phosphate buffered saline (PBS), bovine serum albumin (BSA), formic acid (for mass spectrometry), N-ethylmaleimide (NEM) and all standard compounds, including $^{13}$C-labeled L-glutamic acid, $^{13}$C, $^{15}$N-labeled GSH and non-labeled 5-oxoproline, L-glutamic acid, GSH and GSSG, were purchased from Sigma-Aldrich (Zwijndrecht, The Netherlands). Ultrapure water was obtained from a Milli-Q Advantage A10 water purification system at a resistivity of 18.2 MΩ cm (Millipore SAS, Molsheim, France).

### Permanent myocardial infarction in wild-type mice

The animal protocol was approved by the Animal Ethical Committee of the University of Groningen (permit number: DEC6632). The animal experiments were performed conform the ARRIVE guidelines (14). A total of 24 wild-type mice were included in the MI study. All mice were 14-20 weeks of age and 35-40 g of body weight. The WT mice were randomized into two groups, the SHAM-operated group and the MI group. Animals were anesthetized with isoflurane and medical oxygen, followed by the administration of 5mg/kg of carprofen. The MI group (n = 13) underwent permanent ligation of the left anterior descending branch (LAD) of the left coronary artery. The ligation of the LAD was placed to achieve a ±30% area at risk of the left ventricle (LV). The SHAM operated group (n = 11) underwent the same procedure without ligation of the LAD. After 4 weeks, animals were sacrificed and blood, urine, and organs were collected and immediately placed in liquid nitrogen, and stored for

further sample preparation and subsequent LC-MS analysis.

**Production of isotopically-labeled internal standards (IS)**

The 5-oxoproline internal standard (IS) was prepared from $^{13}C$-labeled L-glutamic acid. Briefly, L-glutamic acid (250mg) was dissolved in 0.1 N HCl and heated at 80°C for 72hrs, to convert $^{13}C$-L-glutamic acid into $^{13}C$-5-oxoproline, as previously described (15). Later, the solution was placed under a stream of nitrogen to remove the 0.1 N HCl and re-dissolved in 50 mL water. This method resulted in a mixed internal standard of $^{13}C$-5-oxoproline and $^{13}C$-L-glutamic acid.

GSSG (IS) was prepared by a controlled oxidation of $^{13}C$, $^{15}N$-labeled GSH. Briefly, 10 mg of $^{13}C$, $^{15}N$-labeled GSH were dissolved in 1 mL water. Half of the solution (0.5 mL) was mixed with of 0.5 mg NaI (final concentration 6.7 mM) and 1 µL 30 % $H_2O_2$. The mixture was placed in a thermomixer at 25°C for 60 min to allow oxidation. Excess $H_2O_2$ was eliminated by increasing the temperature of the mixture to 65°C for 5 min according to Haberhauer-Troyer et al (2013) (16).

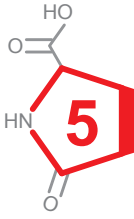


Later, both solutions (one containing $^{13}C$-5-oxoproline and $^{13}C$-L-glutamic acid, and the other containing $^{13}C$, $^{15}N$-labeled GSH and $^{13}C$, $^{15}N$-GSSG) were mixed and the solvent was evaporated. Finally, the mixture was resuspended in 1 mL water and used as IS for further experimental work. The final ratio of the components in the internal standard solution was 1:1,5:6:12 for $^{13}C$-L-glutamic acid, $^{13}C$-5-oxoproline, $^{13}C$, $^{15}N$-GSSG and $^{13}C$, $^{15}N$-labeled GSH respectively.

**Preparation of extraction solution**

A mixture containing 0.5 µL isotopically-labeled IS and 1.25 mg of NEM in 75% methanol was prepared and used for 3 purposes, including extraction of the analytes (5-oxoproline, L-glutamate GSH and GSSG), precipitation of proteins present in the samples and derivatization of GSH with NEM.

**Sample preparation**

Murine plasma and urine was prepared by adding 200 µL of cold (-20°C) extraction solution to 25 µL of either plasma or urine. The snap frozen murine tissues (heart, kidney, and liver) were powdered by means of a mortar and pestle and ±1 mg of powdered tissue was mixed with 200 µL of cold (-20°C) extraction solution. Plasma and urine samples were vortexed for 5 min, and tissue samples were sonicated for 5 min, followed by incubation for 45 min in a thermomixer at room temperature and 900 rpm to allow the formation of the GSH-NEM conjugate. The samples were centrifuged at 4°C and 20800g for 20 min. The supernatant was collected and dried under a flow of nitrogen gas at room temperature, followed by resuspension in 100 µL water. At this stage, samples were stored at -80°C until LC-MS measurements

were performed. For tissue samples, pellets formed after centrifugation were homogenized in 200 µL ice-cold RIPA buffer [50 mM Tris pH 8.0, 1% Nonidet P40, 0.5% deoxycholate, 0.1% SDS, 150 mM NaCl). Protein concentrations were determined with the Pierce BCA Protein Assay Kit (ThermoFisher Scientific), following manufacturer instructions. 5-Oxoproline, L-glutamic acid, GSH-NEM and GSSG concentrations were normalized by using the protein content (µg) of the measured samples.

**LC-MS**

5-Oxoproline, L-glutamic acid, GSH-NEM and GSSG were separated in the reverse phase mode using an Acquity HSS T3 column (1.8 µm, 100 × 2.1 mm; Waters) on an Agilent 1290 Infinity LC system (Santa Clara, CA, United States). Mobile phases consisted of a mixture of 0.1% formic acid in water (eluent A) and methanol (eluent B). The following elution gradient was applied: 0 min – 100%A, 2.5 min – 100%A, 5 min – 95%A, 6 min – 15%A, 8 min – 15%A and 10 min – 100%A. The column temperature was set at 30°C, the flow rate was 0.3 mL/min, and the injection volume per sample was 10 µL.

Mass spectrometry detection was performed using an Agilent 6410 Triple Quadrupole MS system. The analytes were detected by electrospray ionization in positive (ESI+) and Multiple Reaction Monitoring (MRM) mode. The optimized MS source parameters were as following: ionspray voltage: +1500V, drying gas flow ($N_2$): 6 L/min, drying gas temperature 300°C, and nebulizer pressure: 15 psi. The mass spectrometer was set to unit resolution and the electron multiplier was set to 2400 V. The run was divided into 4 segments looking for the MS/MS transitions 130/84 for 5-oxoproline, 135/88 for $^{13}$C-labeled 5-oxoproline (internal standard), 148/84 for L-glutamic acid, 153/88 for $^{13}$C-labeled L-glutamic acid (internal standard), 433/304 for GSH-NEM, 436/307 for $^{13}$C, $^{15}$N-labeled GSH-NEM (internal standard), 613/355 for GSSG and 619/361 for $^{13}$C, $^{15}$N-labeled GSSG (internal standard). Fragmentor and collision energies were optimized to 100 V and 9 V for 5-oxoproline; 100 V and 13 V for L-glutamic acid; 125 V and 9 V for GSH-NEM and 200 V and 21 V for GSSG, respectively. The dwell time for each transition was 100 ms. Separation (UPLC) and detection (MS) systems were controlled by Agilent MassHunter Workstation software (Santa Clara, CA, United States).

**Analysis of surrogate matrices**

Matrix effects were evaluated by spiking 5-oxoproline, L-glutamic acid, GSH and GSSG (primary standards) into heart, kidney and liver tissue as well as plasma and urine from mice, and comparing the results with those obtained for surrogate matrices (2% BSA in PBS and PBS alone). Snap-frozen tissue samples were suspended in PBS (appr. 10% $^{w}/_{v}$) and maintained on dry ice during the experiment. Twenty-five µL

of each tissue suspension, plasma and urine were spiked with the primary standards across the same range of concentrations as for the linearity test (see below). Each sample was extracted following the sample preparation procedure described above. Calibration curves were constructed based on the peak area ratios of unlabeled metabolites to their corresponding 13C-labeled standards.

**Validation**

For validation purposes 5-oxoproline, L-glutamic acid and GSSG (primary standards) were weighed, dissolved in PBS containing 2% BSA and mixed to obtain a single analyte stock solution with a concentration of 200 µM. GSH was also included in this stock solution but its final concentration was 4000 µM. The stock solution was diluted with PBS containing 2% BSA to obtain 10 calibration points with concentrations of the analytes ranging from 200 to 0.12 µM for 5-oxoproline, L-glutamic acid and GSSG, and from 4000 to 2.4 µM for GSH. These calibrants were subjected to the previously defined same sample preparation procedure (see above). After the extraction procedure, the final concentrations of the calibration points ranged from 50 to 0.03 µM for 5-oxoproline, L-glutamic acid and GSSG, and from 1000 to 0.6 µM for GSH-NEM. Calibration curves were constructed based on the peak area ratios of unlabeled metabolites to their corresponding $^{13}$C-labeled standards.

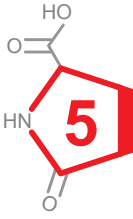


Following international guidelines (17,18), method validation was performed by evaluating the following parameters: intra-day variability (repeatability), inter-day variability (intermediate precision), lower limit of quantitation (LLOQ), linearity, accuracy, recovery and stability. Three quality control samples (QC) were prepared by spiking a solution of PBS containing 2% BSA with 5-oxoproline, L-glutamic acid and GSSG at 40, 12 and 3 µM, and GSH at 800, 240 and 60 µM. These were defined as High, Medium (Med) and Low QC samples, respectively. The QC samples were used to evaluate accuracy, recovery and precision (repeatability and intermediate precision). Accuracy, recovery and repeatability were assessed by independently extracting the 3 QC samples and measuring them 3 times in one batch. Intermediate precision was evaluated by repeating the previous experimental procedure on 3 different days. For stability studies, QC samples were prepared in human plasma and analyzed as follows. Three QC samples were prepared and measured 3 times in one batch after leaving them on the bench for 25 and 51 hrs at room temperature. Storage stability was assessed by freezing the previously prepared QC samples at -40°C, thawing and LC-MS analysis. This process was repeated 5 times on different days. The LLOQ was set to the lowest point on the calibration curves where the analyte responses were at least 5-times higher than a blank and where the coefficient of variation (CV) was less than 20%.

## Results and discussion

### LC-MS

Multiple LC-MS methods have been developed for the determination of key molecules of the γ-glutamyl cycle (8–10,13,19). We selected reverse phase chromatography on a $C_{18}$ column (Acquity HSS T3 column) as the separation approach for the simultaneous determination of L-glutamate, 5-oxoproline, GSSG and GSH-NEM, since it avoided drawbacks of other types of separation, such as strong contamination of the ionization source and short column life-time (20,21).

L-glutamate, 5-oxoproline, GSSG and GSH-NEM were separated in 10 min with retention times of 0.90, 2.75, 5.85 and 6.90 min, respectively (Fig. S1). Although the peak for L-glutamate is rather close to the dead volume of the column, this did not affect the quantitative response of the analyte (see validation results below). For the quantitative analysis of GSH and GSSG a derivatization process with NEM was required to prevent oxidation during sample preparation (22). Moreover, GSH-NEM is more easily detected by positive ESI compared to the nonalkylated form and displays better chromatographic properties (8).

### Evaluation of matrix effects on the analytical response

An essential part of method development is the selection of a proper way to prepare calibrants and QC samples (23). Generally, the use of calibration standards in authentic matrix is preferred for accurate quantitation. However, the quantitative determination of endogenous compounds, such as L-glutamate, 5-oxoproline, GSSG and GSH, in biological samples is complicated due to the lack of analyte-free authentic biological matrices (23,24). While the standard addition method, in which a calibration curve is created by adding increasing concentrations of the analyte to individual aliquots of the sample of interest, is a well-known but tedious approach to overcome this problem (23), using a so-called surrogate matrix, is more practical provided a suitable matrix can be found (24). In order to test the effect of the different biological matrices on the quantitation of L-glutamate, 5-oxoproline, GSSG and GSH, we used the standard addition method in authentic matrix and compared the results with two widely used surrogate matrices, PBS containing 2% BSA and PBS alone.

The suitability of a surrogate matrix to replace the authentic matrix was evaluated by comparing the slopes of the calibration curves (23) and by calculating the signal suppression/enhancement (SSE) factor proposed by Smith et al. (25). An SSE higher than 100% indicates enhancement of a particular signal, while the opposite indicates a suppression effect. As there is no acceptance criterion in regulatory guidelines, we set 3 thresholds for the SSE. An SSE of 100±20% was considered to show that the analyte response in the surrogate matrix is identical to that in authentic matrix. An

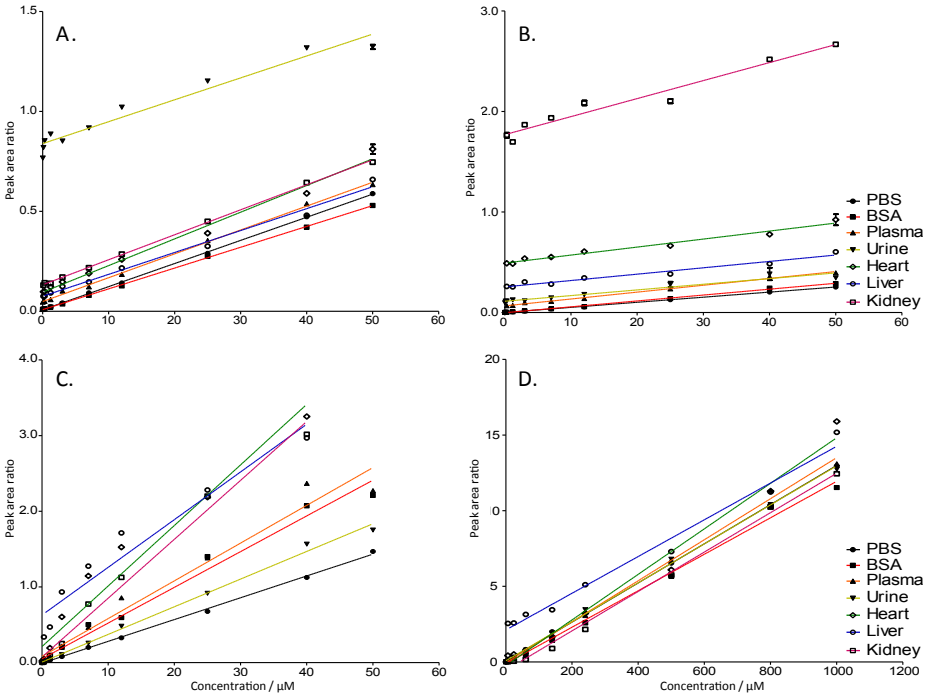


**Fig. 2. Evaluation of matrix effects on the quantitative response of 5-oxoproline (A), L-glutamate (B), GSSG (C) and GSH-NEM (D) in tissues and body fluids from healthy mice.**
PBS 1X (black lines,black circles), 2% BSA in PBS (red lines,black squares), plasma (orange lines,black triangles), urine (yellow lines,black triangles), heart (green lines,white diamonds), liver (blue lines,white circles) and kidney (pink lines,white squares).

SSE of 100±30% was considered to be acceptable for quantification, although slight enhancement or suppression effects may bias the results. Deviations of the SSE from 100% beyond 30% were considered unacceptable for quantitative bioanalysis and the results were not considered for further interpretation. We realize that this is somewhat arbitrary and recommend establishing generally accepted guidelines.

Calibration curves in each of the tested matrices are shown in Fig. 2 and the numerical values are given in Table S1. The corresponding SSE factors can be found in Table 1. 5-Oxoproline and GSH-NEM can be measured in all biological matrices using PBS and in most of them using 2% BSA in PBS as surrogate matrix (SSE = 128,24% in heart tissue). L-Glutamate should be preferably measured with 2% BSA in PBS as surrogate matrix except for kidney, were none of the two surrogate matrices proved satisfactory according to our criteria. For GSSG, 2% BSA in PBS proved satisfactory as surrogate matrix for plasma and urine, while none of the surrogate matrices was within ±30% of 100% SSE for the tissue extracts.

**Table 1. Signal suppression/enhancement (SSE) factors for 5-oxoproline, L-glutamate, GSSG and GSH-NEM prepared in murine plasma or urine and heart, liver and kidney tissue.**

| SEE (%) | 5-Oxoproline | | L-Glutamate | | GSSG | | GSH-NEM | |
|---|---|---|---|---|---|---|---|---|
| | PBS | BSA | PBS | BSA | PBS | BSA | PBS | BSA |
| Plasma | **103,20** | **114,70** | 134,82 | **116,54** | 173,13 | **105,65** | **104,71** | **112,44** |
| Urine | **94,73** | **105,28** | **111,34** | **96,24** | ***126,90*** | ***77,44*** | **99,46** | **106,80** |
| Heart | **115,38** | ***128,24*** | 157,22 | **92,88** | 277,78 | 169,52 | **116,22** | ***124,79*** |
| Liver | **94,73** | **105,28** | ***125,24*** | **108,26** | 218,81 | 133,53 | **93,75** | **100,66** |
| Kidney | **108,04** | **120,08** | 353,94 | 305,96 | 270,18 | 164,88 | **100,54** | **107,96** |

The signal suppression/enhancement effect was calculated as follows: SSE(%)=(slope$_{matrix-diluted}$ /slope$_{surrogate\ matrix}$) x 100.
Values in bold face fulfill the set criterion of being within ±20% of the SSE value for the authentic matrix.
Values in bold and italic face fulfill the set criterion of being within ±30% of the SSE value for the authentic matrix.

The higher y-axis intercepts of the calibration curves for 5-oxoproline in urine (Fig. 2A and Table S1) and for L-glutamate in kidney tissue indicate that these matrices contain comparatively high endogenous levels. Furthermore, there was a considerable enhancement effect of the L-glutamate signal (SSE > 300%) in kidney tissue in comparison with both surrogate matrices (Table 1), a phenomenon that remains currently unexplained. The signal for GSSG was enhanced in all biological matrices except for urine. The reason for this enhancement is currently unclear, notably since we quenched interconversion of GSH to GSSG immediately during sample preparation.

The coefficient of determination ($r^2$), as a measure of linearity, is another important parameter to compare calibration curves in the different matrices (Table S1). When validating analytical methods, an $r^2 \geq 0.99$ is recommended as an acceptance criterion for quantitative purposes (17,18). Based on this criterion, we classified calibration curves into those with an $r^2 \geq 0.99$ (bold face in Table S1) and those with an $r^2 \leq 0.99$. The results show that complex matrices, such as tissue extracts or biofluids, lead to a reduced linear fit in comparison to the surrogate matrices. Both surrogate matrices allow accurate quantitation of 5-oxoproline, L-glutamate and GSH-NEM. For GSSG only PBS gave an acceptable linear fit while 2% BSA in PBS showed an $r^2$ of 0.9833. The reason for this discrepancy is currently not clear.

Based on these results, we chose 2% BSA in PBS as the most suitable surrogate matrix, allowing reliable analysis of 5-oxoproline in plasma, urine, heart, liver and kidney, L-glutamate in plasma, urine, heart and liver, GSH-NEM in plasma, urine, heart, liver and kidney and GSSG in plasma and urine according to an SSE of 100 ± 30% (Fig. 2, Tables 1 and S1).

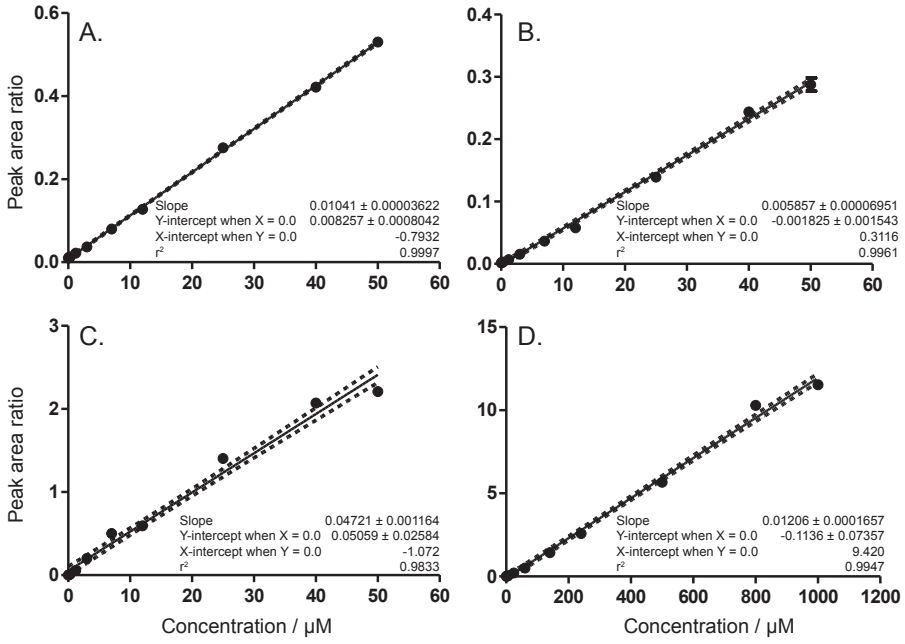


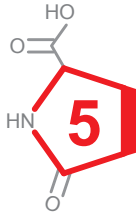


**Fig. 3. Linear responses of 5-Oxoproline (A), L-Glutamate (B), GSSG (C), and GSH (D) prepared in PBS 1X with 2% BSA.**
Calibration curves are based on peak area ratios of unlabeled to stable-isotope-labeled internal standards.

## Method validation

Based on the results above, we validated the methodology to quantify key components of the γ-glutamyl cycle (L-glutamate, 5-oxoproline and GSH-NEM) in biofluids and tissues, using 2% BSA in PBS as surrogate matrix. Linearity was tested across a dynamic range of 0.03 to 50 µM for 5-oxoproline, L-glutamate, and GSSG, and 0.6 to 1000 µM for GSH-NEM (Fig. 3) and the $r^2$ values are reported in Table S1. The lower limits of quantitation (LLOQ) were set to the lowest point on the calibration curves where the analyte response was at least 5-times higher than a blank and where the coefficient of variation (CV) was less than 20% in accordance with international guidelines (17,18). Results for accuracy, precision and stability are summarized in Table 2. The bias for the quantitation of 5-oxoproline, L-glutamate, GSH-NEM and GSSG ranged from 1.2 to -9.3%, 4.4 to -10.0%, 4.1 to -10.2% and 7.0 to -4.0%, respectively. Recoveries were within the range of 89.8–107% for all target analytes for High, Med and Low QC samples. CVs were below ±15% satisfying validation criteria for repeatability, intermediate precision and stability (Table 2).

## Analysis of the γ-glutamyl cycle in animals with heart failure

To study the effect of an induced myocardial infarct (MI) on the γ-glutamyl cycle

**Table 2. Accuracy, precision (intra- and inter-day) and stability of of 5-Oxoproline, L-Glutamate, GSSG, and GSH.**

| | | 5-Oxoproline | | | L-Glutamate | | |
|---|---|---|---|---|---|---|---|
| | | High QC | Med QC | Low QC | High QC | Med QC | Low QC |
| **Accuracy** | | | | | | | |
| Nominal Concentration | (µM) | 40 | 12 | 3 | 40 | 12 | 3 |
| Mean Concentration | (µM) | 404,670 | 115,354 | 27,219 | 417,440 | 107,991 | 29,001 |
| Bias | (%) | 1,2 | -3,9 | -9,3 | 4,4 | -10,0 | -3,3 |
| Recovery | (%) | 101,2 | 96,1 | 90,7 | 104,4 | 90,0 | 96,7 |
| **Precision** | | | | | | | |
| Intra-day RSD | (%) | 0,3 | 0,8 | 4,8 | 1,0 | 0,4 | 4,8 |
| Inter-day RSD | (%) | 3,0 | 4,3 | 0,6 | 1,9 | 8,8 | 4,7 |
| **Stability** | | | | | | | |
| Bench-top (25 h) RSD | (%) | 2,9 | 7,8 | 3,1 | 6,2 | 7,2 | 3,0 |
| Bench-top (51 h) RSD | (%) | 2,0 | 5,1 | 9,9 | 3,9 | 9,5 | 9,0 |
| Freeze-thaw (5 cycles) RSD | (%) | 5,3 | 5,3 | 6,0 | 8,7 | 4,4 | 9,0 |

| | | GSSG | | | GSH-NEM | | |
|---|---|---|---|---|---|---|---|
| | | High QC | Med QC | Low QC | High QC | Med QC | Low QC |
| **Accuracy** | | | | | | | |
| Nominal Concentration | (µM) | 40 | 12 | 3 | 800 | 240 | 60 |
| Mean Concentration | (µM) | 427,937 | 115,235 | 31,730 | 8,330,421 | 2,327,737 | 5,387,827 |
| Bias | (%) | 7,0 | -4,0 | 5,8 | 4,1 | -3,0 | -10,2 |
| Recovery | (%) | 107,0 | 96,0 | 105,8 | 104,1 | 97,0 | 89,8 |
| **Precision** | | | | | | | |
| Intra-day RSD | (%) | 0,3 | 0,7 | 0,8 | 0,9 | 3,3 | 2,0 |
| Inter-day RSD | (%) | 6,0 | 9,0 | 15,5 | 4,5 | 6,0 | 4,9 |
| **Stability** | | | | | | | |
| Bench-top (25 h) RSD | (%) | 8,1 | 2,8 | 6,9 | 3,9 | 2,2 | 5,0 |
| Bench-top (51 h) RSD | (%) | 9,7 | 11,1 | 10,0 | 1,1 | 3,5 | 6,8 |
| Freeze-thaw (5 cycles) RSD | (%) | 6,5 | 5,9 | 8,0 | 2,5 | 3,1 | 3,2 |

in mice, we determined the concentrations of 5-oxoproline, L-glutamate, GSH and GSSG in plasma, urine, heart tissue, kidney tissue and liver tissue of SHAM-operated mice (N = 11) and mice that were subjected to MI (N = 13). 5-Oxoproline concentrations were significantly increased in all samples of MI-mice compared to control animals [plasma (5.99 vs 3.72 µM/µg protein), urine (460.43 vs 191.89 µM/µg protein), heart tissue (16.26 vs 4.80 nM/µg protein) and kidney tissue (84.50

vs 20.02 nM/µg protein)] ($p \leq 0.05$), with the exception of liver tissue, where the increase was not statistically significant (20.89 vs 11.42 nM/µg protein, $p \geq 0.05$) (Fig. 4). A similar pattern was found for L-glutamate, however, statistical significance was only reached in kidney tissue (914.31 vs 555.27 nM/µg protein, $p \leq 0.05$) (Fig. 4). The levels of GSH were not significantly different between SHAM-operated mice and mice with MI in any of the samples (Fig. 4). GSSG was elevated in all tissue samples from MI animals when compared to the control animals (heart: 4.70 vs 0.60; $p = 0.06$, kidney: 8.47 vs 4.46 and liver: 20.81 vs 18.24 nM/µg protein), however, this difference was not statistically significant (Fig. 4). GSSG was undetectable in plasma and urine from all animals.

A well-established parameter to measure oxidative stress in biological systems is the ratio between GSH and GSSG, where a decrease is indicative of an increase in oxidative stress (10). While individual measurements of GSH and GSSG did not reach statistical significance between the MI and control groups, we found that the GSH/GSSG ratio was significantly reduced in heart tissue after MI (Fig. 4).

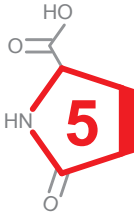


In a previous study we demonstrated that the expression of OPLAH, the enzyme responsible for the conversion of 5-oxoproline into L-glutamate, is reduced in cardiac tissue exposed to MI (3). Reduction in OPLAH expression was shown to be linked to increased levels of 5-oxoproline and oxidative stress (3). This is in line with the data presented in the current study, where we observed that 5-oxoproline is significantly elevated in cardiac tissue and that the GSH/GSSG ratio is significantly reduced, suggesting an increase in oxidative stress. While we observed a similar increase in 5-oxoproline in renal and liver tissue, there was no difference in the GSH/GSSG ratio, suggesting that these organs have a higher capacity to compensate for oxidative stress than the heart.

Based on our knowledge of the γ-glutamyl cycle (Fig. 1), 5-oxoproline, a degradation product of glutathione, is converted back to L-glutamate by OPLAH. Therefore, a reduction of OPLAH coupled to an increase in 5-oxoproline in heart failure would suggest a reduction in the availability of L-glutamate for the *de novo* synthesis of GSH. However, the results obtained in this study do not support this hypothesis. It rather seems that, upon the induction of heart failure, L-glutamate and total GSH levels are increased. This suggests that OPLAH is not a key regulator with respect to recycling L-glutamate to maintain GSH levels in animal tissue but rather an inducer of oxidative stress.

These findings shed new light on the role of the γ-glutamyl cycle in myocardial infarction further stressing the importance of 5-oxoproline in inducing oxidative

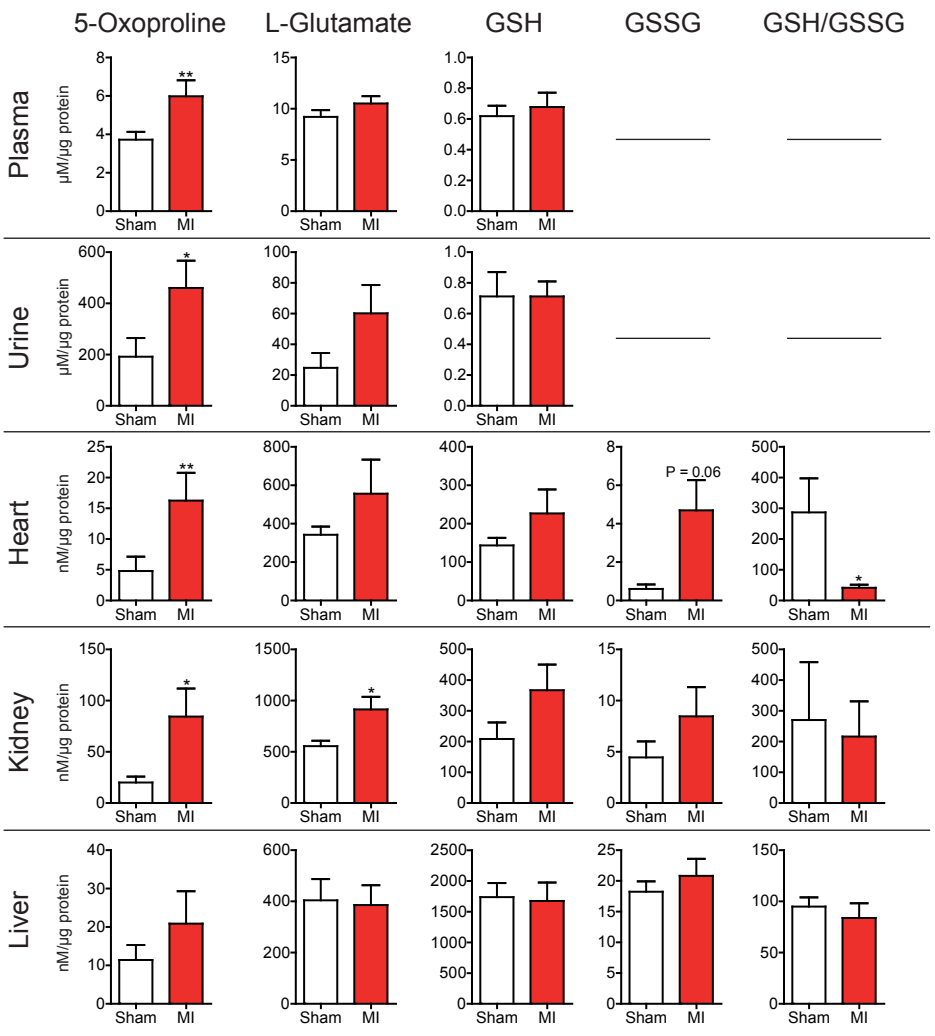


**Fig. 4. Comparison of the concentration of key components of the γ-glutamyl cycle in different organs and biofluids from healthy controls (SHAM) and mice with myocardial infarction (MI).** The lines for GSSG and the GSH/GSSG ratio in plasma and urine indicate the analyte was not detected. Data are presented as means ± SEM. Significance level according to Student's t test: *p<0.05, **p <0.01.

stress. Previously, we demonstrated that plasma 5-oxoproline levels are related to outcome after heart failure in humans, with elevated levels associating with a worse outcome (3). The findings reported here confirm these results and suggest that plasma 5-oxoproline levels may serve as a biomarker for outcome after heart failure.

## Conclusion

We developed and validated an LC-MS method for the quantitation of 5-oxoproline, L-glutamate, GSH-NEM and GSSG, key components of the γ-glutamyl cycle, in plasma, urine and three different kinds of animal tissue (heart, kidney, liver). Using this methodology, effects on the γ-glutamyl cycle were studied following the induction of heart failure in mice. Besides the clinical usefulness of the GSH/GSSG ratio as an index of oxidative stress, our results suggest that 5-oxoproline is an easily measurable biomarker of oxidative stress related to cardiovascular disease.

## Acknowledgements

Dr. Ranieri Rossi (Department of Life Sciences, Laboratory of Pharmacology and Toxicology, University of Siena, Via A. Moro 4, 53100 Siena, Italy) is acknowledged for advice with respect to the sample preparation procedure. Jos Hermans (Department of Analytical Biochemistry, University of Groningen) is acknowledged for help with operating the LC-MS instrumentation.

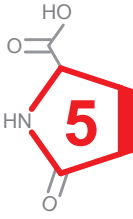

# References


1. Pollack M, Leeuwenburgh C. Molecular mechanisms of oxidative stress in aging: free radicals, aging, antioxidants and disease. Handb Oxid Antioxidants Exerc [Internet]. 1999;881–923. Available from: http://plaza.ufl.edu/cleeuwen/Pollack.PDF
2. Del Valle LG. Oxidative stress in aging: Theoretical outcomes and clinical evidences in humans. Biomed. Aging Pathol. 2011. page 1–7.
3. van der Pol A, Gil A, Silljé HHW, Tromp J, Ovchinnikova ES, Vreeswijk-Baudoin I, et al. Accumulation of 5-oxoproline in myocardial dysfunction and the protective effects of OPLAH. Sci Transl Med. 2017;9:eaam8574.
4. Meister A, Anderson ME. Glutathione. Annu Rev Biochem. Annual Reviews 4139 El Camino Way, P.O. Box 10139, Palo Alto, CA 94303-0139, USA ; 1983;52:711–60.
5. Liu Y, Hyde AS, Simpson MA, Barycki JJ. Emerging regulatory paradigms in glutathione metabolism. Adv Cancer Res. 2014;122:69–101.
6. Pederzolli CD, Sgaravatti AM, Braum CA, Prestes CC, Zorzi GK, Sgarbi MB, et al. 5-Oxoproline reduces non-enzymatic antioxidant defenses in vitro in rat brain. Metab Brain Dis. 2007;22:51–65.
7. Pederzolli CD, Mescka CP, Zandoná BR, de Moura Coelho D, Sgaravatti AM, Sgarbi MB, et al. Acute administration of 5-oxoproline induces oxidative damage to lipids and proteins and impairs antioxidant defenses in cerebral cortex and cerebellum of young rats. Metab Brain Dis. 2010;25:145–54.
8. Harwood DT, Kettle AJ, Brennan S, Winterbourn CC. Simultaneous determination of reduced glutathione, glutathione disulphide and glutathione sulphonamide in cells and physiological fluids by isotope dilution liquid chromatography-tandem mass spectrometry. J Chromatogr B Anal Technol Biomed Life Sci. 2009;877:3393–9.
9. Moore T, Le A, Niemi A-K, Kwan T, Cusmano-Ozog K, Enns GM, et al. A new LC–MS/MS method for the clinical determination of reduced and oxidized glutathione from whole blood. J Chromatogr B. Elsevier; 2013;929:51–5.
10. Lee S-G, Yim J, Lim Y, Kim J-H. Validation of a liquid chromatography tandem mass spectrometry method to measure oxidized and reduced forms of glutathione in whole blood and verification in a mouse model as an indicator of oxidative stress. J Chromatogr B. Elsevier; 2016;1019:45–50.
11. Florholmen-Kjær Å, Lyså RA ndre, Fuskevåg OM, Goll R, Revhaug A, Mortensen KE rlend. A sensitive method for the analysis of glutathione in porcine hepatocytes. Scand J Gastroenterol. 2014;49:1359–66.
12. Geenen S, Guallar-Hoyas C, Michopoulos F, Kenna JG, Kolaja KL, Westerhoff H V., et al. HPLC–MS/MS methods for the quantitative analysis of 5-oxoproline (pyroglutamate) in rat plasma and hepatic cell line culture medium. J Pharm Biomed Anal. Elsevier; 2011;56:655–63.
13. Eckstein JA, Ammerman GM, Reveles JM, Ackermann BL. Analysis of glutamine, glutamate, pyroglutamate, and GABA in cerebrospinal fluid using ion pairing HPLC with positive electrospray LC/MS/MS. J Neurosci Methods. 2008;171:190–6.
14. Kilkenny C, Browne WJ, Cuthill IC, Emerson M, Altman DG. Improving Bioscience Research Reporting: The ARRIVE Guidelines for Reporting Animal Research. PLoS Biol. Public Library of Science; 2010;8:e1000412.
15. Eckstein JA, Ammerman GM, Reveles JM, Ackermann BL. Analysis of glutamine, glutamate, pyroglutamate, and GABA in cerebrospinal fluid using ion pairing HPLC with positive electrospray LC/MS/MS. J Neurosci Methods. 2008;171:190–6.
16. Haberhauer-Troyer C, Delic M, Gasser B, Mattanovich D, Hann S, Koellensperger G. Accurate quantification of the redox-sensitive GSH/GSSG ratios in the yeast Pichia pastoris by HILIC-MS/MS. Anal Bioanal Chem. 2013;405:2031–9.
17. European Medicines Agency (EMA) - Committee for Medicinal Products for Human Use. Guideline on bioanalytical method validation. London, UK; 2012.
18. US Department of Health and Human Services, Food and Drug Administration - Center for Drug Evaluation and Research C for VM. Guidance for Industry: Bioanalytical Method Validation. Rockville, MD, USA.; 2001.
19. Joo K-M, Han JY, Son ED, Nam G-W, Chung HY, Jeong H-J, et al. Rapid, simultaneous and nanomolar determination of pyroglutamic acid and cis-/trans-urocanic acid in human stratum corneum by hydrophilic interaction liquid chromatography (HILIC)–electrospray ionization tandem mass spectrometry. J Chromatogr B. Elsevier; 2012;897:55–63.

20. Paglia G, Hrafnsdóttir S, Magnúsdóttir M, Fleming RMT, Thorlacius S, Palsson B, et al. Monitoring metabolites consumption and secretion in cultured cells using ultra-performance liquid chromatography quadrupole-time of flight mass spectrometry (UPLC-Q-ToF-MS). Anal Bioanal Chem. 2012;402:1183–98.
21. Yuan M, Breitkopf SB, Yang X, Asara JM. A positive/negative ion–switching, targeted mass spectrometry–based metabolomics platform for bodily fluids, cells, and fresh and fixed tissue. Nat Protoc. Nature Publishing Group; 2012;7:872–81.
22. Giustarini D, Tsikas D, Colombo G, Milzani A, Dalle-Donne I, Fanti P, et al. Pitfalls in the analysis of the physiological antioxidant glutathione (GSH) and its disulfide (GSSG) in biological samples: An elephant in the room. J Chromatogr B Anal Technol Biomed Life Sci. 2016;1019:21–8.
23. van de Merbel NC. Quantitative determination of endogenous compounds in biological samples using chromatographic techniques. TrAC - Trends Anal Chem. 2008;27:924–33.
24. Ho S, Gao H. Surrogate matrix: opportunities and challenges for tissue sample analysis. Bioanalysis. 2015;7:2419–33.
25. Smith D, Smith L, Shafer W, Klotz J, Strickland J. Development and validation of an lc-ms method for quantitation of ergot alkaloids in lateral saphenous vein tissue. J Agric Food Chem. 2009;57:7213–20.

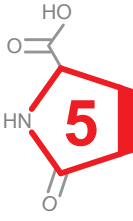

# Supplementary Material

## *Supplementary Figures*

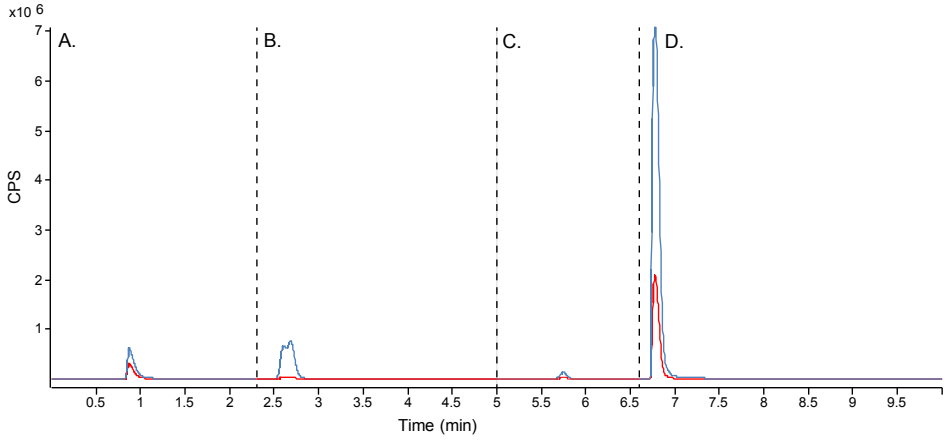


**Fig. S1. Representative MRM chromatogram in a kidney matrix.**
L-Glutamate (**A**), 5-Oxoproline (**B**) and GSSG (**C**) were analyzed at 0.12 µM, and GSH-NEM (**D**) was analyzed at 2.4 µM. The vertical lines represent the change of the MS/MS transitions for each metabolite as follows: 130/84 for 5-oxoproline and 135/88 for $^{13}$C-labeled 5-oxoproline (internal standard), 148/84 for L-glutamic acid and 153/88 for $^{13}$C-labeled L-glutamic acid (internal standard), 433/304 for GSH-NEM and 436/307 for $^{13}$C, $^{15}$N-labeled GSH-NEM (internal standard), 613/355 for GSSG and 619/361 for $^{13}$C, 15N-labeled GSSG (internal standard). Blue lines represent the isotopically labeled internal standards and red lines represent the unlabeled analytes.

**Table S1. Matrix effect on the linear response of 5-Oxoproline, L-Glutamate, GSSG, and GSH-NEM in plasma, urine, heart, kidney and liver tissues and evaluation of 2% BSA in PBS and PBS alone as surrogate matrices. * values in bold face show $r^2$ values > 0.99.**

| | | | | | | | |
|---|---|---|---|---|---|---|---|
| **5-Oxoproline** | | | | | | | |
| **Best-fit values** | **PBS** | **BSA** | **Plasma** | **Urine** | **Heart** | **Liver** | **Kidney** |
| Slope | 0.01157 ± 0.00003828 | 0.01041 ± 0.00003622 | 0.01194 ± 0.00009715 | 0.01096 ± 0.0004563 | 0.01335 ± 0.0002928 | 0.01096 ± 0.0002215 | 0.01250 ± 0.00007915 |
| Y-intercept when X=0.0 | 0.007948 ± 0.0008498 | 0.008257 ± 0.0008042 | 0.04886 ± 0.002157 | 0.8393 ± 0.01013 | 0.09537 ± 0.006852 | 0.07540 ± 0.005182 | 0.1329 ± 0.001852 |
| X-intercept when Y=0.0 | -0,6871 | -0,7932 | -4,093 | -76,60 | -7,142 | -6,882 | -10,63 |
| $r^2$ | **0,9997** | **0,9997** | **0,9981** | 0,9537 | 0,9881 | 0,9899 | **0,9990** |
| **L-Glutamate** | | | | | | | |
| Slope | 0.005063 ± 0.00002915 | 0.005857 ± 0.00006951 | 0.006826 ± 0.0001210 | 0.005637 ± 0.0003275 | 0.007960 ± 0.0003305 | 0.006341 ± 0.0002669 | 0.01792 ± 0.0008298 |
| Y-intercept when X=0.0 | 0.0006489 ± 0.0006471 | -0.001825 ± 0.001543 | 0.06639 ± 0.003003 | 0.1122 ± 0.007272 | 0.4920 ± 0.008203 | 0.2549 ± 0.006623 | 1.770 ± 0.02060 |
| X-intercept when Y=0.0 | -0,1282 | 0,3116 | -9,727 | -19,90 | -61,81 | -40,20 | -98,75 |
| $r^2$ | **0,9991** | **0,9961** | **0,9931** | 0,9136 | 0,9635 | 0,9625 | 0,9550 |
| **GSSG** | | | | | | | |
| Slope | 0.02881 ± 0.0002021 | 0.04721 ± 0.001164 | 0.04988 ± 0.001638 | 0.03656 ± 0.0004632 | 0.08003 ± 0.003359 | 0.06304 ± 0.003769 | 0.07784 ± 0.001957 |
| Y-intercept when X=0.0 | -0.007075 ± 0.004487 | 0.05059 ± 0.02584 | 0.08299 ± 0.03636 | 0.007194 ± 0.01028 | 0.2121 ± 0.05517 | 0.6288 ± 0.07020 | 0.07289 ± 0.03409 |
| X-intercept when Y=0.0 | 0,2456 | -1,072 | -1,664 | -0,1968 | -2,651 | -9,975 | -0,9364 |
| $r^2$ | **0,9986** | 0,9833 | 0,9707 | **0,9955** | 0,9578 | 0,9364 | 0,9863 |
| **GSH-NEM** | | | | | | | |
| Slope | 0.01295 ± 0.00003311 | 0.01206 ± 0.0001657 | 0.01356 ± 0.0001249 | 0.01288 ± 0.00008667 | 0.01505 ± 0.0003922 | 0.01214 ± 0.0003269 | 0.01302 ± 0.0001929 |
| Y-intercept when X=0.0 | 0.04696 ± 0.01470 | -0.1136 ± 0.07357 | -0.05354 ± 0.05544 | 0.07948 ± 0.03848 | -0.2269 ± 0.1947 | 2.114 ± 0.1623 | -0.5458 ± 0.09574 |
| X-intercept when Y=0.0 | -3,627 | 9,420 | 3,948 | -6,170 | 15,07 | -174,1 | 41,91 |
| $r^2$ | **0,9998** | **0,9947** | **0,9976** | **0,9987** | 0,9853 | 0,9843 | **0,9952** |





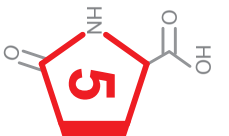

# Chapter 6

## Treating oxidative stress in heart failure: past, present and future

Atze van der Pol[1], Wiek H. van Gilst[1], Adriaan A. Voors[1], Peter van der Meer[1]

[1]Department of Cardiology, University Medical Center Groningen, University of Groningen

*Under review at the European Journal of Heart Failure*

## Abstract

Advances in cardiovascular research have identified oxidative stress as an important pathophysiological pathway in the development and progression of heart failure. Oxidative stress is defined as the imbalance between the production of reactive oxygen species (ROS), and the endogenous antioxidant defense system. Under physiological conditions, small quantities of ROS are produced intracellularly, which function in cell signaling, and can be readily reduced by the antioxidant defense system. However under pathophysiological conditions, the production of ROS exceeds the buffering capacity of the antioxidant defense system, resulting in cell damage and death. Over the last decades several studies have tried to target oxidative stress with the aim to improve outcome in patients with heart failure  However, these studies have shown no to limited beneficial effects of these strategies. The exact reasons as to why these studies failed to demonstrate any beneficial effects remains unclear. However, one plausible explanation lies in that currently employed strategies target oxidative stress by exogenous inhibition of ROS production or supplementation of exogenous antioxidants, thereby disregarding the endogenous antioxidant system. Therefore, bolstering the endogenous antioxidant capacity might be a novel avenue for therapeutic intervention. In this review we provide an overview of oxidative stress in the heart and the strategies utilized to date to target this pathophysiological pathway. We provide novel insights into how modulating the endogenous antioxidants, in particular the γ-Glutamyl cycle, responsible for the formation of the major antioxidant glutathione, may lead to novel therapeutic strategies to improve patient outcome.

## Introduction

Oxidative stress has been identified as a pathophysiological pathway involved in the development and progression of clinical and experimental heart failure (1–3). Oxidative stress is defined as a dysregulation between the production of reactive oxygen species (ROS) and the endogenous antioxidant defense mechanisms, the so called “redox state”. When present in low concentrations ROS plays a critical function in cell homeostasis, however, when available in excess ROS cause cellular dysfunction, protein and lipid peroxidation, DNA damage, and eventually lead to irreversible cell damage and death. This is also evident in the heart where high sensitive troponin assays have demonstrated an increase in troponin release during heart failure progression, suggesting a gradual loss in cardiomyocytes (4).

In the heart an overabundance of ROS can lead to the development and progression of maladaptive myocardial remodeling and heart failure (Fig. 1). ROS directly impairs the electrophysiology and the contractile machinery of cardiomyocytes by modifying proteins central to excitation-contraction coupling, including L-type calcium channels, sodium channels, potassium channels, and the sodium-calcium exchanger (5). ROS can also alter the activity of the sarcoplasmic reticulum $Ca^{2+}$-adenosine triphosphatase (SERCA) as well as reduce myofilament calcium sensitivity. Furthermore, ROS induces an energy deficit by affecting the function of proteins involved in energy metabolism. Finally, ROS has a pro-fibrotic function, by inducing cardiac fibroblast proliferation and matrix metalloproteinases (MMPs) resulting in extracellular remodeling (5).

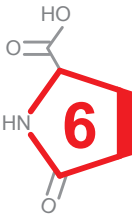


This review will summarize the current knowledge regarding oxidative stress production and the antioxidant defense mechanism in the heart, under physiological and pathophysiological conditions. Furthermore, we recapitulate the current knowledge, failures and successes, regarding the treatment of heart failure by targeting oxidative stress. Finally, we discuss the future potential of targeting endogenous oxidative stress defense mechanisms, in particular the γ-Glutamyl cycle, as potential targets for therapeutic intervention to improve clinical outcome in patients with heart failure.

**Reactive oxygen species in heart failure: a brief summary**

ROS production in the heart is primarily achieved by the mitochondria, NADPH oxidases, xanthine oxidase, and uncoupled nitric oxide synthase (Fig. 2). Under pathological conditions the electron transport chain of the mitochondria is leading to the formation of large quantities of superoxide. This increase has been shown to contribute to cardiomyocyte damage and larger infarct sizes (6,7). ROS production is also enhanced due to an increased expression and activity of NADPH oxidase,

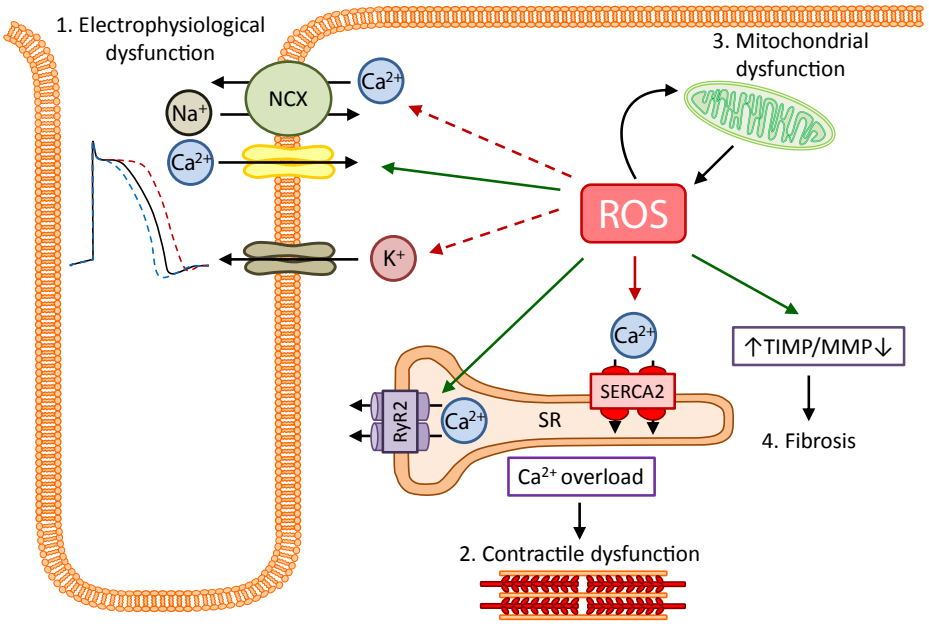


**Fig. 1. The effects of excessive oxidative stress on the myocardium.**
As a result of cardiac injury there is a severe accumulation of oxidative stress (ROS), which has several detrimental effects on the myocardium. 1. Cardiomyocyte electrophysiology is severely affected by increased ROS. ROS reverses the function of the $Na^+/Ca^{2+}$ exchanger (NCX), leading to $Ca^{2+}$ influx and $Na^+$ efflux. ROS also increases the influx of $Ca^{2+}$ via the L-type calcium channels. Increase ROS also increases sarcKATP currents, leading to action potential duration shortening, while also reducing $K_V$ currents and increasing late Na currents leading to prolonged action potential durations. 2. Excessive ROS promotes RyR2 activity and inhibits SERCA2 activity, resulting in calcium overload and reduced myofilament calcium sensitivity. Eventually leading to contractile dysfunction. 3. The mitochondria reacts to ischemic injury by producing increased levels of ROS, however the overabundance of ROS inversely results in further mitochondrial and energy metabolism dysfunction. 4. The increase in ROS is also responsible for an increased fibrosis resulting from an increase in TIMP (tissue inhibitors of metalloproteinases) and reduction in MMP (matrix metalloproteinases) expression.

resulting from several pathological stimuli, including mechanical stretch, angiotensin II, endothelin-1, and TNF-α (8–10). Similarly, xanthine oxidase expression and activity is also increased in the failing heart, again leading to an increased production of ROS (11). Finally, as a result of cardiac injury, nitric oxide synthase (NOS), becomes uncoupled and structurally unstable leading to an increased generation of ROS. In mice, increased generation of ROS has been shown to lead to LV dilatation, contractile dysfunction and LV remodeling (12).

Besides the drastic increase in oxidative stress production, heart failure is also characterized by an exhaustion of the innate antioxidant defense mechanism. In

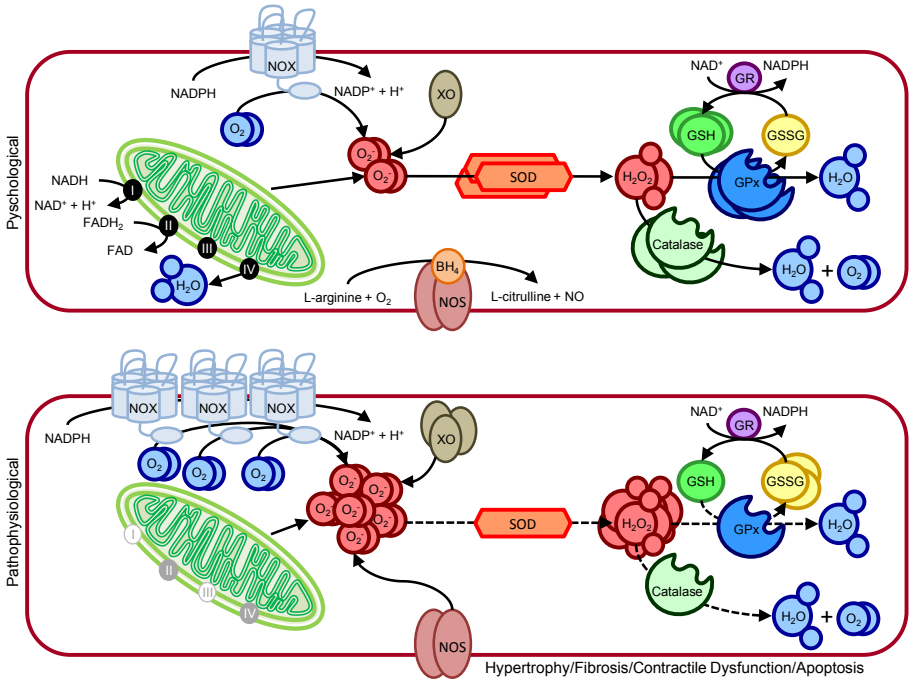


**Fig. 2. Oxidative stress production and scavenging in cardiomyocytes under physiological and pathophysiological conditions.**
(**TOP**) Under physiological conditions oxidative stress in the form of ROS is produced in small quantities by the mitochondrial electron chain, NADPH oxidase (NOX), xanthine oxidase (XO), and Nitric Oxide Synthase (NOS). Mitochondrial respiration converts oxygen to water, resulting in the production of small quantities of superoxide ($O_{2}^{-}$) as a by-product. The process starts with electrons derived from $NADH_2$ and $FADH_2$ moving along the respiratory transport chain through a series of cytochrome-based complexes (I, III, and IV). These complexes eventually transport electrons to molecular oxygen. The high free energy of the electrons is gradually extracted and converted into ATP. NOX is a multimeric complex composed of a plasma membrane spanning cytochrome $b_{558}$ (NOX2) and cytosolic components (Rac1, $p47^{phox}$, $p67^{phox}$, $p40^{phox}$). Under physiological conditions this complex is in a resting state, producing minimal $O_{2}^{-}$, by transferring an electron from NADPH to molecular oxygen. XO, which is a cytoplasmic enzyme that catalyzes the oxidation of hypoxanthine and xanthine to uric acid using molecular oxygen as an electron receptor, and in the process produces $O_{2}^{-}$ and hydrogen peroxide ($H_2O_2$). NOS oxidizes the NOS cofactor $BH_4$ utilizing NADPH to generate nitric oxide and L-citrulline from L-argenine and oxygen. Superoxide dismutase (SOD) initiates the detoxification of ROS, by scavenging $O_{2}^{-}$ and converting it to $H_2O_2$. Both catalase and glutathione peroxidase (GPx) further detoxify the $H_2O_2$ to water and oxygen. GPx utilizes two glutathione (GSH) molecules as electron donors in the reduction of $H_2O_2$ to water, producing oxidized glutathione (GSSG) in the process. Once GPx oxidizes GSH to GSSG, GSH reductase (GR) can reduce GSSG back to GSH at the expense of NADPH, forming the GSH redox cycle. The ratio of GSH to GSSG largely determines the intracellular redox potential. (**BOTTOM**) Under pathophysiological conditions, oxidative stress production is increased as a result of increased NOX and XO expression, coupled to blockage of the mitochondrial electron chain and uncoupling of NOS. Furthermore, the expression and activity (dotted lines) of SOD, catalase, and GPx is reduced. The levels of GSH are also reduced, while the levels of GSSG are increased. This severe increase in oxidative stress eventually leads to hypertrophy, fibrosis, apoptosis, and contractile dysfunction in the myocardium.

cardiomyocytes, as in most cell types, the major endogenous components of the antioxidant defense mechanism responsible for the inactivation of ROS are superoxide dismutase (SOD), catalase, glutathione peroxidase (GPx) and glutathione (GSH) (Fig. 2). Several studies have observed a significant decrease in the activities of SOD, catalase, and GPx in animal models for heart failure (13–15). Furthermore, mice lacking SOD or GPx exposed to cardiac injury have demonstrated worse outcomes when compared to their wild type littermates (16–20). GSH is the major antioxidant of mammalian cells, by scavenging radicals and the elimination of lipid peroxidation products (21). Interestingly, a reduction in total GSH has been observed in animals post cardiac injury (22,23). Furthermore, depletion of GSH was highly correlated to serum TNF-α levels (23). In LV tissue of end-stage dilated or ischemic cardiomyopathy patients total GSH was decreased by 54% when compared to controls (22). In another study, serum GSH levels highly correlated with the severity of heart failure symptoms in patients (24).

## Lessons to be learned from previous oxidative stress treatments in heart failure

Based on the observation that redox state is in disarray during heart failure, several experimental and clinical studies have aimed at treating heart failure by targeting oxidative stress producers (i.e. NADPH oxidases, xanthine oxidase, and uncoupled NOS) or scavengers [i.e. SOD, catalase, exogenous antioxidant (vitamin A, vitamin C, vitamin E, or folic acid), and GPx].

**Targeting oxidative stress production**

Initial experimental animal studies demonstrated that by targeting NADPH oxidases, xanthine oxidase, or NOS uncoupling, resulted in improved survival and cardiac function following cardiac injury. NADPH oxidase inhibition in mice lacking the cytosolic NADPH oxidase component p47phox, was shown to protect the heart from LV remodeling and dysfunction post-myocardial infarction (MI) (25). Inhibition of xanthine oxidase, by means of oxypurinol (rats) or allopurinol (dogs), was found to protect the heart from LV remodeling, improve LV contractile function, and myocardial efficiency post cardiac injury (26,27). The production of ROS by the uncoupling of NOS has also been studied as a possible target for heart failure. In mice, treatment with BH4, a substrate of NOS, improved cardiac function (12). Due to these promising results in the animal setting, several clinical trials targeting oxidative stress production have been conducted.

Inhibition of xanthine oxidase by the administration allopurinol or oxypurinol is at present the best studied therapy in patients with heart failure (11,28–34). The initial

clinical trials were small studies (N=9-60) on patients with dilated cardiomyopathy and chronic heart failure. These trials all demonstrated that treatment with allopurinol or oxypurinol improved myocardial function, peripheral vasodilation capacity, blood flow, endothelial dysfunction, reduced plasma BNP levels, and increased LV ejection fraction (LVEF) (11,28,29,31–33). However, the largest trial (N=405) in patients with heart failure found that the inhibition of xanthine oxidase by means of oxypurinol administration did not result in improved clinical outcome, the OPT-CHF (The Efficacy and Safety Study of Oxypurinol Added to Standard Therapy in Patients With New York Heart Association Class III-IV Congestive Heart Failure) study. The primary end point of the study was a combined clinical end point that classified the patient's clinical status as improved, worsened, or unchanged 24 weeks after the initiation of the study. Compared to the placebo group, patients demonstrated no improvement in clinical status following the oxypurinol treatment (30,34).

Similarly, several clinical trials have been performed with oral BH4 treatments (sapropterin) in patients (N=18-49) with systemic or pulmonary hypertension (35–37). However, these trials all failed to demonstrate any significant differences in nitric oxide synthesis, oxidative stress, systemic hemodynamics, vascular redox state or endothelial function. Taken together, these findings suggest that although targeting oxidative stress production seems theoretically logical, so far these strategies have failed to improve prognosis in the clinical setting.

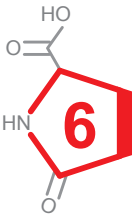


Why is there such a discrepancy between experimental studies and the subsequent clinical trials? The reason as to why inhibition of xanthine oxidase by means of allopurinol or oxypurinol did not lead to the expected beneficial effects could be due patient to patient physiological differences. A post-hoc analysis of OPT-CHF study demonstrated that a sub-set of patients with elevated uric acid, the product of xanthine oxidase, levels did demonstrate mild improvement in heart failure symptoms (34). That is to say, patients with the highest xanthine oxidase activity, and therefore, the highest uric acid levels, did seem to benefit from oxypurinol administration. Thus, targeting xanthine oxidase could be further characterized in heart failure patients with proven increases in xanthine oxidase activity or elevated uric acid levels. Targeting oxidative stress production from NOS uncoupling by means of sapropterin administration also demonstrated no beneficial effects in the clinical setting. The administration of sapropterin was found to increase the BH4 levels in the blood, but there was also a significant oxidation of exogenous BH4 to BH2, a competitive inhibitor of BH4 that promotes NOS uncoupling (37,38). Several studies have demonstrated that it is the ratio between BH4 and BH2 that regulate NOS coupling, and sapropterin had no net effect on the ratio (37,38). Therefore, there was no increase in NOS coupling, which may have resulted in the lack of

improvement on patient outcome (37,38).

**Administration of exogenous antioxidants**

Besides targeting oxidative stress production, early experimental studies demonstrated that increasing the endogenous antioxidant capacity lead to improved outcome following cardiac injury. Mainly, studies focused on overexpressing SOD, catalase, and GPx, which all three were found to improve cardiac function post-cardiac injury (18,39,40). These findings suggest that by increasing the antioxidant capacity of the heart, cardiomyocyte survival is improved, and the myocardium is better able to cope with injury. To further assess the potential of increasing the antioxidant capacity in heart failure, experimental studies have demonstrated that the supplementation of vitamin A, vitamin C, vitamin E, and folic acid can lead to improved cardiac function (41–44). Following these experimental findings, a multitude of clinical studies have focused on reducing oxidative stress by the supplementation of exogenous antioxidants vitamin A, vitamin C, vitamin E, or folic acid (45–49).

Initial studies found that the supplementation of exogenous antioxidants lead to a reduction in cardiovascular events, infarct sizes, and oxidative stress (45,46). However, a recent meta-analysis of 50 randomized control trials studying the effects of vitamin and antioxidant supplementation, including 294,478 participants, concluded that supplementation with exogenous vitamins and antioxidants was not associated with reductions in the risk of major CVDs (50). The underlying reasons as to the discrepancy between the beneficial effects of exogenous antioxidant supplementation in the experimental setting versus the clinical setting is not yet fully understood. It has however been speculated that antioxidant supplementation may only be beneficial to a subset of patients with a proven increase in oxidative stress. Therefore, a better understanding of the individual variability in human antioxidant defenses is essential to identify the patient population that may benefit from these treatments. Furthermore, efforts should be made into the identification of compounds capable of directly influencing the endogenous antioxidants (i.e. SOD, catalase and GPx), which have demonstrated highly beneficial effects in the experimental setting.

## The future of oxidative stress as a therapeutic target in heart failure

Although the findings of clinical trials aimed at reducing ROS production and increasing exogenous antioxidants have been disappointing, targeting oxidative stress, specifically the endogenous antioxidant capacity, in heart failure should not be entirely disregarded. The major endogenous antioxidant in mammalian cells is GSH, which is formed by the γ-Glutamyl cycle. GSH protects cells against oxidative stress, and GSH levels have been shown to be highly associated with heart failure

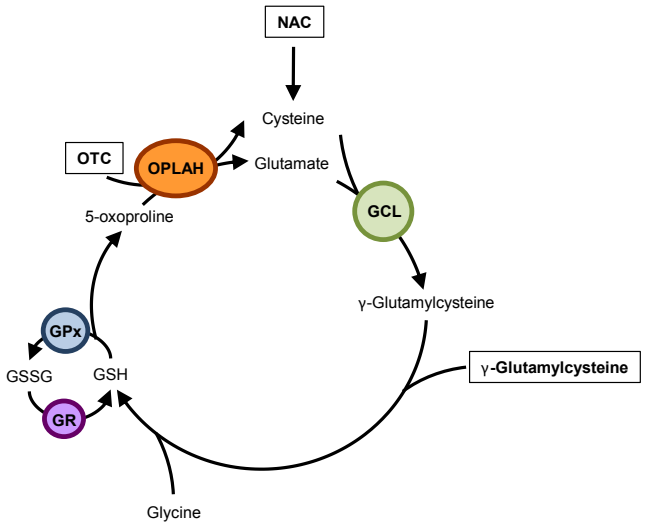


**Fig. 3. Drug therapies targeting endogenous glutathione synthesis.**
Glutathione (GSH) is synthesized from cysteine (the rate limiting amino acid), glutamate, and glycine by the γ-Glutamyl cycle. GSH is then utilized by GSH peroxidase (GPx) to reduce oxidative stress, and in the process forming oxidized GSH (GSSG). GSSG is then reduced by action of GSH reductase (GR). Improving the γ-Glutamyl cycle's ability to produce GSH has been characterized as a treatment target in heart failure. N-acetylcysteine (NAC), γ-glutamylcysteine, and 2-oxothiazolidine-4-carboxylate (OTC, also known as pro-cysteine) are compounds which have demonstrated the capacity to increase the endogenous production of GSH. OTC is converted to cysteine, by action of 5-oxoprolinase (OPLAH), to be used for *de novo* synthesis of GSH. Similarly, NAC is converted to cysteine intracellularly, and used for GSH synthesis. γ-Glutamylcysteine is utilized by the γ-Glutamyl cycle to form GSH, by addition of glycine.

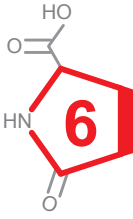


severity in the experimental and clinical setting (21–24). Therefore, bolstering the levels of endogenous GSH or increasing the activity of the γ-Glutamyl cycle may be a novel approach to dealing with oxidative stress and improving outcome of heart failure patients.

### Improving endogenous glutathione levels in heart failure

Increasing the endogenous GSH levels can be primarily achieved by supplementation with GSH precursors which can be utilized by the γ-Glutamyl cycle for de novo GSH synthesis (Fig. 3). A previously studied approach has been the supplementation of N-acetylcysteine, a precursor of GSH. N-acetylcysteine is readily absorbed into cells, where it is converted into cysteine, the rate limiting amino acid in the synthesis of GSH. Experimental studies have demonstrated that N-acetylcysteine can improve GSH levels, reduce oxidative stress, and improve cardiac function post injury (22,23). Based on these observation, clinical trials in patients with heart failure have been conducted with the administration of N-acetylcysteine (51–54). N-acetylcysteine was found to reduce oxidative stress, as measured by an increase in the GSH/GSSG

ratio. Furthermore, N-acetylcysteine reduced infarct size and improved cardiac function (51–54). Thus, improving the endogenous levels of GSH seems to be a promising target for treating oxidative stress increases in heart failure.

Besides N-acetylcysteine, γ-glutamylcysteine, another GSH precursor, and 2-oxothiazolidine-4-carboxylate (OTC), an analogue of 5-oxproline, also seem to have the potential to increase endogenous GSH levels. Both of these compounds have been demonstrated to increase GSH and reduce oxidative stress in the experimental and clinical setting (55–61). Similar to N-acetylcysteine, supplementation of γ-glutamylcysteine increased the levels of GSH, with no adverse effects, in cancer patients (55). OTC, which is converted to cysteine by 5-oxoprolinase (OPLAH), increases GSH levels in the experimental setting (56,57). Interestingly, early experimental studies have shown that OTC improved cardiac function following cardiac injury (58,59). Furthermore, in several clinical trials OTC treatment was found to have no adverse effects and increased GSH concentrations and decreased oxidative stress in patients with acute respiratory distress syndrome and HIV patients (60,61).

Although limited studies have focused on increasing the endogenous GSH levels in heart failure patients, studies with N-acetylcysteine supplementation do suggest this to be a potential strategy for combating the increase in oxidative stress resulting from cardiac injury. Future studies should focus on further characterizing the beneficial effects of N-acetylcysteine, γ-glutamylcysteine, and OTC on heart failure patient outcome.

**Targeting the γ-Glutamyl cycle in heart failure**

Besides improving the endogenous GSH levels by administration of GSH precursors, another avenue for reducing oxidative stress in heart failure is to improve the expression and/or activity of the γ-Glutamyl cycle. Recent experimental studies have demonstrated that several components of the γ-Glutamyl cycle are strongly associated with the development and progression of heart failure (including γ-glutamylcysteine synthetase, GPx, and OPLAH). Furthermore, modulation of these enzymes, by overexpression has resulted in cardio-protection (18,19,62–64). Of particular interest is OPLAH, a cytoplasmic enzyme of the GSH cycle whose only function is the conversion of 5-oxoproline, a degradation product of GSH, into glutamate (Fig. 4). Interestingly, studies have demonstrated that excessive 5-oxoproline accumulation can lead to the induction of intracellular oxidative stress (64–66). Therefore, OPLAH plays a pivotal role not only in the γ-Glutamyl cycle, by producing glutamate for *de novo* GSH synthesis, but also as an antioxidant by scavenging 5-oxoproline.

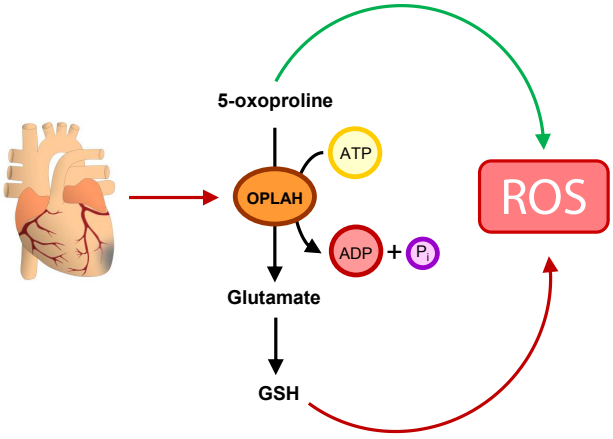


**Fig. 4. Targeting 5-oxoprolinase to reduce oxidative stress in heart failure.**
Following cardiac injury, 5-oxoprolinase (OPLAH) expression is reduced, leading to the accumulation of 5-oxoproline. 5-Oxoproline then leads to drastic increase in oxidative stress (ROS). To help reduce the insult of 5-oxoproline to the injured myocardium, two strategies could be developed: [1]pharmacologically improve the remaining OPLAH's ability to reduce 5-oxoproline or [2]by means of gene therapy increase OPLAH expression.

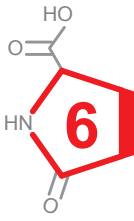


OPLAH expression has been found to be suppressed in heart failure, in the experimental and clinical setting (64,67). In the murine setting, this reduction in OPLAH was found to results in an increase in cardiac tissue and plasma 5-oxoproline levels, which coincided with an increase in oxidative stress (64). Interestingly, elevated levels of plasma 5-oxoproline in chronic heart failure patients was found to be associated with worsened outcome64. In a recent study, OPLAH overexpression mice exposed to I/R injury or permanent MI showed improved cardiac function, reduced infarct size and fibrosis, when compared to wild type littermates (64). Improved cardiac function in the OPLAH overexpression mice was coupled to reduced 5-oxoproline levels and improved GSH/GSSG ratio post cardiac injury (64). Thus, bolstering the expression and/or activity of OPLAH could lead to novel therapeutic strategies for patients with heart failure.

To date there are no known pharmacological agents (i.e. drugs or small molecules) that have the capacity to induce OPLAH activity. Future studies should therefore focus on identifying novel pharmacological agents that specifically target OPLAH. Similarly, the development of an OPLAH gene therapy, as recently described for SERCA2, could also serve as a viable therapeutic strategy (68,69). Furthermore, besides OPLAH, other members of the γ-Glutamyl cycle should also be screened for their potential use as therapeutic targets in heart failure.

## Conclusion

In this review we present current evidence for the role of oxidative stress and the antioxidant defense mechanisms, with a particular focus on GSH and the γ-Glutamyl cycle, in heart failure. Both the modulation of GSH levels and the γ-Glutamyl cycle seem to be novel and interesting new targets in the treatment of heart failure. In particular the development of medications capable of interacting with the components of the γ-Glutamyl cycle may lead to novel treatment options for heart failure in the future.

## References


1. Karimi Galougahi K, Antoniades C, Nicholls SJ, Channon KM, Figtree GA. Redox biomarkers in cardiovascular medicine. Eur Heart J 2015;
2. Kayama Y, Raaz U, Jagger A, Adam M, Schellinger IN, Sakamoto M, Suzuki H, Toyama K, Spin JM, Tsao PS. Diabetic Cardiovascular Disease Induced by Oxidative Stress. Int J Mol Sci 2015;16:25234–25263.
3. Tsutsui H, Kinugawa S, Matsushima S. Oxidative stress and heart failure. Am J Physiol Heart Circ Physiol 2011;301:H2181–H2190.
4. Sato Y, Fujiwara H, Takatsu Y. Cardiac troponin and heart failure in the era of high-sensitivity assays. J Cardiol Elsevier; 2012;60:160–167.
5. Takimoto E, Kass DA. Role of Oxidative Stress in Cardiac Hypertrophy and Remodeling. Hypertension 2007;49.
6. Sawyer DB, Colucci WS. Mitochondrial Oxidative Stress in Heart Failure : 'Oxygen Wastage' Revisited. Circ Res 2000;86:119–120.
7. Perrelli M, Pagliaro P, Penna C. Ischemia/reperfusion injury and cardioprotective mechanisms: Role of mitochondria and reactive oxygen species. World J Cardiol 2011;3:186–200.
8. Doughan AK, Harrison DG, Dikalov SI. Molecular mechanisms of angiotensin II-mediated mitochondrial dysfunction: Linking mitochondrial oxidative damage and vascular endothelial dysfunction. Circ Res 2008;102:488–496.
9. Heymes C, Bendall JK, Ratajczak P, Cave AC, Samuel JL, Hasenfuss G, Shah AM. Increased myocardial NADPH oxidase activity in human heart failure. J Am Coll Cardiol Elsevier Masson SAS; 2003;41:2164–2171.
10. Cappola TP, Kass DA, Nelson GS, Berger RD, Rosas GO, Kobeissi ZA, Marbán E, Hare JM. Allopurinol improves myocardial efficiency in patients with idiopathic dilated cardiomyopathy. Circulation 2001;104:2407–2411.
11. Cappola TP, Kass DA, Nelson GS, Berger RD, Rosas GO, Kobeissi ZA, Marban E, Hare JM, T.P. C, D.A. K, G.S. N, R.D. B, G.O. R, Z.A. K, E. M, J.M. H. Allopurinol improves myocardial efficiency in patients with idiopathic dilated cardiomyopathy. Circulation 2001;104:2407–2411.
12. Takimoto E, Champion HC, Li M, Ren S, Rodriguez ER, Tavazzi B, Lazzarino G, Paolocci N, Gabrielson KL, Wang Y, Kass DA. Oxidant stress from nitric oxide synthase-3 uncoupling stimulates cardiac pathologic remodeling from chronic pressure load. J Clin Invest 2005;115:1221–1231.
13. Hill MF, Singal PK. Antioxidant and oxidative stress changes during heart failure subsequent to myocardial infarction in rats. Am J Pathol 1996;148:291–300.
14. Khaper N, Singal PK. Effects of afterload-reducing drugs on pathogenesis of antioxidant changes and congestive heart failure in rats. J Am Coll Cardiol 1997;29:856–861.
15. Khaper N, Kaur K, Li T, Farahmand F, Singal PK. Antioxidant enzyme gene expression in congestive heart failure following mycardial infarction. Mol Cell Biochem Kluwer Academic Publishers; 2003;251:9–15.
16. Deel ED van, Lu Z, Xu X, Zhu G, Hu X, Oury TD, Bache RJ, Duncker DJ, Chen Y. Extracellular superoxide dismutase protects the heart against oxidative stress and hypertrophy after myocardial infarction. Free Radic Biol Med NIH Public Access; 2008;44:1305–1313.
17. Ding Y, Li Y-L, Zimmerman MC, Davisson RL, Schultz HD. Role of CuZn superoxide dismutase on carotid body function in heart failure rabbits. Cardiovasc Res 2009;81.
18. Shiomi T, Tsutsui H, Matsusaka H, Murakami K, Hayashidani S, Ikeuchi M, Wen J, Kubota T, Utsumi H, Takeshita A. Overexpression of glutathione peroxidase prevents left ventricular remodeling and failure after myocardial infarction in mice. Circulation 2004;109:544–549.
19. Yoshida T, Watanabe M, Engelman DT, Engelman RM, Schley JA, Maulik N, Ho YS, Oberley TD, Das DK. Transgenic mice overexpressing glutathione peroxidase are resistant to myocardial ischemia reperfusion injury. J Mol Cell Cardiol 1996;28:1759–1767.
20. Forgione MA, Cap A, Liao R, Moldovan NI, Eberhardt RT, Lim CC, Jones J, Goldschmidt-Clermont PJ, Loscalzo J. Heterozygous cellular glutathione peroxidase deficiency in the mouse: abnormalities in vascular and cardiac function and structure. Circulation 2002;106:1154–1158.
21. Townsend DM, Tew KD, Tapiero H. The importance of glutathione in human disease. Biomed Pharmacother = Biomédecine pharmacothérapie 57:145–155.
22. Adamy C, Mulder P, Khouzami L, Andrieu-abadie N, Defer N, Candiani G, Pavoine C, Caramelle P,

Souktani R, Corvoisier P Le, Perier M, Kirsch M, Damy T, Berdeaux A, Levade T, Thuillez C, Hittinger L, Pecker F. Neutral sphingomyelinase inhibition participates to the benefits of N-acetylcysteine treatment in post-myocardial infarction failing heart rats. J. Mol. Cell. Cardiol. 2007. p. 344–353.
23. Bourraindeloup M, Adamy C, Candiani G, Cailleret M, Bourin M-C, Badoual T, Su JB, Adubeiro S, Roudot-Thoraval F, Dubois-Rande J-L, Hittinger L, Pecker F. N-acetylcysteine treatment normalizes serum tumor necrosis factor-alpha level and hinders the progression of cardiac injury in hypertensive rats. Circulation 2004;110:2003–2009.
24. Damy T, Kirsch M, Khouzami L, Caramelle P, Corvoisier P Le, Roudot-Thoraval F, Dubois-Randé J-L, Hittinger L, Pavoine C, Pecker F. Glutathione deficiency in cardiac patients is related to the functional status and structural cardiac abnormalities. PLoS One 2009;4:e4871.
25. Doerries C, Grote K, Hilfiker-Kleiner D, Luchtefeld M, Schaefer A, Holland SM, Sorrentino S, Manes C, Schieffer B, Drexler H, Landmesser U. Critical role of the NAD(P)H oxidase subunit p47phox for left ventricular remodeling/dysfunction and survival after myocardial infarction. Circ Res 2007;100:894–903.
26. Ukai T, Cheng CP, Tachibana H, Igawa A, Zhang ZS, Cheng HJ, Little WC. Allopurinol enhances the contractile response to dobutamine and exercise in dogs with pacing-induced heart failure. Circulation 2001;103:750–755.
27. Minhas KM, Saraiva RM, Schuleri KH, Lehrke S, Zheng M, Saliaris AP, Berry CE, Vandegaer KM, Li D, Hare JM. Xanthine oxidoreductase inhibition causes reverse remodeling in rats with dilated cardiomyopathy. Circ Res 2006;98:271–279.
28. Gavin AD, Struthers AD. Allopurinol reduces B-type natriuretic peptide concentrations and haemoglobin but does not alter exercise capacity in chronic heart failure. Heart 2005;91:749–753.
29. Guan W, Osanai T, Kamada T, Hanada H, Ishizaka H, Onodera H, Iwasa A, Fujita N, Kudo S, Ohkubo T, Okumura K. Effect of allopurinol pretreatment on free radical generation after primary coronary angioplasty for acute myocardial infarction. J Cardiovasc Pharmacol 2003;41:699–705.
30. Freudenberger RS, Schwarz RP, Brown J, Moore A, Mann D, Givertz MM, Colucci WS, Hare JM. Rationale, design and organisation of an efficacy and safety study of oxypurinol added to standard therapy in patients with NYHA class III - IV congestive heart failure. Expert Opin Investig Drugs 2004;13:1509–1516.
31. Cingolani HE, Plastino JA, Escudero EM, Mangal B, Brown J, Pérez NG. The Effect of Xanthine Oxidase Inhibition Upon Ejection Fraction in Heart Failure Patients: La Plata Study. J Card Fail 2006;12:491–498.
32. Doehner W, Schoene N, Rauchhaus M, Leyva-Leon F, Pavitt D V, Reaveley DA, Schuler G, Coats AJS, Anker SD, Hambrecht R. Effects of xanthine oxidase inhibition with allopurinol on endothelial function and peripheral blood flow in hyperuricemic patients with chronic heart failure: results from 2 placebo-controlled studies. Circulation 2002;105:2619–2624.
33. Farquharson CAJ, Butler R, Hill A, Belch JJF, Struthers AD. Allopurinol improves endothelial dysfunction in chronic heart failure. Circulation 2002;106:221–226.
34. Hare JM, Mangal B, Brown J, Fisher C, Freudenberger R, Colucci WS, Mann DL, Liu P, Givertz MM, Schwarz RP, OPT-CHF Investigators. Impact of Oxypurinol in Patients With Symptomatic Heart Failure. J Am Coll Cardiol 2008;51:2301–2309.
35. Reverter E, Mesonero F, Seijo S, Martínez J, Abraldes JG, Peñas B, Berzigotti A, Deulofeu R, Bosch J, Albillos A, Carles García-Pagán J. Effects of Sapropterin on Portal and Systemic Hemodynamics in Patients With Cirrhosis and Portal Hypertension: A Bicentric Double-Blind Placebo-Controlled Study. Am J Gastroenterol 2015;110:985–992.
36. Robbins IM, Hemnes AR, Simon Gibbs J, Christman BW, Howard L, Meehan S, Cabrita I, Gonzalez R, Oyler T, Zhao L, Du R-H, Mendes LA, Wilkins MR. Safety of sapropterin dihydrochloride (6r–bh4) in patients with pulmonary hypertension. Exp Lung Res 2011;37:26–34.
37. Cunnington C, Assche T Van, Shirodaria C, Kylintireas I, Lindsay AC, Lee JM, Antoniades C, Margaritis M, Lee R, Cerrato R, Crabtree MJ, Francis JM, Sayeed R, Ratnatunga C, Pillai R, Choudhury RP, Neubauer S, Channon KM. Systemic and Vascular Oxidation Limits the Efficacy of Oral Tetrahydrobiopterin Treatment in Patients With Coronary Artery DiseaseClinical Perspective. Circulation 2012;125.
38. Vásquez-Vivar J, Martásek P, Whitsett J, Joseph J, Kalyanaraman B. The ratio between tetrahydrobiopterin and oxidized tetrahydrobiopterin analogues controls superoxide release from endothelial nitric oxide synthase: an EPR spin trapping study. Biochem J 2002;362:733–739.
39. Qin F, Lennon-Edwards S, Lancel S, Biolo A, Siwik DA, Pimentel DR, Dorn GW, Kang YJ, Colucci

WS. Cardiac-specific overexpression of catalase identifies hydrogen peroxide-dependent and -independent phases of myocardial remodeling and prevents the progression to overt heart failure in G(alpha)q-overexpressing transgenic mice. Circ Heart Fail 2010;3:306–313.
40. Wang P, Chen H, Qin H, Sankarapandi S, Becher MW, Wong PC, Zweier JL. Overexpression of human copper, zinc-superoxide dismutase (SOD1) prevents postischemic injury. Proc Natl Acad Sci U S A 1998;95:4556–4560.
41. Dhalla AK, Hill MF, Singal PK. Role of oxidative stress in transition of hypertrophy to heart failure. J Am Coll Cardiol 1996;28:506–514.
42. Hamblin M, Smith HM, Hill MF. Dietary supplementation with vitamin E ameliorates cardiac failure in type I diabetic cardiomyopathy by suppressing myocardial generation of 8-iso-prostaglandin F2alpha and oxidized glutathione. J Card Fail NIH Public Access; 2007;13:884–892.
43. Prasad K, Gupta JB, Kalra J, Lee P, Mantha S V, Bharadwaj B. Oxidative Stress as a Mechanism of Cardiac Failure in Chronic Volume Overload in Canine Model. J Mol Cell Cardiol 1996;28:375–385.
44. Li W, Tang R, Ouyang S, Ma F, Liu Z, Wu J. Folic acid prevents cardiac dysfunction and reduces myocardial fibrosis in a mouse model of high-fat diet-induced obesity. Nutr Metab (Lond) BioMed Central; 2017;14:68.
45. Stephens NG, Parsons A, Schofield PM, Kelly F, Cheeseman K, Mitchinson MJ. Randomised controlled trial of vitamin E in patients with coronary disease: Cambridge Heart Antioxidant Study (CHAOS). Lancet (London, England) 1996;347:781–786.
46. Singh RB, Niaz MA, Rastogi SS, Rastogi S. Usefulness of antioxidant vitamins in suspected acute myocardial infarction (the Indian experiment of infarct survival-3). Am J Cardiol 1996;77:232–236.
47. MARCHIOLI R. ANTIOXIDANT VITAMINS AND PREVENTION OF CARDIOVASCULAR DISEASE: LABORATORY, EPIDEMIOLOGICAL AND CLINICAL TRIAL DATA. Pharmacol Res 1999;40:227–238.
48. Tomasian D, Keaney JF, Vita JA. Antioxidants and the bioactivity of endothelium-derived nitric oxide. Cardiovasc Res 2000;47:426–435.
49. Albert CM, Cook NR, Gaziano JM, Zaharris E, MacFadyen J, Danielson E, Buring JE, Manson JE. Effect of folic acid and B vitamins on risk of cardiovascular events and total mortality among women at high risk for cardiovascular disease: a randomized trial. JAMA NIH Public Access; 2008;299:2027–2036.
50. Myung S-K, Ju W, Cho B, Oh S-W, Park SM, Koo B-K, Park B-J. Efficacy of vitamin and antioxidant supplements in prevention of cardiovascular disease: systematic review and meta-analysis of randomised controlled trials. BMJ 2013;346.
51. Mehra A, Shotan A, Ostrzega E, Hsueh W, Vasquez-Johnson J, Elkayam U. Potentiation of isosorbide dinitrate effects with N-acetylcysteine in patients with chronic heart failure. Circulation 1994;89:2595–2600.
52. Šochman J, Vrbská J, Musilová B, Roček M. Infarct size limitation: Acute N-acetylcysteine defense (ISLAND trial): Preliminary analysis and report after the first 30 patients. Clin Cardiol Wiley Periodicals, Inc.; 1996;19:94–100.
53. Sochman J, Peregrin JH. Total recovery of left ventricular function after acute myocardial infarction: comprehensive therapy with streptokinase, N-acetylcysteine and percutaneous transluminal coronary angioplasty. Intrrnational J Cardiol 1992;35:116–118.
54. Arstall MA, Yang J, Stafford I, Betts WH, Horowitz JD. N-Acetylcysteine in Combination With Nitroglycerin and Streptokinase for the Treatment of Evolving Acute Myocardial Infarction. Circulation 1995;92.
55. Zarka MH, Bridge WJ. Oral administration of γ-glutamylcysteine increases intracellular glutathione levels above homeostasis in a randomised human trial pilot study. Redox Biol 2017;11:631–636.
56. Williamson JM, Meister A. New substrates of 5-oxo-L-prolinase. J Biol Chem 1982;257:12039–12042.
57. Weitberg AB. The effect of L-2-oxothiazolidine on glutathione levels in cultured mammalian cells. Mutat Res 191:189–191.
58. Shug A, Madsen D. Protection of the ischemic rat heart by procysteine and amino acids. J Nutr Biochem 1994;5:356–359.
59. POON BY, GODDARD CM, LEAF CD, RUSSELL JA, WALLEY KR. l -2-Oxothiazolidine-4-Carboxylic Acid Prevents Endotoxin-induced Cardiac Dysfunction. Am J Respir Crit Care Med American Thoracic SocietyNew York, NY; 1998;158:1109–1113.
60. Bernard GR, Wheeler AP, Arons MM, Morris PE, Paz HL, Russell JA, Wright PE. A trial of antioxidants N-acetylcysteine and procysteine in ARDS. The Antioxidant in ARDS Study Group. Chest

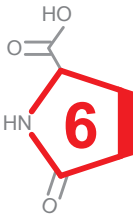

1997;112:164–172.
61. Kalayjian RC, Skowron G, Emgushov RT, Chance M, Spell SA, Borum PR, Webb LS, Mayer KH, Jackson JB, Yen-Lieberman B. A phase I/II trial of intravenous L-2-oxothiazolidine-4-carboxylic acid (procysteine) in asymptomatic HIV-infected subjects. J Acquir Immune Defic Syndr 1994;7:369–374.
62. Schupp N, Schmid U, Heidland A, Stopper H. Rosuvastatin protects against oxidative stress and DNA damage in vitro via upregulation of glutathione synthesis. Atherosclerosis 2008;199:278–287.
63. Costa S, Reina-Couto M, Albino-Teixeira A, Sousa T. Statins and oxidative stress in chronic heart failure PALAVRAS-CHAVE. Rev Port Cardiol 2015;35:41–57.
64. Pol A van der, Gil A, Silljé HHW, Tromp J, Ovchinnikova ES, Vreeswijk-Baudoin I, Hoes M, Domian IJ, Sluis B van de, Deursen JM van, Voors AA, Veldhuisen DJ van, Gilst WH van, Berezikov E, Harst P van der, Boer RA de, Bischoff R, Meer P van der. Accumulation of 5-oxoproline in myocardial dysfunction and the protective effects of OPLAH. Sci Transl Med 2017;9:eaam8574.
65. Pederzolli CD, Sgaravatti AM, Braum CA, Prestes CC, Zorzi GK, Sgarbi MB, Wyse ATS, Wannmacher CMD, Wajner M, Dutra-Filho CS. 5-Oxoproline reduces non-enzymatic antioxidant defenses in vitro in rat brain. Metab Brain Dis 2007;22:51–65.
66. Pederzolli CD, Mescka CP, Zandoná BR, Moura Coelho D de, Sgaravatti AM, Sgarbi MB, Souza Wyse AT de, Duval Wannmacher CM, Wajner M, Vargas CR, Dutra-Filho CS. Acute administration of 5-oxoproline induces oxidative damage to lipids and proteins and impairs antioxidant defenses in cerebral cortex and cerebellum of young rats. Metab Brain Dis 2010;25:145–154.
67. Yang K-C, Yamada KA, Patel AY, Topkara VK, George I, Cheema FH, Ewald GA, Mann DL, Nerbonne JM. Deep RNA sequencing reveals dynamic regulation of myocardial noncoding RNAs in failing human heart and remodeling with mechanical circulatory support. Circulation 2014;129:1009–1021.
68. Jessup M, Greenberg B, Mancini D, Cappola T, Pauly DF, Jaski B, Yaroshinsky A, Zsebo KM, Dittrich H, Hajjar RJ, Calcium Upregulation by Percutaneous Administration of Gene Therapy in Cardiac Disease (CUPID) Investigators. Calcium Upregulation by Percutaneous Administration of Gene Therapy in Cardiac Disease (CUPID): A Phase 2 Trial of Intracoronary Gene Therapy of Sarcoplasmic Reticulum Ca2+-ATPase in Patients With Advanced Heart Failure. Circulation 2011;124:304–313.
69. Zsebo K, Yaroshinsky A, Rudy JJ, Wagner K, Greenberg B, Jessup M, Hajjar RJ. Long-Term Effects of AAV1/SERCA2a Gene Transfer in Patients With Severe Heart FailureNovelty and Significance. Circ Res 2014;114:101–108.

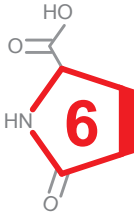
HO
O
HN
6
O

# Chapter 7

Discussion & future perspectives

Heart failure (HF) is the most prominent health challenge of the developed world, with a five year survival rate of less than 50% 1. HF is defined as the complex end stage clinical syndrome that can result from numerous cardiac disorders, including myocardial infarction (MI), hypertension, cardiomyopathies, and valvular disease. Although, many breakthroughs have been made, the fundamental mechanisms responsible for the development and progression of HF have not yet been fully elucidated. In recent years it has been observed that cardiac injury in the adult heart leads to a switch in gene expression which to some extend resembles the expression pattern observed in the fetal heart. This process has been described as cardiac fetal reprogramming, and is defined as the suppression of adult and re-expression of fetal genes in the diseased myocardium. The exact reasons and mechanisms as to why the adult heart reverts back to a fetal-like expression pattern and the consequences here of remain unknown. With this thesis we provide a large body of evidence suggesting that a better understanding of cardiac fetal reprogramming can lead to novel therapeutic strategies for patients with HF. We describe the identification of OPLAH, a novel member of the cardiac fetal gene program, which possesses a cardio-protective effect by scavenging the oxidative stress inducing metabolite, 5-oxoproline. In turn, we demonstrate 5-oxoproline to be a putative novel biomarker for patients with HF.

**Cardiac fetal reprogramming: a tool to exploit novel treatment targets for the failing heart**

In **chapter 2**, we reviewed the current knowledge regarding cardiac fetal reprogramming in HF, by looking at the expression profiles during cardiac development and disease, with a particular focus on cardiac metabolism, contractile machinery, electrophysiology, and neurohormonal expression.

In terms of cardiac metabolism we describe how during development the heart reverts to a fetal pattern in which glycolysis primarily contributes to ATP production as opposed to fatty acid oxidation (2,3). This switch in energy substrates has been suggested to result from a reduction in PPAR-α and PGC-1α levels due to rising levels of HIF-1α (4). Once HIF-1α levels increase in the adult heart, expression of 6-phosphofructo-2-kinase (PFK2) increases, resulting in increased levels of fructose-2,6-biphosphate, thereby activating PFK1 and ultimately glycolysis (5).

Besides the switch in energy metabolism, cardiac fetal reprogramming also occurs in the contractile machinery. Maturation from a fetal to an adult heart involves a steady shift from compliant (fetal) to stiffer (adult) contractile proteins. As a result of cardiac disease, the adult heart undergoes a reversion to a more compliant fetal contractile machinery. This turnover has been highly studied in the sarcomere, where several components of the sarcomere revert to a more fetal like state upon cardiac injury.

Myosin heavy chain (MHC) and light chain (MLC) are part of the “molecular motor” of the sarcomere, and both have isoforms that are mainly expressed in the fetal and mature heart. Studies have demonstrated that an isoform switch takes place as a result from cardiac injury that resembles the fetal heart for both the MHC and the MLC (6–11). Similar isoform switches have been observed for actin (10–14), troponin (14–16) and titin (14,17–19).

The reversion to a more fetal-like state in response to cardiac injury has also been observed in the mechanisms regulating the electrophysiology of cardiomyocytes. Cardiomyocyte electrophysiology is in large part governed by the expression of ion channels, gap junctions, and the calcium homeostasis. It has been observed that the immature and mature heart differ from each other in terms of excitability, action potential properties, contractility, and relaxation (20). As a result the fetal heart expresses different genes involved in the generation and propagation of the action potential then the adult heart. Sodium channels ($I_{Na}$), potassium channels ($I_{to}$, $I_{K1}$, $I_{Kr}$, and $I_{Ks}$), and calcium channels ($I_{ca,L}$, and NCX) are expressed lower in the fetal heart then in the adult heart, on the other hand the $I_{Ca,T}$ (*CACNA1H*) and $I_f$ (*HCN4*) ion channels are significantly higher expressed in the fetal heart then the adults heart (20). Interestingly, in cardiac tissue of patients diagnosed with end stage HF, the major sodium ($I_{Na}$), potassium ($I_{to}$, $I_{K1}$, $I_{Kr}$, and $I_{Ks}$), and calcium ($I_{ca,L}$, and NCX) ion channels are significantly repressed, while $I_{ca,T}$ and $I_f$ (*HCN4*) are up-regulated (21–23). These findings suggest that as a result of cardiac injury, the heart undergoes ion channel remodeling, resulting in an expression profile similar to that of the fetal heart. Likewise, it has been well established that during cardiac development in both rodent models and in the human setting, the expression of connexin 43, connexin 40, and connexin 45 are progressively increased as the heart matures (24–27). This developmental increase in the density of gap junctions in the heart correlates well with the developmental increase in conduction velocity. Upon cardiac damage in both rodent models and in the human setting, connexin 43 expression is not only drastically reduced (±50%), but the remaining connexin 43 gap junctions are also highly disorganized (27–29). This decrease in connexin 43 expression is also associated with an increase in connexin 40 expression (27–29).

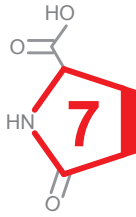


Finally, cardiac fetal reprogramming is not only limited to metabolism, contractile machinery, and electrophysiological, but also occurs in the expression of cardiac neurohormones. Specifically fetal reprogramming has been observed in the expression of atrial and brain natriuretic peptides (ANP and BNP, respectively). Both ANP and BNP are highly expressed in the fetal heart, and as the heart matures these levels drop rapidly. Following cardiac injury, these two neurohormones are re-expressed. In recent years it has been well established that the re-expression of

both ANP and BNP has a cardioprotective effect in the failing myocardium.

Combined these observations all suggest that cardiac fetal reprogramming is an integral part of the pathophysiology of HF. Although there is plethora of evidence regarding cardiac fetal reprogramming and its importance during HF, there still remains much to be uncovered regarding this process. In this thesis I describe how understanding the process of cardiac fetal reprogramming can lead to novel therapeutic strategies for HF patients.

**Identification of OPLAH as a novel member of the cardiac fetal gene program, and its cardio-protective effect in myocardial dysfunction**

In **chapter 3** we sought to identify new members of the cardiac fetal gene program and investigate whether these genes could serve as therapeutic targets in the human setting. By means of RNA sequencing analysis on different stages of murine cardiac development and disease, we identified 68 genes which behaved like cardiac fetal genes (demonstrating inverse expression during cardiac disease as compared to cardiac development). Of these 68 putative cardiac fetal genes, 39 had already been described in the literature as associated with cardiac disease or development (including *Ryr2*, *Cacna2d1*, *Fstl1* and *Bambi*) (30–33). The remaining 29 genes had been associated with neither cardiac development nor cardiac disease to date, and were considered novel genes associated with the cardiac fetal-like gene program. To evaluate whether these 29 putative cardiac fetal-like genes were also relevant in humans, we screened the expression of these genes across an adult human organ panel using qRT-PCR. *ANXA11*, *HADH*, *CD300LG*, and *OPLAH* were predominantly expressed in the human heart. Of these four genes, *OPLAH*, was found to be the more cardiac specific and as such we further explored the role of OPLAH in the heart.

*OPLAH* is a gene which encodes for 5-oxoprolinase an enzyme involved in the γ-Glutamyl cycle, where it specifically converts 5-oxoproline, a degradation product of glutathione (GSH), into glutamate (34,35). We identify *OPLAH* as a novel cardiac gene involved in HF, which is at least in part regulated by the PGC-1α/ERRα axis. Both PGC-1α and ERRα are key transcriptional regulators of antioxidant protection genes (36). It has been well established that PGC-1α regulates ERRα expression, and that the expression of PGC-1α is induced in cardiac development and repressed in HF (36,37). Our data support the interaction between PGC-1α and ERRα by demonstrating that direct inhibition of ERRα activity results in an increase in PGC-1α and ERRα mRNA, suggesting a compensatory mechanism. Furthermore, the decreased activity of ERRα was shown to reduce OPLAH expression and enhance oxidative stress. These observations are in line with a recent study, which demonstrated by microarray analysis on RNA isolated from ERRα knockout mouse

hearts that these mice had significantly increased expression of PGC-1α and reduced OPLAH (38).

In **chapter 3** we also investigated the consequence of OPLAH depletion in HF resulting in an increase in oxidative stress and 5-oxoproline. Furthermore, exogenous administration of 5-oxoproline to cardiomyocytes also led to increased oxidative stress. This finding is supported by a previous study that identified 5-oxoproline as an inducer of oxidative stress in brain tissue (39,40). We propose that HF leads to the reduction of PGC-1α, which, as a consequence, results in a decrease in ERRα and antioxidant protection genes, including OPLAH. Due to reduced OPLAH expression, 5-oxoproline cannot be processed into glutamate, and the excessive accumulation of 5-oxoproline leads to increases in oxidative stress, adding further insult to the progression of the disease. By exposing mice with cardiac-specific OPLAH overexpression to cardiac injury, we demonstrate that these mice have less oxidative stress, lower 5-oxoproline, and reduced fibrosis, resulting in improved cardiac function. Thus, we posit that OPLAH is a potential target for therapeutic intervention in HF.

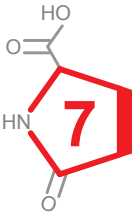


To further stress the involvement of OPLAH and 5-oxoproline in HF, we measured 5-oxoproline in plasma of both experimental and clinical HF. In rats with pressure overload–induced HF (REN2) where LV tissue 5-oxoproline was ~20-fold higher than in control rats, circulating 5-oxoproline was also found to be about six fold higher. To determine whether these findings could be extrapolated to the human setting, we measured 5-oxoproline in the plasma of healthy controls (n = 10) and patients with acute HF (n = 10) (24). Plasma 5-oxoproline was increased about four fold in acute HF patients compared to healthy controls. To assess the potential of 5-oxoproline to serve as a circulating biomarker in clinical HF, we we tested the prognostic potential of 5-oxoproline in a cohort of 535 patients who had been hospitalized for acute HF. Interestingly, we found that higher 5-oxoproline was associated with a worse outcome. These findings suggest that circulating 5-oxoproline, the substrate of OPLAH, can serve as a potential biomarker in patients with HF, further stressing the involvement of OPLAH and 5-oxoproline in HF.

**OPLAH ablation leads to accumulation of 5-oxoproline, oxidative stress, fibrosis and elevated fillings pressures in a murine model for heart failure with a preserved ejection fraction.**

In **chapter 4**, we sought to further characterize the role of OPLAH in HF. In **chapter 3** we found OPLAH to possess a cardio-protective effect in an over-expression mouse model (41). Furthermore, in our in vitro work we demonstrated that a reduction in OPLAH resulted in increased susceptibility towards oxidative stress (41). To further address this observation, in **chapter 4** we describe the development of an *Oplah* full

body knock-out (KO) mouse and the effects ischemia/reperfusion (IR) injury has on these mice.

OPLAH ablation in mice was observed to result in increased 5-oxoproline, oxidative stress, atrial enlargement, fibrosis, ventricular filling pressures, and impaired LV relaxation coupled to a preserved LV ejection fraction. Interestingly, at baseline these mice did not only develop a cardiac phenotype, but we also observed an increase in renal fibrosis, suggesting the increase in 5-oxoproline was resulting in renal damage. Interestingly, when challenged, these mice were found to be more susceptible to cardiac damage and sudden death, following cardiac IR injury. Furthermore, genetic disruption of *Oplah* not only led to an increase in cardiac damage, but we also observed that the *Oplah* KO mice developed proteinuria following IR injury. Combined these findings suggested that OPLAH ablation in mice resulted in a phenotype reminiscent of patients with HF with preserved ejection fraction (HFpEF). This in its self is novel since to date there are no strong animal models to study HFpEF. Thus utilizing these mice my serve to better understand this disease and uncover novel therapeutic strategies to treat the disease.

As described in **chapter 3**, we identified that 5-oxoproline was not only elevated in the myocardium but also in the plasma of animals with HF. In acute HF, circulating 5-oxoproline was independently associated with patient outcome and associated with known markers for cardiac remodeling, stretch, and oxidative stress, but not with markers for inflammation (41). To further explore the potential of 5-oxoproline as a biomarker in HF, and in particular with regards towards its involvement in HFpEF, in **chapter 4** we measured this metabolite in a small cohort of patients with HFpEF. Similar to our observations in **chapter 3** where 5-oxoproline levels were increased in patients with acute HF when compared to healthy controls, we found that plasma levels of 5-oxoproline were also higher in HFpEF patients then healthy controls. Furthermore, higher levels of circulating 5-oxoproline were found to independently associate with more concentric remodeling, a hallmark of HFpEF.

Although our proposed murine model for HFpEF mimics HFpEF in the human setting, there remain several limitations to this model. The main limitation is that in this model HFpEF is developed as a result of direct genetic manipulation. Thus, it is uncertain whether the pathophysiological pathway, implicating OPLAH and 5-oxoproline, is also involved in the onset of HFpEF in humans. Rather one could also speculate that the effects we observe in the *Oplah* KO mice are a result of the severe oxidative stress, due to accumulation of the oxidative stress inducing agent 5-oxoproline. Additionally, circulating 5-oxoproline was measured in a very specific cohort of HFpEF patients with pulmonary hypertension, and therefore it is

uncertain to which extent findings of this patient cohort can be extrapolated to other patients with HFpEF. Furthermore, the sample size was rather small, inhibiting us from performing more extensive analyses.

**LC-MS analysis of key components of the γ-Glutamyl cycle in tissues and body fluids from mice with Myocardial Infarction**

In **chapter 3** and **chapter 4** we utilized a LC-MS method that enabled us to measure 5-oxoproline and glutamate. However to obtain a better understanding of the involvement of the γ-glutamyl cycle in heart failure, in **chapter 5**, we sought out to develop a LC-MS method for the quantification of 5-oxoproline, glutamate, GSH and GSSG (oxidized GSH), key components of the γ-glutamyl cycle, in biological samples. The method we developed and validated, accurately and reliable quantified 5-oxoproline, glutamate, and GSH. The levels of GSSG were quantifiable in murine tissues, however this was not the case for plasma and urine of these animals. The fact that GSSG was not detectable in the plasma and urine samples suggest that within these samples GSSG is either unstable or the GSSG levels within the samples falls out of the lower limits of the detection of the method.

Utilizing the developed methodology, we assessed the effects on the γ-glutamyl cycle following the induction of HF in mice. Specifically in the heart we found increases in 5-oxoproline together with a decrease in the GSH/GSSG ratio in mice exposed to HF, further strengthening the notion that 5-oxoproline is an oxidative stress inducing agent (39–41). In addition to being elevated in the heart, 5-oxoproline levels were found to be increased in the kidney, liver, plasma and urine of all mice exposed to HF. However, the GSH/GSSG ratios in the kidney and liver of these animals remained stable, suggesting that these tissues have a higher buffering capacity for oxidative stress. Interestingly, we found 5-oxoproline levels in urine to be elevated following cardiac injury, suggesting that, like plasma, urine 5-oxoproline levels could serve as a possible HF biomarker.

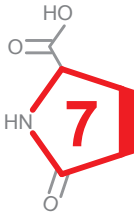


**Treating oxidative stress in heart failure: past, present, and future**

OPLAH is a member of the γ-Glutamyl cycle, and following the observations made in this thesis, we were interested in further characterizing this cycle in HF and uncover whether other members of this cycle could also serve as possible therapeutic targets for patients with HF. To this end, in **chapter 6** we reviewed the current knowledge regarding the γ-Glutamyl cycle and its association to oxidative stress and HF.

The γ-Glutamyl cycle is responsible for the GSH metabolism. GSH is synthesized from glutamate, cysteine, and glycine by γ-glutamylcysteine synthetase (GCL) and glutathione synthetase (GS) (42). Upon synthesis, GSH can be utilized internally by the cell, or be exported to the extra-cellular matrix. The primary means of recovering

the exported GSH is by a scavenging pathway, involving γ-Glutamyltransferase (GGT), γ-glutamylcyclotransferase (GGCT), OPLAH, and dipeptidase (42).

GSH is the major source of non-enzymatic antioxidants, but also participates in biosynthetic pathways, signaling processes, detoxification, and storage and transport of key metabolites (35). Its function as an antioxidant is regulated by glutathione peroxidase (GPx) and glutathione reductase (GR). GPx utilizes two GSH molecules as electron donors in the reduction of hydrogen peroxide to water, producing glutathione disulfide (GSSG) in the process (43). Once GPx oxidizes GSH to GSSG, GSH reductase (GR) can reduce GSSG back to GSH at the expense of NADPH. The ratio of GSH to GSSG largely determines the intracellular redox potential. When oxidative stress overcomes the cells ability to reduce GSSG to GSH, GSSG is actively exported out of the cell to prevent a major shift in the redox equilibrium (44). Therefore, severe oxidative stress depletes the intracellular GSH pool (45).

Several studies focused on the γ-Glutamyl cycle have uncovered that certain enzymes involved in this cycle have cardio-protective properties, including GCL, GPx, and OPLAH. However, clinical strategies for targeting these steps have not yet been explored, which is in large part due to the lack of drugs or small molecules that specifically target these enzymes. The research focused on dissecting the involvement of the γ-Glutamyl cycle and GSH in HF has not only resulted in the identification of novel therapeutic targets for this disease, but has also lead to the characterization of several novel oxidative stress associated HF biomarkers. Plasma GSH concentrations have been shown to be highly associated with cardiac disease severity (46–48). 5-oxoproline, a degradation product of GSH and an oxidative stress inducing metabolite, has recently also been shown to associate with outcome in patients with HF. Likewise, serum GGT levels were found to be significantly associated with CVDs risk. Finally, both GR and GPx-1 activity, measured in patient plasma, were shown to be predictors for cardiovascular risk. These findings further address the importance GSH and the γ-Glutamyl cycle have in the development and progression of HF.

**Future Perspectives**

Given the high morbidity and mortality rate in heart failure the identification of new pathways and therapeutic targets is crucial. These efforts may eventually lead to the discovery of novel therapies for HF. To this end in the work described in this thesis we tried to uncover novel therapeutic candidates by looking at the process of fetal reprogramming, a process where the gene expression profile of the diseased heart resembles that of the developing heart, leading to the discovery of OPLAH and 5-oxoproline.

Besides the work covered in this thesis, limited information is available in the current scientific literature regarding OPLAH in particular in the HF setting. Furthermore, to date there are no known compounds which have the capacity to specifically increase the expression or activity of OPLAH. Thus the development of an innovative drug screening tool for OPLAH expression or activity may lead to the identification of novel therapeutic strategies and improved prognosis for patients with HF. The most applicable technique to increase the expression of OPLAH in patient hearts would involve some form of genetic manipulation, such as gene therapy. However, this technique carries a high risk to it, and its safety and effectiveness remains unproven (49). One could also induce OPLAH expression by targeting ERRα, however this transcription factor targets a large number of other genes (including genes involved in energy metabolism, mitochondrial oxidative metabolism, mitochondrial biogenesis, lipid metabolism and carbohydrate metabolism) and it is uncertain what the safety, effectiveness, and whether this would lead to any beneficial effects. Thus, the most clinically viable therapeutic option would be to identify a highly specific and selective compound capable of increasing the endogenous OPLAH activity.

Another way one could envision the work covered in this thesis to translate into the clinic would be in utilizing 5-oxoproline as a diagnostic and/or prognostic biomarker for patient with HF. Although it is still not certain whether the 5-oxoproline present in plasma is directly linked to the reduction of OPLAH in the myocardium, the association we show throughout this thesis is that plasma 5-oxoproline is clearly elevated in HF patients. In patients with acute HF plasma 5-oxoproline is highly associated with patient outcome. Interestingly, since 5-oxoproline is associated with oxidative stress, and a reduction in OPLAH and an accumulation of 5-oxoproline lead to the development of a HFpEF-like phenotype in mice, suggests a possible link to HFpEF. When measured in a cohort of HFpEF 5-oxoproline was found to be elevated and associate with concentric remodeling. This observation suggest that 5-oxoproline is also involved in the onset of clinical HFpEF. However, it is still not certain whether 5-oxoproline is a good biomarker to distinguish between HF patients with HFpEF and patients with reduced ejection fraction (HFrEF). To fully characterize 5-oxoproline as a HF biomarker it would be of interest to measure the plasma 5-oxoproline levels in a large cohort of HF patients, including both HFpEF and HFrEF patients. Finding 5-oxoproline to be selective for patients with HFpEF, would be a major breakthough since to date there are no available biomarkers that can specifically distinguish HFpEF from HFrEF. Furthermore we also demonstrate that 5-oxoproline levels in the urine of mice exposed to HF is also elevated. This is an interesting observation and could lead to a novel family of HF biomarkers which could be measured in the urine of HF patients, facilitating the ease of measurement and diagnosis. Thus, although the work in this thesis describes a novel putative

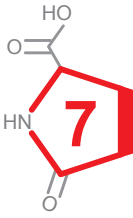

HF biomarker, much remains unknown about the potential of 5-oxoproline as a diagnostic or prognostic marker in cardiovascular diseases.

**Concluding remarks**

With this thesis we aimed to provide a better understanding of fetal reprogramming in HF and how further unraveling this process may lead to novel therapeutic strategies that can benefit HF patients. To this end our work-flow consisted of four distinct steps. Firstly, we performed an RNA sequencing analysis on cardiac development and disease to help identify possible members of the cardiac fetal gene program. Secondly, putative candidate genes were screened in both in vitro and in vivo disease models to identify their importance in cardiac disease. Thirdly, we developed over-expression and knock-out murine models of our top candidate gene (*OPLAH*) to help unravel its role in myocardial dysfunction. Finally, by studying the pathophysiology of OPLAH we uncovered that its substrate, 5-oxoproline, could function as a possible novel biomarker in HF.

In this highly translational study, we went from gene discovery by means of RNA sequencing to in vitro and in vivo HF disease models, and finally transitioning into the clinical setting with the identification of a novel HF biomarker. Thus, this thesis offers a novel pathophysiological avenue in HF, that if further explored, could aid in the development of new therapeutic options for HF patients.

# References


1. Stewart S, MacIntyre K, MacLeod MM., Bailey AE., Capewell S, McMurray JJ. Trends in hospitalization for heart failure in Scotland, 1990–1996. An epidemic that has reached its peak? Eur Heart J 2001;22.
2. Clerk A, Cullingford TE, Fuller SJ, Giraldo A, Markou T, Pikkarainen S, Sugden PH. Signaling pathways mediating cardiac myocyte gene expression in physiological and stress responses. J Cell Physiol 2007;212:311–322.
3. Bilsen M van, Smeets PJH, Gilde AJ, Vusse GJ van der. Metabolic remodelling of the failing heart: the cardiac burn-out syndrome? Cardiovasc Res 2004;61:218–226.
4. Young ME, Patil S, Ying J, Depre C, Ahuja HS, Shipley GL, Stepkowski SM, Davies PJ, Taegtmeyer H. Uncoupling protein 3 transcription is regulated by peroxisome proliferator-activated receptor (alpha) in the adult rodent heart. FASEB J 2001;15:833–845.
5. Minchenko O, Opentanova I, Caro J. Hypoxic regulation of the 6-phosphofructo-2-kinase/fructose-2,6-bisphosphatase gene family (PFKFB-1-4) expression in vivo. FEBS Lett 2003;554:264–270.
6. Miyata S, Minobe W, Bristow MR, Leinwand LA. Myosin heavy chain isoform expression in the failing and nonfailing human heart. Circ Res 2000;86:386–390.
7. Lompre AM, Schwartz K, d'Albis A, Lacombe G, Thiem N Van, Swynghedauw B. Myosin isoenzyme redistribution in chronic heart overload. Nature 1979;282:105–107.
8. Morano I. Tuning the human heart molecular motors by myosin light chains. J Mol Med 1999;77:544–555.
9. Razeghi P, Young ME, Alcorn JL, Moravec CS, Frazier OH, Taegtmeyer H. Metabolic gene expression in fetal and failing human heart. Circulation 2001;104:2923–2931.
10. Schwartz K, Carrier L, Chassagne C, Wisnewsky C, Boheler KR. Regulation of myosin heavy chain and actin isogenes during cardiac growth and hypertrophy. Symp Soc Exp Biol 1992;46:265–272.
11. Schwartz K, Boheler KR, la Bastie D de, Lompre AM, Mercadier JJ. Switches in cardiac muscle gene expression as a result of pressure and volume overload. Am J Physiol 1992;262:R364–R369.
12. Boheler KR, Carrier L, La Bastie D De, Allen PD, Komajda M, Mercadier JJ, Schwartz K. Skeletal actin mRNA increases in the human heart during ontogenic development and is the major isoform of control and failing adult hearts. J Clin Invest 1991;88:323–330.
13. Kuwahara K, Nishikimi T, Nakao K. Transcriptional regulation of the fetal cardiac gene program. J Pharmacol Sci 2012;119:198–203.
14. Yin Z, Ren J, Guo W. Sarcomeric protein isoform transitions in cardiac muscle: A journey to heart failure. Biochim Biophys Acta - Mol Basis Dis 2015;1852:47–52.
15. Kim S-H, Kim H-S, Lee M-M. Re-expression of fetal troponin isoforms in the postinfarction failing heart of the rat. Circ J 2002;66:959–964.
16. Schiaffino S, Gorza L, Ausoni S. Troponin isoform switching in the developing heart and its functional consequences. Trends Cardiovasc Med 1993;3:12–17.
17. Rajabi M, Kassiotis C, Razeghi P, Taegtmeyer H. Return to the fetal gene program protects the stressed heart: a strong hypothesis. Heart Fail Rev 2007;12:331–343.
18. Lahmers S, Wu Y, Call DR, Labeit S, Granzier H. Developmental Control of Titin Isoform Expression and Passive Stiffness in Fetal and Neonatal Myocardium. Circ Res 2004;94:505–513.
19. Neagoe C, Kulke M, Monte F Del, Gwathmey JK, Tombe PP De, Hajjar RJ, Linke WA. Titin isoform switch in ischemic human heart disease. Circulation 2002;106:1333–1341.
20. Harrell MD, Harbi S, Hoffman JF, Zavadil J, Coetzee WA. Large-scale analysis of ion channel gene expression in the mouse heart during perinatal development. Genomics 2007;273–283.
21. Borlak J, Thum T. Hallmarks of ion channel gene expression in end-stage heart failure. FASEB J 2003;17:1592–1608.
22. Nattel S, Maguy A, Bouter S Le, Yeh Y-H. Arrhythmogenic ion-channel remodeling in the heart: heart failure, myocardial infarction, and atrial fibrillation. Physiol Rev 2007;87:425–456.
23. Nattel S, Frelin Y, Gaborit N, Louault C, Demolombe S. Ion-channel mRNA-expression profiling: Insights into cardiac remodeling and arrhythmic substrates. J Mol Cell Cardiol Elsevier Inc.; 2010;48:96–105.
24. Kempen MJA Van, Fromaget C, Gros D, Moorman AFM, Lamers WH. Spatial Distribution of Connexin43 , the Major Cardiac Gap Junction Protein , in the Developing and Adult Rat Heart. 1991;1638–1651.
25. Fromaget C, Aoumari A el, Dupont E, Briand JP, Gros D. Changes in the expression of connexin 43,


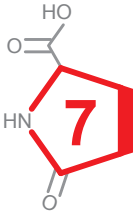

a cardiac gap junctional protein, during mouse heart development. J Mol Cell Cardiol 1990;22:1245–1258.
26. Hertzberg EL, Spray DC, Leinwand LA. Expression of Connexin43 in the Developing Rat Heart. Circ Res 1991;68:782–787.
27. Severs NJ, Coppen SR, Dupont E, Yeh HI, Ko YS, Matsushita T. Gap junction alterations in human cardiac disease. Cardiovasc Res 2004;62:368–377.
28. Wang Y, Hill JA. Electrophysiological remodeling in heart failure. J Mol Cell Cardiol 2010;48:619–632.
29. Severs NJ, Bruce AF, Dupont E, Rothery S. Remodelling of gap junctions and connexin expression in diseased myocardium. Cardiovasc Res 2008;80:9–19.
30. Taur Y, Frishman WH. The cardiac ryanodine receptor (RyR2) and its role in heart disease. Cardiol Rev 2005;13:142–146.
31. Antzelevitch C, Pollevick GD, Cordeiro JM, Casis O, Sanguinetti MC, Aizawa Y, Guerchicoff A, Pfeiffer R, Oliva A, Wollnik B, Gelber P, Bonaros EP, Burashnikov E, Wu Y, Sargent JD, Schickel S, Oberheiden R, Bhatia A, Hsu L-F, Haïssaguerre M, Schimpf R, Borggrefe M, Wolpert C. Loss-of-function mutations in the cardiac calcium channel underlie a new clinical entity characterized by ST-segment elevation, short QT intervals, and sudden cardiac death. Circulation 2007;115:442–449.
32. El-Armouche A, Ouchi N, Tanaka K, Doros G, Wittköpper K, Schulze T, Eschenhagen T, Walsh K, Sam F. Follistatin-like 1 in chronic systolic heart failure: a marker of left ventricular remodeling. Circ Heart Fail 2011;4:621–627.
33. Villar A V, García R, Llano M, Cobo M, Merino D, Lantero A, Tramullas M, Hurlé JM, Hurlé MA, Nistal JF. BAMBI (BMP and activin membrane-bound inhibitor) protects the murine heart from pressure-overload biomechanical stress by restraining TGF-β signaling. Biochim Biophys Acta 2013;1832:323–335.
34. Meister A, Anderson ME. Glutathione. Annu Rev Biochem Annual Reviews 4139 El Camino Way, P.O. Box 10139, Palo Alto, CA 94303-0139, USA ; 1983;52:711–760.
35. Liu Y, Hyde AS, Simpson MA, Barycki JJ. Emerging regulatory paradigms in glutathione metabolism. Adv Cancer Res 2014;122:69–101.
36. Huss JM, Torra IP, Staels B, Giguere V, Kelly DP. Estrogen-Related Receptor Directs Peroxisome Proliferator-Activated Receptor Signaling in the Transcriptional Control of Energy Metabolism in Cardiac and Skeletal Muscle. Mol Cell Biol 2004;24:9079–9091.
37. Rowe GC, Jiang A, Arany Z. PGC-1 coactivators in cardiac development and disease. Circ Res NIH Public Access; 2010;107:825–838.
38. Dufour CR, Wilson BJ, Huss JM, Kelly DP, Alaynick WA, Downes M, Evans RM, Blanchette M, Giguère V. Genome-wide orchestration of cardiac functions by the orphan nuclear receptors ERRalpha and gamma. Cell Metab 2007;5:345–356.
39. Pederzolli CD, Sgaravatti AM, Braum CA, Prestes CC, Zorzi GK, Sgarbi MB, Wyse ATS, Wannmacher CMD, Wajner M, Dutra-Filho CS. 5-Oxoproline reduces non-enzymatic antioxidant defenses in vitro in rat brain. Metab Brain Dis 2007;22:51–65.
40. Pederzolli CD, Mescka CP, Zandoná BR, Moura Coelho D de, Sgaravatti AM, Sgarbi MB, Souza Wyse AT de, Duval Wannmacher CM, Wajner M, Vargas CR, Dutra-Filho CS. Acute administration of 5-oxoproline induces oxidative damage to lipids and proteins and impairs antioxidant defenses in cerebral cortex and cerebellum of young rats. Metab Brain Dis 2010;25:145–154.
41. Pol A van der, Gil A, Silljé HHW, Tromp J, Ovchinnikova ES, Vreeswijk-Baudoin I, Hoes M, Domian IJ, Sluis B van de, Deursen JM van, Voors AA, Veldhuisen DJ van, Gilst WH van, Berezikov E, Harst P van der, Boer RA de, Bischoff R, Meer P van der. Accumulation of 5-oxoproline in myocardial dysfunction and the protective effects of OPLAH. Sci Transl Med 2017;9:eaam8574.
42. Lu SC. Glutathione synthesis. Biochim Biophys Acta 2013;1830:3143–3153.
43. Arthur JR. The glutathione peroxidases. Cell Mol Life Sci 2000;57:1825–1835.
44. Bachhawat AK, Thakur A, Kaur J, Zulkifli M. Glutathione transporters. Biochim Biophys Acta 2013;1830:3154–3164.
45. Lu SC. Regulation of glutathione synthesis. Mol Aspects Med 30:42–59.
46. Adamy C, Mulder P, Khouzami L, Andrieu-abadie N, Defer N, Candiani G, Pavoine C, Caramelle P, Souktani R, Corvoisier P Le, Perier M, Kirsch M, Damy T, Berdeaux A, Levade T, Thuillez C, Hittinger L, Pecker F. Neutral sphingomyelinase inhibition participates to the benefits of N-acetylcysteine treatment in post-myocardial infarction failing heart rats. J. Mol. Cell. Cardiol. 2007. p. 344–353.
47. Bourraindeloup M, Adamy C, Candiani G, Cailleret M, Bourin M-C, Badoual T, Su JB, Adubeiro S, Roudot-Thoraval F, Dubois-Rande J-L, Hittinger L, Pecker F. N-acetylcysteine treatment normalizes

serum tumor necrosis factor-alpha level and hinders the progression of cardiac injury in hypertensive rats. Circulation 2004;110:2003–2009.

48. Damy T, Kirsch M, Khouzami L, Caramelle P, Corvoisier P Le, Roudot-Thoraval F, Dubois-Randé J-L, Hittinger L, Pavoine C, Pecker F. Glutathione deficiency in cardiac patients is related to the functional status and structural cardiac abnormalities. PLoS One 2009;4:e4871.
49. Hulot J-S, Salem J-E, Redheuil A, Collet J-P, Varnous S, Jourdain P, Logeart D, Gandjbakhch E, Bernard C, Hatem SN, Isnard R, Cluzel P, Feuvre C Le, Leprince P, Hammoudi N, Lemoine FM, Klatzmann D, Vicaut E, Komajda M, Montalescot G, Lompré A-M, Hajjar RJ, AGENT-HF Investigators. Effect of intracoronary administration of AAV1/SERCA2a on ventricular remodelling in patients with advanced systolic heart failure: results from the AGENT-HF randomized phase 2 trial. Eur J Heart Fail 2017;19:1534–1541.

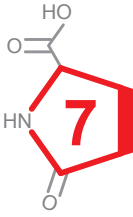

# Chapter 8

## Summary

Heart failure (HF) as a result of myocardial infarction (MI) and ischaemic heart disease remains the most prominent health challenge of the developed world, with a five year survival rate of less than 50%. Although, many breakthroughs have been made, the fundamental mechanisms responsible for the development and progression of HF have not yet been fully elucidated. In recent years it has been observed that cardiac injury in the adult heart leads to a switch in gene expression which to some extend resembles the expression pattern observed in the fetal heart. This process has been described as cardiac fetal reprogramming, and is defined as the suppression of adult and re-expression of fetal genes in the diseased myocardium. The exact reasons and mechanisms as to why the adult heart reverts back to a fetal-like expression pattern and the consequences here of remain unknown.

In **chapter 2**, we reviewed the current knowledge regarding cardiac fetal reprogramming in HF, by looking at the expression profiles during cardiac development and disease, with a particular focus on cardiac metabolism, contractile machinery, electrophysiology, and neurohormonal expression. The findings discussed in **chapter 2**, suggest that cardiac fetal reprogramming is an integral part of the pathophysiology of HF. Although there is plethora of evidence regarding cardiac fetal reprogramming and its importance during HF, there still remains much to be uncovered regarding this process and its involvement in the development and/or progression of HF.

With this thesis we tried to further characterize cardiac fetal reprogramming in HF, and how a better understanding of this process can lead to novel therapeutic strategies for patients with HF. In **chapter 3**, we identified several novel genes of the cardiac fetal gene program, by looking expression at different stages of cardiac development and disease in mice. Of the identified genes, *OPLAH* encoding 5-oxoprolinase a member of the γ-Glutamyl cycle, was found to be the most cardiac specific. Further investigation revealed that OPLAH possessed a cardio-protective function by scavenging 5-oxoproline, an oxidative stress inducing metabolite formed by de degradation of glutathione. In turn, we also demonstrate that 5-oxoproline is a novel biomarker for patients with HF. Together these findings suggest *OPLAH*, a novel member of the cardiac fetal gene program, to be an ideal target for therapeutic intervention in HF.

To further study the importance of OPLAH in the heart, in **chapter 4**, we describe the development of an *Oplah* full body knock-out (KO) mouse and the effects ischemia/reperfusion (IR) injury has on these mice. At baseline, KO mice were found to have a cardiac and renal phenotype resembling the clinical manifestation of HF with preserved ejection fraction (HFpEF). To date, there is limited knowledge regarding the pathophysiology of HFpEF, and more importantly there are no known treatment

options for patients with this disease. Therefore, developing a murine model for HFpEF by means of OPLAH ablation, leading to increased oxidative stress from 5-oxoproline accumulation, may eventually lead to a better understanding of the disease and possible new therapeutic strategies to treat the disease. By stressing these KO mice by inducing HF, we found these mice to be more susceptible to cardiac injury. Finally, we also demonstrate that 5-oxoproline is elevated in the plasma of HFpEF patients and associates with more concentric remodeling, a hallmark of HFpEF. Although, highly interesting, it still remains uncertain to what extend OPLAH and 5-oxoproline are involved in the onset of clinical HFpEF. Additionally, it still remains unclear as to what extend circulating 5-oxoproline is specific for HFpEF, or whether it is a marker for HF in general.

In **chapter 3** and **chapter 4** we utilized a LC-MS method that enabled us to measure 5-oxoproline and glutamate. However to obtain a better understand of the involvement of the γ-glutamyl cycle in heart failure, in **chapter 5**, we sought out to develop a LC-MS method for the quantification of 5-oxoproline, glutamate, GSH and GSSG (oxidized GSH), key components of the γ-glutamyl cycle, in biological samples. Utilizing the developed methodology, we assessed the effects on the γ-glutamyl cycle following the induction of HF in mice. Specifically in the heart we found increases in 5-oxoproline together with a decrease in the GSH/GSSG ratio in mice exposed to HF, further strengthening the notion that 5-oxoproline is an oxidative stress inducing agent. In addition to being elevated in the heart, 5-oxoproline levels were found to be increased in the kidney, liver, plasma and urine of all mice exposed to HF. However, the GSH/GSSG ratios in the kidney and liver of these animals remained stable, suggesting that these tissues have a higher buffering capacity for oxidative stress. Interestingly, we found 5-oxoproline levels in urine to be elevated following cardiac injury, suggesting that, like plasma, urine 5-oxoproline levels could serve as a possible HF biomarker.

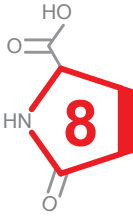


OPLAH is a member of the γ-Glutamyl cycle, and following the observations made in this thesis, we were interested in further characterizing this cycle in HF and uncover whether other members of this cycle could also serve as possible therapeutic targets for patients with HF. To this end, in **chapter 6** we reviewed the current knowledge regarding the γ-Glutamyl cycle and its association to oxidative stress and HF. Several studies focused on the γ-Glutamyl cycle have uncovered that certain enzymes involved in this cycle have cardio-protective properties, including GCL, GPx, and OPLAH. However, clinical strategies for targeting these steps have not been explored, which is in large part due to the lack of drugs or small molecules that specifically target these enzyme. The research focused on dissecting the involvement of the γ-Glutamyl cycle and GSH in HF has not only resulted in the

identification of novel therapeutic targets for this disease, but has also lead to the characterization of several novel oxidative stress associated HF biomarkers. These findings further address the importance GSH and the γ-Glutamyl cycle have in the development and progression of HF.

In summary, we show that, by further characterizing the cardiac fetal gene program, novel targets for therapeutic intervention in HF can be identified. We demonstrate that *OPLAH*, a novel cardiac fetal gene, has a cardio-protective effect in HF and that the ablation of this gene results in the development of HFpEF in mice. Furthermore, we characterize the substrate of OPLAH, 5-oxoproline, as being a novel HF biomarker. Together these findings identify OPLAH and 5-oxoproline as novel pathophysiological pathway in HF, and targeting the expression and/or activity of OPLAH may lead to new therapeutic options of HF patients.

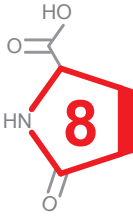
HO
O
HN
8
O

# Chapter 9

## Nederlandse samenvatting

Hartfalen als gevolg van een myocardiaal infarct (MI) of ischemische hartziekte blijft de prominentste uitdaging van de ontwikkelde wereld met slechts 50% overlevingskans in de eerste vijf jaren na diagnose. Ondanks de vele doorbraken zijn de onderliggende mechanismen voor de ontwikkeling en progressie van hartfalen tot op heden nog niet opgehelderd. In recente jaren is gebleken dat cardiale schade leidt tot het omschakelen van een volwassen genprofiel naar een genprofiel dat kenmerkend is voor een foetaal hart. Dit proces wordt omschreven als foetale herprogrammering (fetal reprogramming) en wordt omschreven als het onderdrukken van adulte genen, terwijl foetale genen opnieuw tot expressie komen in de aangedane hartspier. De exacte reden waarom het hiertoe leidt en het mechanisme hier achter zijn vooralsnog onbekend.

In **hoofdstuk 1** hebben we de huidige kennis besproken met betrekking tot cardiale foetale reprogrammering tijdens hartfalen door de genprofielen die aanwezig zijn tijdens ziekte en gezondheid te bestuderen. We hebben voornamelijk aandacht geschonken aan cardiaal metabolisme, het contractieapparaat, elektrofysiologie en neurohormonaal. De bevindingen in **hoofdstuk 1** suggereren dat foetale reprogrammering een integraal deel is van de pathofysiologie van hartfalen. Hoewel er een overvloedig is aan data die deze processen beschrijven, er is nog veel te ontdekken over de mate waarin foetale reprogrammering bijdraagt aan de ontwikkeling van hartfalen en het verdere verloop van de ziekte.

In dit proefschrift hebben we proberen te karakteriseren welke rol cardiale foetale reprogrammering speelt tijdens hartfalen en hoe een beter begrip van dit proces kan leiden tot nieuwe behandelmethodes voor hartfalenpatiënten. In **hoofdstuk 2** hebben we enkele genen ontdekt binnen het foetale cardiale genprofiel door de verschillende genexpressiepatronen te bestuderen tijdens de ontwikkeling van de muis en in zieke muizen. Tussen deze nieuwe genen was specifiek in het hart *OPLAH* het prominentst aanwezig. *OPLAH* is een gen dat codeert voor 5-oxoprolinase en speelt een rol in de γ-Glutamyl cyclus. Na aanvullend onderzoek bleek dat OPLAH een beschermende functie heeft in hart door het schadelijke 5-oxoproline om te zetten tot een onschadelijk product. 5-oxoproline is een metaboliet dat oxidatieve stress veroorzaakt in het lichaam en wordt gevormd door de afbraak van een belangrijke afweermolecuul: gluthathione. OPLAH kan van het afgebroken van 5-oxoproline weer functioneel gluthathione maken. Daarnaast toonden we aan dat 5-oxoproline een nieuwe biomarker kan zijn voor hartfalen. Uit dit onderzoek blijkt dat *OPLAH* (een nieuw gen binnen het cardiale foetale genprofiel) een ideaal onderwerp kan zijn voor nieuwe behandelingen.

In **hoofdstuk 3** beschreven we de ontwikkeling van een algehele *Oplah*-knockout muis

en de effecten van ischemie-reperfusieschade in deze muizen. De uitgangswaarden in de knockout muis suggereerden dat de muizen een cardiale en renale stoornis hadden zoals ook wordt gezien in patiënten met hartfalen met een behouden kamerfunctie (ook wel HFpEF genoemd). Tot op heden is er maar beperkte kennis over the pathofysiologie van HFpEF en er zijn geen effectieve behandelmethodes beschikbaar. Om deze reden was het ontwikkelen van een muismodel door middel van het uitschakelen van OPLAH waardoor 5-oxoproline stapeling optrad een eerste stap in de richting van het beter leren begrijpen van HFpEF en mogelijk heeft dit een behandelmethode tot gevolg. Door deze *Oplah*-knockout muizen bloot te stellen aan hartfalen konden we bevestigen dat ze tevens vatbaarder waren voor cardiale schade. Uiteindelijk lieten we ook zien dat het 5-oxoproline niveau in het bloed van HFpEF-patiënten verhoogd was en dat ze (net als de *Oplah*-knockout muizen) meer concentrische ventrikelremodelering hadden. Hoewel het zeer interessant is, blijft het onduidelijk in welke mate OPLAH en 5-oxoproline betrokken zijn bij de ontwikkeling van HFpEF. Met dit onderzoek is het ook niet duidelijk hoe specifiek 5-oxoproline in het bloed specifiek geassocieerd is met HFpEF; mogelijk is het een kenmerk voor hartfalen in het algemeen.

In **hoofdstuk 2** en **hoofdstuk 3** hebben we gebruik gemaakt van vloeistof chromatografie-massa spectrometrie (Engelse afkorting: LC-MS). Hiermee waren we in staat 5-oxoproline- en glutamaatwaardes in bloed kunnen te meten. Om een beter begrip te krijgen van de mate van betrokkenheid van de γ-glutamylcyclus tijdens hartfalen hebben we in **hoofdstuk 4** een nieuwe LC-MS-methode ontwikkeld om de belangrijkste stoffen van deze cyclus te kunnen meten: 5-oxoproline, glutamaat, gluthathione (GSH) en geoxideerd gluthathione (GSSG). Met deze nieuwe methode konden we de γ-glutamylcyclus bestuderen in muizen met hartfalen. We observeerden dat er in verhouding meer GSSG aanwezig was in het hart van muizen met hartfalen; een waarneming die de hypothese dat 5-oxoproline oxidatieve stress veroorzaakt verder ondersteunt. Bovendien vonden we verhoogde 5-oxorpolinewaardes in de nieren, lever, plasma en urine van muizen met hartfalen. De GSH/GSSG balans in de nieren en lever bleef stabiel; dit duidt op een verhoogde buffercapaciteit voor oxidatieve stress in deze organen tijdens hartfalen. Tevens waren de 5-oxoprolineniveaus verhoogd in de urine tijdens hartfalen. Dit is een sterke suggestie dat urinewaardes (net als in het plasma) gebruikt kunnen worden als biomarker voor hartfalen.

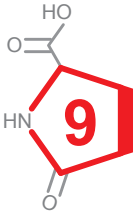


OPLAH is deel van de γ-glutamylcyclus en – op basis van de bevindingen in dit proefschrift – waren we geïnteresseerd in het karakteriseren van deze cyclus tijdens hartfalen zodat we andere delen van de cyclus konden identificeren die als mogelijk behandeld kunnen worden in patiënten met hartfalen. Om deze reden hebben we

de huidige stand van zaken rondom de γ-glutamylcyclus nauwkeurig uiteengezet in **hoofdstuk 5**. Diverse studies richtte zich tot enkele enzymen in de cyclus die een beschermende functie hebben in het hart, waaronder: GCL, GPx en OPLAH. Ongeacht deze kennis is de therapeutische potentie van deze enzymen nooit onderzocht, omdat er een gebrek is aan medicijnen of andere moleculen waarmee deze enzymen specifiek beïnvloed worden. Dit onderzoek richtte zich voornamelijk op het ontleden van de γ-glutamylcyclus met als doel om nieuwe behandelingen te ontwikkelen, maar ook om nieuwe oxdatieve stress biomarkers te ontdekken die een rol spelen bij hartfalen. Onze bevindingen geven een duidelijke noodzaak weer van de rol van GSH en de γ-glutamylcyclus tijdens het ontstaan en verloop van hartfalen.

In dit proefschrift hebben we aangetoond dat nieuwe behandelstrategieën mogelijk zijn als gevolg van het karakteriseren van het cardiale foetale genenprofiel. We hebben bewezen dat *OPLAH* (als nieuwe cardiaal foetaal gen) een beschermende rol speelt in het hart tijdens hartfalen en dat een verminderde expressie van het gen HFpEF tot gevolg heeft in muizen. Bovendien hebben we 5-oxoproline geïdentificeerd als nieuwe biomarker voor hartfalen. Alles bij elkaar genomen hebben we de pathway met OPLAH en 5-oxoproline geïdentificeerd als een nieuw proces binnen de pathofysiologie van hartfalen en zou het een mogelijk onderwerp voor behandeling kunnen zijn in patiënten met hartfalen.

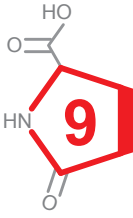
HO
O
HN
9
O

# Appendices

# Curriculum vitae & publications

## Biography

The author of this thesis, Atze van der Pol, was born on April 28th 1986 in Yaoundé, Cameroon. After finishing his high school degree, at the American International School of Guatemala, in 2004, he enrolled at the University of Groningen, The Netherlands, in pursuit of a B.Sc in Biology. In 2009 Atze obtained his B.Sc in Biology double majoring in Medical Biology and Molecular Biology. It was during his second undergraduate research at the lab of Dr. Marcel Behr (McGill University, Montreal, Canada) that Atze developed a keen interest in clinical research directed at curing human afflictions. In 2011, Atze acquired his M.Sc in Molecular Biology and Biotechnology at the University of Groningen. In November 2011 he started his PhD project in the laboratory of Prof. dr. Wiek van Gilst, under supervision of Dr. Peter van der Meer, at the University Medical Center Groningen (The Netherlands). The central focus of his research were to elucidate novel mechanisms implicating cardiac fetal reprogramming in Cardiovascular Diseases, with a particular interest in discovering putative therapeutic targets for clinical intervention. During his PhD project, Atze was awarded the first runner-up prize at the European Society of Cardiology, Young Investigator Award Sessions (Paris, France, 2017). The outcome of his research is presented in this thesis.

## Attended Meetings

1. European Society of Cardiology, Young Investigator Award Sessions, Paris, France, 2017
2. American Heart Association, Scientific Sessions, Chicago (Illinois), USA, 2014
3. American Heart Association, Scientific Sessions, Dallas (Texas), USA, 2013

## Awards

First runner up Award at the European Society of Cardiology, Young Investigator Award Sessions, Paris, France, 2017

## Publications

1. Accumulation of 5-oxoproline in myocardial dysfunction and the protective effects of OPLAH. Sci Transl Med. 2017;9:eaam8574
2. Rodent heart failure models do not reflect the human circulating microRNA signature in heart failure, PLoS One 2017 May; 12(5):1-14
3. Fibrosis Marker Syndecan-1 and Outcome in Patients With Heart Failure With Reduced and Preserved Ejection Fraction, Circ Heart Fail. 2014 May;7(3):457-462
4. Cardiac regeneration in left ventricular dysfunction: are we asking the right questions?, Eur J Heart Fail. 2012 January;14(1):1-4

# Acknowledgements

The successful completion of a PhD is no small feat, and I can speak of my own experience, that this would not have been possible without the help, friendship, support, and guidance of many people whom I would like to acknowledge below.

Foremost, I would like to express my sincerest gratitude towards Prof. dr. Peter van der Meer. Dear Peter, from the beginning of my PhD project you were my co-promotor and only in the last few months did you also become my promotor. I want to thank you for the opportunity and the faith you placed in me throughout the rollercoaster that was my PhD. In the beginning you entrusted me with setting up the murine stem cell culture in our lab, and although this was highly interesting and we managed to obtain some nice results in the end we moved off of this project in pursuit of novel therapeutic targets in cardiac disease. Upon choosing a gene of interest from our initial screenings we had a difference of opinion concerning which gene to further pursue, GRB7 or OPLAH. In the end I managed to convince you about OPLAH and you basically gave me “carte blanche” to unravel the role of this gene in heart failure. By enabling me to work very independently on this project I have learned a lot about what it means to set up a research project from scratch. In many ways the researcher I am today is in no small part due to your guidance, support, and positive re-enforcement, and for that I would like to thank you!

I would like to thank my promotor Prof. dr. Wiek van Gilst. Dear Wiek, I would like to thank you for all your support over the years. Your positive attitude and your critical thinking in regards to science have had a great influence on me. It was always a great support to know that your door was always open for me if needed. For this I would like to thank you!

I would also like to thank my promotor Prof. dr. Rudolf A. de Boer. Dear Rudolf, I would like to thank you for all your help in regards to my PhD work. Over the years you always brought great input into my projects. All of your comments and questions during Lunch meetings and PhD meetings always helped me to look at my work from a different perspective. For this I am very grateful!

I would like to thank Dr. Herman Silljé. Dear Herman, from the very beginning of my PhD project you were a great source of knowledge and experience which were invaluable for me. I came to the department with a background mainly focused on microbiology, and it was thanks to you that I developed the skills required to fully develop my project, eventually leading to the work in this thesis. I learned a lot from you, and appreciate your help and overall contribution.

I want to also thank Prof. dr. Rainer Bischoff. Dear Rainer, without your knowledge

and hands-on experience in the field of mass-spectrometry, I would have never been able to elevate the research in this thesis to the level it currently has. For that and all the constructive discussions, I give you my sincerest gratitude.

To the members of my reading committee, Prof. dr. Joost P.G. Sluijter, Prof. dr. Ellen A.A. Nollen and Prof. dr. Gerjan Navis, thank you for your critical evaluation of my work.

To my paranymphs and good friends Martijn and Jasper, thank you for all the support over the years. Jasper, you started out working as a student for me and we spend many hours (even on weekends) working in the lab, and from the very beginning it was always a blast to work with you. I am very thankful to you for all the support, humor and interesting conversations we have had over the years! Martijn, you have been a great support for me over the years, both in and outside the lab. You were always available to help me out and for this I am very grateful. Both of you have been a great influence of the years!

To all my colleagues who supported me over the years: Janny, Linda, and Silke, thank you for all your help. I would like to also thank Martin for sharing all his knowledge and expertise, and for your willingness to always help me out! To Inge and Marloes, you two were an integral part of my projects, and we worked for many long hours together in the CDP performing all the required animal experiments for my studies. I thank you two for all the great work and for always being willing to help me out when I needed it! To Kees, I thank you for all the effort you put in performing the murine MRI's for me. We worked long days doing these measurements, and you were always willing to put in the extra hours just to make it possible for me to finish all the animals. I really appreciate your help. Thank you all for your hard work!

To all the post docs, PhDs, and students – past and present – a very big thank you to you all! To Hasan (you really helped me settle in when I first started my PhD at the department), Bo, Meimei, Mariusz, Lili, Hongjuan (you were a great roommate with an amazing sense of humor! Thank you!), Frank, Anne-Margreet and Wardit (thank you for teaching me all the ropes when I first started!), Reinout, Mathilde, Harmen, Rogier, Wouter M, Wouter t' R and Niek (thank you for putting up with me on our travels to various congresses), Weijie, Edgar and Mohsin (thank you for all the great conversations regarding science and life!), Diederik, Guido, Yanick, Nils, Katya, Pedro, Arnold, David, Lysanne (As my roommate who has the same sense of humor as me, we had some very interesting conversations), Hanna, Johanneke, Sebastian, Eline, Aad and Mario.

To Mr. Peder Aune and Mr. Tim Bond I would like to give a special thanks to you! It was thanks to your support, motivation, and enthusiasm that helped me choose for a scientific career and in many ways anecdotes form your high school classes have stuck with me through my university studies. I would like to extend my sincerest gratitude to the both of you!

I would also like to thank Prof. dr. Marcel A. Behr. Dear Marcel, I would like to thank you for giving me the opportunity to work at your lab at the McGill University during my Masters. It is due to this project that I became highly interested in doing research directed at curing human afflictions. Although the project we worked on together was mainly in the field of Medical Microbiology, I learned a lot from you, and it is thanks to that experience that I ended up doing the work presented in this thesis. For that you have my sincerest gratitude.

I would like to thank friends and acquaintances outside of the department. To Tom and Gerard you were the first friends I made here in Groningen, and you have stuck with me throughout all these years. Some of my fondest memories of my time here in Groningen revolve around the three of us and all the crazy things we experienced on and off the lacrosse field! For that I really want to thank you guys. To Rutger, we have known each other since our time studying Biology and I have always appreciated our discussions (most of the time about our own work, since we were both quit passionate about what we did), and Liza thank you for all the great conversations. To Mat, you are one of my oldest friends and I have always enjoyed your way of looking at the world. Andres, without your help in setting up and performing the LC-MS measurements the work I present in this thesis would not have been what it is today.

To my family you have always been there for me and for this you have my sincerest gratitude and love. Mem, tu siempre me has empujado para que yo logre sacar lo máximo de mí mismo y es por esa misma razón que yo he llegado a donde estoy hoy. Gracias por siempre estar ahí en las buenas y en las malas, tú has sido un gran apoyo durante toda mi vida y te lo agradezco muchísimo. Heit, do bist altyd in grut foarbyld foar my west. Ik wolsto graach betankje foar alle motivaasje de ôfrûne jierren. Ik wit dat ik net altyd maklik bin west mar Heit en Mem binne der altyd foar my west, en dêr foar sil ik jimme altyd tankber foar wêzen. To my dear sister, Clara, I would like to say thank you! Since we were kids I always knew you had my back and when I first moved here you were there for me and have been there ever since. For this and all your support over the years I would like to thank you! I also want to thank Juan for helping me out when needed. I have always known I could rely on the two of you. To my beautiful niece, Irene, I can't wait to see what path your life will take you, and knowing the smart and enthusiastic kid that you are I am sure you

will be successful no matter what you do. Bauke, my one and only brother, I can't begin to describe how much I appreciate you. Like me you have a very scientifically oriented mind, and I have always enjoyed our conversations and discussions about science. For this and for always being willing to help me out I would like to thank you. Pake en Beppe, it is jimme net gund om it beheljen fan myn doctoraat te oansjen. Jimme binne der altyd foar my west en dêrfoar sil ik jimme altyd tankber foar wêzen. Mamama, tu tampoco lograste llegar a ver que yo obtuviera mi doctorado. Y aunque no estés aquí yo nunca te olvidare y te quiero agradecer por todo el amor y apoyo que me has dado.

Finally I would like to thank the greatest loves of my life. Azi, you are my love, my wife, my best friend, azizam. I would have never imagined that I would meet the love of my life during my PhD, but here we are seven years later! You have always supported and managed to motivate me throughout all these years. You have had to sacrifice a lot as a result of my workaholic nature, but it is your everlasting patience that has allowed me to finally finalize my PhD. I can't wait to see what the rest of our life has in store for us! Alma Bahar, my most beautiful and loved daughter. You truly have brought a great happiness and an indescribable love to my life. I look forward to seeing you grow, and no matter what you will do in life, I want you to know that I will always be there for you.

Atze